Faculty of Aerospace Engineering

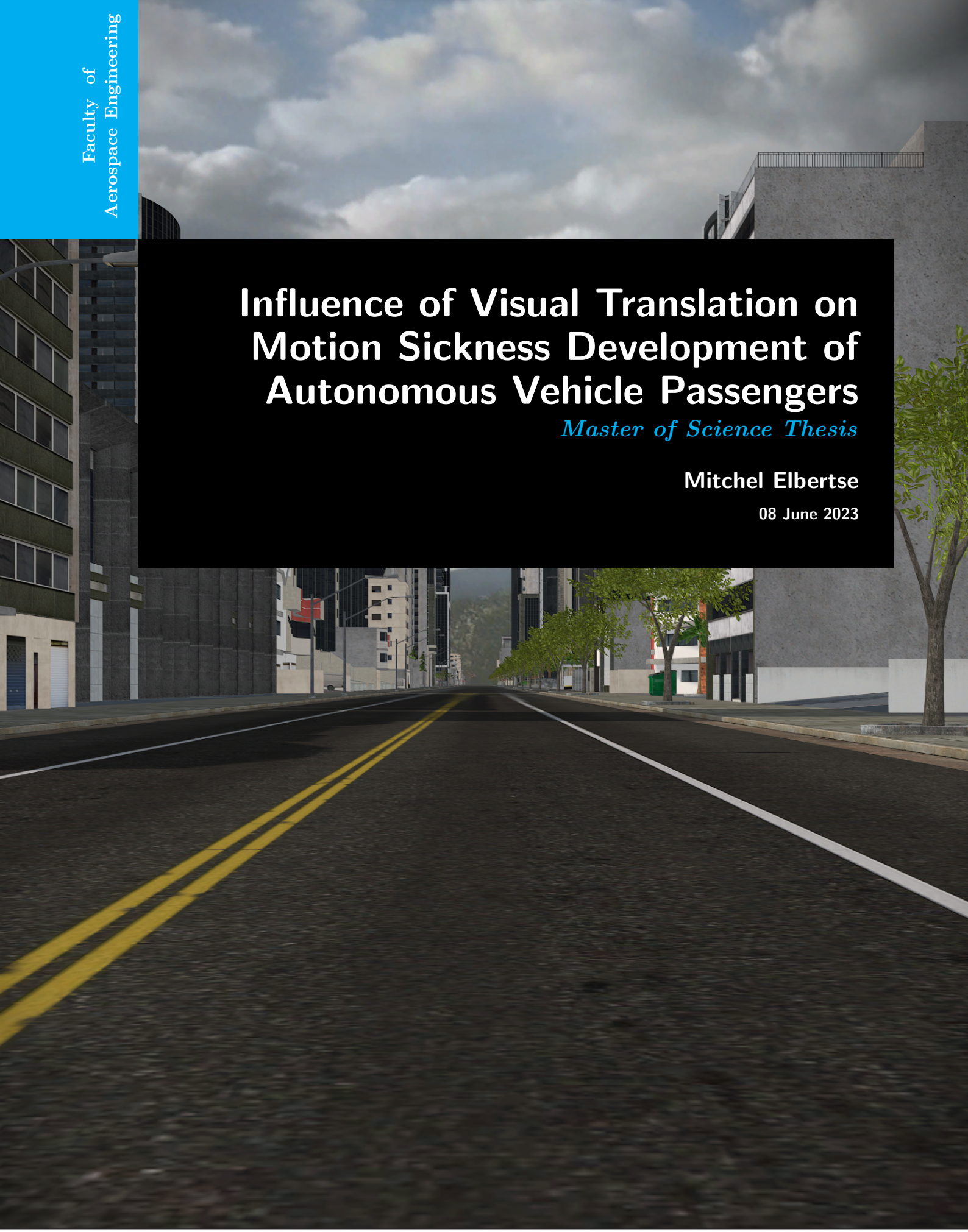

Influence of Visual Translation on Motion Sickness Development of Autonomous Vehicle Passengers

Master of Science Thesis

Mitchel Elbertse

08 June 2023

TU Delft Delft University of Technology

Challenge the future

Influence of Visual Translation on Motion Sickness Development of Autonomous Vehicle Passengers

Master of Science Thesis

Master of Science Thesis

For obtaining the degree of Master of Science in Aerospace Engineering
at Delft University of Technology

Mitchel Elbertse

08 June 2023

Faculty of Aerospace Engineering · Delft University of Technology

Delft University of Technology

Copyright © Mitchel Elbertse
All rights reserved.

Delft University Of Technology
Department Of
Control and Simulation

The undersigned hereby certify that they have read and recommend to the Faculty of Aerospace Engineering for acceptance a thesis entitled **"Influence of Visual Translation on Motion Sickness Development of Autonomous Vehicle Passengers"** by **Mitchel Elbertse** in partial fulfillment of the requirements for the degree of **Master of Science**.

Dated: 08 June 2023

Readers:

prof. dr. ir. M. Mulder

prof. dr. ir. J. C. F. de Winter

dr. ir. M. M. van Paassen

ir. O. Stroosma

ir. R. Wijlens

Acronyms

AV	Automated Vehicle
BL	Baseline
CI	Confidence Interval
CNS	Central Nervous System
DERP	Design Eye-height Reference Point
DLP	Digital Light Processing
DOF	Degrees of Freedom
EM	Eye Movement
FoV	Field of View
GIA	Gravito-Inertial Acceleration
HOF	High Optical Flow
LOF	Low Optical Flow
MISC	MIsery SCale
MS	Motion Sickness
MSI	Motion Sickness Incidence
MSSQ	Motion Sickness Susceptibility Questionnaire
OF	Optical Flow
RMS	Root Mean Square
SCC	Semicircular Canals
SD	Standard Deviation
SEM	Standard Error of the Mean
SeMo	Sensory Model
SRS	SIMONA Research Simulator
SVC	Subjective Vertical Conflict
VIMS	Visually Induced Motion Sickness
VVMS	Visual-Vestibular Motion Sickness

List of Symbols

Roman Symbols

Symbol	Description	Unit
$\boldsymbol{a}$	Inertial acceleration vector	$[m/s^2]$
a_m	maximum acceleration	$[m/s^2]$
a^{SeMo}	Combined visual-vestibular inertial acceleration	$[m/s^2]$
b	Hill function fitting parameter	$[-]$
d	Conflict signal	$[m/s^2]$
e	Error signal	$[-]$
$\boldsymbol{f}$	Specific force vector	$[m/s^2]$
$\boldsymbol{g}$	Subjective vertical vector	$[m/s^2]$
H_{OK}	Transfer function of optokinetic influence	$[-]$
$\boldsymbol{I}$	Camera image signal	$[-]$
$\boldsymbol{i}$	Idiotropic vector	$[m/s^2]$
K_a	Accuracy of inertial acceleration anticipation	$[-]$
K_{ac}	Inertial acceleration conflict loop gain	$[-]$
K_{avis}	Visual acceleration gain	$[-]$
K_{flow}	Optical flow gain	$[-]$
K_{gc}	Subjective vertical conflict loop gain	$[-]$
K_{gvis}	Visual subjective vertical conflict loop gain	$[-]$
K_{OTO}	Otolith dynamics gain	$[-]$
K_{vc}	Subjective vertical conflict loop gain	$[-]$
K_{vis}	Visual gain	$[-]$
K_ω	Accuracy of rotational velocity anticipation	$[-]$
$K_{\omega c}$	Rotational velocity conflict loop gain	$[-]$
$K_{\omega vis}$	Visual rotational velocity conflict loop gain	$[-]$
k_i	Inertial acceleration conflict loop gain for $x-$, $y-$, or $z-$axis	$[-]$
m	Model parameter of polynomial acceleration model	$[-]$
n	Parameter accounting for steepness of Hill function	$[-]$
n	Model parameter of polynomial acceleration model	$[-]$
P	Maximum percentage of people who become motion sick under given circumstances	$[\%]$
$\boldsymbol{p}$	Visual vertical vector	$[m/s^2]$

Symbol	Description	Unit
R	Reduction factor	$[-]$
r	Model parameter of polynomial acceleration model	$[-]$
s	Laplace variable	$[-]$
t	Time	$[s]$
$\boldsymbol{u_d}$	Desired body state	$[-]$
$\boldsymbol{u_s}$	Sensed body state	$[-]$
V_a	Expected vertical signal	$[m/s^2]$
V_p	Perceived vertical signal	$[m/s^2]$
$\boldsymbol{v}$	Subjective vertical vector	$[m/s^2]$
$\boldsymbol{v}$	Velocity vector	$[m/s]$
v_{err}	Washed-out error signal	$[m/s]$
w	Weight	$[-]$

Greek Symbols

Symbol	Description	Unit
$\boldsymbol{\Delta a}$	Inertial acceleration conflict vector	$[m/s^2]$
$\boldsymbol{\Delta g}$	Subjective vertical conflict vector	$[m/s^2]$
$\boldsymbol{\Delta v}$	Subjective vertical conflict vector	$[m/s^2]$
$\boldsymbol{\Delta\omega}$	Rotational velocity conflict vector	$[rad/s]$
ε	Conflict threshold value for cosine bell operator	$[rad/s]$
ζ	Damping factor	$[-]$
θ	Time ratio of polynomial acceleration model	[-]
μ	Time constant of leaky integrator	$[s]$
μ	Average	$[-]$
ρ	Correlation coefficient	$[-]$
σ	Standard deviation	$[-]$
τ_1	First order time constant of otoliths	$[s]$
τ_2	Second order time constant of otoliths	$[s]$
τ_A	Adaptation time constant of semicircular canals	$[s]$
τ_a	Adaptation time constant of semicircular canals	$[s]$
τ_c	Adaptation time constant of visual-vestibular error	$[s]$
τ_d	Decay time constant of semicircular canals	$[s]$
τ_d	Time delay of visual system	$[s]$
τ_{delay}	Time delay of visual system	$[s]$
τ_I	Time constant of leaky integrator	$[s]$
τ_i	Time constant corresponding to visual-vestibular error on the $x-$, $y-$, or $z-$axis	$[s]$
τ_L	Decay time constant of otolithss	$[s]$
τ_l	Decay time constant of semicircular canals	$[s]$
τ_{lp}	Time constant of low-pass filter	$[s]$
τ_{OK}	Time constant of transfer function of optokinetic influence	$[s]$
τ_{va}	Time constant of visual attractor dynamics	$[s]$
τ_w	Adaptation time constant of visual-vestibular error	$[s]$

Symbol	Description	Unit
$\boldsymbol{\omega}$	Rotational velocity vector	$[rad/s]$
ω_{err}	Washed-out error signal	$[rad/s]$
ω_n	Natural frequency	$[rad/s]$

Subscripts

Symbol	Description
HP	High-Pass filter
i	$x-$, $y-$, or $z-$axis
i	participant
LP	Low-Pass filter
s	Sensed by the sensory systems
t	Time point
$vest$	Vestibular system
vis	Visual system

Superscripts

Symbol	Description
i	$x-$, $y-$, or $z-$axis

Accents

Symbol	Description
$\hat{.}$	Expected signal
$\tilde{.}$	Internally estimated signal
$\bar{.}$	(Weighted) average

Contents

List of Figures

List of Tables

Chapter 1

Introduction

Automated Vehicles (AVs) have the potential to bring numerous benefits to society, including a reduction in the number of accidents on the road, alleviation of traffic congestion problems, regulation of fuel consumption and pollution, and reduction in driving times (Begg, 2014). Although the concept of automation in vehicles is not new, with the earliest versions of cruise control having been introduced in the late fifties (Akamatsu, Green, & Bengler, 2013), modern vehicle automation technologies offer a more comprehensive range of features, spanning from anti-lock brakes, adaptive cruise control, and lane keeping to fully automated driving (Diels & Bos, 2016). The primary difference between fully automated driving and the other technologies is that in the former, the car is capable of monitoring, reading, and responding to the environment without driver intervention. As a result, drivers can engage in non-driving-related activities, such as reading a book, watching a display, or conversing with passengers in the back seat, which in theory makes vehicle travel more productive and comfortable (Diels & Bos, 2016).

Despite the potential benefits of automation in vehicles, there is a significant issue surrounding the transition from active driver to passive passenger, which is an increase in the likelihood and severity of Motion Sickness (MS) (Diels & Bos, 2016). A worldwide survey conducted by Schmidt, Kuiper, Wolter, Diels, and Bos (2020) highlights that car passengers are more prone to experiencing MS than car drivers. As such, drivers are typically able to align their head with the direction of motion, as they can anticipate the forthcoming motions (Fukuda, 1976). Such alignment has been shown to alleviate MS (Wada, Fujisawa, & Doi, 2018). On the contrary, vehicle passengers can predict and anticipate these movements to a lesser extent. Therefore, they are unable to align their heads with the direction of motion, making them more susceptible to MS.

It is evident from the previous discussion that motion anticipation plays a crucial role in reducing the occurrence of MS. In this context, Diels, Ye, Bos, and Maeda (2022) suggest that vision is the most crucial modulating factor that is associated with anticipating future motion. However, future scenarios for AVs envision several factors that could potentially impact motion anticipation and MS, such as occluded windows, multimedia displays, passengers engaging in secondary activities, and backward-oriented seats, all of which can directly

influence the out-of-window view (Diels & Bos, 2016). Despite the significance of vision in motion anticipation and MS reduction, the precise role of visual factors, such as Field of View (FoV), optical flow characteristics, and vertical observation from the visual scene, is yet to be understood (Diels et al., 2022). Research is required to address these questions and clarify the importance of the visual field characteristics in reducing MS.

Section 1-1 will go into more detail about the problem statement and the knowledge gap that the current study tries to fill. The research objective and the research question that logically follow from these are provided in Section 1-2. Finally, a complete outline of the Master of Science Thesis report is given in Section 1-3.

1-1 Problem Statement

MS is a malady caused by passive self-motion[1] that contains certain types of dynamic and kinematic properties (Bertolini & Straumann, 2016; Money, 1970). It is suggested that MS occurs when motion-sensitive sensors (i.e., vestibular system, visual system, and somatosensory system) are exposed to conflicting motion signals (Bertolini & Straumann, 2016). It is interesting that subjects who do not have a functional vestibular system are not susceptible to MS (Cheung, Howard, & Money, 1991), indicating the important role of the vestibular system in the nauseogenic stimulus. Each sensory system has its own shortcomings, which our Central Nervous System (CNS) is trying to solve. The CNS has evolved to combine these sensory signals into a best estimate of self-propelled motion. However, passive motion leads to a combination of sensory signals that is impossible for the CNS to interpret, leading to MS (T. Brandt & Daroff, 1980). In addition, individual MS susceptibility depends on many different factors, e.g., gender, age, ethnicity, and physiological factors. However, universal trends in the development of MS could be observed within the population (Bos et al., 2008), which will be the main focus of this research.

The sensory mismatch theory is most widely accepted to explain MS (Bertolini & Straumann, 2016). This theory states that a conflict between sensory systems is only provocative if the present sensory signals are at variance with the expected sensory signals in the CNS. These signals are theorized to be generated by an internal model, which is a copy of the actual sensory dynamics. This internal model is created and updated by previous experiences (Reason & Brand, 1975), and is derived from the observer model theory (Oman, 1982) (see Bos et al. (2008) for a schematic overview). Bles, Bos, De Graaf, Groen, and Wertheim (1998) suggested that only the Subjective Vertical Conflict (SVC) is sufficient to explain MS. The SVC theory directly relates the conflict between the expected sensed vertical and the vertical provided by the sensory signals to MS. This theory becomes apparent when comparing the following two situations. Humans rotating around an Earth-vertical axis barely experience MS because the subjective vertical is not at play.[2] However, rotating around an Earth-horizontal axis does provoke MS since the subjective vertical constantly changes direction (Bos et al., 2008).

Diels et al. (2022) suggest that vision is the most crucial modulating factor associated with anticipating future motion and is therefore thought to have a beneficial effect on the ex-

[1] Active self-motion can create some uncomfortable feelings but cannot cause MS (Bos, Bles, & Groen, 2008).

[2] Bos et al. (2008) do mention that susceptible people can get sick from rotation around an Earth-vertical axis. However, MS is usually weak and takes a long time to develop in this condition.

pected sensed vertical discussed above. Previous research indicates that visual factors can have a significant impact on the occurrence of MS. Early studies by Probst, Krafczyk, and Büchele (1982) showed that having a wide peripheral view of the environment during repetitive breaking maneuvers in a car can reduce MS. Turner and Griffin (1999) conducted a large-scale public transport survey and found that passengers who have low visibility of the environment, such as those sitting towards the rear of the vehicle, experience more MS. In another study with more than 300 subjects, Griffin and Newman (2004) investigated the influence of different viewing conditions on MS while in the back seat of a car, and similarly found that providing a clear view of the road ahead reduces MS. Additionally, the positioning of in-vehicle multimedia displays which provide peripheral view also appears to be relevant, as these can reduce MS (Kuiper, Bos, & Diels, 2018). Obstruction of the view ahead by rotating the passenger seats backward led to significantly higher MS (Salter, Diels, Herriotts, Kanarachos, & Thake, 2019). Furthermore, showing an artificial earth-fixed reference frame has been shown to alleviate feelings of MS (Feenstra, Bos, & van Gent, 2011; Rolnick & Bles, 1989).

The above suggests that the visual field has a significant impact on the occurrence and severity of MS. Different types of visual information can be distinguished from the visual field, including visual translation, visual rotation, and visual verticality of the environment (Bos et al., 2008). The first two depend on optical flow patterns of the visual image, whereas the latter is based on previous knowledge of structures in the visual scene. For visual translation, the optical flow depends on the distance between the visual observer and the object, also known as motion parallax (Correia Grácio, Bos, van Paassen, & Mulder, 2014). Gibson (1950) explains this effect with the global optical flow rate, which is directly proportional to the velocity and inversely proportional to the height or distance of the observer relative to the visual plane when traveling through a visual environment.

Recent research has focused on quantifying MS development using computational models, with the aim of predicting the incidence and severity of MS based on physical signals (Kamiji, Kurata, Wada, & Doi, 2007). The goal of these models is to gain a better understanding of MS and reduce its risk in AV passengers by identifying the most influential aspects of physical motions. Although current MS models can reasonably predict MS based on physical movements (Inoue, Liu, & Wada, 2023; Kamiji et al., 2007), the impact of the visual field is still not fully incorporated in those models. Researchers have attempted to include the influence of visual rotation (Jalgaonkar, Schulman, Ojha, & Awtar, 2021; Wada, Kawano, Okafuji, Takamatsu, & Makita, 2020), visual vertical (Liu, Inoue, & Wada, 2022), and visual translation (Braccesi & Cianetti, 2011), but experimental data that validate these models are lacking.

The preceding discussion reveals that the influence of visual information in MS models has only recently received attention. However, which specific aspects of the visual field influence MS is still not well understood (Diels et al., 2022). The following section will discuss how the current research will aim to investigate and fill this knowledge gap.

1-2 Research Objective and Research Questions

The problem statement in Section 1-1 identified that the precise role of visual factors in the development of MS is yet to be understood and that the influence of visual information in MS models is still underrepresented. The current research will fill this knowledge gap by investigating the effect of visual translation on MS and quantifying this effect in a MS prediction model. An experiment will be carried out to test the reliability of this model and to contribute to the scarce availability of data representing MS development based on physical and visual translational motions. Therefore, the research objective can be defined as follows:

Research objective

- *"The objective of this research is to quantify the influence of visual translation on motion sickness development in autonomous vehicle passengers, by capturing this effect in a mathematical model and performing a human-out-of-the-loop experiment to verify the reliability of this model."*

From this research objective, a main research question was formulated. Answering this research question aims to meet the research objective mentioned above.

Research question

- *"How can the influence of visual translational information on the development of motion sickness of autonomous vehicle passengers be quantified?"*

To answer the main research question fully, three sub-questions were defined. These sub-questions will help to formulate an extensive answer to the main research question. The research was divided into the influence of visual translation on motion perception, the influence of visual translation on MS, and to what extent this influenced can be modeled. The sub-questions are listed below.

Research sub-questions

- *"How do humans use visual translational information for motion perception in autonomous vehicles?"*
- *"What is the influence of visual translational information on motion sickness of autonomous vehicles passengers?"*
- *"To what extent can the influence of visual translation on motion sickness be captured in a mathematical model?"*

Before answering the research question(s), a literature study was carried out to acquire all relevant knowledge and state-of-the-art technology that is currently available. To guide this literature study, a set of questions was set up and is shown below.

Literature research questions

- *"What is motion sickness?"*
- *"What causes motion sickness and what are the underlying theories?"*
- *"What visual information is used for motion perception?"*
- *"How does visual information influence motion sickness development?"*
- *"What are the current efforts in capturing the effect of visual information in motion sickness prediction models?"*

1-3 Thesis Outline

This Master of Science Thesis report is structured in parts. Part I contains the thesis paper that summarizes the main findings of the current research formatted as a standalone academic paper. This paper is regarded as the main and final result of the complete graduation project. Section I provides an introduction to the subject of MS in AVs. Section II offers a detailed explanation of MS and the visual factors that can influence its occurrence and severity. It also describes the MS prediction model developed by Wada et al. (2020) and proposes an extension to incorporate the effect of visual translation. Section III outlines the experiment carried out to validate the proposed visual translation extension. The results of the experiment are presented in Section IV, followed by a discussion of their implications in Section V. Finally, Section VI provides the main conclusions of the study.

Part II contains the preliminary research report that includes answers to the literature research questions from the previous section, together with a research proposal that was made to help answer the main research and research sub-questions. This report was handed in halfway during the graduation project and has already been graded for the course AE4020. Note that the research proposal in the preliminary research report could deviate from the actual research presented in Part I. The first two literature research questions of Section 1-2 are answered in Chapter 2, where a detailed definition of MS and MS theories are given. Furthermore, this section tackles the problem of AV passengers experiencing more MS. Chapter 3 discuses what visual information is used in motion perception, and how this information is combined with information from the vestibular system. This answers the third literature research question. Additionally, the fourth question about the visual influence on MS is answered in the same chapter. The last literature research question is answered in Chapter 4 by explaining the current efforts to include visual information in MS prediction models. The approaches used in these models, together with the information from the previous questions, are used as motivation for the research proposal presented in Chapter 5.

A book of appendices that includes more detailed analyses of the MS model proposal and parts of the experiment and its results are shown in Part III. Appendix A describes a more in-depth analysis of the proposal for adding the effect visual translation to the 6DOF-SVC model. More information on the motion profile and motion tuning is included in Appendix B. Furthermore, all results of the experiment (which are not shown in Part I) and individual results per participant are shown in Appendix C and Appendix D, respectively. In addition,

documents that show the complete briefing of the participants are presented in Appendix E. Finally, the Appendices F-H contain the experiment checklists, the experiment rating card, and the questionnaires that were completed by the participants after the experiment sessions.

Part I

Thesis Paper

Influence of Visual Translation on Motion Sickness Development of Autonomous Vehicle Passengers

Mitchel Elbertse
MSc student Control and Simulation
Delft University of Technology
Delft, Netherlands

***Abstract*—Autonomous vehicles are becoming increasingly prevalent in society, but the transition from active driver to passive passenger is known to increase the risk and severity of motion sickness. Motion anticipation is a critical factor in this difference, and visual information is known to be a major contributor to motion anticipation. However, the underlying mechanisms of how visual information influences motion sickness remain largely unknown. This study aims to investigate the effect of visual translation on motion sickness development. To accomplish this, a proposal was made to extend an existing motion sickness prediction model with visual translational components. A human-out-of-the-loop experiment was conducted in a moving-base simulator to test the proposed model's reliability and determine whether visual translation influences motion sickness. The experiment simulated an urban ride that featured repetitive accelerating and breaking maneuvers on a straight road. Eighteen participants were subjected to three different visual conditions that varied in the amount of global optical flow, while the simulator's motion was identical. The results suggest that congruent visual translation may lead to a minor, non-significant reduction of motion sickness, while the amount of optical flow does not seem to affect it. The proposed motion sickness model was able to predict a slight decrease in motion sickness for conditions with visual optical flow, as demonstrated by the experiment. Nonetheless, it is still debatable whether congruent visual translation may influence the onset and severity of motion sickness, as the results of this study could not confirm this.**

***Index Terms*—motion sickness, motion sickness modeling, autonomous vehicles, visual translation, optical flow**

I. Introduction

Autonomous Vehicles (AVs) have the potential to bring numerous benefits to society, including a reduction in the number of accidents on the road, alleviation of traffic congestion problems, regulation of fuel consumption and pollution, and reduction in driving times [1]. Although the concept of automation in vehicles is not new, with the earliest versions of cruise control having been introduced in the late fifties [2], modern vehicle automation technologies offer a more comprehensive range of features, spanning from anti-lock brakes, adaptive cruise control, and lane keeping to fully automated driving [3]. The primary difference between fully automated driving and the other technologies is that in the former, the car is capable of monitoring, reading, and responding to the environment without driver intervention. As a result, drivers can engage in non-driving-related activities, such as reading a book, watching a display, or conversing with passengers in the back seat, which in theory makes vehicle travel more productive and comfortable [3].

Despite the potential benefits of automation in vehicles, there is a significant issue surrounding the transition from active driver to passive passenger, which is an increase in the likelihood and severity of Motion Sickness (MS) [3]. A worldwide survey conducted by Schmidt et al. [4] highlights that car passengers are more prone to experience MS than car drivers. This difference has been investigated by Rolnick et al. [5], who found that individuals who are in control of a moving vehicle experience significantly less MS than those who are not. This is because drivers can adapt to the dynamics of the vehicle, allowing them to predict upcoming motions following their input, while vehicle passengers cannot do this. Additionally, drivers typically align their head with the direction of motion, as they can anticipate the forthcoming motions [6]. Such alignment has been shown to alleviate MS [7]. In contrast, vehicle passengers can predict and anticipate these movements to a lesser extent. Therefore, they are unable to align their heads with the direction of motion, making them more susceptible to MS.

It is evident from the previous discussion that motion anticipation plays a crucial role in reducing the occurrence of MS. In this context, Diels et al. [8] suggest that vision is the most crucial modulating factor associated with anticipating future motion. Future scenarios for AVs envision several factors that could potentially impact motion anticipation and MS, such as occluded windows, multimedia displays, passengers engaging in secondary activities, and backward-oriented seats, all of which can directly influence the out-of-window view [3]. Despite the significance of vision in motion anticipation and MS reduction, the precise role of visual factors, such as Field of View (FoV), optical flow characteristics, and vertical observation from the visual scene, is yet to be understood [8]. Research is required to address these questions and clarify the importance of the visual field characteristics in reducing MS.

Previous research indicates that visual factors can have a significant impact on the occurrence of MS. Early studies by Probst et al. [9] showed that having a wide peripheral view of the environment during repetitive breaking maneuvers in a car can reduce MS. Turner et al. [10] conducted a large-scale public transport survey and found that passengers who have low visibility of the environment, such as those sitting towards the rear of the vehicle, experience more MS. In another study

with more than 300 subjects, Griffin et al. [11] investigated the influence of different viewing conditions on MS while in the back seat of a car, and similarly found that providing a clear view of the road ahead reduces MS. Additionally, the positioning of in-vehicle multimedia displays that provide a peripheral view of the environment also appears to be relevant, as these can reduce MS [12]. Furthermore, obstruction of the view ahead by rotating the passenger seats backwards led to significantly higher MS [13]. Finally, showing an artificial earth-fixed reference frame has also been shown to alleviate feelings of MS [14, 15].

Recent research has been focused on quantifying MS development using computational models, aiming to predict the incidence and severity of MS based on physical and visual motion signals [16]. The goal of these models is to gain a better understanding of MS and reduce its risk in AV passengers by identifying the most influential aspects of visual and physical motions. While current MS models can reasonably predict MS based on physical movements [16, 17], the impact of the visual field is still not fully incorporated in those models. Researchers have attempted to include the influence of visual rotation [18, 19], visual vertical [20], and visual translation [21], but experimental data validating these models are lacking.

The preceding discussion reveals that the influence of visual information in MS models has only recently received attention. However, which specific aspects of the visual field influence MS is still not well understood [8]. In light of this knowledge gap, the present study aims to investigate the effect of visual translation on MS development. The objective of this research is to quantify the influence of visual translation on motion sickness development in autonomous vehicle passengers, by capturing this effect in a mathematical model and performing a human-out-of-the-loop experiment to verify the reliability and accuracy of this model. Ultimately, the findings of this study will provide insights into the role of visual translational information in MS and contribute to the development of design strategies for AVs.

This paper provides an in-depth exploration of the phenomenon of MS, its relationship with visual perception and specifically visual translation, the use of a computational model to predict MS based on different amounts of visual translation, and an experiment validating this model. Section II offers a detailed explanation of MS and the visual factors that can influence its occurrence and severity. It also describes the MS prediction model developed by Wada et al. [18] and proposes an extension to incorporate the effect of visual translation. Section III outlines the experiment performed to validate the proposed visual translation extension. The results of the experiment are presented in Section IV, followed by a discussion of their implications in Section V. Finally, Section VI provides the main conclusions of the study.

II. Background

A. Motion Sickness

MS is a malady caused by passive self-motion[1] that contains certain types of dynamic and kinematic properties [23, 24]. It is suggested that MS occurs when motion-sensitive sensors (i.e., vestibular system, visual system, and somatosensory system) are exposed to conflicting motion signals [24]. It is interesting that subjects who do not have a functional vestibular system are not susceptible to MS [25], indicating the important role of the vestibular system in the nauseogenic stimulus. In addition, individual MS susceptibility depends on many different factors, e.g., gender, age, ethnicity, and physiological factors. However, universal trends in the development of MS could be observed within the population [22], which are of interest in the current study.

The sensory mismatch theory is widely accepted to explain MS [24]. This theory states that a conflict between sensory systems is only provocative if the present sensory signals are at variance with the expected sensory signals in the Central Nervous System (CNS). These signals are theorized to be generated by an internal model, which is a copy of the actual sensory dynamics. This internal model is created and updated by previous experiences [26], and is derived from the observer model theory [27] (see [22] for a schematic overview). Bles et al. [28] suggested that only the Subjective Vertical Conflict (SVC) is sufficient to explain MS. The SVC theory directly relates the conflict between the expected sensed vertical and the vertical provided by the sensory signals to MS, which becomes apparent when comparing the following two situations. Humans rotating around an Earth-vertical axis barely experience MS because the subjective vertical is not at play.[2] However, rotating around an Earth-horizontal axis does provoke MS in humans since the subjective vertical constantly changes direction [22].

The SVC theory is still hypothetical, and it has not yet been proven that this theory explains the underlying mechanisms of MS. However, it can explain many types of sickness that are caused by motion [22]. Therefore, for the current study, the SVC theory is taken as a basis for investigating the influence of visual translation on MS.

B. Visual Influence in Motion Sickness

Humans perceive motion through different sensory signals that the CNS integrates into a combined perception of self-motion [29]. Motion perception is important for explaining MS, as present and expected motion signals play a key role in the SVC theory. The role of the visual system in motion perception is well understood, whereas the role of the visual system in MS is still unclear [22].

Different types of visual information contribute to self-motion perception, including visual translation, visual rotation,

[1] Active self-motion can create uncomfortable feelings but cannot cause MS [22].

[2] Bos et al. [22] do mention that susceptible people can get sick from rotation around an Earth-vertical axis. However, MS is usually weak and takes a long time to develop under this condition

and visual verticality of the environment [22].[3] The first two depend on optical flow patterns within the visual field, while the latter is based on previous knowledge of structures in the visual scene. For visual translation, the optical flow depends on the distance between the visual observer and the object, also known as motion parallax [31]. Gibson [32] explains this effect with the global optical flow rate, which is directly proportional to the velocity and inversely proportional to the height or distance of the observer relative to the visual plane when traveling through a visual environment.

Griffin and Butler have conducted several experiments in which they investigated the effect of visual information on MS. Griffin et al. [11] investigated the effects of different types of restricted views of the environment while subjects were driven around in a real car. The results showed that providing a wide or narrow forward view reduced the subject's illness ratings, indicating that a view of the road ahead is important to diminish MS. Butler et al. [33] performed their MS experiment in a motion-based simulator. They subjected their participants to for-and-aft oscillatory movements while changing the visual condition. The authors concluded that there is no significant difference in terms of MS between internal, external, or collimated visual fields. A follow-up experiment [34] included for-aft motion in combination with pitch oscillations. Unlike the previous experiment, these results showed that there were significantly lower mean illness ratings with an external view, compared to internal or blindfolded views. The authors suggested that the presence of rotational motion is necessary for a congruent visual field to have a possitive effect on MS.

The latter two experiments only used narrow forward views of the environment, but did not include a condition with visual motion in the peripheral view. Therefore, the experiment conducted in the current research included a full 180 degree horizontal FoV of the environment, to better investigate the influence of visual translation, independent of forward or peripheral view, on MS.

C. Motion Sickness and Visual Translation Modeling

Human self-motion control cannot be performed with a simple feedback control system, as neural delays and imperfect human motion sensors would cause self-motion control to become unstable [22]. Instead, to overcome these shortcomings, it is hypothesized that a desired body state is compared to an expected body state that is produced within the human CNS [27]. These expected motion signals are computed within an internal model that contains a copy of the actual body and sensor dynamics that are created and updated by previous experiences. The internal body dynamics compute the expected body state, while the internal sensor dynamics produce an expected sensed body state. The latter is compared to the present sensed body state, in which the resulting conflict is used to update the input to the internal body dynamics. This theory is capable of describing human self-motion control despite the imperfect human motion sensors, as these are also included within the internal model (see [22] for a schematic overview of the observer model theory).

Bles et al. [28] developed a 1 Degree of Freedom (DOF)-SVC model for passive vertical motion that uses the observer model theory. The model computes a sensed vertical signal with a vestibular system model and compares this signal with an expected sensed vertical signal calculated by the internal model (i.e., a copy of the vestibular system dynamics). This conflict signal is used to update the estimated vertical that is produced by the body dynamics within the internal model. This update is believed to be a mechanism within the CNS that reduces the SVC and models the adaptive learning behavior of humans [28]. The conflict signal between the expected sensed vertical and the vertical provided by the sensory signals is integrated over time and transformed into a measure of MS, which is the Motion Sickness Incidence (MSI). This is defined as the percentage of people who would vomit, given a certain motion stimulus over time [35].

Wada et al. [18] extended this model to the 6DOF-SVC model, which includes translational and rotational physical motions (both in three DOFs) and an extension for the influence of visual rotation. This model still adheres to the observer model theory, since it has an internal model, i.e., a copy of the primary vestibular and visual dynamics. This internal model calculates expected sensed motion signals for vestibular acceleration, vestibular rotational velocity, vestibular vertical, and visual rotational velocity. These signals are compared to the actual sensory signals, which creates conflict signals that are used to update the estimated motion signals (input of the internal model). The SVC is still used by the model to compute the MSI. A hill function and a leaky integrator convert the SVC signal to a value between 0% (no vomiting) and 100% (everyone vomits). The leaky integrator is also responsible for the accumulation of MSI over time. For a more in-depth elaboration of the 6DOF-SVC model, see [18].[4]

D. Motion Sickness Model with Visual Translation

A proposal for including the influence of visual translation in the 6DOF-SVC model is shown in Fig. 1. The parts shown in black are the original 6DOF-SVC model of [18], whereas the visual translation extension is shown in red. Experiments by Monen et al. [37] showed that the human visual system is insensitive to visual acceleration, meaning that the visual translational input should be visual velocity v_{vis}. Correia Grácio et al. [31] showed that the amplitude of visual cues is not equally perceived as the amplitude of initial cues,

[3] Visual translation and visual rotation are sometimes referred to as linear and circular vection, respectively. However, since vection is defined as the sense of self-motion from visual images in the absence of physical self-motion [30], vection is not considered in the current research, since passengers in autonomous vehicles experience physical self-motion.

[4] Liu et al. [20] extended the 6DOF-SVC model with visual vertical dynamics (which are experimentally tested in [36]) and Inoue et al. [17] revisited the 6DOF-SVC model with a parameter optimization that takes experimental data from motion perception into account. The results of these are not considered in the current research, since a first proposal is made to add visual translation to the original model of [18].

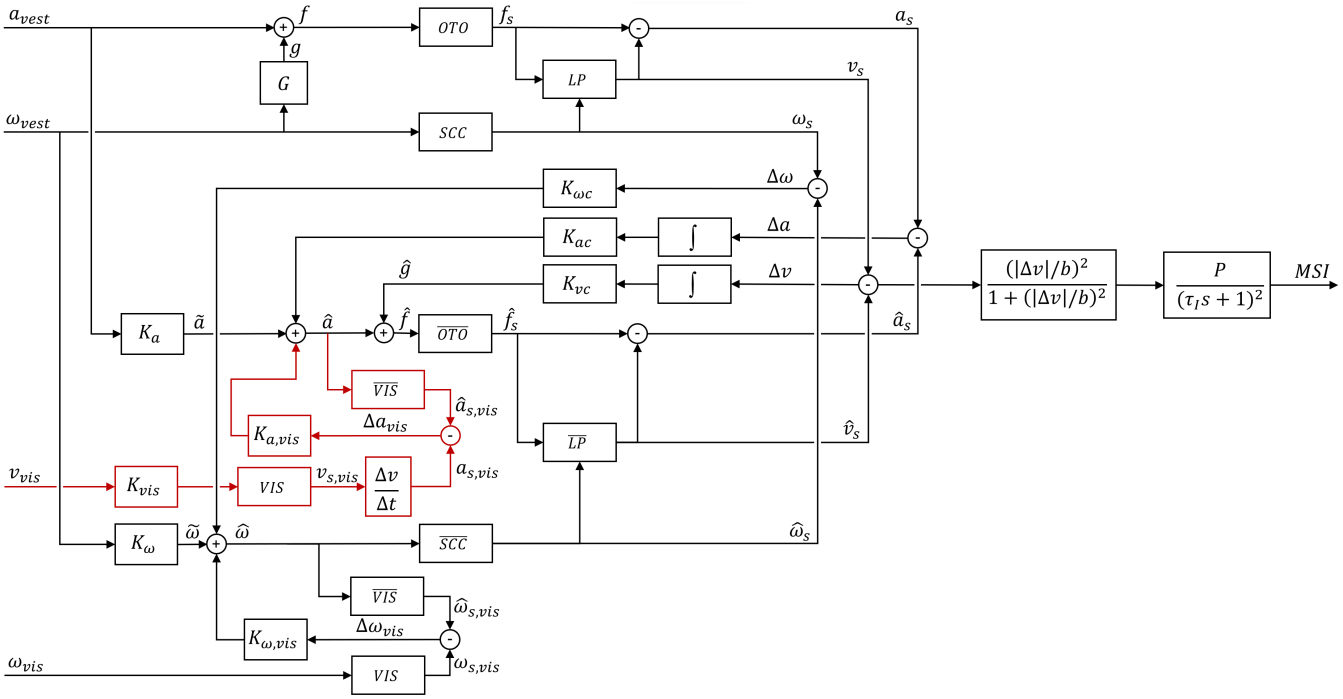

Fig. 1. 6DOF-SVC model with visual translation extension (shown in red)

especially in simulated environments. They state that the visual gain (i.e., perceptual scaling factor between visual and intertial cues) in the surge direction is mainly depended on the quality and amount of depth cues in the visual field. As visual cues could be perceived as less strong than inertial cues [31], visual velocity v_{vis} must be scaled down to be integrated with inertial cues. The visual velocity is scaled by visual gain K_{vis} that has a value between zero (no global optical flow rate and low visual fidelity) and one (high optical flow rate and high visual fidelity). The value of K_{vis} can never be higher than one as visual cues are never experiences as more strong than inertial cues [31].

A similar approach as Wada et al. [18] used to add the influence of visual rotation to the 6DOF-SVC model, is used to model the influence of visual translation. The sensed visual velocity $v_{s,vis}$ is calculated by the visual dynamics VIS. As suggested with the motion perception model of Bos et al. [22], the visual dynamics for translational motion VIS is modeled as a first-order low-pass filter as shown in Eq. 1.

$$H_{\mathrm{LP}}(s) = \frac{1}{\tau_{vis}s + 1}, \qquad \text{with } \tau_{vis} = 2 \text{ s} \tag{1}$$

The expected sensed visual signal is calculated by the visual dynamics in the internal model $\overline{VIS}$, which uses the estimated inertial acceleration signal $\hat{a}$ to calculate the expected sensed visual acceleration $\hat{a}_{s,vis}$. It must be noted that the visual gain K_{vis} is intentionally left out of the internal dynamics path, as it is believed that the CNS expects an increase in visual velocity (independent of visual field characteristics) after an inertial acceleration. Values of K_{vis} close to zero would remove this expectation, lowering the desired effect of the visual translation extension. The internal visual dynamics $\overline{VIS}$ are equal to the primary visual dynamics VIS and therefore should also have a velocity signal as input and output. Therefore the estimated inertial acceleration signal $\hat{a}$ should be integrated to an estimated velocity signal which would be transformed to an estimated sensed visual velocity signal by the internal visual dynamics $\overline{VIS}$. This sensed visual velocity signal should be compared to the actual sensed visual velocity $v_{s,vis}$ which creates a conflict signal in the velocity domain. To update the estimated inertial acceleration signal $\hat{a}$ accordingly, this visual velocity conflict signal needs to be differentiated to an visual acceleration conflict signal. However, for simplicity, the conflict signal is calculated in the acceleration domain. The sensed visual velocity $v_{s,vis}$ is differentiated to the sensed visual acceleration $a_{s,vis}$, so that it can be compared to the expected sensed visual acceleration $\hat{a}_{s,vis}$. The resulting visual acceleration conflict Δa_{vis} is scaled by the visual acceleration gain $K_{a,vis}$ and used to update the estimated inertial acceleration signal $\hat{a}$.[5] The value of $K_{a,vis}$ is based on the type of visual information (e.g., congruent, conflicting or eyes closed), similar to how the value of $K_{\omega,vis}$ is determined in [18]. For now, the value is set to zero for closed eyes (canceling the influence of visual acceleration because the CNS does not expect visual signals) and to unity for open eyes (visual acceleration affects

[5] As integration, differentiation and the visual dynamics are all linear operators, the output of the 6DOF-SVC model with visual translation would be the same if the visual acceleration conflict signal was calculated in the velocity domain.

the estimated inertial acceleration signal $\hat{a}$). Further research is required to investigate whether this gain should also be dependent on conflicting or congruent information, similar to [18].

III. Method

A human out-of-the-loop experiment was performed to study the effect of visual translation on MS. The experiment was carried out to test the reliability and accuracy of the proposed visual translation extension to the 6DOF-SVC model, and to collect more data on the influence of visual translation on MS, as this information is scarce in the literature.[6] A simulated urban ride was performed in a moving-base simulator. The experiment participants were subjected to three different visual conditions in three different sessions, while the motion of the simulator was kept the same. These visual conditions varied in the amount of optical flow.

A. Apparatus

To subject the participants to visual and physical motion cues, the SIMONA Research Simulator (SRS) at Delft University of Technology was used (see Fig. 2). The SRS has a 6-DOF hydraulic motion base, while the visual system consists of three digital light processing projectors capable of creating a collimated 180 degree horizontal by 40 degree vertical FoV. A computer generated outside view of the three visual conditions was shown to the participants.

Fig. 2. SIMONA Research Simulator

An inside view of the simulator cabin during the experiment is shown in Fig. 3. Since the objective of this research was to investigate the influence of visual translation on MS, head rotations induced by neck movements were kept to a minimum by asking participants to wear a neck brace. A pre-test in which one participant was asked to perform an experiment run with and without a neck brace while wearing a head angular rate sensor showed that the neck brace indeed reduced head rotations. The Standard Deviation (SD) of the head pitch rate for sessions with and without neck brace was 1.97 deg/s and 8.71 deg/s, respectively. In addition, a noise canceling headset was worn to mask actuator noise from the motion system by playing a monotone engine sound and used for communication with the simulator operator. A display just below the exterior visuals showed the MIsery SCale (MISC) table (an 11-point scale based on the typical progression of MS symptoms [38]) to the participants.

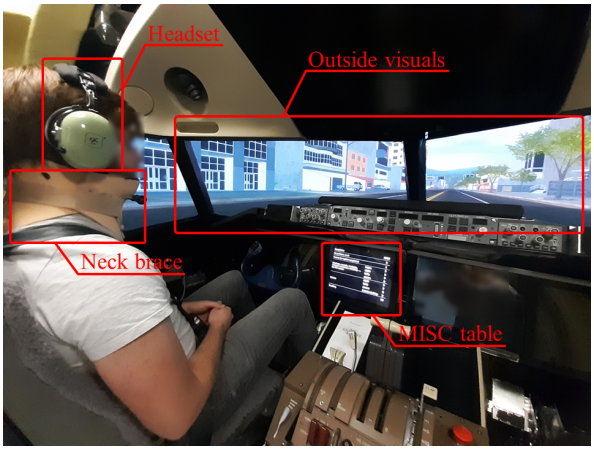

Fig. 3. Experiment setup inside the simulator cabin

B. Motion Profile

All three conditions featured the same 30-minute motion profile that simulated 134 maneuvers, either braking or accelerating, on a straight road. Therefore, the motion profile only contained longitudinal accelerations and decelerations. As the research objective was to capture the influence of visual translation on MS, no corners were incorporated into the motion profile.

To simulate an urban driving scenario, three velocities that usually appear in urban driving were chosen. These velocities were 30, 50 and 70 km/h, which are represented as red lines in the complete experimental velocity profile shown in Fig. 4. These three velocities resulted in three types of acceleration (30→50, 50→70, 30→70) and three types of deceleration maneuvers (50→30, 70→50, 70→30), which were pseudo-randomly ordered.[7] Each type of maneuver occurred 22 times, which, together with the start and end maneuvers, made a total of 134 maneuvers. The simulation started and ended at zero velocity, making these maneuvers an acceleration from 0 km/h to 30 km/h and a deceleration from 30 km/h to 0 km/h, respectively.

The kinematic polynomial acceleration model of Akçelik and Biggs [39] (Eqs. 2-4) was used to design the experimental

[6] Much research has been performed on Visually Induced Motion Sickness (VIMS) and its relation to vection (see [30] for an overview). However, VIMS is defined as MS that is provoked by visual movement in the absence of physical motion. Therefore, VIMS is not within the scope of the current research, as physical motion is present.

[7] Actually there were two types of acceleration, since the acceleration profiles for 30 to 50 km/h and 50 to 70 km/h were equal (similar for the deceleration profiles). However, since visual velocities were different, these two acceleration profiles were treated as different types of motion.

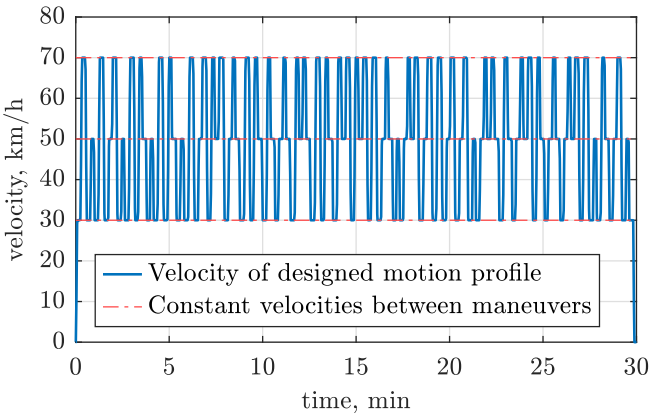

Fig. 4. Velocity profile of designed motion profile

vehicle acceleration profiles. In Eq. 2, a_m represents the maximum acceleration reached in the maneuver in m/s^2 and θ corresponds to the ratio of time from the start of acceleration to the total acceleration time t_a. The free parameter m determines the time ratio of the maximum acceleration θ_m as shown in Eq. 3. The fixed parameter n was set to 1.0 (as recommended by Akçelik and Biggs [39]), while the parameter m was set to a value that corresponds to the maximum acceleration value being reached halfway during the maneuver (i.e., $\theta_m = 0.5$, $m = 2.66$). The latter was chosen to create symmetric acceleration profiles, as other values of θ_m caused unnaturally high jerk values at the start or end of the acceleration profile. The parameter r depends solely on m, as shown in Eq. 4. The maximum acceleration values used in these equations were chosen to mimic a slightly assertive driving style according to the values found by Karjanto et al. [40]. This resulted in a maximum acceleration value (a_m) of 0.3g and a maximum deceleration value of 0.38g for all acceleration and deceleration maneuvers, respectively. An assertive driving style was chosen to ensure that the simulated motion was sufficiently provocative in terms of MS. The duration of the vehicle acceleration and deceleration profiles t_a was determined by the desired velocity differences.

$$a(t) = r a_m \theta^n (1-\theta^m)^2, \qquad \text{with } n > 0,\ m > -0.5n \quad (2)$$

$$\theta(t) = t/t_a, \qquad \theta_m = (1+2m)^{-1/m} \quad (3)$$

$$r = ((1+2m)^{2+1/m})/4m^2 \quad (4)$$

All vehicle acceleration and deceleration profiles were run through a second-order low-pass filter (Eq. 5) to limit excessively high jerk values that appear at the beginning of the profiles.

$$H_{\text{LP}}(s) = \frac{1}{(\tau_s s + 1)^2}, \qquad \text{with } \tau_s = 0.05 \text{ s} \quad (5)$$

The duration of the constant-velocity phases in between maneuvers was set between six and twelve seconds. The value was dependent on the minimum amount of time required for prepositioning of the simulator (discussed in Subsection III-C), combined with some variation time to prevent anticipation of upcoming maneuvers. With the pseudo-random order of maneuvers and varying times in between maneuvers, it was attempted to create an unpredictable motion profile.

C. Motion Cueing

The motion space of the SRS is limited, requiring the use of a motion filter to translate the designed vehicle motion profile into simulator motions that remain within the simulator motion envelope. For this purpose, a classical washout filter [41] was used. As low-frequency motions are difficult to simulate with the SRS, the designed vehicle motion profile was passed through a first-order high-pass filter after being scaled down by a gain ($K = 0.47$). This filter with the chosen break frequency is shown in Eq. 6 and determined the translational motion of the simulator. To better simulate low-frequency motions, tilt coordination was used.[8] For this, the designed vehicle motion profile was passed through a second-order low-pass filter with the corresponding filter settings as shown in Eq. 7, after being scaled down by the same gain K. This filter determined the pitch movements of the simulator. The maximum pitch rate was established at 2.2 deg/s, which is below the human vestibular threshold of 3 deg/s [43]. Furthermore, the filtering point was chosen so that the motion felt in the left seat of the SRS corresponded to the motions that would have been felt in the left-hand front seat of the autonomous vehicle.[9]

$$H_{\text{HP}}(s) = \frac{s}{s + \omega_{n,\text{HP}}}, \qquad \text{with } \omega_{n,\text{HP}} = 1.8 \text{ rad/s} \quad (6)$$

$$H_{\text{LP}}(s) = \frac{\omega_{n,\text{LP}}^2}{s^2 + 2\zeta_{\text{LP}}\omega_{n,\text{LP}} s + \omega_{n,\text{LP}}^2}, \qquad \text{with } \omega_{n,\text{LP}} = 3.6 \text{ rad/s}, \quad \zeta_{\text{LP}} = 1 \quad (7)$$

Additionally, prepositioning was applied to virtually enlarge the motion space of the SRS. The simulator moved backward when the upcoming maneuver was an acceleration, while the simulator moved forward when the upcoming maneuver was a deceleration. The maximum prepositioning accelerations and jerk values were 0.0367 m/s^2 and 0.0917 m/s^3, respectively, which are below the human vestibular threshold values of 0.04 m/s^2 and 0.1 m/s^3 (only tested experimentally) [44, 45]. This ensured that prepositioning was not felt by participants, and this prevented false motion cues.

[8]Tilt coordination was not required to simulate the designed vehicle motions. However, only translational motions of the simulator would barely have caused any motion discomfort, as the amplitude of the specific force would become very low [42]. Therefore, it was chosen to use tilt coordination.

[9]As the designed vehicle motion profile only featured longitudinal inertial accelerations, the specific forces felt inside the vehicle are equal at every position. Hence, only the height of the filter point inside the SRS is important. This was set 35 cm below the participants' eye height, as otherwise too much motion space of the SRS would be lost.

The motion filter and prepositioning parameters presented above were tuned to make optimal use of the available motion space of the SRS. Multiple parameter settings were pre-tested in the simulator. Parameters that felt close to real-life urban driving were chosen for the experiment.

D. Visual Stimuli

The subjects were exposed to three visual conditions with varying amounts of global optical flow, corresponding to the designed acceleration profiles. Fig. 5 displays static images of these visual conditions, only showing the images generated by the forward-facing projector of the visual system of the SRS. The left- and right-hand projectors generated an extension of these views, making a full 180 degree horizontal FoV of the environment. Visual stimuli representing realistic driving scenarios were designed using the Unity game engine and the Fantastic City Generator package [46]. These scenarios included a typical four-lane road design with solid road markings to avoid edge rate phenomena, i.e., subjects could not directly identify the speed at which they traveled from dashed road lines. A relatively wide road was chosen as the visual system of the SRS used collimated visuals. Objects too close to the observer would otherwise still be presented at infinity, making the simulation less realistic. The driver's eye height in the visual environment was fixed at 110 cm above the surface of the road [47], while the lateral position was 50 cm to the left of a 370-cm-wide lane's centerline. This gave the participants the impression that they were sitting in the left-hand front seat.

The first condition, called the Baseline (BL) condition (Fig. 5(a)), showed a four-lane road design without textures. Consequently, this condition did not include any visual movement. The second condition, called the Low Optical Flow (LOF) condition (Fig. 5(b)), represented a rural road and contained road, grass, and dirt textures, as well as some trees on the side of the road to give participants a sense of their velocity. Additionally, a mountain landscape and a sky background were added for increased realism, but did not move. The third and final condition, called the High Optical Flow (HOF) condition (Fig. 5(c)), simulated an urban city drive and featured tall buildings, city lanterns, and trees close to the road. This created higher rates of optical flow, especially in the peripheral view, as visual velocity is directly related to the distance from the observer [32, 48]. The buildings were generated in random order, so there were no repetitive blocks in the visual scene. In addition, no traffic and road crossings were incorporated in the visual conditions to keep motion predictability to a minimum.

The BL condition only showed a static image of the road ahead. An image of a road, rather than a black screen, was chosen to have the same brightness and color settings as in the Optical Flow (OF) conditions and to suppress the sensation of tilt coordination. The BL condition served as a control for the two OF conditions. The camera position in the visual scene was calculated by double integration of the designed acceleration profile.

E. Predicted MSI

The predicted MSI values for the experimental conditions computed by the 6DOF-SVC model with visual translation extension (Fig. 1) are shown in Table I. These values represent the MSI value after the 30-minute motion exposure. MSI_{des} indicates the predicted MSI for the designed acceleration profile before motion filtering, while MSI_{sim} indicates the predicted MSI for the simulator motion after motion filtering. For both predictions, the visual velocity input was set to the visual cues shown to the subjects, while the visual rotation input was set to zero. The values used for the visual gain K_{vis} were derived from the findings of Correia Grácio et al. [31]. They used similar LOF and HOF conditions to investigate the perceptual scaling between visual and inertial cues in a simulated environment. This was done by letting the participants determine the best match between visual and inertial cues, by changing the visual gain, i.e., the amplitude of the visual cues divided by the amplitude of the inertial cues. As the 6DOF-SVC model with visual translation needs to transform visual cues into inertial cues, the inverses of the visual gains found by [31] in the surge direction were used as a first guess for the values of K_{vis} used for LOF and HOF. The visual gain for BL was set to zero because no visual flow was present in this condition. As stated before, the visual acceleration gain $K_{a,vis}$ was set to unity for all conditions (open-eye condition). All other parameters and dynamics used in the 6DOF-SVC model with visual translation were kept equal to those used in [18].

TABLE I
MSI VALUES FOR THE EXPERIMENTAL CONDITIONS, PREDICTED BY THE 6DOF-SVC MODEL WITH VISUAL TRANSLATION EXTENSION

	K_{vis} [-]	$K_{a,vis}$ [-]	MSI_{des} [%]	MSI_{sim} [%]
BL	0	1	4.24	2.41
LOF	0.25	1	3.69	1.91
HOF	0.3	1	3.59	1.82

The simulated MSI values for the designed and simulated motion profile showed a reduction for LOF and HOF compared to BL, while only a slightly reduced value was observed between the OF conditions. Furthermore, the predicted MSI for the simulator motion profile was considerably lower than the predicted MSI for the designed motion profile. This is the effect of the applied motion filter, which greatly reduces the motion amplitude.

F. Participants

Eighteen participants completed the experiment, of whom nine were women and nine were men.[10] The 18 participants were students or recent graduates of Delft University of Technology, and were between 18 and 27 years of age ($\mu = 22.5$

[10]A total of 25 participants took part in the experiment. However, seven of them were unable to complete the full experiment. Five of these participants got too sick and did not want to continue the experiment. Data collected from participants who dropped out were not used in the analysis.

(a) Baseline condition (b) Low optical flow condition (c) High optical flow condition

Fig. 5. Forward views of the three different visual driving scenarios

years, $\sigma = 2.28$ years). All participants completed the Motion Sickness Susceptibility Questionnaire (MSSQ) developed by Golding [49] before participating in the experiment. The median MSSQ score of the participants was 6.2 ($\mu = 7.33$, $\sigma = 6.35$) which is around the 30th percentile of MS susceptibility [49]. This value is quite low compared to the general population, but as some participants were unable to complete the entire experiment due to severe MS symptoms, it was decided not to invite people who are highly susceptible to MS (i.e., people with high MSSQ values).

Participants were instructed not to consume alcohol or products with comparable physical effects 24 hours before the experiment sessions. Furthermore, participants had no knowledge about the purpose of the experiment and did not know which conditions were part of the experiment. Additionally, the experiment was approved by the Human Research Ethics Committee of Delft University of Technology and all participants provided their written informed consent prior to participation.

G. Procedures

To minimize the effect of individual motion sickness susceptibility on the results, a within-subject experiment design was chosen, which meant that each participant executed all three conditions. It was expected that, regardless of the condition, the first experiment session would cause more discomfort compared to the second and third sessions.[11] To mitigate this effect, different condition orders were chosen. From three conditions, six different order groups were formed, resulting in three participants per order group. The experiment sessions took place on three different days to minimize MS symptoms carrying over from one session onto another. To ensure that the participants could better compare the different experiment conditions, a best effort was made to schedule the sessions close to each other. However, for logistical reasons, some participants had multiple days between sessions, with a maximum of 12 days between the first and last sessions.

Before the first session, participants were briefed about the experiment procedures, safety instructions, and their tasks during the experiment. The participants were seated in the left-hand seat of the SRS (Fig. 3) and instructed to wear a neck brace. The seat height was adjusted so that the eye height of the participants was equal to the designed eye height of the SRS. In addition, participants were instructed to keep a relaxed body posture and look forward.

Each experiment session consisted of 30 minutes of motion followed by a 10-minute recovery period in which participants were instructed to remain seated while the simulator was not moving. During the 40 minutes, a beeping sound was played at an interval of 30 seconds that instructed the participants to verbally communicate their MISC score. If a participant communicated four consecutive sixes or one seven, the simulation was stopped, but the recovery period was still carried out. At the beginning of the recovery period, participants were advised to remove the neck brace and, if preferred, the headset to stimulate their recovery. Participant communication without headset was continued through the intercom system of the SRS.

After the recovery period, participants completed an electronic survey that contained questions about the experienced MS symptoms, physical motion assessment, visual motion assessment, and an open question about their general experience. The last session contained an additional survey with comparative questions about the level of comfort and driving behavior in all conditions.

H. Dependent Measures

1) MSSQ scores: Before the participants were selected for the experiment, they filled in the MSSQ, resulting in a number that indicates their susceptibility to MS.

2) MISC scores: During the 30 minutes of motion and the 10-minute recovery period, participants verbally communicated a MISC value between 0 and 10 at an interval of 30 seconds, giving a measure of the development of MS [38]. When participants were in doubt about their MISC score, they were allowed to communicate a score between two integer MISC values (e.g., 1.5, 2.5).

3) MS symptoms checklist: After each experiment session, participants completed a checklist that contained 24 commonly experienced MS symptoms. They gave a rating of the severity of their symptoms on a four-point ordinal scale ranging from 'none' to 'severe'.

[11] This was expected as participants are usually a bit more nervous in the first session and they have not yet been familiarized with the simulator.

4) Physical and visual motion assessment questionnaires: Per session the participants were asked to what extent they agreed with statements about their perceived realism of the physical and visual motion and the predictability of the simulator motion. They rated the statements on a seven-point Likert scale [50].

5) Subjective comfort assessment: After all three sessions, participants rated the conditions in terms of level of comfort and driving behavior. Both questions asked for a rating between one and seven, which ranged from 'extremely uncomfortable' to 'extremely comfortable' and 'extremely aggressive driving behavior' to 'extremely defensive driving behavior', respectively.

I. Data Analysis

1) MISC scores: The mean MISC value at each time point was calculated by taking the average of the MISC values given by all participants at that time point. The last communicated MISC score of participants who were unable to complete the full 30 minutes of motion exposure was repeated for the remaining data points, for the mean MISC analysis. Furthermore, the Standard Error of the Mean (SEM) was calculated to give an indication of the variation between participants.

To capture the effect of high or low OF on MS in a single number, the approach developed by Reuten et al. [51] was used. The reduction R_{ti} per time point t and participant i is given by Eq. 8. Here, OF_{ti} indicates the MISC score given in the LOF or HOF condition and BL_{ti} indicates the MISC score given in the BL condition. The reduction has a value between -1 (maximum worsening) and +1 (maximum mitigation) and was calculated for the 30 minutes of exposure to motion. When OF_{ti} = BL_{ti} = 0, R_{ti} is set to zero. Furthermore, R_{ti} is not calculated for the missing time points of the participants who were unable to complete the full 30 minute motion exposure, which is different from the mean MISC analysis.

$$R_{ti} = \frac{(\text{BL}_{ti} - \text{OF}_{ti})}{(\text{BL}_{ti} + \text{OF}_{ti})} \tag{8}$$

As the resolution of R_{ti} was low for the first time points, each reduction point was weighted by w_{ti}.[12] The average reduction per participant i and the average reduction per time point t are given by:

$$\overline{R}_i = \frac{\sum_t w_{ti} R_{ti}}{\sum_t w_{ti}}, \qquad \overline{R}_t = \frac{\sum_i w_{ti} R_{ti}}{\sum_i w_{ti}}, \quad \text{with } w_{ti} = \text{BL}_{ti} + \text{OF}_{ti} \tag{9}$$

To capture the effectiveness of high or low OF on MS development across all time points and participants in a single number, the overall weighted average reduction $\overline{R}_{\text{LOF/HOF}}$ for one condition was given by:

$$\overline{R}_{\text{LOF/HOF}} = \frac{\sum_i w_i \overline{R}_i}{\sum_i w_i}, \qquad \text{with } w_i = \sum_t w_{ti} \tag{10}$$

To see whether OF (independent of low or high) influences MS, the grand mean $\overline{R}$ across both conditions was defined by the average of the grand mean per participant $\overline{R}_i$ weighted by their sum of the weights w_i of the LOF and HOF reductions. A weighted one-sided t-test (α = 0.05) was performed to see if the grand mean was greater than zero, indicating a positive reduction in MISC scores. To examine whether there was a difference in MS mitigation between LOF and HOF, again a weighted one-sided t-test (α = 0.05) was performed on the $\overline{R}_{\text{LOF}}$ and $\overline{R}_{\text{HOF}}$ values. Furthermore, all 95% Confidence Intervals (CIs) presented in the next section were calculated with bootstrapping of R_{ti} and the corresponding weights.

To investigate the influence of the order effect in the results, the overall reduction values for session two $\overline{R}_{\text{ses2}}$ and session three $\overline{R}_{\text{ses3}}$ were calculated in the same way as the overall reductions $\overline{R}_{\text{LOF}}$ and $\overline{R}_{\text{HOF}}$. The reduction R_{ti} was calculated by comparing the MISC values of the second and third sessions with the first session (instead of comparing LOF and HOF with BL). Weighted one-sided t-tests (α = 0.05) were performed to see if the reduction values $\overline{R}_{\text{ses2}}$ and $\overline{R}_{\text{ses3}}$ were greater than zero.

2) Subjective comfort assessment: Subjective comfort was measured with the level of comfort and driving behavior scoring. As these variables could be considered ordinal data, a Friedman test was used to find significant differences between all conditions. Post-hoc analysis with a Wilcoxon signed-rank test was performed to identify which condition pairs could be considered significantly different.

J. Hypotheses

Visual information plays an important role in the occurrence and severity of MS symptoms [22]. Visual rotational and vertical information (congruent with physical movements) is shown to be capable of decreasing MS [22]. Therefore, correct visual translational information was expected to have a mitigating effect on MS. Furthermore, it was expected that the amount of optical flow will also influence MS. The HOF condition was predicted to increase the velocity sensation, providing more information on ego-motion. Therefore, the hypotheses of the experiment were as follows.

1) Hypothesis I: Congruent visual translational information will reduce the occurrence and severity of motion sickness.

2) Hypothesis II: The occurrence and severity of motion sickness will decrease with increasing global optical flow rates.

[12] The first time points usually had a MISC score of 0 or 1, resulting in a lower resolution of R_{ti}, as these values of R_{ti} would quickly become -1 or +1.

IV. Results

A. MISC Scores

The average MISC scores and the corresponding SEM for the 30-minute simulated motion and the 10-minute recovery period are shown in Fig. 6.[13] A first observation shows a slightly lower mean MISC of LOF and HOF compared to BL. The development of the mean MISC scores is especially different in the initial minutes of the motion exposure. Here, the MISC scores in BL show more motion discomfort compared to LOF and HOF. Especially MISC ratings in HOF take some time to develop. The development of the mean MISC scores of all conditions is similar between 11 and 19 minutes. However, while the mean MISC score for BL is still increasing in the last 11 minutes, the mean MISC scores for LOF and HOF remain more or less constant. This results in a higher mean MISC value for BL at the end of the simulation. Finally, the mean MISC scores in the recovery period show a similar exponential decline.

Fig. 6 also shows the SD of the jerk of the specific force in the x-direction of the head reference frame for the corresponding 30 seconds. An attempt was made to investigate whether the aggressiveness of the motion (assumed to be related to the SD of the jerk) could explain the spikes in the mean MISC trend. To some extent, a high SD corresponds to an increase in mean MISC, however, this is not consistent within one condition or between the conditions (e.g., the high jerk values located at 3.5, 11, and 16.5 minutes only cause an increase in mean MISC in one or two conditions). Furthermore, not all MISC score spikes correspond to a high SD of specific force jerk. Therefore, no clear correlation could be found between the aggressiveness of the motion and an increase in mean MISC.

The weighted reduction at each time point $\overline{R}_t$ is shown in Fig. 7. As is clearly visible, the weighted reduction is most prominent in the initial minutes for both conditions, whereas a more or less constant value is reached after 20 minutes. Here, a value of $\overline{R}_t < 0$ indicates a worsening of MS, which only occurs for LOF at some points in time.

Fig. 8 shows the average weighted reduction for each participant ($\overline{R}_i$) and condition. Twelve participants had a positive reduction $\overline{R}_i$ in LOF and ten participants had a positive reduction in HOF. This also indicates a slight advantage of the OF conditions over BL. However, there are participants who had negative reduction values (worse than BL) for the OF conditions. To investigate whether this was caused by an order effect, minus signs were added for conditions that occurred before BL. As visible from the graph, some negative reduction values could have been caused by this effect, however, not for all participants. Participants 8 and 12 had negative reduction values even though the conditions occurred after BL. The size of the markers is proportional to the participant weights w_i, indicating the total amount of MISC scores given in BL and corresponding OF condition. These weights determine the influence of a participant on the overall average reduction values $\overline{R}$, which means that the reduction of participants with more MS symptoms has more of an effect on the total reduction value. For example, participants 13, 16, and 18 had a reduction value of 1, meaning that they did not experience MS symptoms in the corresponding OF condition, i.e., only MISC scores of zero for LOF/HOF, while they had some symptoms in BL. However, since their weights w_i are relatively small (a total of 1-10 MISC scores in both conditions summed over the entire 30 minutes of motion exposure), their reduction values barely contribute to the overall reduction $\overline{R}$ compared to participants who did experience severe MS symptoms.

The overall reductions $\overline{R}_{\text{LOF}}$ and $\overline{R}_{\text{HOF}}$ (also indicated by the dashed lines in Figs. 7 and 8) were 0.095 (95% CI, 0.077 to 0.113) and 0.158 (95% CI, 0.141 to 0.176), respectively. These results show that a positive reduction was caused by the OF conditions, since the lower bounds of the 95% CIs for both conditions are greater than zero.

The grand mean reduction $\overline{R}$ (weighted average of both conditions) was calculated to be 0.126 (95% CI, 0.111 to 0.140). Again, as the lower bound of the CI is higher than zero, a positive reduction of the OF conditions over BL is observed. However, a one-sided weighted t-test did not show a significant greater value than zero (t = 1.714, p = 0.052), meaning that no significant difference was found between the OF conditions and BL.

To test if a difference in MISC scores between LOF and HOF was present, again a weighted one-sided t-test was performed to see if the overall reduction $\overline{R}_{\text{HOF}}$ is greater than the total reduction $\overline{R}_{\text{LOF}}$. The test did not show a significant difference (t = 0.520, p = 0.697), indicating that no difference in terms of MS could be found between LOF and HOF.

An attempt was made to investigate the order effect on the MISC values by calculating the overall reduction values for session two $\overline{R}_{\text{ses2}}$ and session three $\overline{R}_{\text{ses3}}$. This resulted in an overall reduction value for session two $\overline{R}_{\text{ses2}}$ of 0.225 (95% CI, 0.208 to 0.245) and an overall reduction value for session three $\overline{R}_{\text{ses3}}$ of 0.098 (95% CI, 0.081 to 0.115). Sessions two and three scored lower MISC scores compared to the first session. As both CIs do not include zero, it suggests that the MISC scores of session two and three deviate from those of the first session. Weighted one-sided t-tests showed that the reduction in session two was significantly greater than zero (t = 3.134, p = 0.003) and showed that the reduction in session three was not significantly greater than zero (t = 0.972, p = 0.172). It is striking, that the reduction in the third session is not significantly different. Increasing reduction values were expected with increasing session numbers, as participants are more familiar with the motion of the simulator.

[13] From the 18 participants who performed all three sessions, two participants prematurely stopped all three conditions and one participant did not go higher than a MISC score of zero in all sessions. All other participants were able to complete the 30 minutes of motion and had at least one session that caused a MISC score of one or higher.

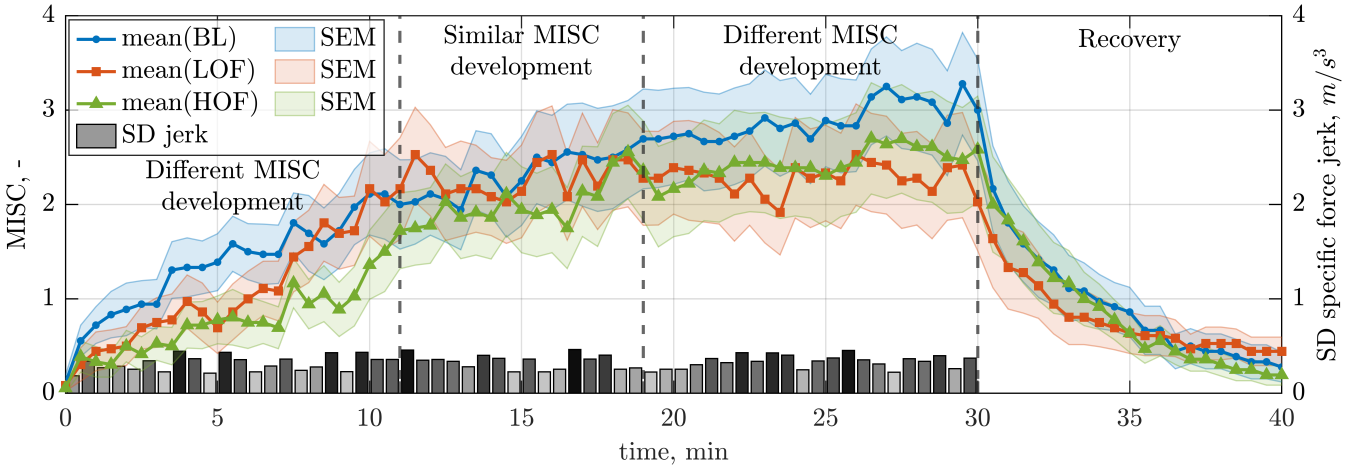

Fig. 6. Mean MISC scores and corresponding SEM over the 30-minute simulator motion and 10-minute recovery period, and the SD of the jerk of the specific force in the x-direction of the head reference frame

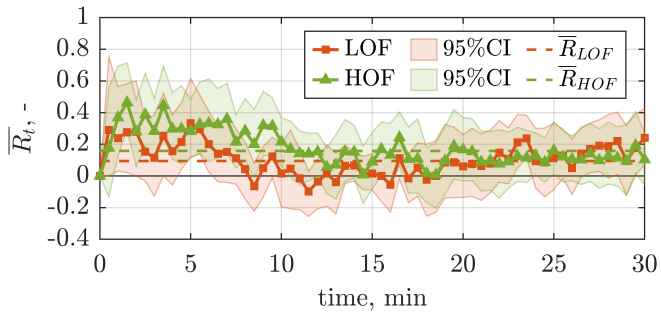

Fig. 7. Average weighted reduction for each time point ($\overline{R_t}$), including 95% confidence intervals, and overall weighted average reduction $\overline{R}$

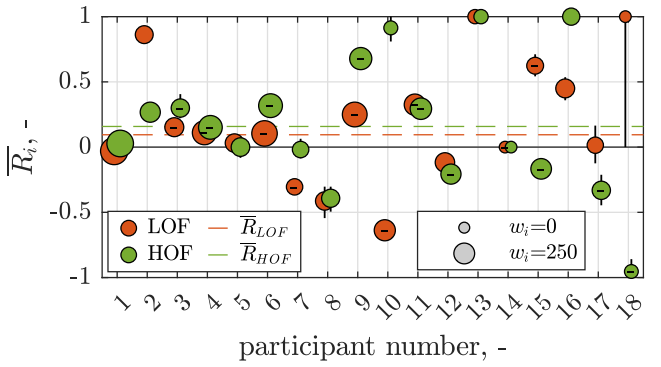

Fig. 8. Average weighted reduction for each participant ($\overline{R_i}$), including 95% confidence intervals (indicated by the vertical lines) and overall weighted average reduction $\overline{R}$. Participant weights w_i are illustrated with the marker size. A minus sign indicates that the specific condition took place before the BL condition

B. Motion Sickness Susceptibility

Fig. 9 shows the maximum MISC scores plotted against the MSSQ percentile score per individual participant for each condition. A moderate positive correlation could be observed between the maximum MISC score and the MSSQ percentile score, indicated by the correlation coefficients ρ. More interestingly, the means of the maximum MISC score for BL, LOF, and HOF were, 4.1, 3.1, and 3.4, respectively. These results indicate that the severity of MS symptoms are higher in BL compared to both OF conditions, while the participants experienced marginally more severe symptoms in HOF compared to LOF. Again, a small influence of visual translation on MS is showing, while a clear difference is missing between LOF and HOF.

C. Subjective Motion Comfort

Fig. 10 shows the results of the MS symptoms checklist. The first six groups of bars represent commonly observed MS symptoms. Except for some minor variation in the frequency of symptoms, no clear differences between the experimental conditions could be observed here. All other symptoms asked for in the questionnaire showed similar minor variations, except for eyestrain (also shown in Fig. 10). Participants experienced more eyestrain in BL compared to LOF and HOF. When evaluating the participants' comments given in the open questions, it became clear that the visuals shown in BL were difficult to focus on, which explains the increase in eyestrain.

Furthermore, the results of the level of comfort scoring performed at the end of all the experiment trials are shown in Fig. 11. A clear difference could be observed between the BL and the OF conditions, which means that the participants had a clear preference for LOF and HOF over BL. A Friedman test showed that there was a statistically significant difference in the level of comfort scores, depending on the type of visual condition (χ^2 = 11.662, p = 0.003). Post hoc analyses with Wilcoxon signed rank tests were performed with a Bonferroni correction, resulting in a significance level set at $p < 0.017$. These tests showed that a statistically significant difference could be found between BL and LOF (Z = -2.952, p = 0.003) and between BL and HOF (Z = -2.544, p = 0.011). No significant differences were found between LOF and HOF (Z = -0.797, p = 0.425).

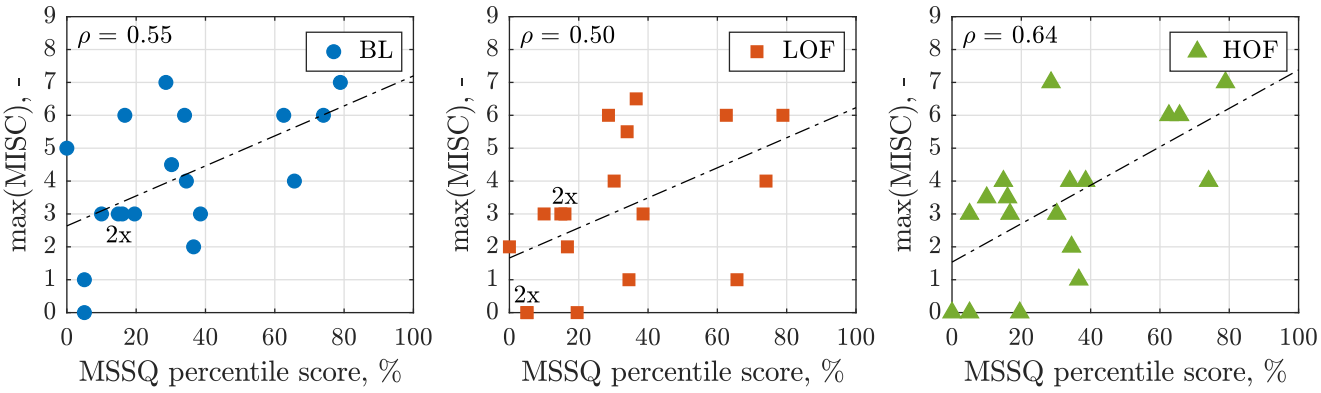

(a) Baseline condition (b) Low optical flow condition (c) High optical flow condition

Fig. 9. Maximum MISC scores plotted against the MSSQ percentile score per individual participant

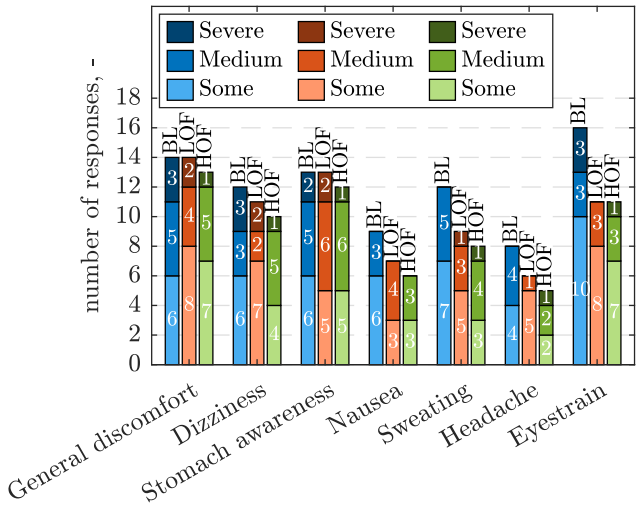

Fig. 10. Frequency and severity of MS symptoms experienced during all three experiment conditions

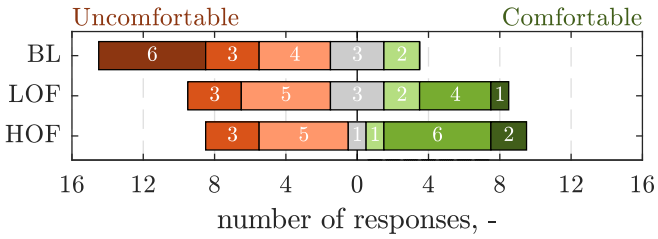

Fig. 11. Subjective level of comfort ratings for each condition

To investigate how the participants rated the level of comfort of the OF conditions compared to BL, the differences in the comfort scores between LOF/HOF and BL for each participant are visualized in Fig. 12. For reference, the blue number indicates the comfort score given for BL. As could be observed, 15 participants rated LOF as more comfortable than BL, while

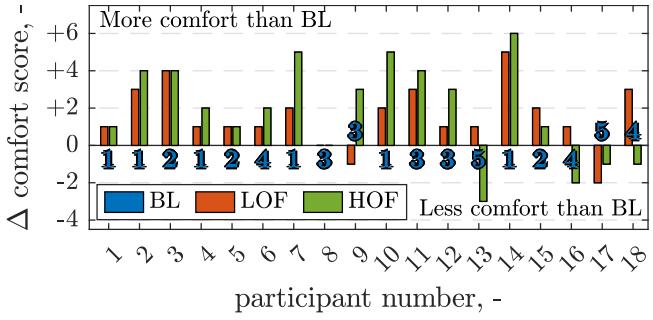

Fig. 12. The differences in comfort scores between the OF conditions and BL

13 participants rated HOF as more comfortable than BL. This indicates that the participants preferred the conditions with optical flow over the condition without optical flow. Again, only minor differences are observed between LOF and HOF.

To examine whether there was a correlation between reduction $\overline{R}_i$ and the difference in comfort score, both parameters are plotted against each other in Fig. 13. As shown in the figure, the weighted correlations (with weights w_i) for LOF and HOF were 0.14 and 0.15, respectively. Therefore, there was almost no correlation between the reduction $\overline{R}_i$ and the difference in comfort score. This could mainly be explained by the fact that some participants who had a negative reduction still scored the OF conditions as more comfortable than BL (all dots located in the second quadrant of Fig. 13). This figure shows that greater motion comfort does not necessarily mean lower MISC scores. More interestingly, most of the outliers (located near the edges of the figure) were participants with low susceptibility to MS (smaller marker sizes). This makes their individual results less credible.

Finally, the post-session questionnaire asked participants to give their level of agreement to statements about visual and physical motions. Statements asking the participant to rate the realism of physical motion explicitly are shown in Fig. 14. Two opposing questions were asked to check the

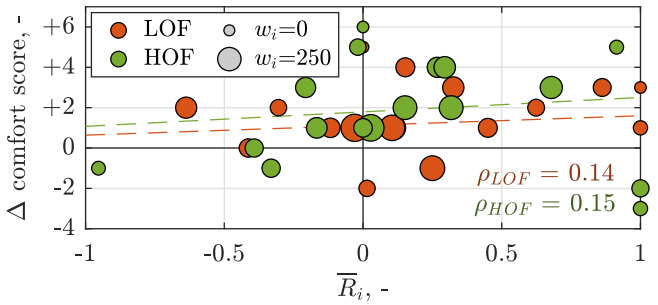

Fig. 13. The difference in comfort score between the OF conditions and BL plotted against reduction $\overline{R}_i$ for LOF and HOF. Participant weights w_i are illustrated with the marker size

Q1: I felt as if I was being driven around in a car.
Q2: The motion I was exposed to did not resemble that of a vehicle on the road.

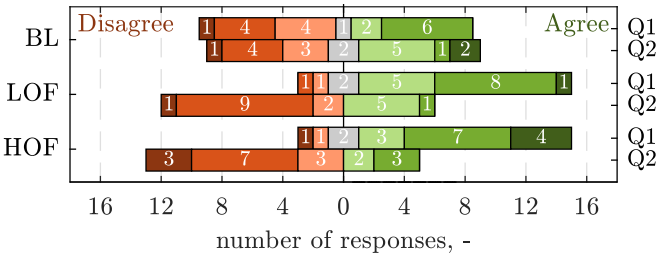

Fig. 14. Responses to the statements of the realism of the simulator motion in the post-session questionnaire

validity of the participant's answers. Interestingly, participants rated the physical motions of LOF and HOF to resemble real-life driving substantially better than the physical motion in BL, while the simulator motion was exactly the same in all conditions. The opposing question confirmed the validity of the participants' answers as the number of responses is roughly symmetric around zero for all conditions. This statement showed that the visual condition had a great influence on the fidelity of the simulation.

V. Discussion

A human-out-of-the-loop experiment was conducted in a moving-base simulator to investigate the influence of visual translation on MS. The experiment aimed to test the reliability and accuracy of the proposed visual translation extension to the 6DOF-SVC model and to contribute to the knowledge in the literature about the influence of visual translation on MS. To achieve these objectives, the experiment featured three different visual conditions with varying amounts of optical flow while keeping the physical motion of the simulator identical. The severity of MS in participants was assessed with MISC scores during the experiment, while subjective comfort ratings were obtained through post-experiment questionnaires.

The mean MISC scores and the grand mean reduction value demonstrated a slight improvement of the OF conditions over BL, indicating that there is a (small) influence of visual translation on MS. However, no significant differences were found, as a large spread was observed in individual reduction values. Moreover, the MS symptoms checklist exhibited only minor variations between conditions, indicating that there is no evidence for reduced MS severity with congruent visual translation. On the contrary, in terms of comfort level, a significant difference was found between the OF conditions and BL. Additionally, the weighted reduction factors and comfort analysis did not show a significant difference between LOF and HOF, suggesting that the amount of optical flow has little to no impact on MS.

As the MISC analysis and the subjective level of comfort analysis did not agree with each other, Hypothesis I, which stated that congruent visual translational information would reduce the occurrence and severity of MS, could neither be accepted nor rejected. Furthermore, as the MISC analysis, symptoms checklist and the subjective level of comfort ratings provided evidence that there were no differences between LOF and HOF, Hypothesis II, which postulated that higher global optical flow rates would decrease the occurrence and severity of MS, was rejected.

Regarding the participants who were unable to finish the complete 30-minute motion exposure, their last communicated MISC score was repeated for the remaining time points to calculate the mean MISC scores of all three conditions. This approach was employed to prevent a sudden decline in the mean MISC score when a participants stopped the experiment. However, due to this choice, the resulting mean MISC scores are an underestimate of the actual mean MISC scores, as the MISC scores of these participants would have been higher if they had continued. Furthermore, the reduction values were not calculated for the missing time points. This is because the repetitions of the last communicated MISC score only contained sixes or sevens due to the stopping criteria, which would result in unrealistic reduction values. Consequently, the participants' weights are also underestimated. Therefore, the reductions of the participants who were unable to complete the experiment exerted a lesser impact on the overall reduction values of LOF and HOF than they should have. This limitation underscores the need to identify an alternative and improved solution to address this issue.

The contrasting results between the MISC scores and the subjective level of comfort ratings may potentially be clarified by the fact that there was almost no correlation between these two parameters. Some participants who scored negative reduction values in an OF condition still rated that condition as more comfortable. The missing correlation could potentially be explained by one of the limitations of the MISC used to measure MS. MISC values between two and five resemble all MS symptoms, except for nausea. These values correspond to vague, slight, fairly, and severe levels of symptoms. However, the type of symptom is irrelevant, resulting in equal MISC scores for symptoms that may not be considered equally uncomfortable. For example, fairly warm and fairly dizzy have the same MISC score, even though these symptoms may not be experienced as equally (un)comfortable. Research by Reuten et

al. [52] already showed that the progression of MS symptoms and feelings of unpleasantness do not necessarily develop in an equal way. This may have created a confounding effect on the results and could give an explanation to participants who rated conditions with a reduction value lower than zero as more comfortable. On the contrary, a different experiment [53] showed that MISC and discomfort have a monotonous relationship, which opposes the results found in the current study and those of [52].

Regarding the slower response of the mean MISC score of HOF in the initial minutes of the simulation, an explanation could be found in the content of the visual scene. Some participants reported in open questions that the initial minutes of HOF were less boring and provided more distraction due to the visually attracting scene, making them less aware of the motion of the simulator compared to the other two conditions. Bos [54] has shown that (mental) distraction can indeed cause a reduction in MS. In addition, the responses to the statements asking the participants for the realism of the simulator motion revealed that the visual scenes in the OF conditions made the physical movements more representative of real-life driving, which made the motion more familiar and thus, as commented by the participants, more predictable.[14] The physical motion felt in BL was experienced as less realistic compared to the physical motion in the OF conditions, making them more difficult to predict and therefore harder to anticipate on. This could have caused the higher mean MISC scores for BL. On the other hand, participants commented that sudden braking and acceleration maneuvers without indications in the visual scene did not resemble real-life driving. This was especially experienced in LOF because the visual scene represented a highway without any other traffic. This compromised the fidelity of the simulation.

The preceding discussion reveals the need for further investigation to determine the specific factors that contributed to the observed differences in MISC scores between the experimental conditions. Specifically, it remains unclear whether the discrepancies were caused by variations in the amount of visual optical flow or the type of visual content presented to the participants. To address this issue, a follow-up study should be conducted in which the visual scene does not include known objects. A random dot field, as used by Diels et al. [55], would eliminate any known content from the scene, while the amount of optical flow can still be manipulated by changing the number of dots.

The process of simulating realistic road vehicle acceleration and brake maneuvers in the SRS was a challenging task. Participants reported that the use of tilt coordination to mimic low-frequency longitudinal accelerations was felt, as multiple comments about the simulator motion feeling like driving on a bumpy road, tilting of the car's nose, and a rollercoaster ride appeared in the open questions of the survey. Although the tilt rate was set to a lower value than human vestibular thresholds, the tilt acceleration was not limited and could have caused awareness of rotational motions in participants. Colombet et al. [56] have shown that the acceptance of simulator motion decreases as the maximum tilt acceleration increases. As a result, there was a mismatch between visual and inertial cues in the CNS, as rotational motions were absent in the visual cues. Zacharias [57] discovered that a steady-state conflict between visual and inertial cues leads to a reduced weighting of visual cues in the signal integration of self-motion perception.[15] Since the steady-state conflict was always present in BL (as there was no visual motion), the weight given to visual cues in the signal integration was low. Therefore, the visual-vestibular conflict could have had less effect on MS in this condition. More weight was given to the visual cues in LOF and HOF compared to BL, as these visual cues matched the inertial acceleration of the simulator better. Given this, the visual-vestibular mismatch arising from tilt coordination could have had a greater impact on the MISC values in the OF conditions than in BL.

Furthermore, the motion filter settings created an unrealistic specific force profile for the short acceleration and deceleration maneuvers, which had more aggressive acceleration changes in the designed motion profile compared to the longer acceleration and deceleration maneuvers. As the pitch rate limiter was set to a relatively low value, the low-frequency accelerations created by tilt coordination were lagging behind the designed motion profile, causing false motion cues in the experiment. This effect could compromise the reliability of the experiment results. To address this limitation, an alternative (and better) method of computing the simulator motion is a motion cueing algorithm based on a model predictive controller, which has been shown to perform better than a classical washout filter [59].

In another experiment that investigated the effect of visual translation on MS [33], participants were subjected to for-and-aft oscillatory motion while the visual environment was altered. They also found little to no differences in mean illness ratings between blindfolded, internal, external, and collimated views of the environment. However, a follow-up experiment [34] that included for-and-aft oscillatory motion with pitching motion found that an external view resulted in significantly lower mean illness ratings than blindfolded and internal views, suggesting that congruent visual rotation is more crucial than congruent visual translation. Moreover, Correia Grácio et al. [31] investigated the perceptual scaling of visual and inertial cues in the surge, sway, and yaw directions. They observed that visual and inertial cues were perceived as equally strong in yaw rotations, whereas in surge and sway, the inertial cues dominated. These findings suggest that accurate visual information in rotational motions is more critical to self-motion perception than accurate visual information in translational motions. Consequently, accurate visual rotations would increase the accuracy of the expected subjectective vertical, leading to a reduction in MS. However, it should be

[14] It is worth noting that comments of the participants also confirmed that the tilt coordination was felt the most in BL, confirming that the visual scenes of LOF and HOF suppressed the sensation of tilt coordination the most.

[15] Telban et al. [58] have modeled this effect mathematically.

noted that the fidelity of the visual cues in the current study and that of Correia Grácio et al. [31] could have influenced the results. For instance, stereopsis (i.e., depth perception retrieved through binocular vision) was missing in the visual cues, which plays an important role in depth perception and is crucial for visual translational motion perception [31]. Additionally, Correia Grácio et al. [31] examined the effect of the amount of optical flow on perceptual scaling and found only minor differences between the LOF and HOF conditions, similar to the findings of the current study.

One drawback of using the same participants for all conditions is that they become more familiar with the motion of the simulator as the number of sessions performed increases. The order effect analysis showed that the MISC values of session two and three (irrespective of the visual condition) were lower compared to session one. Furthermore, since Correia Grácio et al. [31] found high CIs for the visual gains in the surge direction, individual participants could have experienced the amplitude of the visual cues in the current experiment differently. A potential solution to this issue is to allow participants to manually adjust their visual gains before the start the experiment by turning a knob until the visual and inertial cues match according to their perception. This ensures that each participant experiences the visual velocity in a similar way.

Since the conflict between the sensed vertical and expected sensed vertical is the root cause of MS in the SVC theory [28], it is essential to investigate which visual information could influence the conflict between these two signals. According to Bos et al. [22], who developed a visual-vestibular motion perception model, visual rotation and visual verticality directly influence the perceived subjective vertical, while visual translation does not. Bos et al. [22] assume that visual translational information is combined with inertial accelerations after low-pass filtering of the otolith response. This filter translates the sensed specific force to sensed inertial acceleration and sensed vertical signals [60]. Therefore, visual translation does not affect the SVC, hence, in the visual-vestibular motion perception model of Bos et al. [22], visual translation would not have an influence on MS. The results of the current research could support this, as only small decreases in MS were observed for conditions with visual translation compared to the condition without visual translation. However, due to the limited fidelity of visual and inertial cues in the current study, there is no conclusive evidence for this.

The proposed 6DOF-SVC model with visual translation extension was able to predict a slight decrease in MS for conditions with visual optical flow, similar to the results of the experiment. However, a direct comparison between the model's predicted MSI (percentage of people who would vomit) and the experiment's measured MISC (a scale based on the typical progression of MS symptoms) is challenging. To compare these two results, the reduction factors for the predicted MSI values were calculated by comparing the MSI predicted for LOF and HOF with the MSI predicted for BL. The resulting reduction factors of 0.117 and 0.141, respectively, are close to the overall reductions $\overline{R}_{\text{LOF}}$ of 0.095 and $\overline{R}_{\text{HOF}}$ of 0.158 found in the experiment. This indicates that the 6DOF-SVC model with visual translation extension is capable of predicting the slight decrease in MS for LOF and HOF compared to the MS in BL. However, validating this model using only the results of the current experiment is not possible, as multiple factors have not been tested. For example, the combination of visual rotation and visual translation may require the gains from the (visual) rotation paths to be altered with the introduction of visual translation. Additionally, visual translation in heave and sway directions may result in different visual motion perception. Therefore, further research is required to confirm the workings of the model.

The decrease in predicted MS by the 6DOF-SVC model primarily depends on the visual acceleration gain $K_{a,vis}$ and the visual gain K_{vis}. When $K_{a,vis}$ has values higher than one and K_{vis} values are close to one, the model can better estimate the inertial acceleration signal $\hat{a}$ when the correct visual velocity is presented. However, using simulated physical and visual motions as input can lead to an increased visual acceleration conflict signal Δa_{vis} when K_{vis} is set too high. This increase is due to the different amplitudes of vestibular acceleration a_{vest} and visual velocity v_{vis}, as the motion filter alters the amplitude of the designed motion profile. Despite this, it is still a matter of discussion whether the CNS uses visual velocity to better estimate the inertial acceleration and if the (small) decrease in MS is due to the addition of visual translation. Both the current experiment and Butler et al.'s study [33] suggest that there is no or only a small influence of visual translation on MS. Thus, the value of the visual acceleration gain $K_{a,vis}$ should be close to zero.

An out-of-the-window view is a critical component of AV design, since visual information is one of the most important factors that modulates motion anticipation [8]. Several studies [9]–[15] have demonstrated that visual information can significantly decrease MS. However, based on the current research, it appears that visual translation does not have a significant impact on MS. Visual rotation, vertical visual cues, or even displaying a path that shows future motions may have a greater influence in reducing MS. Therefore, window design and seating arrangements remain relevant in AV design, but providing only visual information that displays passengers' (change in) velocity may not be sufficient to reduce the occurrence and severity of MS.

VI. Conclusion

This study aimed to investigate the effect of showing visual translation on MS by developing a MS prediction model that integrated visual translation, and then verifying the model in a human-out-of-the-loop experiment utilizing a moving-base simulator. Three different visual conditions, which varied in the amount of optical flow, were used, while the physical motion of the simulator was identical.

The experiment results indicate that visual translation may have a slight impact on MS, as evidenced by the decrease

in MS symptoms for the conditions with optical flow in comparison to the baseline condition. However, no significant differences are observed. Additionally, subjective comfort ratings vary significantly between the baseline and optical flow conditions, with the baseline condition being rated as more uncomfortable. Nevertheless, since the MS symptoms and subjective comfort analysis do not correspond with each other, the hypothesis that congruent visual translational information would reduce the occurrence and severity of MS can neither be accepted nor rejected. Furthermore, the amount of global optical flow appeares to have no influence on MS, as there were no significant differences between the low and high optical flow conditions in the experienced MS symptoms and subjective comfort ratings.

The MS model, with a proposal for a visual translation extension, was able to predict the slight decrease in MS for conditions with visual optical flow, as was demonstrated by the experiment. However, it is still up for discussion whether congruent visual translational information would have a significant influence on the occurrence and severity of MS as this study could not confirm this.

REFERENCES

[1] D. Begg, "A 2050 vision for London: What are the implications of driverless transport?," tech. rep., Clear Chanel, 2014.

[2] M. Akamatsu, P. Green, and K. Bengler, "Automotive technology and human factors research: Past, present, and future," *International Journal of Vehicular Technology*, vol. 2013, pp. 1–27, 2013.

[3] C. Diels and J. E. Bos, "Self-driving carsickness," *Applied Ergonomics*, vol. 53, pp. 374–382, 2016.

[4] E. A. Schmidt, O. X. Kuiper, S. Wolter, C. Diels, and J. E. Bos, "An international survey on the incidence and modulating factors of carsickness," *Transportation Research Part F: Traffic Psychology and Behaviour*, vol. 71, pp. 76–87, 2020.

[5] A. Rolnick and R. E. Lubow, "Why is the driver rarely motion sick? The role of controllability in motion sickness," *Ergonomics*, vol. 34, no. 7, pp. 867–879, 1991.

[6] T. Fukuda, "Postural behaviour and motion sickness," *Acta Oto-Laryngologica*, vol. 81, no. 3-6, pp. 237–241, 1976.

[7] T. Wada, S. Fujisawa, and S. Doi, "Analysis of driver's head tilt using a mathematical model of motion sickness," *International Journal of Industrial Ergonomics*, vol. 63, pp. 89–97, 2018.

[8] C. Diels, Y. Ye, J. E. Bos, and S. Maeda, "Motion sickness in automated vehicles: Principal research questions and the need for common protocols," *SAE International*, vol. 5, no. 2, pp. 1–14, 2022.

[9] T. Probst, S. Krafczyk, and W. Büchele, "Visuelle prävention der bewegungskrankheit im auto," *Archiv für Psychiatrie und Nervenkrankheiten*, vol. 231, pp. 409–421, 1982.

[10] M. Turner and M. J. Griffin, "Motion sickness in public road transport: Passenger behaviour and susceptibility," *Ergonomics*, vol. 42, no. 3, pp. 444–461, 1999.

[11] M. J. Griffin and M. M. Newman, "Visual field effects on motion sickness in cars," *Aviation, Space, and Environmental Medicine*, vol. 75, no. 9, pp. 739–748, 2004.

[12] O. X. Kuiper, J. E. Bos, and C. Diels, "Looking forward: In-vehicle auxiliary display positioning affects carsickness," *Applied Ergonomics*, vol. 68, pp. 169–175, 2018.

[13] S. Salter, C. Diels, P. Herriotts, S. Kanarachos, and D. Thake, "Motion sickness in automated vehicles with forward and rearward facing seating orientations," *Applied Ergonomics*, vol. 78, pp. 54–61, 2019.

[14] A. Rolnick and W. Bles, "Performance and well-being under tilting conditions: The effects of visual reference and artificial horizon.," *Aviation, Space, and Environmental Medicine*, vol. 60, no. 8, pp. 779—-785, 1989.

[15] P. J. Feenstra, J. E. Bos, and R. N. H. W. van Gent, "A visual display enhancing comfort by counteracting airsickness," *Displays*, vol. 32, no. 4, pp. 194–200, 2011.

[16] N. Kamiji, Y. Kurata, T. Wada, and S. Doi, "Modeling and validation of carsickness mechanism," in *SICE Annual Conference 2007*, pp. 1138–1143, IEEE, 2007.

[17] S. Inoue, H. Liu, and T. Wada, "Revisiting motion sickness models based on SVC theory considering motion perception," tech. rep., SAE Technical Paper, 2023.

[18] T. Wada, J. Kawano, Y. Okafuji, A. Takamatsu, and M. Makita, "A computational model of motion sickness considering visual and vestibular information," in *2020 IEEE International Conference on Systems, Man, and Cybernetics (SMC)*, pp. 1758–1763, IEEE, 2020.

[19] N. Jalgaonkar, D. S. Schulman, S. Ojha, and S. Awtar, "A visual-vestibular model to predict motion sickness response in passengers of autonomous vehicles," *SAE International Journal of Advances and Current Practices in Mobility*, vol. 3, no. 5, pp. 2421–2432, 2021.

[20] H. Liu, S. Inoue, and T. Wada, "Motion sickness modeling with visual vertical estimation and its application to autonomous personal mobility vehicles," in *2022 IEEE Intelligent Vehicles Symposium (IV)*, pp. 1415–1422, IEEE, 2022.

[21] C. Braccesi and F. Cianetti, "Motion sickness. Part I: Development of a model for predicting motion sickness incidence," *International Journal of Human Factors Modelling and Simulation*, vol. 2, no. 3, pp. 163–187, 2011.

[22] J. E. Bos, W. Bles, and E. L. Groen, "A theory on visually induced motion sickness," *Displays*, vol. 29, no. 2, pp. 47–57, 2008.

[23] K. E. Money, "Motion sickness," *Physiological Reviews*, vol. 50, no. 1, pp. 1–39, 1970.

[24] G. Bertolini and D. Straumann, "Moving in a moving world: A review on vestibular motion sickness," *Frontiers in Neurology*, vol. 7, no. 14, pp. 1–11, 2016.

[25] B. S. Cheung, I. P. Howard, and K. E. Money, "Visually-induced sickness in normal and bilaterally labyrinthine-defective subjects," *Aviation, Space, and Environmental Medicine*, vol. 62, no. 6, pp. 527–531, 1991.

[26] J. T. Reason and J. J. Brand, *Motion sickness*. Academic Press, 1975.

[27] C. M. Oman, "A heuristic mathematical model for the dynamics of sensory conflict and motion sickness," *Acta Oto-Laryngologica*, vol. 94, no. sup392, pp. 4–44, 1982.

[28] W. Bles, J. E. Bos, B. De Graaf, E. Groen, and A. H. Wertheim, "Motion sickness: Only one provocative conflict?," *Brain Research Bulletin*, vol. 47, no. 5, pp. 481–487, 1998.

[29] F. Cardullo, B. Sweet, R. Hosman, and C. Coon, "The human visual system and its role in motion perception," in *AIAA Modeling and Simulation Technologies Conference*, 2011.

[30] B. Keshavarz, B. E. Riecke, L. J. Hettinger, and J. L. Campos, "Vection and visually induced motion sickness: How are they related?," *Frontiers in Psychology*, vol. 6, p. 472, 2015.

[31] B. J. Correia Grácio, J. E. Bos, M. M. van Paassen, and M. Mulder, "Perceptual scaling of visual and inertial cues," *Experimental Brain Research*, vol. 232, no. 2, pp. 637–646, 2014.

[32] J. J. Gibson, *The perception of the visual world*. Houghton Mifflin, 1950.

[33] C. A. Butler and M. J. Griffin, "Motion sickness during fore-and-aft oscillation: Effect of the visual scene," *Aviation, Space, and Environmental Medicine*, vol. 77, no. 12, pp. 1236–1243, 2006.

[34] C. A. Butler and M. J. Griffin, "Motion sickness with combined fore-aft and pitch oscillation: Effect of phase and the visual scene," *Aviation, Space, and Environmental Medicine*, vol. 80, no. 11, pp. 946–954, 2009.

[35] J. F. O'Hanlon and M. E. McCauley, "Motion sickness incidence as a function of vertical sinusoidal motion," *Aerospace Medicine*, vol. 45, no. 4, pp. 336–369, 1974.

[36] H. Liu, S. Inoue, and T. Wada, "Subjective vertical conflict model with visual vertical: Predicting motion sickness on autonomous personal mobility vehicles," *arXiv preprint arXiv:2302.08642*, 2023.

[37] J. Monen and E. Brenner, "Detecting changes in one's own velocity from the optic flow," *Perception*, vol. 23, no. 6, pp. 681–690, 1994.

[38] J. E. Bos, S. N. MacKinnon, and A. Patterson, "Motion sickness symptoms in a ship motion simulator: Effects of inside, outside and no view," *Aviation, Space, and Environmental Medicine*, vol. 76, no. 12, pp. 1111–1118, 2005.

[39] R. Akçelik and D. C. Biggs, "Acceleration profile models for vehicles in road traffic," *Transportation Science*, vol. 21, no. 1, pp. 36–54, 1987.

[40] J. Karjanto, N. Md. Yusof, J. Terken, F. Delbressine, M. Z. Hassan, and M. Rauterberg, "Simulating autonomous driving styles: Accelerations for three road profiles," in *MATEC Web of Conferences*, vol. 90, p. 01005, 2017.

[41] L. D. Reid and M. A. Nahon, "Flight simulation motion-base drive algorithms: Part 1. Developing and testing equations," tech. rep., University of Toronto, 1985.
[42] M. E. McCauley, J. W. Royal, C. D. Wylie, J. F. O'Hanlon, and R. R. Mackie, "Motion sickness incidence: Exploratory studies of habituation, pitch and roll, and the refinement of a mathematical model," tech. rep., Human Factors Research Inc., 1976.
[43] E. L. Groen and W. Bles, "How to use body tilt for the simulation of linear self motion," *Journal of Vestibular Research*, vol. 14, no. 5, pp. 375–385, 2004.
[44] H. M. Heerspink, W. R. Berkouwer, O. Stroosma, M. M. van Paassen, M. Mulder, and J. A. Mulder, "Evaluation of vestibular thresholds for motion detection in the SIMONA research simulator," in *AIAA Modeling and Simulation Technologies Conference and Exhibit*, 2005.
[45] P. Hansson, A. Stenbeck, A. Kusachov, F. Bruzelius, and B. Augusto, "Prepositioning of driving simulator motion systems," *International Journal of Vehicle Systems Modelling and Testing*, vol. 10, no. 3, pp. 288–304, 2015.
[46] MasterPixel3D, "Fantastic city generator." https://assetstore.unity.com/packages/3d/environments/urban/fantastic-city-generator-157625, 2022. Accessed: 2023-04-12.
[47] F. S. Capaldo, "Driver eye height: Experimental determination and implications on sight distances," *Procedia - Social and Behavioral Sciences*, vol. 43, pp. 375–383, 2012.
[48] M. Lappe, F. Bremmer, and A. V. van den Berg, "Perception of self-motion from visual flow," *Trends in Cognitive Sciences*, vol. 3, no. 9, pp. 329–336, 1999.
[49] J. F. Golding, "Predicting individual differences in motion sickness susceptibility by questionnaire," *Personality and Individual Differences*, vol. 41, no. 2, pp. 237–248, 2006.
[50] R. Likert, "A technique for the measurement of attitudes," *Archives of Psychology*, vol. 22, no. 140, pp. 5–55, 1932.
[51] A. J. C. Reuten, J. B. J. Smeets, J. Rausch, M. H. Martens, E. A. Schmidt, and J. E. Bos, "The (in)effectiveness of anticipatory vibrotactile cues in mitigating motion sickness," *Experimental Brain Research*, vol. 241, p. 1251–1261, 2023.
[52] A. J. C. Reuten, S. A. E. Nooij, J. E. Bos, and J. B. J. Smeets, "How feelings of unpleasantness develop during the progression of motion sickness symptoms," *Experimental Brain Research*, vol. 239, no. 12, pp. 3615–3624, 2021.
[53] K. N. de Winkel, T. Irmak, V. Kotian, D. M. Pool, and R. Happee, "Relating individual motion sickness levels to subjective discomfort ratings," *Experimental Brain Research*, vol. 240, no. 4, pp. 1231–1240, 2022.
[54] J. E. Bos, "Less sickness with more motion and/or mental distraction," *Journal of Vestibular Research*, vol. 25, no. 1, pp. 23–33, 2015.
[55] C. Diels, K. Ukai, and P. A. Howarth, "Visually induced motion sickness with radial displays: Effects of gaze angle and fixation," *Aviation, Space, and Environmental Medicine*, vol. 78, no. 7, pp. 659–665, 2007.
[56] F. Colombet, Z. Fang, and A. Kemeny, "Tilt thresholds for acceleration rendering in driving simulation," *Simulation*, vol. 93, no. 7, pp. 595–603, 2017.
[57] G. Zacharias, *Motion sensation dependence on visual and vestibular cues*. PhD thesis, Massachusetts Institute of Technology, 1977.
[58] R. J. Telban and F. M. Cardullo, "Motion cueing algorithm development: Human-centered linear and nonlinear approaches," tech. rep., State University of New York, 2005.
[59] Y. R. Khusro, Y. Zheng, M. Grottoli, and B. Shyrokau, "MPC-based motion-cueing algorithm for a 6-DOF driving simulator with actuator constraints," *Vehicles*, vol. 2, no. 4, pp. 625–647, 2020.
[60] R. Mayne, "A systems concept of the vestibular organs," in *Vestibular System Part 2: Psychophysics, Applied Aspects and General Interpretations. Handbook of Sensory Physiology, vol 6 / 2* (H. H. Kornhuber, ed.), pp. 493–580, Springer, 1974.

Part II

Preliminary Thesis

(This part has already been graded for the course AE4020)

Chapter 2

Motion Sickness

Considerations of MS have been around for a long time. In the past, boats provided one of the few forms of passive motion to individuals. Translational and rotational motions caused sea sickness in sailors. Nowadays, there are many new forms of passive motion, for example, buses, cars, trains, and planes, which make MS a prominent research topic again (Bertolini & Straumann, 2016). This chapter will give a brief definition of MS in Section 2-1, causes and current theories of MS in Section 2-2, and the problem of AVs with MS in Section 2-3. Section 2-4 briefly sums up the main findings.

2-1 Motion Sickness Definition

MS is a malady caused by passive self-motion that contains certain types of dynamic and kinematic properties (Bertolini & Straumann, 2016; Money, 1970). Motion illusions, i.e., moving visual surroundings, could also be a cause of MS. It should be noted that subjects who do not have a functional vestibular system are not susceptible to MS (Cheung et al., 1991). This indicates that the vestibular system plays an important role in the nauseogenic stimulus. A quick observation of the above suggests that MS occurs when motion-sensitive sensors (i.e., the vestibular system, the visual system, and the somatosensory system) are exposed to conflicting motion signals (Bertolini & Straumann, 2016).

Signs and symptoms of MS can include various combinations of the following: drowsiness, dizziness, discomfort, restiveness, repetitive yawning, stomach awareness, nausea, pallor, sweating, headache, malaise, bradycardia, arterial hypotension, vomiting, and apathy (Reason & Brand, 1975). These are sorted according to MS severity. Although responses differ between individuals, they usually develop in a fixed order (Tyler & Bard, 1949). The severity and duration of the motion stimulus required for any MS symptoms vary significantly between individuals. Furthermore, susceptibility to MS varies, where age and genetic factors play an important role (Golding & Gresty, 2015; Reavley, Golding, Cherkas, Spector, & MacGregor, 2006).

Sensory systems involved in motion stimuli are the vestibular system, the visual system and the somatosensory system. Each system has its own role in motion perception and is sensitive to different aspects of motion stimuli. Vision cannot distinguish between self-motion or motion of the observed scene (e.g., moving train illusion), and is highly dependent on brightness conditions. The Semicircular Canals (SCC) within the vestibular system are only sensitive to rotational velocity changes and cannot measure constant velocities, whereas the otoliths can only measure the specific force and cannot differentiate between inertial accelerations and gravity. It becomes clear that every sensor has its shortcomings, which the CNS is trying to solve. The CNS combines all sensory signals into a best estimate of the **self-propelled motion**, weighing them according to their reliability. MS arises when a subject experiences **passive self-motion**, that is, being moved around by an external force (e.g., being driven around in an autonomous car). These unnatural motion stimuli lead to a combination of sensory signals that is impossible for the CNS to interpret, resulting in MS (Bertolini & Straumann, 2016).

2-2 Motion Sickness Theories

The most often mentioned explanation for MS is the **sensory mismatch theory** (Bertolini & Straumann, 2016). This theory states that a conflict in sensory motion signals (e.g., signals from the visual and vestibular systems) is not enough to cause MS (Reason & Brand, 1975). This conflict is only provocative if the present sensory signals are at variance with the expected sensory signals. This explains why humans rarely get sick when subjected to a constant visual angular velocity in an optokinetic drum (Bos et al., 2008). In this condition the CNS does not expect a signal from the vestibular sytem, since the SCC are not sensitive to constant angular velocities (Angelaki & Cullen, 2008). Hence, present sensory signals in this situation are not at variance with the expected sensory signals. In a mathematical model (see Oman (1982) for an example), this conflict vector would be represented by the difference between **all** sensory afferent signals and the expected sensory afferent signals from the CNS.

Bles et al. (1998) state that the **SVC** only, is enough to explain the cause of MS. The SVC theory only considers the conflict between the expected subjective vertical and the vertical provided by the sensory signals. This means that the rotational velocity and the linear acceleration conflicts do not (directly) influence MS. This assumption can be made since people barely get sick when rotating around an Earth-vertical axis, while they do develop sickness when being rotated around an Earth-horizontal axis (Bos et al., 2008).[1] The sensory conflict and SVC theories look similar, but when considering a subject that is accelerating around an Earth-vertical axis at constant angular velocity, they differ. The sensory mismatch theory labels this motion provocative since the visual and vestibular dynamics are different, while this motion would not cause MS according to the SVC theory.

A third theory exists which is based on the angular vestibulo-ocular reflex and the relation with the Gravito-Inertial Acceleration (GIA). The underlying mechanism in the CNS is the **velocity storage**. This mechanism integrates and coordinates sensory rotational signals for

[1] Bos et al. (2008) do mention that susceptible people can get sick from rotation around an Earth-vertical axis. However MS is usually weak and takes a long time to develop in this condition. MS in this situation could be explained by a misperception of the center of rotation, an uncertainty in sensor outputs, or incorrectly perceived vertical when the head is held still for a longer time.

self-motion perception (Raphan, Matsuo, & Cohen, 1979). This integrated signal gives the subject an estimate of the current rotational velocity vector. The theory states that MS is related to the difference of the yaw eigenvector of this rotational velocity estimate, which is close to the spatial vertical, and the actual sensed rotational velocity signal from the SCC (Bertolini & Straumann, 2016). This difference is equal to the conflict signal as defined by the SVC theory. However, transitional motions are not taken into account in the velocity storage theory, which makes it less valuable than the SVC theory.

Riccio and Stoffregen (1991) presented an alternative approach to explain MS. They state that MS is provoked when a motion stimulus triggers **postural instability**. Therefore the authors move the focus from motion perception to a sensory-motor process. To support this theory, experiments did find a correlation between postural instability and MS (Stoffregen & Smart Jr, 1998). Again, verticality perception plays a major role in causing MS in the postural instability theory. However, this theory can only be used when a subject requires postural stabilization. Therefore, it is less useful for predicting MS of passengers seated in AVs.

Note that all theories that are mentioned above are not necessarily exclusive. Elements of these theories overlap or may be true in different kind of motion conditions.

2-3 Motion Sickness in Automated Vehicles

AVs could have different levels of automation technologies. Low-level automation includes anti-lock brakes and forward collision warning, while high-level automation includes adaptive cruise control and automatic lane keeping (Diels & Bos, 2016). The driver's role changes with the level of automation, starting from an active driver, to a supervisory role, to a passenger. With full automation, the driver is able to engage in secondary tasks (e.g., reading a book, watching a movie) and can be oriented backwards to have a conversation with the back-seat passengers.

However, there is one problem with automation that did not get a lot of attention, namely motion sickness. AVs do increase the likelihood and incidence of MS due to several reasons (Diels & Bos, 2016). A visual-vestibular conflict arises when the driver engages in non-driving related activities, that is, visual motion does not correspond to the vehicle motion. The CNS commonly integrates congruent visual and vestibular signals, so visual motion that conflicts with the physical motion is not as expected. As explained in Section 2-2, this sensory conflict is thought to be the main reason for MS.

Another problem that arises with automation is motion anticipation. Rolnick and Lubow (1991) noticed that the driver rarely experiences motion sickness, indicating that the CNS also uses previous experiences to make a prediction about self-motion. A car driver learns the transition from steering wheel and pedals to the actual vehicle motion. This makes the CNS capable of making a better self-motion prediction, thus minimizing the sensory conflict responsible for motion sickness. Next to the "learned" vehicle dynamics, visual information also plays a key role in motion anticipation. A clear view of the road ahead improves future motion predictions and consequently reduces the occurrence of motion sickness. Again, secondary activities or rearward facing seating positions prevent this unobstructed view of the road ahead.

From the above, it becomes clear that controllability and visual information of future motions are important for diminishing MS. The current designs of AVs take away both factors. The driver is unable to predict upcoming motions from their own input, and secondary activities or rear-facing seats obstruct a clear view of the road ahead, which normally helps people predict future motion. Therefore, AV occupants are more likely to experience MS.

2-4 Conclusions

Considerations of MS in sailors have been around for a long time. However, today there are many new forms of passive motion (e.g., buses, trains, cars), increasing the demand for MS research. MS is defined as a malady caused by passive self-motion that contains certain types of dynamic and kinematic properties, in which the vestibular system plays an important role (Money, 1970).

Several theories exist to explain MS, including the sensory mismatch theory, SVC theory, velocity storage theory, and the postural instability theory. In all theories verticality perception plays an important role, that is, when the sensed and expected vertical differ, MS arises. The SVC theory is best suited for the application to autonomous vehicles, since both rotational and translational motions are taken into account and seated passengers do not require postural stabilization.

Due to the driver losing the control of the vehicle and engaging in non-driving related activities, MS becomes a problem in autonomous vehicles. Clear visual information, in accordance with the physical motion, could help minimize the Motion Sickness Incidence (MSI) of AV passengers. The exact role of visual motion on self-motion perception and MS will be discussed in Chapter 3.

Chapter 3

Visual Motion

As stated in Chapter 2, vision is one of the sensory systems involved in motion perception. This chapter will elaborate on the role of visual information in motion perception, and what the influence of visual information is on MS. First, the visual sensor and the types of motion distinguishable from vision will be discussed in Section 3-1. This chapter also contains an explanation of the integration of visual and vestibular sensory signals and how these can be used in an observer model. Section 3-2 and Section 3-3 focus on a number of experiments where the role of vision on MS and Visually Induced Motion Sickness (VIMS) was examined.

3-1 Visual Information in Motion Perception

Humans perceive motion through different sensory signals including the visual system, vestibular system, somatosensory system, and auditory system (Cardullo, Sweet, Hosman, & Coon, 2011). The human CNS integrates these sensory signals into a combined perception of self-motion. Multiple layers of organisation are present in this perceptual process. Motion perception is important for understanding MS, as expected motion signals play a key role in the SVC theory. This section focuses on human motion perception and in particular on the role of the visual system.

3-1-1 Visual Sensor

Humans use the eyes as a visual sensor to their environment. Light enters the eye via the cornea, which acts as a protective layer. After propagating through the pupil, lens, and protective clear liquids, the light hits the retina. All these layers act as optical elements that reflect and focus light onto the retina (see Figure 3-1 for a schematic overview). Rods and cones in the retina convert the incoming light into small electrical currents that are sent to the visual centers in the CNS. A higher density of cones, responsible for color vision, can be found inside the fovea, while the rods, sensitive to light intensity only, vastly outnumber the cones in the periphery. These rods and cones produce a neuronal signal that passes through

several layers of signal processing in the CNS. The visual cortex, located at the backside of the human brain, is responsible for the visual processing. Its tasks are spatial organization, pattern recognition, and visual recognition and memory. This is a complex process, which makes visual perception the slowest perceptual process dealing with self-motion (Cardullo et al., 2011).

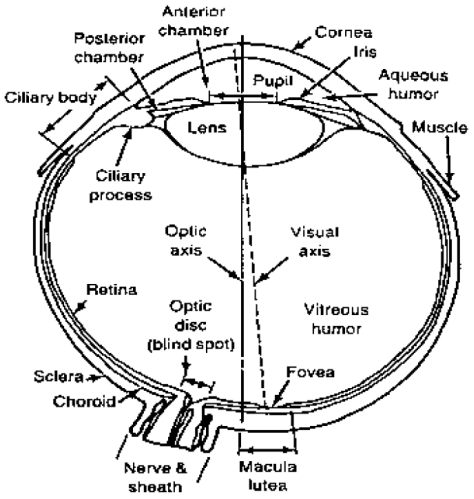

Figure 3-1: Systematic view of the human eye (Cardullo et al., 2011)

3-1-2 Visual Field

Vision can be used for static perception, that is, the ability to resolve details of an image. For depth perception, recognition of objects of known size is important. However, for the current research project, it is more interesting to look at the motion perception capabilities of the human eye. The CNS is capable of detecting motion from visual input. There is a dedicated part of the human brain responsible for visual motion perception (Cardullo et al., 2011). This part is not only able to process object motion in the visual field, but can also subtract information from the visual environment about self-motion.

Information about self-motion or self-orientation can be distinguished from the visual environment, including: (1) **visual translation** which is often referred to as linear vection, (2) **visual rotation**, often referred to as circular vection and (3) **visual vertical** of the environment.[1] The first two depend on optical flow patterns of the visual image, whereas the latter is based on previous knowledge of structures in the visual scene. For visual translation, the optical flow depends on the distance between the visual observer and the object (Correia Grácio et al., 2014). Figure 3-2a-b shows this phenomenon, where distant objects close to the horizon barely move (indicated by a small arrow), whereas objects close to the observer move relatively fast (indicated by a large arrow). This effect is known as motion parallax (Lappe, Bremmer, & van den Berg, 1999) and is responsible for the fact that driving a sports car low to the ground has a greater sense of motion than flying an aircraft at altitude. Gibson (1950) also explains this effect with the global optical flow rate. This is directly proportional

[1]Vection is defined as the sense of self-motion from visual images, in the absence of physical self-motion (Keshavarz, Riecke, Hettinger, & Campos, 2015).

with the velocity and inversely proportional with the height of the observer traveling through a visual environment. On the other hand, with visual rotation, the whole visual scene has a constant optical flow and is independent of the distance; see Figure 3-2c. This only holds for the pitch and yaw movements of the head, since roll movement rotates the whole visual scene around its center point. To distinguish visual translation and visual rotation from each other, motion parallax is used, therefore depth variation in the visual field is required to differentiate between the two (Lappe et al., 1999). Lastly, humans use visual field patterns to determine subjective verticality (Bos et al., 2008). For example, a tilted house or horizon gives information about the subjects' roll orientation. It is interesting that this also holds in tilted houses due to earthquakes. Humans can experience MS when navigating through these environments (Kitahara & Uno, 1967).

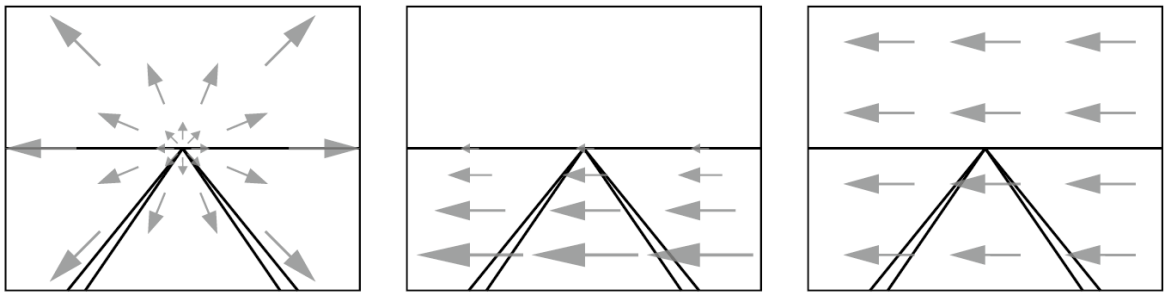

Figure 3-2: Example of the optic flow field for surge, sway, and yaw (Correia Grácio et al., 2014)

Contrast within the visual field is important to distinguish optical flow patterns. This contrast is defined as luminence differences within an image. Our eyes need a certain contrast intensity to recognize patters, however, this value is almost ten times lower when a visual stimulus is in motion (Cardullo et al., 2011), indicating that our CNS is trained to recognize visual motion. Additionally, it must be noted that humans can hardly see visual acceleration and can only see visual velocity. Experiments by Calderone and Kaiser (1989) showed that high acceleration thresholds are needed for visual acceleration detection. This is important for the integration of visual and vestibular information, since the vestibular system is sensitive to acceleration. This will be further eleborated on in subsection 3-1-3.

3-1-3 Visual-Vestibular Interactions

Visual motion information is integrated with other sensory signals, e.g., vestibular and somatosensory systems, to a combined perception of self-motion. Bos et al. (2008) created a mathematical model of this integration process, depicted in Figure 3-3. The inputs of the model are the physical and visual motions experienced by the head. Thus, the model uses a head-fixed reference frame with the positive x-axis pointing out of the nose, the positive y-axis pointing out of the left ear and the positive z-axis is pointing up, out of the head, orthogonal to the other axes.

The vestibular system consists of the otoliths (OTO block) and the semicircular canals (SCC block), sensitive to linear accelerations and rotational rates, respectively. In particular, the otoliths are sensitive to the three-dimensional specific force $\boldsymbol{f}$, which is a combination of

inertial and gravitational accelerations. The otolith dynamics are modeled as unity, since the otoliths are capable of sensing low-frequency accelerations almost perfectly (Merfeld, Young, Oman, & Shelhamert, 1993). The input to the SCC block is the three-dimensional rotational velocity vector $\boldsymbol{\omega}$. The SCC are modeled as a high-pass filter, since they can only measure changes in rotational velocity. Mayne (1974) suggested that the gravity component $\boldsymbol{g}$ is resolved in the CNS, by low-pass filtering the sensed specific force $\boldsymbol{f}$ in the earth-fixed reference frame ($\boldsymbol{g}$ is constant in an earth-fixed reference frame). This low-pass filtering is implemented in the model with the $\mathbf{R}\ \mathbf{LP}\ \mathbf{R}^{-1}$ path, where the sensed rotational velocity ($\boldsymbol{\omega}$) is used for the reference frame conversion. This concludes the vestibular part of the motion perception model.

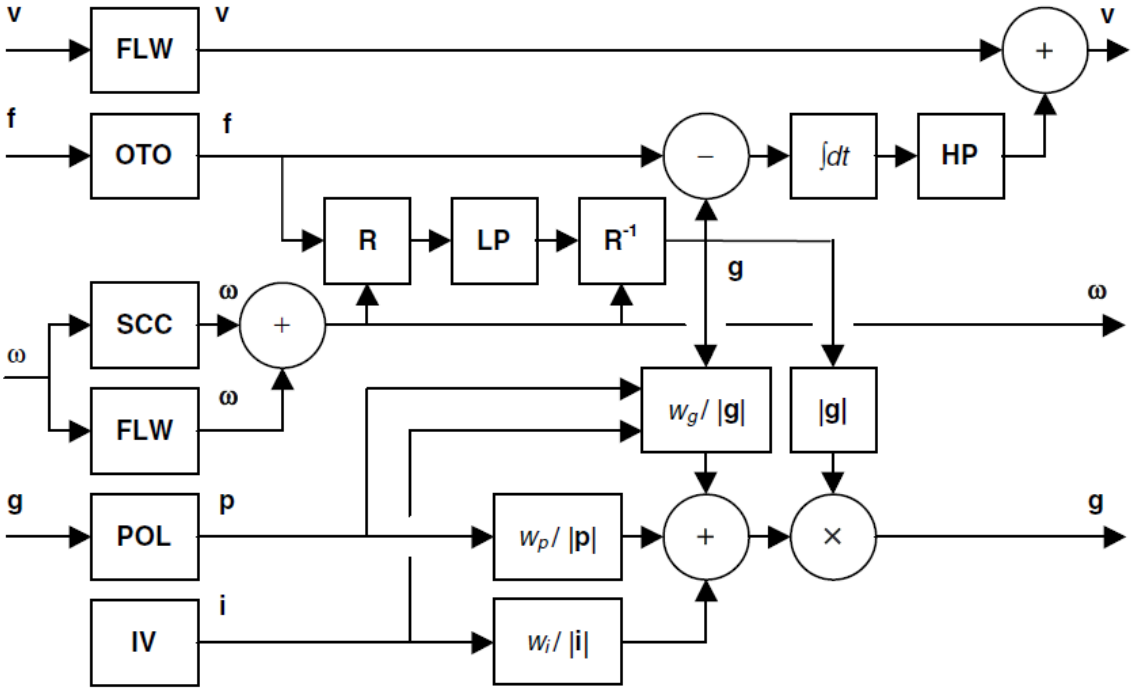

Figure 3-3: Visual-vestibular interaction model by Bos et al. (2008)

The three different sources of visual information discussed in subsection 3-1-2 are added to this model as well. Humans cannot detect visual acceleration directly (Monen & Brenner, 1994), but can only sense visual velocity. Linear vection $\boldsymbol{v}$ (1) is calculated using a low-pass filter in the upper FLW block. The time constant of this filter is in a similar range as the time constant of the low-pass filter used to distinguish between inertial and gravitational acceleration ($\tau_{lp} = 5$). Consequently, the visual sensed velocity can be added to the integrated high-pass-filtered inertial acceleration felt by the otoliths, resulting in an integrated visual-vestibular velocity perception.[2] Circular vection $\boldsymbol{\omega}$ (2) typically shows low-pass behaviour (Dichgans & Brandt, 1978), while the SCC can be modelled as a high-pass filter. Hence, these two sensor afferents can also be linearly added (Robinson, 1977), as seen by the SCC

[2]The high-pass filter after the integration of the inertial acceleration felt by the otoliths will be omitted in later models. Bos and Correia Grácio (2015) showed that humans have a constant velocity perception during constant centrifugal acceleration. Hence, integrating an already high-pass filtered version of the specific force $\boldsymbol{f}$ is enough to calculate the vestibular velocity perseption.

and the lower FLW block in Figure 3-3. The visual vertical vector (3), or visual polarity, is added to the model in the POL block at the bottom. Vertical information from the vestibular system $\boldsymbol{g}$, visual system $\boldsymbol{p}$, and idiotropic vector $\boldsymbol{i}$ are weighted and added to calculate the final perceived attitude $\boldsymbol{g}$ (bottom right).[3] Visual verticality information has been weighted the highest in this model.

Correia Grácio et al. (2014) investigated the effects of FoV, image size, and depth cues on visual gains (i.e., the ratio between visual and inertial cues). Their subjects had to turn a knob, that controlled the amount of visual motion, until they felt the inertial and visual cues to be coherent in a motion-based simulator. They found that visual gains were closer to unity when the FoV was the largest, indicating that the FoV should be as close to the human FoV as possible to have equal visual and vestibular amplitudes. This is related to the important role of the peripheral view in self-motion perception. Furthermore, Correia Grácio et al. (2014) found out that humans need objects of known size in their visual field to correctly estimate linear speed from optic flow. Last, the authors concluded that depth cues are important to correctly perceive visual translation. As explained before, motion parallax is a crucial aspect of visual self-motion perception. But other depth cues (e.g., accommodation, convergence, shading) are also important. All factors mentioned above are important to keep in mind when designing an experiment using a motion-based simulator with a visual system.

3-1-4 Observer model theory

A motion perception model as presented above could be used to explain human body motion control. The integrated visual-vestibular signals ($\mathbf{v}$, ω, $\mathbf{g}$) represent the sensed state $\mathbf{u_s}$. A simple feedback control system would compare the sensed state $\mathbf{u_s}$ to a desired state $\mathbf{u_d}$ (see subsection 4-1-2 for an example). Due to high neural delays and imperfect sensors, an approach to model body motion control in this way would not work.

To overcome these problems and correctly model human body motion control, the observer theory is used. Bos et al. (2008) created a global overview of a body motion control model using the observer theory, as depicted in Figure 3-4. Here a desired state $\mathbf{u_d}$ is fed through a preparatory phase ($\mathbf{P}$) and controller ($\mathbf{C}$) that generates motor commands $\mathbf{m}$. Together with the external perturbations $\mathbf{u_e}$, the motor commands $\mathbf{m}$ form the input to the body ($\mathbf{B}$). These commands produce the actual state $\mathbf{u}$ of our body, which are sensed by the motion sensitive sensors producing the sensed state $\mathbf{u_s}$. These sensor dynamics are shown in the gray block ($SO-Sub$) and could include a motion perception model as shown in Figure 3-3. It is thought that the CNS is expecting certain sensory feedback in self-motion, which is represented as the expected sensed state $\mathbf{u'_s}$. This expectation is produced by an internal model ($SO - Sub' + \mathbf{B'}$), which is a copy of the primary sensor and body dynamics. This internal model is created and updated by previous experiences. It takes as input the efference copy $\mathbf{m'}$ which is a copy of the original motor commands $\mathbf{m}$ send to our muscles. The main idea behind the observer model theory is that the desired state $\mathbf{u_d}$ is compared to an expected state $\mathbf{u'}$, instead of the sensed state $\mathbf{u_s}$. This expected state $\mathbf{u'}$ is the output of the internal body model $\mathbf{B'}$. Hence, humans control their body with their thoughts instead of their senses. The expected state $\mathbf{u'}$ is used for a lot of other processes, like Eye Movement (EM), as well.

[3] The idiotropic vector is related to the body axis of an individual. It has a small influence on the final perceived subjective vertical (Mittelstaedt, 1983).

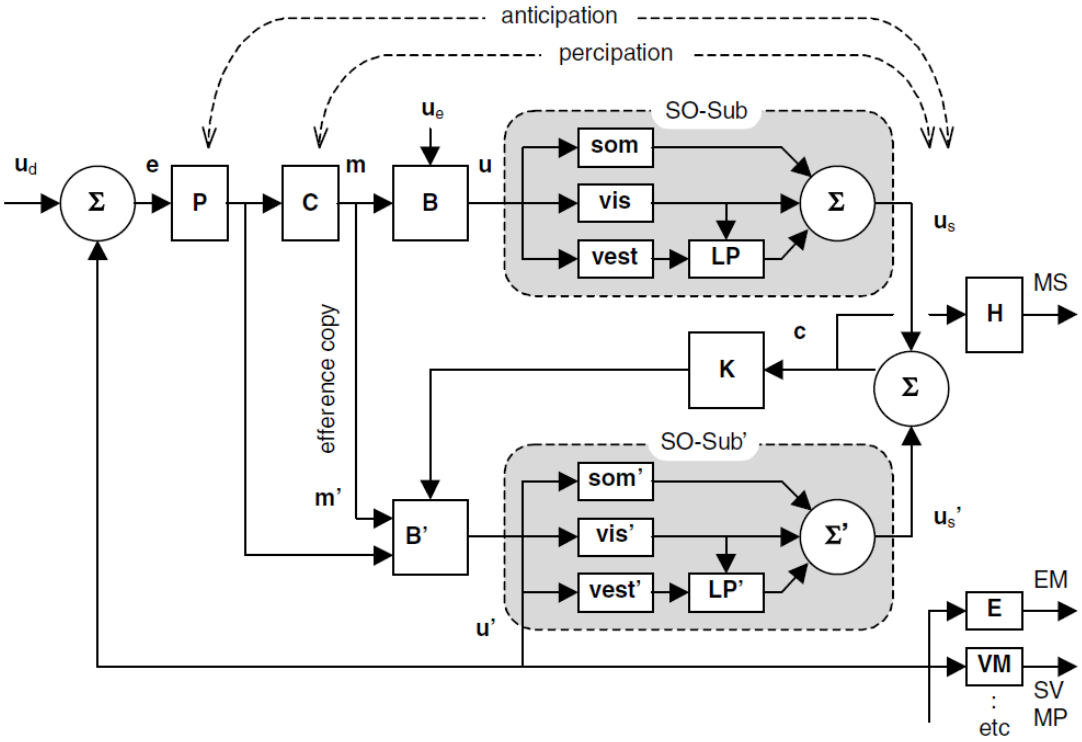

Figure 3-4: Global overview of a body motion control model that adheres to the observer model theory (Bos et al., 2008)

Ideally the sensed state $\mathbf{u_s}$ and the expected sensed state $\mathbf{u'_s}$ are equal. Without external perturbations $\mathbf{u_e}$, the output of the primary sensor and body dynamics is equal to the output of the internal model. However, with external perturbations present, a conflict $\mathbf{c}$ arises between the two aforementioned signals. This conflict is weighted by $\mathbf{K}$ and used by the internal model to drive the conflict $\mathbf{c}$ towards zero.

The observer model theory is key to explain the occurrence of MS in vehicle passengers. It is assumed that the magnitude and duration of the conflict signal $\mathbf{c}$ is related to MS. This signal is a mathematical representation of the sensory conflict theory as explained in Section 2-2. For self-propelled motion the conflict signal will remain relatively low as the input to the primary sensor and body dynamics ($SO - Sub$) is almost equal to the input of the internal model ($SO - Sub'$). Here, only the disturbance signal $\mathbf{u_e}$ slightly changes the primary input. However, during passive motion, i.e., being driven around in an autonomous car, the external force $\mathbf{u_e}$ dominates the input to the primary dynamics as there is no desired state. In this condition the passenger can barely anticipate upcoming motions, as explained in Section 2-3. Since the passenger is not controlling the vehicle theirself (no active muscle commands $\mathbf{m}$), no efference copy is created. Without an efference copy the internal model cannot predict upcoming sensed motion signals $\mathbf{u'_s}$, creating substantial conflicts with the actual sensed motion signals $\mathbf{u_s}$, hence, increasing the occurence of MS.

Anticipation of upcomming motions of autonomous vehicle passengers can still be achieved by letting the passengers know how the car is going to move in the near future. Several solutions

are available, such as a clear view of the road ahead or MS mitigation systems like a display indicating upcoming motions. In this way the antipation path can be restored without the need for an efference copy.

3-2 Visual Information in Motion Sickness

Previously, visual influence on motion perception has been discussed. This is important to understand the underlying mechanisms of MS. The exact relation between inertial or visual motion and MS will be discussed in Chapter 4. This section focuses on a number of experiments found in literature that investigate the visual influence on MS.

Griffin and Butler have performed a number of experiments investigating the visual effect on MS (Butler & Griffin, 2006, 2009; Griffin & Newman, 2004). Griffin and Newman (2004) looked into the effects of restricted views of the environment, different seating positions, and a video view of the road ahead while subjects were driven around in a real car. Results of the effect of different viewing conditions on mean illness ratings are shown in Figure 3-5. Condition 1 included the normal viewing condition, i.e., a passenger seated in the central rear seat of the car with clear forward and side views. In condition 2 the passengers wore a blindfold which eliminates any visual information. Condition 3 obstructed all windows (forward an side windows) with panels, such that only the interior of the car was visible. Conditions 4 and 5 were similar to condition 3, except that the side windows were not obstructed in condition 4, while condition 5 provided a small gap in the forward panel to provide a narrow forward view. Griffin and Newman (2004) found equal amounts of mean illness ratings for blindfolded subjects and restricted forward views (with or without blinded side windows). Providing a wide or narrow forward view reduced subject illness ratings, indicating that a view of the road ahead is important for diminishing MS symptoms. This is an interesting result since passengers of autonomous cars are often oriented backwards to have a conversation with the backseat passengers (Diels & Bos, 2016). This scenario is therefore not realistic, since it will increase MS occurrence and severity. Different seating position and provision of a video of the environment did not have a significant effect on sickness ratings. The distance between the display and the subjects could be an explanation for the latter. Moreover, the video did not show the road exactly as it would have been seen directly out of the window, due to the lateral head movements caused by the vehicle motions.

Butler and Griffin (2006) performed a MS experiment in a motion-based simulator. They subjected their participants to for-and-aft oscillatory movements while changing the visual conditions. Results of this experiment are shown in Figure 3-6. The internal condition only provided a view of the simulator cabin to the participants. The three external conditions provided a narrow forward external view of simple black shapes on a white background (condition 2), six horizontal lines (condition 3), and the laboratory (condition 4). The latter condition was also viewed through a larger window. The collimated condition showed the same simple shapes as condition 2 through a collimated lens to the participants, which eliminated image movement due to translational movements of the head. In the blindfolded condition subjects wore a blindfold and were instructed to close their eyes. A stationary condition was added to serve as a baseline condition. The authors concluded that there is no significant difference between all internal, external or collimated visual conditions. It must be mentioned that they

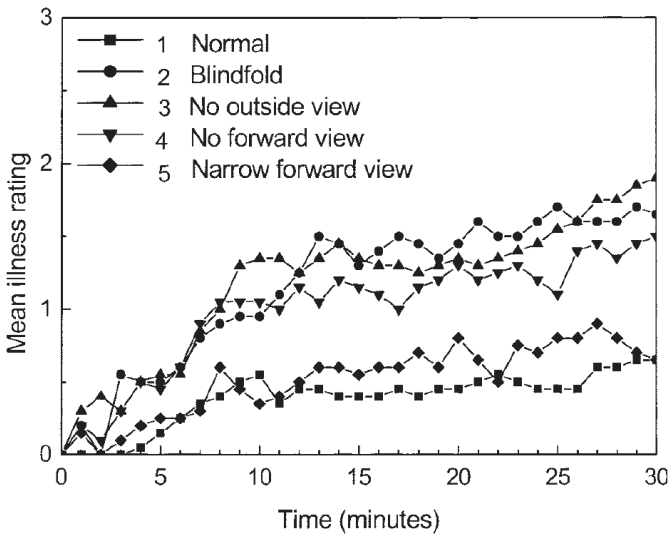

Figure 3-5: Mean illness ratings for different viewing conditions in a moving car, adopted from Griffin and Newman (2004)

did not include a condition where the peripheral field motion was congruent with the physical motion.

A follow-up experiment (Butler & Griffin, 2009) included a combination of for-and-aft oscillatory motion with pitch oscillations (results shown in Figure 3-7. This experiment included three different visual conditions; an internal condition that only shows the simulator interior, a blindfolded condition where participants closed their eyes, and an external condition that showed the laboratory through a window. Butler and Griffin (2009) also analyzed out-of-phase and in-phase conditions of the translational and rotational motions. Unlike the previous experiment, these results did show that there was significantly less sickness with an external view, compared to the internal or blindfolded viewing conditions. The authors suggested that the presence of pitch motion is necessary for the visual field to have an effect on MS. Interestingly, the phase affected the blindfolded condition the most. The out-of-phase condition (forward motion is accompanied by backward pitch and vice versa) produced higher illness ratings. A possible explanation could be that the out-of-phase condition is experienced as unnatural motion stimuli. Wada et al. (2018) found similar results when car passengers tilted their heads towards the direction of the GIA during slalom driving. This conditions corresponds to the in-phase condition of the experiment by Butler and Griffin (2009). Again, the latter experiment only used a narrow forward view and did not include any visual motion in the peripheral view. These experiments show that the visual field can increase or decrease the occurrence of MS.

While Griffin and Newman (2004) showed that peripheral view (side windows only) did not reduce MS compared to no outside view, Kuiper et al. (2018) did show that the amount of peripheral view has an influence on illness. Their experiment participants were given a visual task at two different display positions, either at eye height in front of the windscreen or at the height of the glove compartment. The eye-height condition allowed more peripheral visual field and reduced the MISC-ratings significantly during slalom driving. Jones et al. (2019) did a similar experiment. Passengers were driven along a test track with or without a reading

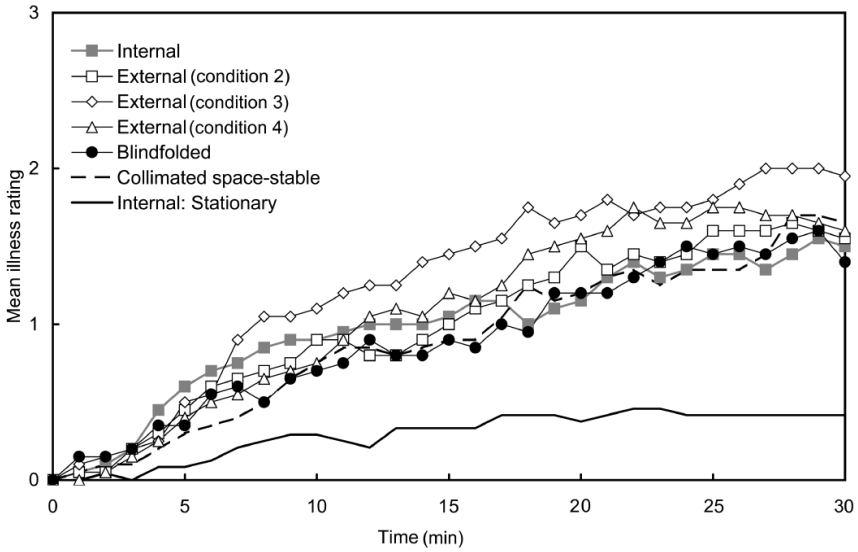

Figure 3-6: Mean illness ratings for different viewing conditions in for-and-aft oscillation, adopted from Butler and Griffin (2006)

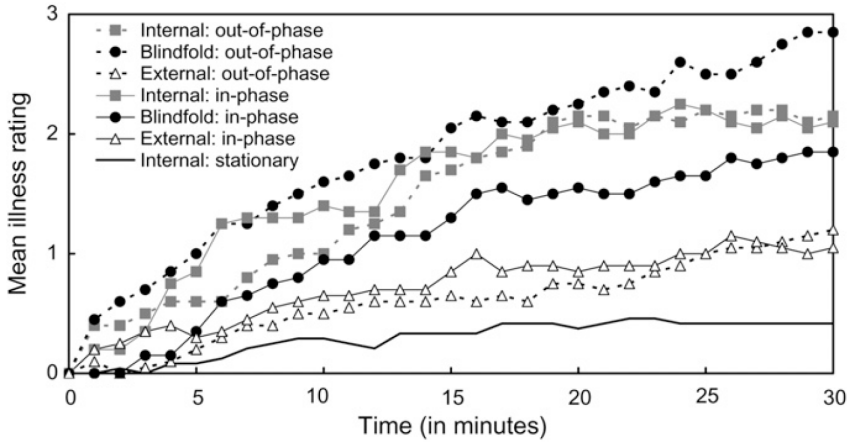

Figure 3-7: Mean illness ratings for different viewing conditions in combined for-and-aft and pitch oscillations, adopted from Butler and Griffin (2009)

task (tablet located on the subjects' lap). For younger participants (age < 60), the no-task condition (no restriction of the outside view) significantly reduced MS ratings.

The experiments mentioned above do indicate that the key to reducing MS with visual-vestibular interactions is having a completely unobstructed view of the outside world. However, with restricted central vision (e.g., working on a laptop, reading a book), motion cues can still be seen in the peripheral field, which plays a key factor in self-motion perception (Kuiper et al., 2018). It must be noted that vection, instead of optical flow, is assumed to play an important role in visual-vestibular MS. But according to Bos et al. (2008) the exact relation of linear vection and MS is still unclear.

3-3 Visually Induced Motion Sickness

VIMS is a sensation that is similar to that of regular MS. The difference is that there usually is no physical motion present and that the visual stimulation is the dominant cause for MS (Keshavarz et al., 2015). VIMS can occur when wearing a virtual reality headset or in fixed-based simulators, for example. This section will shortly discuss the main differences between VIMS and MS, theoretical explanations, and the role of vection in VIMS.

VIMS and MS are similar, but there are subtle differences. For example, symptoms of VIMS and MS are comparable, however, disorientation and optokinetic disturbances are more present during VIMS (Keshavarz et al., 2015). Theories explained in Section 2-2 are also applicable to VIMS. Similar to MS, the most dominant theory being used to describe VIMS is the sensory mismatch theory. A visually induced self-motion perception would drive the CNS to also expect sensory signals from the vestibular and somatosensory systems. If the expected values of these signals are different then the actually sensed signals, people will experience VIMS.

Vection plays an important role in explaining VIMS, however, the exact relation is not clear in the literature. People can experience vection in the absence of VIMS, but the other way around, experiencing VIMS without vection, might not be true. Most experiments found in litterature only focus on either VIMS or vection, but not both. An overview of experiments that do study both can be found in Keshavarz et al. (2015). These experiments did confirm that vection is almost always present during VIMS, however vection alone is not sufficient enough for explaining VIMS. Bonato, Bubka, Palmisano, Phillip, and Moreno (2008) investigated the effect of vection strength and changes in vection speed on VIMS. They found that vection strength had no influence on VIMS, while changes in vection did. These results could be explained using the sensory mismatch theory. During constant vection no accelerations are present, hence expected signals from the vestibular system are zero. However, with changes in vection speed, acceleration information from the vestibular system is expected while this is not present. Therefore, changes in vection speed increases the severity of VIMS.

3-4 Conclusions

This chapter included a brief discussion on what is currently known in the literature about the role of visual information in motion perception and MS. Vision is one of the motion-sensitive systems, which together with the vestibular and somatosensory systems are responsible for motion perception. Signals from all systems are integrated into one perceived motion signal.

Visual information about self-motion or self-orientation can be split up into three categories: visual translation, visual rotation and visual vertical. Translation and rotation depend on visual flow patterns while the vertical is determined by visual field patters. The CNS integrates these visual motion signal with vestibular motion signals. Bos et al. (2008) created a mathematical model of this integration process. This motion perception model transforms actual head motion signals to perceived motion signals. Other factors, such as FoV, image size, and depth cues, can influence visual motion perception as well. It is important to keep these factors in mind when designing an experiment. Additionally, the motion perception model design by Bos et al. (2008) can be used in an observer model. The observer model theory is key to explaining the occurrence of MS.

Most conducted MS experiments focused on motion only and did not include visual information. The influence of inertial motion on MS is well understood, but the influence of the visual system is still unknown. The few MS experiments in literature that did include both inertial and visual motions did not find a clear relation between visual motion and MS. Butler and Griffin (2006) found no significant influence of changing the visual scene on MS. However, it is remarkable that they only used a small forward view in their experiment, while it is known that a wide FoV is important for visual motion perception (Correia Grácio et al., 2014). The research presented in this report will contribute to finding experimental data on the influence of a wide FoV on MS, since this is lacking in the literature.

While experiments including inertial and visual motion are limited, high amounts of experiments including pure visual motion exist. MS provoked by visual motion is often called VIMS and is highly researched, since this is a problem for virtual reality headsets. Although MS and VIMS are different concepts, VIMS research is still interesting for the current research. Research showed that VIMS rarely happens without vection. The role of vection in regular MS is still unclear, therefore more research in this topic is needed.

Chapter 4

Motion Sickness and Motion Perception Modelling

Over the last decades, many models have been developed for self-motion perception and MS. These mathematical models try to capture how the human CNS integrates signals from different sensory systems into perceived self-motion or self-orientation and how combinations of signals can provoke MS, respectively. For the current study, the focus is on the visual and vestibular systems. MS and motion perception models including visual-vestibular interactions are discussed in this chapter. Section 4-1 presents the MS prediction model of Wada et al. (2020). The visual-vestibular motion perception model by Telban and Cardullo (2005) is discussed in Section 4-2. Jalgaonkar et al. (2021) integrated the two aforementioned models, which are elaborated on in Section 4-3. Lastly, Section 4-4 discusses the approach taken by Braccesi and Cianetti (2011) for including visual translational information in a MS prediction model.

4-1 6DOF-SVC Model

Many efforts have been made to capture the development of MS in a mathematical model. Wada et al. (2020) have developed a state-of-the-art computational model that describes MS development of humans subjected to accelerations and rotations. In this study the model is used for autonomous car passengers, but the model is also applicable for other applications.

Figure 4-1 depicts one of the latest versions of the 6Degrees of Freedom (DOF)-SVC model, which already includes visual rotation as an input. Inputs to the model are the specific force $\boldsymbol{f}$, inertial accelerations $\boldsymbol{a}$, and angular velocities of the head $\boldsymbol{\omega}$, combined with the visual angular velocities $\boldsymbol{\omega_{vis}}$. Since the model is dealing with the movement of a passenger's head, a head-fixed right-handed reference frame is used. It is assumed that the positive x-axis is pointing out of the nose, the positive y-axis is pointing out of the left ear and the positive z-axis is pointing out of the head orthogonal to the other axes, see Figure 4-2. All parameters used within this model are shown in Table 4-1. More details are given in the following sections.

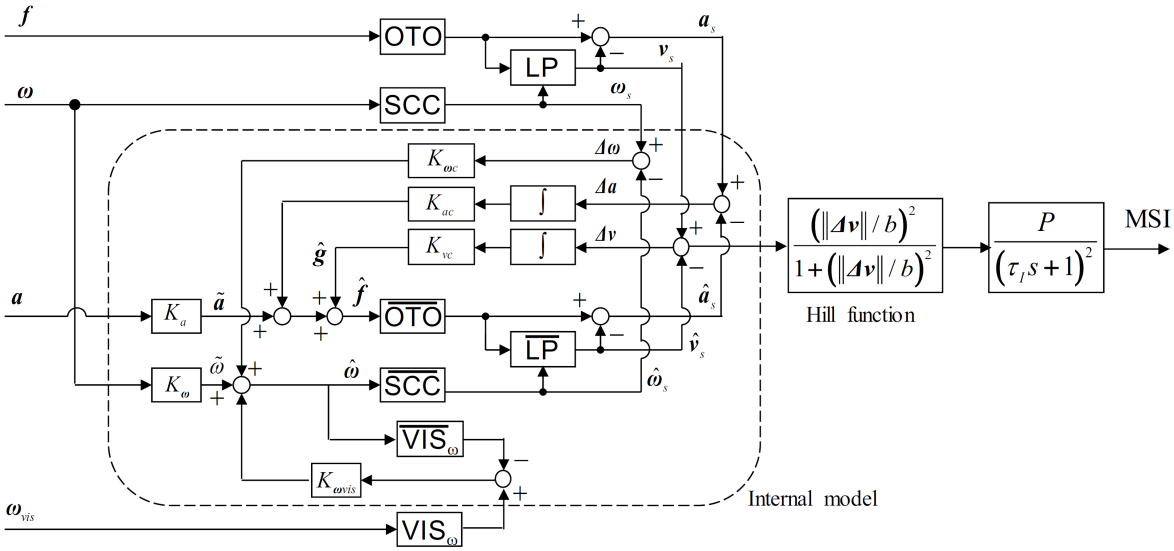

Figure 4-1: 6DOF-SVC MS prediction model (Wada et al., 2020)

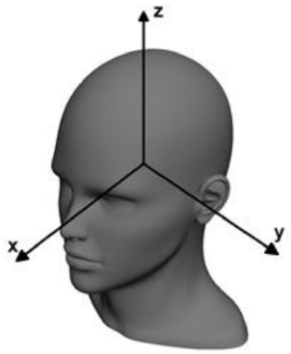

Figure 4-2: Visual-vestibular coordinate frame (Jalgaonkar et al., 2021)

Table 4-1: 6DOF-SVC model parameters (Wada et al., 2020)

Parameter	K_ω [-]	K_a [-]	$K_{\omega c}$ [-]	K_{vc} [-]	K_{ac} [-]	$K_{\omega vis}$ [-] [1]	P [%]	τ_I [s]	b [m/s^2]	τ_d [s]	τ_{lp} [s]
Value	0.1	0.1	10.0	5.0	1.0	10	85	720	0.5	7.0	5.0

4-1-1 Sensory Dynamics

The sensory dynamics consist of the OTO block, the SCC block, the LP block, and the VIS_ω block. These parts of the 6DOF-SVC model represent the dynamics of the human sensors, which translate external motion into internally sensed motion signals. Each block is elaborated on in more detail in the following.

Block OTO

The OTO block (see Figure 4-1) captures the otolith dynamics of the vestibular system located in the inner ear. Since the otoliths cannot feel a difference between the inertial acceleration a and the gravitational acceleration g, the input to the OTO block is the specific force f, or GIA. The specific force is defined as: $f := a + g$. The specific force is a three-dimensional vector, which is translated into a "sensed specific force" f_s by the OTO block. This signal represents the acceleration felt by the otolith organs. In this model, the otolith dynamics are represented by a unity matrix, since the otoliths are capable of sensing low-frequency accelerations almost perfectly (Merfeld et al., 1993). Experiments from McCauley, Royal, Wylie, O'Hanlon, and Mackie (1976) indicate that MS only occurs at low-frequency motion, peaking at 0.16 Hz.

Block SCC

The dynamics of the SCC used in the SCC block are given below in Equation 4-1. These dynamics are based on Merfeld (1995), and can be represented by a high-pass filter (Merfeld et al., 1993).

$$\boldsymbol{\omega}_s^i = \frac{\tau_d \tau_a s^2}{(\tau_d s + 1)(\tau_a s + 1)} \boldsymbol{\omega}^i \tag{4-1}$$

The equation above represents the transfer function for each of the SCC, therefore, the superscript i corresponds to the x-, y-, and z-axes. The dominant decay time constant and the adaptation time constant of the SCC are given by τ_d and τ_a, respectively.[2] The values used are $\tau_d = 7.0$ s and $\tau_a = 190$ s determined by Haslwanter, Jaeger, Mayr, and Fetter (2000), who carried out experiments on humans instead of Merfeld (1995), who carried out experiments on monkeys. The dominant decay time constant ensures that the afferent response to a step input decreases exponentially, as defined by Merfeld et al. (1993). This is important since the SCC cannot measure constant rotational velocities, but only velocity changes. Merfeld found an additional reversal response in the semicircular canals when subjected to eccentric rotations. This effect is modeled by the adaptation time constant.

[1] The value of $K_{\omega vis}$ is not set at 10, its value is determined by the amount of visual information available to the passenger. For example, a value of 10 is chosen when there is an unobstructed view of the outside world, whereas a value of 3 is used when reading a book.

[2] The dynamics of the semicircular canals differ between different versions of the 6DOF-SVC model. Kamiji et al. (2007); Wada, Kamij, et al. (2015) use the dynamics explained in Section 4-1-1. However, later versions of the model (Liu et al., 2022; Wada et al., 2020) only use the dominant decay time constant τ_d and omit the adaptation time constant τ_a. Therefore, the transfer function becomes: $\omega_s^i = \frac{\tau_d s}{\tau_d s + 1} \omega^i$. Since the adaptation time constant τ_a barely had an effect on the subjective vertical, it was left out.

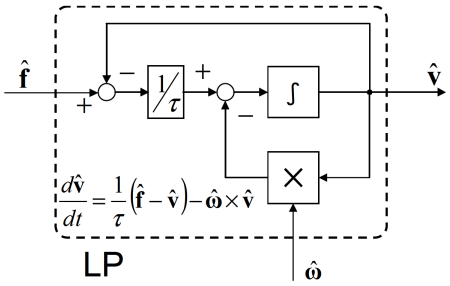

Figure 4-3: Block diagram representation of Equation 4-2 (Kamiji et al., 2007)

The input into the SCC block is the three-dimensional angular velocity vector ω, which is transformed by Equation 4-1 to the sensed angular velocity vector ω_s, also called the semicircular canal afference.

Block LP

As explained in Section 4-1-1, the otoliths cannot differentiate between inertial acceleration and gravitational acceleration. However, the CNS is still able to distinguish between accelerations due to motion and those due to gravity. Therefore, gravitational acceleration must be filtered out of the specific force f. This GIA resolution problem can be solved by low-pass filtering of the otolith afference. As the head is rotated, the direction of the gravitational acceleration changes, hence angular motion as measured by the semicircular canals needs to be taken into account as well (Bos & Bles, 2002). Equation 4-2 incorporates these two effects.

$$\frac{d\mathbf{v_s}}{dt} = \frac{1}{\tau}(\mathbf{f_s} - \mathbf{v_s}) - \boldsymbol{\omega}_s \times \mathbf{v_s} \tag{4-2}$$

Bos and Bles (2002) refer to the above equation as the "Mayne equation", since Mayne (1974) first described this phenomenon mathematically. The first term on the right-hand side of Equation 4-2 represents the low-pass filtering of the otolith afferents. The second term estimates the change of gravity due to rotations of the head. Here, $\mathbf{v_s}$ corresponds to the sensed subjective vertical, $\mathbf{f_s}$ represents the sensed specific force from the otoliths, and $\boldsymbol{\omega}_s$ is the angular velocity sensed by the semicircular canals. The LP block in Figure 4-1 includes Equation 4-2 as a block diagram, that is depicted in Figure 4-3. The LP block has the sensed specific force $\mathbf{f_s}$ and sensed angular velocity $\boldsymbol{\omega}_s$ as inputs and calculates the sensed subjective vertical $\mathbf{v_s}$. The sensed subjective vertical $\mathbf{v_s}$ is subtracted from the sensed specific force $\mathbf{f_s}$ (Figure 4-1) to also create an estimate of the sensed intertial acceleration $\mathbf{a_s}$.

Block VIS

Wada et al. (2020) added visual angular velocity as input to the 6DOF-SVC model. This was the first effort to add visual sensory information to the model. The VIS$_\omega$ block can be found below the internal model in Figure 4-1 and represents the visual sensory dynamics related to the angular velocity. Therefore, it translates perceived visual angular velocity $\boldsymbol{\omega}_{vis}$ retrieved from optical flow patters, to sensed visual angular velocity $\boldsymbol{\omega}_{vis,s}$. In Wada et al. (2020) these

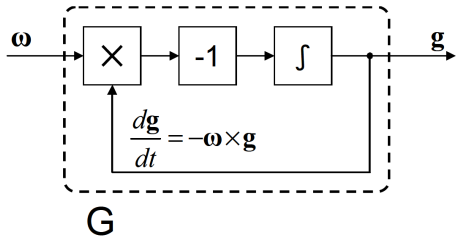

Figure 4-4: Equation block used for determining the direction of the gravity component (Kamiji et al., 2007)

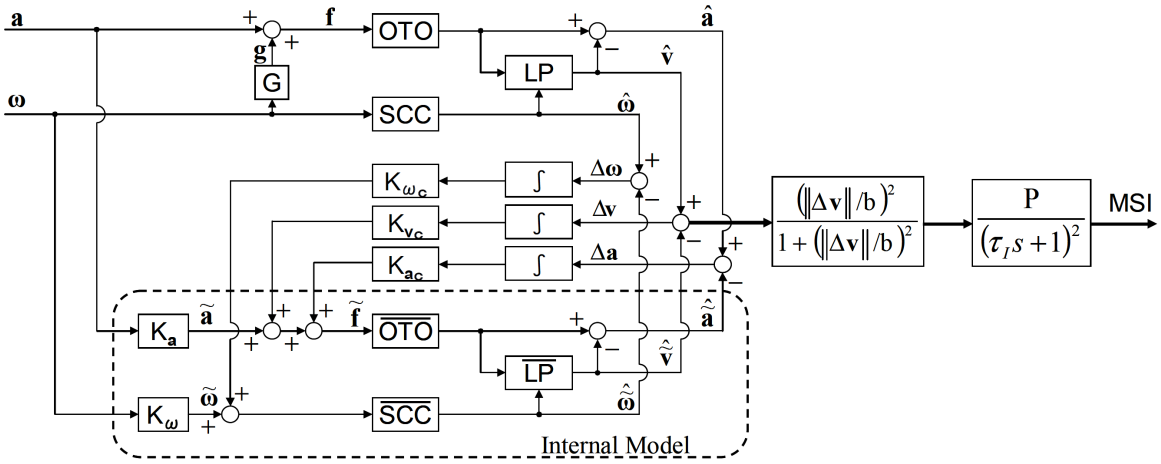

Figure 4-5: Earlier version of the 6DOF-SVC MS prediction model (Kamiji et al., 2007)

dynamics are represented as a unity matrix, since it is assumed that the visual system is able to accurately estimate the visual angular velocity.

Block G

Earlier versions of the 6DOF-SVC model used an extra module to calculate the gravity vector in the head reference frame. This block is used to transform the inertial acceleration $\boldsymbol{a}$ into a specific force $\boldsymbol{f}$ by adding the calculated gravity component $\boldsymbol{g}$, see Figure 4-4. This simplifies the inputs to the original 6DOF-SVC model, since the specific force $\boldsymbol{f}$ can now be left out. Gravity needs to be constant to be able to use the equation in 4-4. This block is located before the sensor dynamic blocks OTO and SCC (see Figure 4-5).

4-1-2 Internal Model

For controlling body motion, a simple single-loop feedback control system is not enough (see Figure 4-6 for an example). In this model, a desired body state $\mathbf{u_d}$ is compared to a sensed body state $\mathbf{u_s}$. In order for this model to work for body motion control, the sensed body state $\mathbf{u_s}$ should be reliable and have negligible delays. However, human motion sensors (otoliths

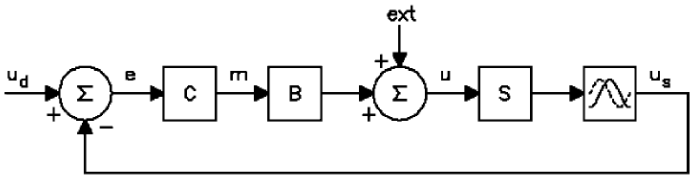

Figure 4-6: A single loop feedback control system to control body motion (Bos & Bles, 2002)

and semicircular canals) cannot accurately capture all types of motions. Moreover, the CNS has internal neural delays which cannot be neglected.

A solution to overcome these problems can be found by using an internal model of the sensory systems parallel to the main sensory systems (Bos & Bles, 2002). This solution is similar to what has been used in the model by Wada et al. (2020) and is also referred to as the observer model theory, see subsection 3-1-4. The internal model is created and updated by previous experiences. In Figure 4-1 the internal model is represented by the dashed lines. Instead of comparing the desired body state $\mathbf{u_d}$ with a sensed body state $\mathbf{u_s}$, the desired body state $\mathbf{u_d}$ is now compared to an expected body state $\hat{\mathbf{u}}$. The latter is calculated by using a copy of the motor commands send to our muscles, also referred to as the efference copy. An internal model of the body dynamics then calculates the expected motion signals $\hat{\mathbf{u}}$. In optimal performance (i.e., self-propelled motion) $\mathbf{u_d}$ and $\hat{\mathbf{u}}$ are equal, since all imperfections in human motion sensors are also captured in the internal model. But passive motion cause these two signals to be different, which causes MS.

The upcoming sections discuss how this internal model is incorporated in the 6DOF-SVC model, and how this internal model is updated.

Internal Sensory Dynamics

It is hypothesized that the CNS uses information about body and sensor dynamics to develop an internal model that produces expected sensory signals (Bos, MacKinnon, & Patterson, 2005). The inputs to the internal model are similar to those of the primary sensor dynamics, which include body accelerations $\mathbf{a}$ and rotational velocities $\boldsymbol{\omega}$. These two signals are scaled down by gains K_a and K_ω, respectively, to the internally estimated body motions $\tilde{\mathbf{a}}$ and $\tilde{\boldsymbol{\omega}}$. The CNS estimates body dynamics from somatic sensors and a copy of the motor commands. Therefore, the gains K_a and K_ω represent the accuracy of self-motion estimation. When a human is controlling their own motion (e.g., walking, running, cycling) these gains are close to one. While being moved due to external forces (e.g., driving in automated vehicles) these gains will be much lower (around 0.1) (Kamiji et al., 2007).

The internally estimated head motions $\tilde{\mathbf{a}}$ and $\tilde{\boldsymbol{\omega}}$ are part of the input to the internal sensory dynamics. Internal sensory dynamics consists of the $\overline{OTO}$ block, the $\overline{SCC}$ block, the $\overline{LP}$ block and the $\overline{VIS_\omega}$ block that are exact copies of the original sensor dynamics. The output of the internal sensory dynamics are the expected sensed motion signals for acceleration $\hat{\boldsymbol{a}}_{\boldsymbol{s}}$, subjective vertical $\hat{\boldsymbol{v}}_{\boldsymbol{s}}$, and rotational velocity $\hat{\boldsymbol{\omega}}_{\boldsymbol{s}}$.

The $\overline{VIS_\omega}$ block uses the expected angular velocity signal $\hat{\boldsymbol{\omega}}$ as input and calculates the expected sensed angular velocity signal $\hat{\boldsymbol{\omega}}_{\boldsymbol{vis,s}}$.

Sensory Feedback Loops

Outputs of the internal model, the expected sensed motion signals $\hat{\boldsymbol{a}}_{\boldsymbol{s}}$, $\hat{\boldsymbol{v}}_{\boldsymbol{s}}$, and $\hat{\boldsymbol{\omega}}_{\boldsymbol{s}}$, are compared to the outputs of the original sensor dynamics, the real sensory afferents $\boldsymbol{a}_{\boldsymbol{s}}$, $\boldsymbol{v}_{\boldsymbol{s}}$, and $\boldsymbol{\omega}_{\boldsymbol{s}}$, respectively. This results in three conflict signals, which are the differences between the expected sensory signals and the actual sensory signals. These conflict signals consist of the angular velocity conflict signal $\boldsymbol{\Delta\omega}$, the inertial acceleration conflict signal $\boldsymbol{\Delta a}$ and the subjective vertical conflict signal $\boldsymbol{\Delta v}$. These errors are used to drive the expected motion signals $\hat{\boldsymbol{a}}$, $\hat{\boldsymbol{f}}$, $\hat{\boldsymbol{v}}$, $\hat{\boldsymbol{\omega}}$ towards their true values $\boldsymbol{a}$, $\boldsymbol{f}$, $\boldsymbol{v}$, $\boldsymbol{\omega}$ (Wada et al., 2020). In this feedback process, the conflict signals are scaled by $K_{\omega c}$, K_{ac}, and K_{vc}, respectively. Moreover, the inertial acceleration conflict $\boldsymbol{\Delta a}$ and the subjective vertical conflict $\boldsymbol{\Delta v}$ are first integrated, so the feedback "gain" increases over time. This results in some "learning" capacity and is also needed for a stable model, as concluded by Bos and Bles (2002). The integration for angular velocity is omitted to allow the angular velocity conflict signal to be in accordance with the results of Khalid, Turan, Bos, and Incecik (2011).[3]

The paper by Wada et al. (2020) introduces the visual angular velocity as input to the 6DOF-SVC model. An extra sensory feedback loop is created at the bottom of Figure 4-1. The actual sensed visual angular velocity $\boldsymbol{\omega_{vis,s}}$ is compared to the expected sensed visual angular velocity $\hat{\boldsymbol{\omega}}_{\boldsymbol{vis,s}}$ to calculate the conflict signal $\boldsymbol{\Delta\omega_{vis}}$. How much of this information is used to correct the expected angular velocity depends on the gain $K_{\omega vis}$. The value of this gain is determined by the visual environment. Low values (0-3) are used when a subject has their eyes closed or is looking down when reading a book, for example (Braccesi & Cianetti, 2011). A value of 10 is used when a subject uses external visual information that is in accordance with vestibular information (e.g., looking outside), based on Newman (2009).

4-1-3 Motion Sickness Calculation

The 6DOF-SVC model depicted in Figure 4-1 uses the subjective vertical conflict signal $\boldsymbol{\Delta v}$ to calculate MS. Bles et al. (1998) concluded that only one type of conflict is sufficient to describe MS. They found that people only get sick when the gravity component is incorrectly anticipated. The subjective vertical conflict signal $\boldsymbol{\Delta v}$ can range from high positive to negative values, while MSI only ranges from 0% (no one vomits) to 100% (every subject vomits), as seen in Bos and Bles (1998). For this reason, a hill function is used to normalize $\boldsymbol{\Delta v}$ to a value between 0 and 1 (see Figure 4-1). The value of b can be changed so that the model best fits the experimental data (Bos & Bles, 1998).

From experiments it is known that MSI accumulates over time and reaches a maximum asymptotically (McCauley et al., 1976). Furthermore, when the subjective vertical conflict is ended, the MSI values gradually go to zero again. To accommodate for these phenomena, a leaky integrator is used to calculate MSI from the output of the hill function (see Figure 4-1). The value of P determines the height of the asymptotic value. The time constant of the leaky-integrator τ_I is set at twelve minutes, to corectly model the slow build of MS.

[3]Earlier versions of the 6DOF-SVC model (Kamiji et al., 2007; Wada et al., 2015) did include an integration in the angular velocity conflict feedback loop. However, it is left out with the addition of the visual angular velocity.

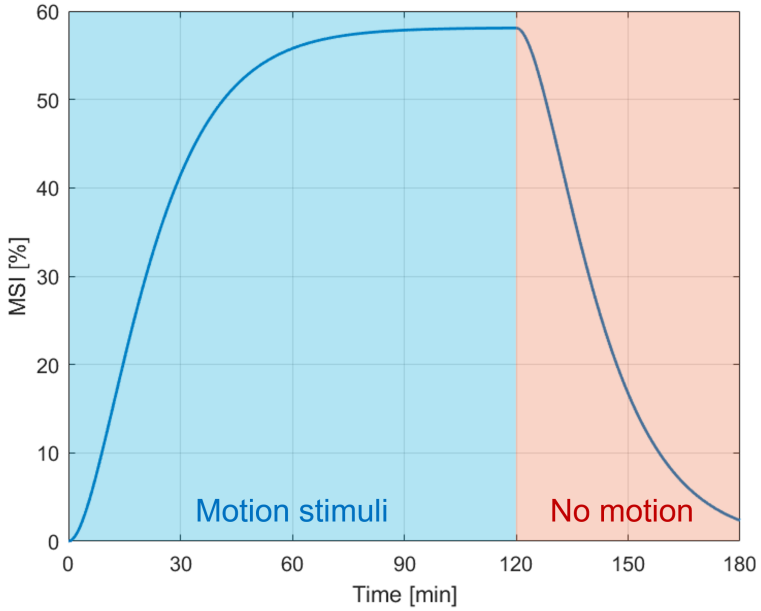

Figure 4-7: Example of a typical MSI profile simulated by the 6DOF-SVC model (Kamiji et al., 2007)

4-1-4 Model Simulations

The 6DOF-SVC model by Kamiji et al. (2007) calculates MSI values given a motion stimulus over time. A typical simulated MSI profile can be seen in Figure 4-7, which is the result of a two-hour sinusoidal acceleration input on the x-axis. This signal has an acceleration amplitude of 10 m/s^2 and a frequency of 0.16 Hz. The MSI gradually rises in the first 60 minutes of the motion stimulus, which is due to the slow time constant of the leaky integrator. A relatively high maximum of 58% is reached, since the motion is acting at the most provocative frequency. After 120 minutes the motion stimulus was stopped, resulting in the MSI gradually going down again. This effect is also caused by the leaky integrator.

The 6DOF-SVC model could also be used to predict MSI values at different frequencies and amplitudes. Figure 4-8a contains the final MSI values after two-hour exposure to a sinusoidal signal with the given frequency and amplitude. Figure 4-8b shows a plotted fit through experimental data from McCauley et al. (1976). The shape of both curves are very similar, both having increasing MSI values with increasing amplitudes. A peak appears around 0.16 Hz in both graphs. The location of this peak is mainly depended on the time constant τ_{lp} of the low-pass filter on the otolith afferents (see Table 4-1). The predicted MSI values are smaller than the actual MSI values found in the experimental data. Values from Table 4-1 were used to create the simulation results, but can be altered to better fit the experimental data.

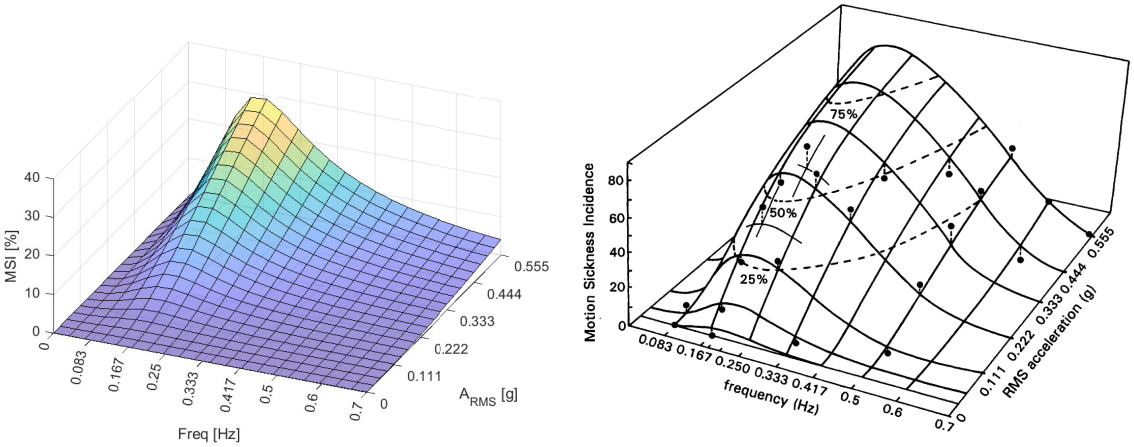

(a) 6DOF-SVC simulation data with varying frequencies and amplitudes.

(b) Fit through experimental MS data with varying frequencies and amplitudes (McCauley et al., 1976)

Figure 4-8: 6DOF-SVC simulation data compared with experimental data from McCauley et al. (1976)

4-1-5 Visual Vertical

Liu et al. (2022) proposed to add the visually perceived vertical to the conventional 6DOF-SVC model by Kamiji et al. (2007). The proposed model is shown in Figure 4-9.[4] Additional blocks and lines are shown in red. Humans use the visual system to determine the visual vertical. This is done by looking for known horizontal or vertical objects (e.g., buildings or the horizon) (Clark, Newman, Karmali, Oman, & Merfeld, 2019).

A new input signal $\boldsymbol{I}$ is added, which consists of color images. The Visually Perceived Vertical block shown in Figure 4-9 extracts gradient angles from the images and converts them to the direction of the visual vertical. The direction is given as a three-dimensional vector, with only nonzero values in the x- and y-directions. The total magnitude of this signal is normalized to 9.81 m/s^2.[5] This signal is then passed to the visual system dynamics, represented by the VIS_g block. For now, these dynamics are represented by a unity matrix. The internally estimated gravity vector $\hat{\boldsymbol{g}}$ is a combination of integrated and scaled conflict errors of the vestibular vertical $\boldsymbol{\Delta v_s}$ and the visual vertical $\boldsymbol{\Delta g_{vis}}$. The dynamics in $\overline{VIS}_g$ discard the z-component of $\hat{\boldsymbol{g}}$, since it is compared to the two-dimensional visual gravity vector $\boldsymbol{g_{vis}}$. Furthermore, it normalizes the magnitude to 9.81 m/s^2 again to create the expected visual vertical signal $\hat{\boldsymbol{g}}_{\boldsymbol{vis}}$. Comparing the expected visual vertical signal to the sensed visual vertical signal results in the conflict signal $\boldsymbol{\Delta g_{vis}}$. Similarly to the other sensory feedback loops, this signal was integrated and scaled by K_{gvis}, and fed back to the internally estimated gravity vector $\hat{\boldsymbol{g}}$ to drive its value to the true value of $\boldsymbol{g}$. Equation 4-3 represents the calculation of $\hat{\boldsymbol{g}}$ in the equation form.

[4]The visual vertical model shown in Figure 4-9 does not include visual angular velocity information shown in the bottom part of Figure 4-1. Integration of both models is still part of the authors' future work.

[5]In this model the sensed visual vertical is represented as the visual gravity vector $\boldsymbol{g_{vis}}$, hence the magnitude of the signal should match the gravitational constant of 9.81 m/s^2.

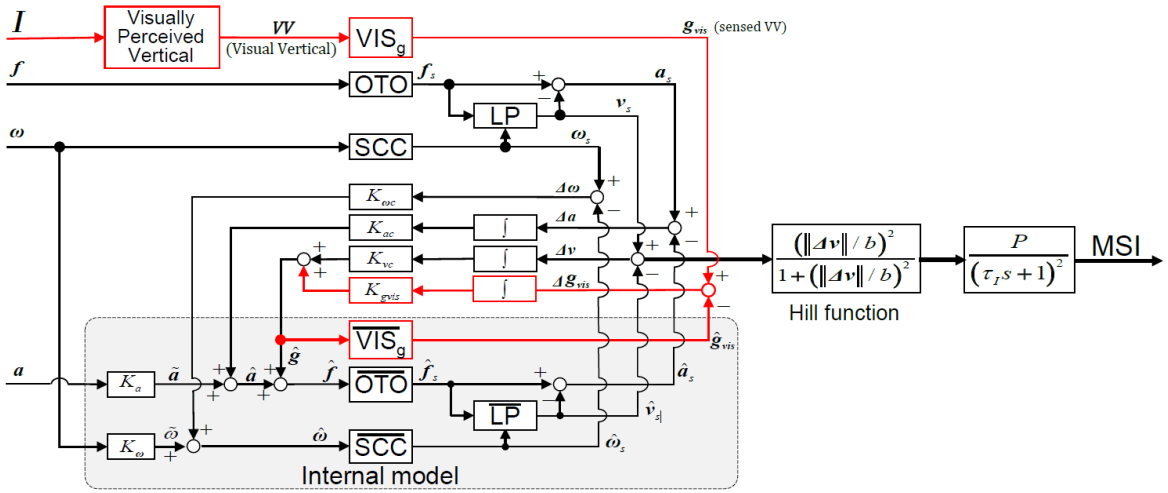

Figure 4-9: 6DOF-SVC MS prediction model including visual vertical conflict (shown in red) (Liu et al., 2022)

All parameters are equal to the ones used in Wada et al. (2020), see Table 4-1, except for the newly added gain K_{gvis}. This gain is set to a value of 5.0, equal to K_{vc}, in order to balance the feedback strength of the two integrated feedback signals.

$$\hat{\boldsymbol{g}} = K_{gvis}\left(\int_0^t (\boldsymbol{g_{vis}}(t) - \hat{\boldsymbol{g}}_{\boldsymbol{vis}}(t))\, dt + C_0\right) + K_{vc}\left(\int_0^t (\boldsymbol{v_s}(t) - \hat{\boldsymbol{v}}_{\boldsymbol{s}}(t))\, dt + C_0\right) \tag{4-3}$$

4-2 Visual-Vestibular Motion Perception Models

Telban and Cardullo (2005) developed a human motion perception model that integrates visual and vestibular motion stimuli and incorporates the interaction between the vestibular and visual stimuli. The model is a combination of the conflict estimation model proposed by Zacharias (1977) and the visual attractor model by Van der Steen (1998), which are elaborated on in the following section. Telban and Cardullo (2005) proposed separate models for rotational and translational motion, which are both discussed at the end of this section.

4-2-1 Visual-Vestibular Conflict Estimator Model

Zacharias (1977) reported that a simple linear addition of the visual and vestibular afferents does not represent the self-motion response when both cues are simultaneously presented. From experiments (Young, 1978) it is known that visual cues dominate the velocity response at low frequencies (< 0.1 Hz), when both signals are in agreement. Moreover, when visual and vestibular cues are in conflict, either in magnitude or direction, the vestibular cues will initially dominate. Young (1978) suggested that when a subject is presented with both cues, the subject will combine the two cues in a non-linear way. The model prioritizes the vestibular response when the two cues are in conflict, while it favors the visual response when the cues are in agreement. Zacharias (1977) made an effort to capture the aforementioned phenomena

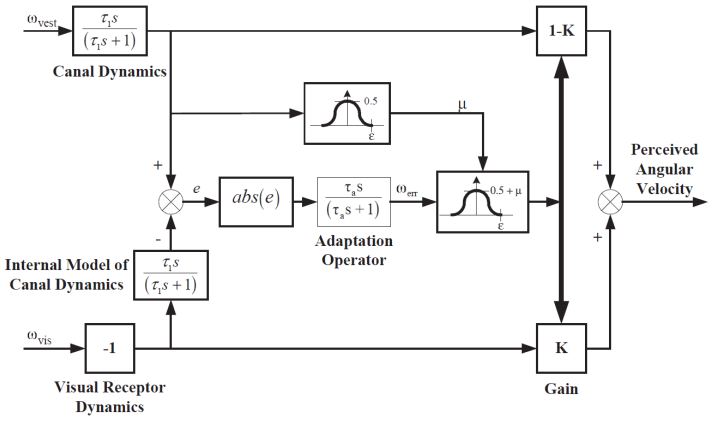

Figure 4-10: Visual-vestibular conflict estimator model (Zacharias, 1977)

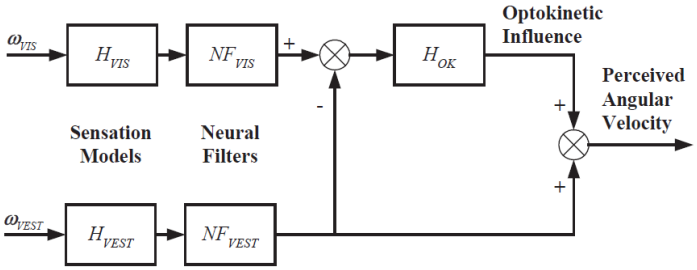

Figure 4-11: Model for self-motion perception with visual attractor (Van der Steen, 1998)

in a mathematical model, illustrated in Figure 4-10. The model structure is explained in more detail in subsection 4-2-3.

4-2-2 Visual Attractor Model

Van der Steen (1998) noted from experiments that the visual estimation of self-motion attracts the vestibular estimation of self-motion for both translational and rotational cues. The author suggested that this attraction effect should be included in a self-motion prediction model. This module is called the visual attractor and is represented as H_{OK} in Figure 4-11. The visual attractor uses the difference in perceived self-motion of the visual and vestibular systems as input, and calculates an optokinetic influence by using a first-order low-pass filter, as shown in Equation 4-4. The total perceived self-motion is then the sum of the vestibular estimate and the optokinetic influence.

$$H_{OK} = \frac{1}{1 + \tau_{OK} s} \tag{4-4}$$

4-2-3 Visual-Vestibular Interaction Model for Rotational Motion

Telban and Cardullo (2005) combined the conflict-based weights on visual and vestibular cues from the model of Zacharias (1977) and the visual attractor model of Van der Steen (1998) into the model illustrated in Figure 4-12. This model merges the vestibular angular velocity signal ω_{VEST} with the visual angular velocity signal ω_{VIS} to a combined perceived angular velocity.[6]

The inputs to this model are one-dimensional, but the model can be applied to the pitch, roll, and yaw movements separately. Vestibular angular velocity ω_{VEST} is passed through the canal dynamics that are modelled as a second-order high-pass filter, with values $\tau_l = 5.73$ s and $\tau_A = 80$ s (Haslwanter et al., 2000). The visual system is modeled as a pure time delay due to neural transmissions, where τ_d is equal to 90 ms (Hosman & Vaart, 1983). The visual system afferent is passed on to an internal model of the canal dynamics, to calculate an expected vestibular response. Subtracting this signal from the actual vestibular response results in the error signal e. The absolute value of this error is passed through an adaptation operator, that allows for long-term resolution of the steady-state conflict. The adaptation time constant τ_c of the first-order high-pass filter was set to 10 seconds by Zacharias (1977). This value is based on typical acceleration latencies observed for a conflicting visual field. The adaptation operator produces a washed-out conflict signal ω_{err}. This conflict signal is used to determine the value of the optokinetic gain K_{OK}, which varies between zero and one. A modified cosine bell function drives this gain to zero when ω_{err} is greater than the conflict threshold value ε, while the value of K_{OK} is between zero and one when ω_{err} is below ε, see Figure 4-13. For negative values of ω_{err}, K_{OK} is equal to one.

The conflict threshold value ε is chosen to be equal to the vestibular indifference motion threshold (Zacharias, 1977). The values obtained by Benson, Hutt, and Brown (1989) are used in this model. For yaw rotations, the conflict threshold value ε is equal to 1.6 deg/s, as also shown in Figure 4-13. For roll and pitch stimuli, a value of 2 deg/s is used. The difference in perceived self-motion of the visual and vestibular systems is scaled by optokinetic gain K_{OK}. Similar to the perception model by Van der Steen (1998) (Figure 4-11), the output of K_{OK} is fed through the visual attractor module represented by a first-order low-pass filter. A value of 2 s is used for τ_{OK}. Lastly, the optokinetic influence is added to the angular velocity perceived by the vestibular system to produce a combined perceived angular velocity.

One of the advantages of the model suggested by Telban and Cardullo (2005) is that the amount of visual influence on perceived angular velocity is determined by the amount of conflict between the vestibular and visual system afferents. As mentioned above, the model of Young (1978) prioritizes signals from the vestibular system with conflicting cues, while it uses visual signals with conforming cues. This effect is also captured in the model of Telban and Cardullo (2005) since high conflicting cues will drive the optokinetic gain K_{OK} to zero, thus blocking the influence of the visual system.

An overview of all parameters used in the model of Telban and Cardullo (2005) is given in Table 4-2.

[6] The visual motion cues in this model are limited to the peripheral visual scene. T. H. Brandt, Dichgans, and Koenig (1973) showed that the peripheral field is primarily used to estimate rotational self-motion. Blocking the central visual field up to 120 degrees barely alters the sensation of circularvection.

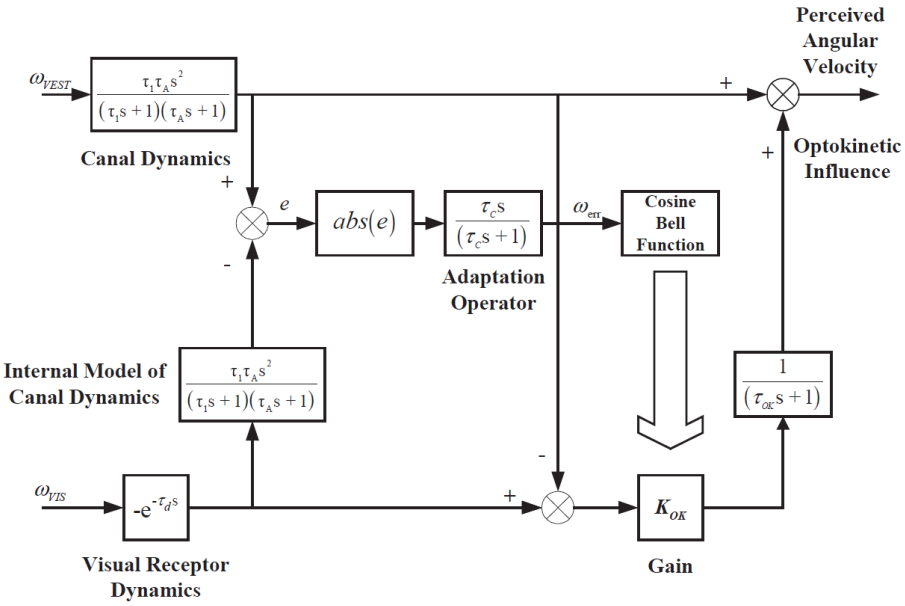

Figure 4-12: Visual-vestibular interaction model for rotational motion (Telban & Cardullo, 2005)

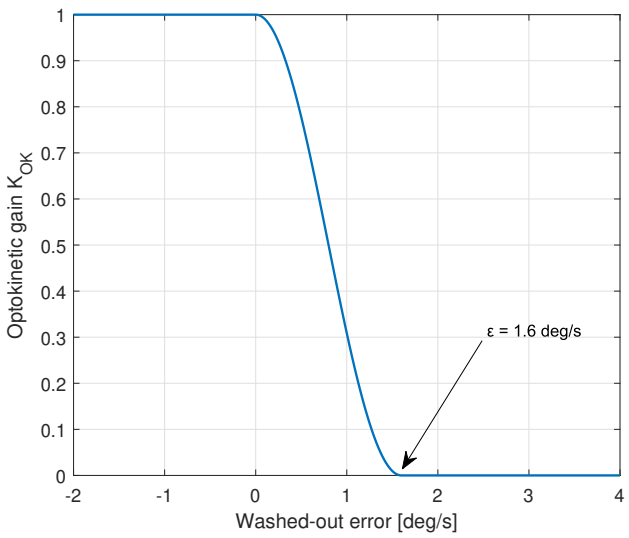

Figure 4-13: Modified cosine bell operator for optokinetic gain (Telban & Cardullo, 2005)

Table 4-2: Visual-vestibular rotational interaction model parameters (Telban & Cardullo, 2005)

Parameter	τ_l [s]	τ_A [s]	τ_d [ms]	τ_c [s]	ε [deg/s]	τ_{OK} [s]
Value	5.73	80	90	10	1.6	2

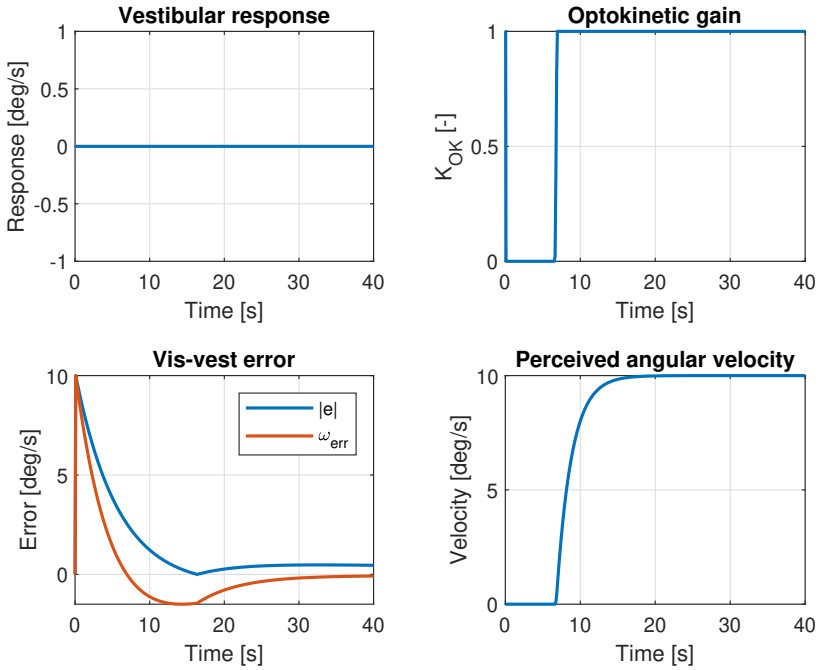

Figure 4-14: Rotational visual-vestibular interaction model responses to visual field step input of 10 deg/s (Telban & Cardullo, 2005)

Figure 4-14 shows the model's response to a visual step input of 10 deg/s, while the vestibular input is kept at zero. Therefore, the absolute error between the vestibular response and visual response (passed through an internal model of the canal dynamics) starts at 10 deg/s, visible in the bottom left graph. Since the internal model of the canal dynamics is modeled as a second-order high-pass filter, the absolute error decays. As the error passes through an adaptation operator, the washout error ω_{err} decays more quickly and even becomes negative. When this washout error is smaller than the conflict threshold value ε (1.6 deg/s), the optokinetic gain increases to a value of one following the curve as shown in Figure 4-14. This activates the visual response and drives the perceived velocity towards the 10 deg/s visual input. The slow build-up of the perceived angular velocity is due to the visual attractor module.

4-2-4 Visual-Vestibular Interaction Model for Translational Motion

Similar to the rotational model described in subsection 4-2-3, Telban and Cardullo (2005) also developed a model for translational motion. The model structure is identical to that of the model for rotational motions. Inputs to the model are the specific force f_{vest} felt by the vestibular system and acceleration a_{vis} seen by the visual system. The perceived linear velocity is the output of the model, which explains the addition of the integration blocks.

The canal dynamics are replaced by otolith dynamics that uses values $K_{OTO} = 0.4$, $\tau_L = 13.2$ s, $\tau_1 = 5.33$, and $\tau_2 = 0.66$ s (Telban & Cardullo, 2005). The washout error v_{err} is used to drive the gain K_{OK}. Values of the visual delay τ_d and the optokinetic time constant τ_{OK} remain equal to those used in the rotational model. However, the adaptation time constant τ_c

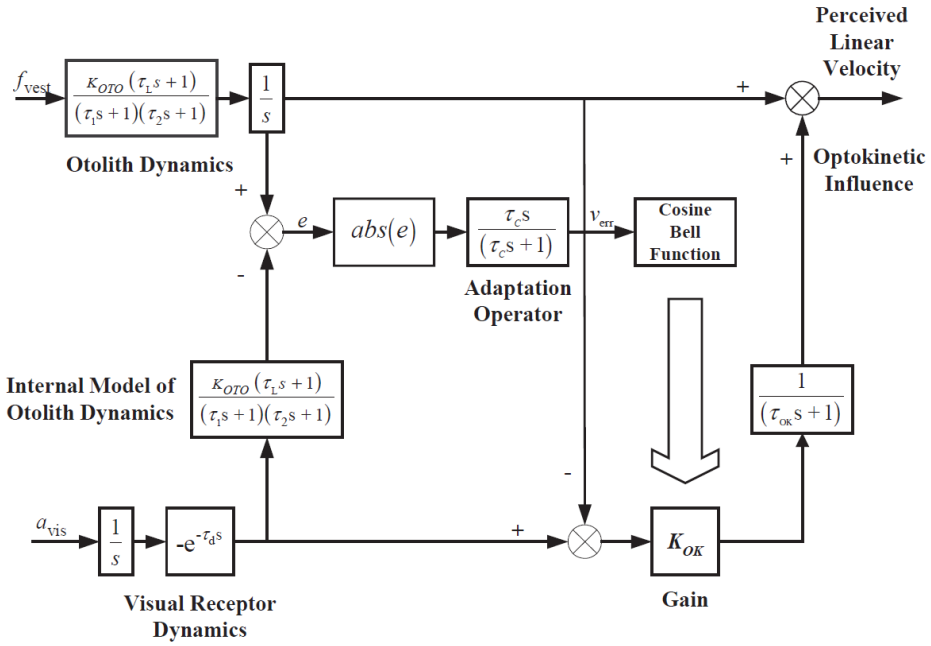

Figure 4-15: Visual-vestibular interaction model for translational motion (Telban & Cardullo, 2005)

Table 4-3: Visual-vestibular translational interaction model parameters (Telban & Cardullo, 2005)

Parameter	K_{OTO} [-]	τ_L [s]	τ_1 [s]	τ_2 [s]	τ_d [ms]	τ_c [s]	ε [deg/s]	τ_{OK} [s]
Value	0.4	13.2	5.33	0.66	90	0.2	0.2	2

and the conflict threshold value ε, were changed to 0.2 seconds and 0.2 m/s, respectively, to match visual motion latencies seen in the experiments of Berthoz, Pavard, and Young (1975). As a result of this smaller time constant, the washout linear velocity error v_{err} decays faster than the washout angular velocity error ω_{err} used in Figure 4-12. Hence, the optokinetic gain K_{OK} will quickly increase to one in a steady-state conflict. For clarity, all the parameters used in the model for translational motion can be found in Table 4-3.

Figure 4-16 shows the model response to a visual step input of 1 m/s (note the different time scale compared to Figure 4-14).[7] Again, the vestibular input was kept at zero. The absolute error increases due to the otolith dynamics included as the internal model. The high-pass filtered washout error v_{err} determines the value of the optokinetic gain K_{OK}. Since the adaptation time constant τ_c decreased with respect to the rotational model, v_{err} remains relatively small and quickly activates the optokinetic gain K_{OK}. This causes smaller perceived velocity-onset latencies compared to the results shown in Figure 4-14 for rotational motion.

[7] Although the model depicted in Figure 4-15 uses visual acceleration as input, it makes more sense to use visual velocity, since humans are not able to see visual acclerations. Thus, the integration block immediately after the visual acceleration input is omitted for these simulations.

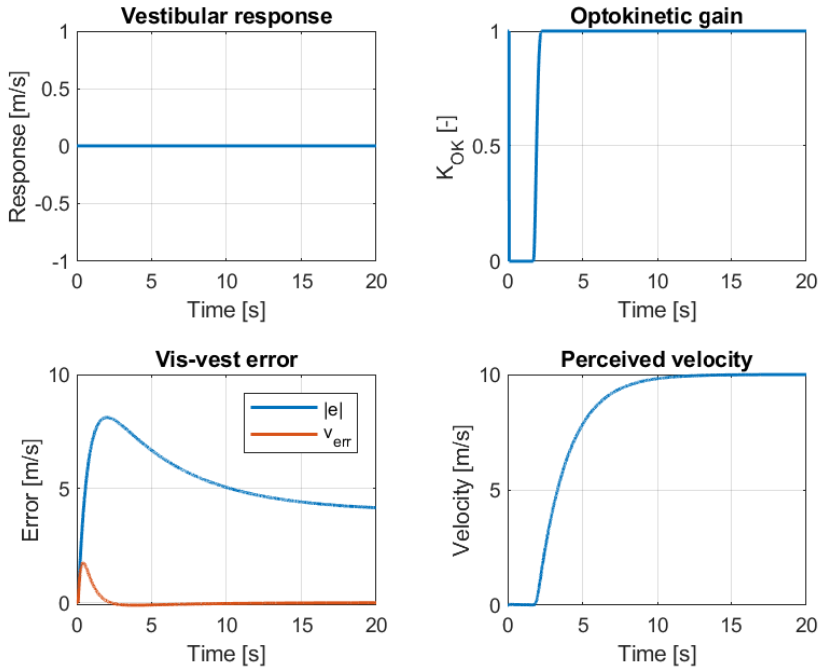

Figure 4-16: Visual-vestibular translational interaction model responses to visual field step input of 1 m/s (Telban & Cardullo, 2005)

4-3 Visual-Vestibular Motion Sicknes Model

Jalgaonkar et al. (2021) proposed the Visual-Vestibular Motion Sickness (VVMS) model that combines the 6DOF-SVC model by Kamiji et al. (2007) with the human motion perception model by Telban and Cardullo (2005), explained in Sections 4-1 and 4-2, respectively. The model can be seen in Figure 4-17. This model uses the same reference frame as the 6DOF-SVC model.

The proposed MS estimation model assumes that the visual system only estimates the angular velocity. A motion perception model is used to take this into account. The model of Wada et al. (2020), depicted in Figure 4-1, only accounts for the visual angular velocity in the internal model. The benefit of the approach taken by Jalgaonkar et al. (2021) is that the visual and vestibular angular velocities are combined into one perceived angular velocity of the head. Furthermore, the amount of influence of the visual system on the perceived angular velocity is determined by the disparity between the visual and vestibular sensed angular velocities, while the model by Wada et al. (2020) (Figure 4-1) needs to be manually tuned by adjusting the gain $K_{\omega vis}$ to be in accordance with the visual condition.

The model of Jalgaonkar et al. (2021) uses the same inputs as the model of Wada et al. (2020). The only difference here is that the former uses the G block, as explained in Section 4-1-1, to calculate the specific force $\boldsymbol{f}$. The SCC_{V-V} block in Figure 4-17 contains the visual-vestibular interaction model for rotational motion by Telban and Cardullo (2005) (Figure 4-12). The output is the visual-vestibular perceived angular velocity $\hat{\boldsymbol{\omega}}$, that replaces the vestibular-only sensed angular velocity signal $\boldsymbol{\omega_s}$ in the model by Wada et al. (2020). It should be noted that

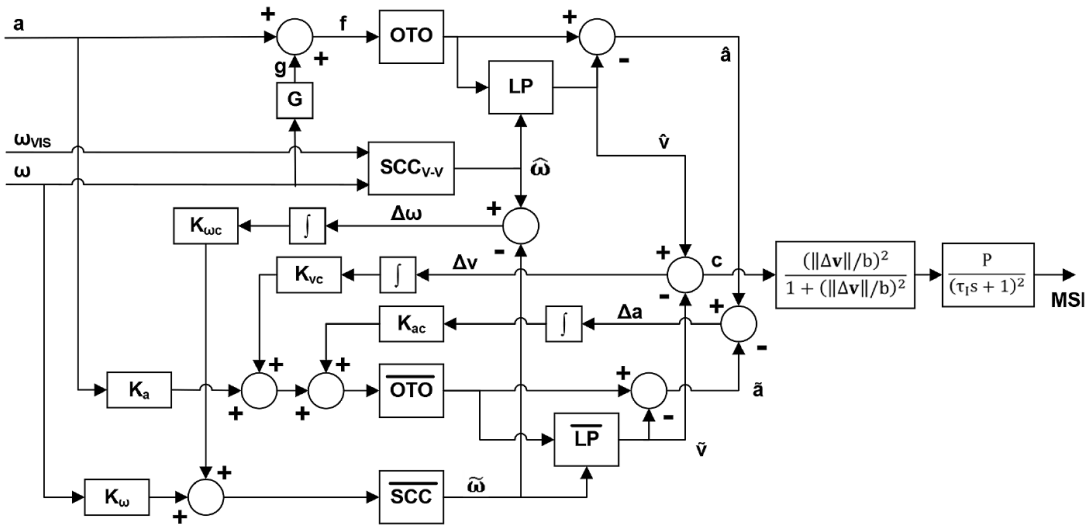

Figure 4-17: Visual-vestibular MS model (Jalgaonkar et al., 2021)

Table 4-4: VVMS model parameters (Jalgaonkar et al., 2021))

Parameter	K_ω [-]	K_a [-]	$K_{\omega c}$ [-]	K_{vc} [-]	K_{ac} [-]	P [%]	τ_l [s]	b [m/s^2]
Value	0.8	0.1	5	5	1	85	720	0.5

Parameter	τ_d [s]	τ_a [s]	τ_{lp} [s]	τ_w [s]	ε [deg/s]	τ_{va} [s]	τ_{delay} [ms]
Value	7	190	5	8	1.6	1.6	90

the SCC dynamics are represented by a second-order high-pass filter in both the SCC_{V-V} and $\overline{SCC}$ blocks, whereas Wada et al. (2020) use a first-order high-pass filter. Furthermore, the model includes similar internal models, sensory feedback loops, and MS calculations.[8] For a more elaborate explanation, the reader is referred to Section 4-1. An overview with all parameters used by Jalgaonkar et al. (2021) can be found in Table 4-4. Note that the values for gains K_ω and $K_{\omega c}$ are equal to those of Kamiji et al. (2007), while these values have changed in a later version of the 6DOF-SVC model (Wada et al., 2020). Furthermore, Jalgaonkar et al. (2021) use different symbols for the adaptation time constant ($\tau_c = \tau_w$) and the visual attractor time constant ($\tau_{OK} = \tau_{va}$), which values are slightly different and taken from Telban and Cardullo (2001).

The 6DOF-SVC model by Kamiji et al. (2007) has shown a close approximation of experimentally observed data (McCauley et al., 1976), except at frequencies lower than 0.16 Hz. Duh, Parker, Philips, and Furness (2004) show that the visual influence on MS is pronounced in the lower frequency ranges. The 6DOF-SVC model is not able to capture this effect correctly. Therefore, adding visual information, as mentioned above, to the 6DOF-SVC model could solve the discrepancies at lower frequencies. Figure 4-18 depicts preliminary simulation results of the VVMS model, that show that adding a visual angular velocity signal (that is in agreement with the physical angular velocity) reduces MSI at low frequencies (0.1 Hz).

[8]Note the integration on the angular velocity feedback loop. This is in accordance with Kamiji et al. (2007).

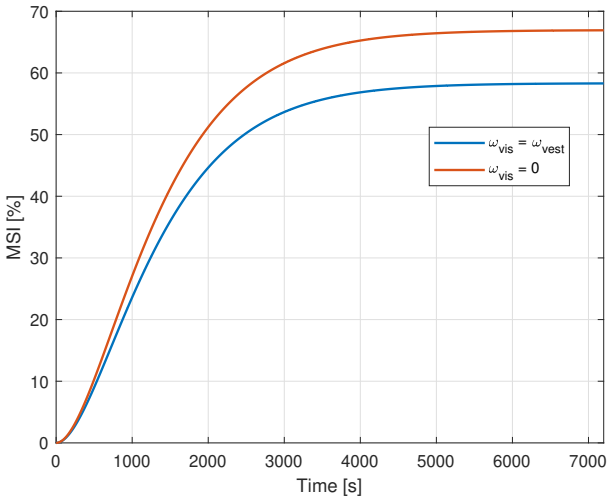

Figure 4-18: Preliminary VVMS model simulation results where the vestibular angular velocity input was set to a sinusoidal signal with 0.5 rad/sec RMS at 0.1 Hz about the y-axis (Jalgaonkar et al., 2021)

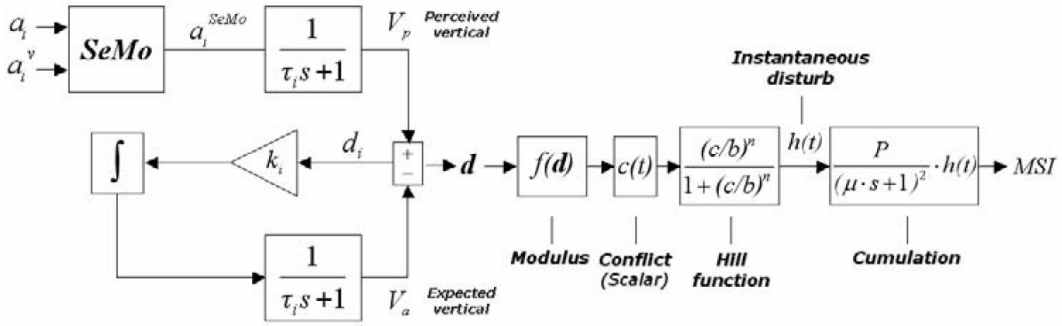

Figure 4-19: MS prediction model including visual accelerations (UNIPG$_{SeMo}$) (Braccesi & Cianetti, 2011)

4-4 UNIPG-SeMo Model

Jalgaonkar et al. (2021) made an effort to add visual angular velocity to a MS prediction model, by using the motion perception model of Telban and Cardullo (2005), as described in Section 4-3. Previous efforts have been made by Braccesi and Cianetti (2011) to add translational visual information to a MS prediction model. They extended the model of Bos and Bles (1998) by including visual linear acceleration as an input.

A representation of the proposed model by Braccesi and Cianetti (2011) is shown in Figure 4-19. Braccesi and Cianetti (2011) used the translational motion perception model of Telban and Cardullo (2005), described in subsection 4-2-4, to calculate a visual-vestibular perceived linear acceleration. This model is included in the SeMo block. The authors made some modifications to the original model from Telban and Cardullo (2005), that can be seen in Figure 4-20. The structure is similar to the original model, but the vestibular input has changed from a specific force f_{vest} to an initial linear acceleration a_i, where i represents one

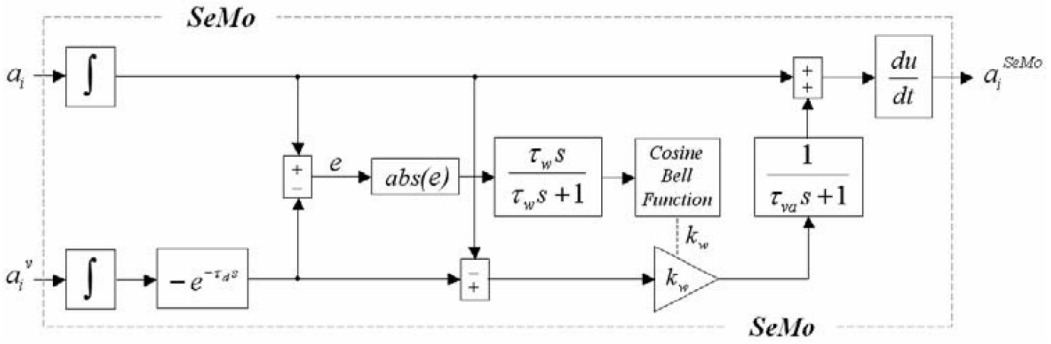

Figure 4-20: detailed representation of the SeMo block in the UNIPG$_{SeMo}$ model (Braccesi & Cianetti, 2011)

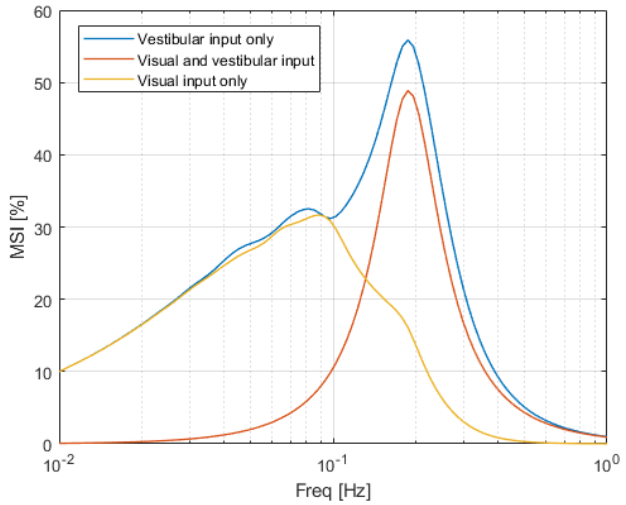

Figure 4-21: UNIPG$_{SeMo}$ model simulation results, two-hour exposure to a vertical sinusoidal motion with an acceleration amplitude of 1.11 m/s^2 RMS (Braccesi & Cianetti, 2011)

of the three translational axes. Furthermore, the perceived linear velocity of the original model is differentiated with respect to time to make this model compatible with the MS prediction model of Bos and Bles (1998). This results in perceived acceleration a_i^{SeMo} as output of the SeMo block. The otolith dynamics have been set to unity, which removes them from the model representation.

In Figure 4-19, the perceived acceleration a_i^{SeMo} is low-pass filtered to the perceived vertical V_p. This signal is compared to the expected vertical signal V_a, which creates conflict signal d_i. This conflict is scaled and integrated to be used as input to the internal model, to update the expected vertical, similar to the model of Wada et al. (2020). This internal model exists is represented by the low-pass filter at the bottom of Figure 4-19. Furthermore, the conflict signal is used to calculate the MSI by first taking the modulus of all three axes. The scalar value resulting from this operation is fed through a hill function, before the signal is integrated by a leaky integrator, which results in the MSI (equal to the 6DOF-SVC model).

As an example, preliminary simulation results of the UNIPG$_{SeMo}$ model are shown in Figure 4-

Table 4-5: UNIPG$_{SeMo}$ model parameters (Braccesi & Cianetti, 2011))

Parameter	τ_x, τ_z [s]	τ_y [s]	k_x, k_z [-]	k_y [-]	b [m/s^2]	n [-]	μ	P [%]	τ_d [s]
Value	0.6	2.4	0.84	3.36	0.7	2	900	85	0.09

Parameter	τ_w [s]	ε [m/s]	τ_{va} [m/s^2]
Value	1.0	0.2	2.0

21.[9] The three different conditions shown are (1) real motion with visual input set to zero, (2) confirming vestibular and visual inputs, and (3) only visual input keeping the vestibular signal at zero. It is clearly visible that the visual contribution to this model is dominant in the lower frequency ranges. Conflicting cues, that is, conditions one and three, result in higher MSI at low frequencies. This is in accordance with the experimental results of Duh et al. (2004). All parameters used for this simulation can be found in Table 4-5.

4-5 Conclusions

The 6DOF-SVC model from Kamiji et al. (2007) is able to accurately predict the MS values and shows a close approximation to the experiment results from McCauley et al. (1976). However, this model only depends on vestibular motion signals (see Section 4-1). Visual motion is still underrepresented in this MS prediction model, while it is known from experiments that the visual condition strongly influences MS (Butler & Griffin, 2006, 2009; Griffin & Newman, 2004). Wada et al. (2020) and Liu et al. (2022) attempted to include visual angular velocity and visual verticallity information, respectively, in the 6DOF-SVC model. These extensions have not been validated with experimental data yet and only work separately for now. Bos et al. (2008) suggested that the visual environment influences motion perception in three ways: visual angular velocity, visual vertical, and visual translation, as discussed in subsection 3-1-3. Extensions to the 6DOF-SVC model have been made for the former two, the latter, however, is still missing in this model. For this reason, the current research topic has been chosen to be the influence of visual translation on motion sickness.

Telban and Cardullo (2005) created a visual-vestibular interaction model that combines motion signals from the visual and vestibular sensors into one perceived motion signal. They proposed separate models for rotational and translational motions. The model merges the visual and vestibular signals based on the conflict value between them. High conflict values increase the influence of the vestibular motion signal on the final perceived motion signal, while low conflict values cause equal contributions of the visual and vestibular signals to the final perceived motion signal.

Jalgaonkar et al. (2021) used the rotational motion model of Telban and Cardullo (2005) and combined it with the 6DOF-SVC model from Kamiji et al. (2007). A different approach is taken to add visual angular velocity to the model, compared to the approach of Wada et al.

[9]UNIPG is an acronym of the university of Perugia (Università degli Studi di Perugia), that the authors have used as the name for the model.

(2020) (see Section 4-3 for a more detailed explanation). The translational motion model of Telban and Cardullo (2005) has been used by Braccesi and Cianetti (2011) in an older MS prediction model from Bos and Bles (1998). They used the combined perceived linear velocity signal as input to the MS model.

Similar to the approaches taken by Braccesi and Cianetti (2011) and Jalgaonkar et al. (2021), an attempt to add visual translation to the 6DOF-SVC model will be made by using the translational model from Telban and Cardullo (2005). A second attempt to include visual translation will use the original 6DOF-SVC model together with the motion perception model explained in subsection 3-1-3. Both attempts will be explained in more detail in Chapter 5.

Chapter 5

Research proposal

Chapters 2 to 4 concluded the literature research on the visual influence on MS. Research on MS became more attractive, since AVs are now rapidly introduces into the society. To help solve the problem of MS in AVs and to contribute to the body of knowledge about this subject, a research proposal is presented in this chapter. The research objective shown in Section 1-2 proposes to capture visual translation in a MS model and verify this model with an experiment. Section 5-1 will discuss two methods for a visual translation extension to the 6DOF-SVC model and Section 5-2 shows the proposed experiment to test the validity of these models.

5-1 Visual Translation Modeling

The role of the vestibular system in MS is well understood, however, the role of the visual system is still unclear. From experiments discussed in Section 3-2 it became evident that the visual system does influence MS. As Wada et al. (2020) and Liu et al. (2022) already started modeling the influence of visual rotation and the visual vertical, respectively, an attempt to model the influence of visual translation on MS will be made in this section. The approach discussed in Subsection 5-1-1 uses the visual-vestibular interaction model of Telban and Cardullo (2005), while the approach in Subsection 5-1-2 uses the motion perception model of Bos et al. (2008). The original 6DOF-SVC model of Kamiji et al. (2007) is used as a baseline, hence, visual rotation and visual vertical are left out. All simulations are performed in MATLAB Simulink.

5-1-1 Modified Acceleration Input

A first attempt to include visual translation to the original 6DOF-SVC model by Kamiji et al. (2007) can be seen in Figure 5-1. All black and blue parts are equal to the original model, and the red parts have been added or modified. Here, a similar approach as Braccesi and Cianetti (2011) used for their model (Section 4-4) is used. The visual-vestibular interaction

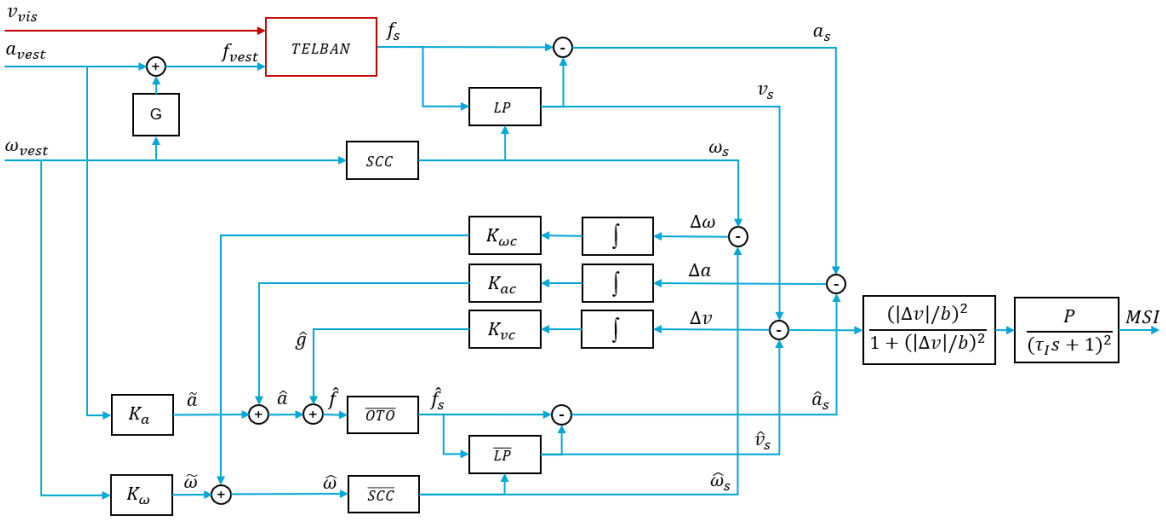

Figure 5-1: 6DOF-SVC model with visual tranlation input by using the model of Telban and Cardullo (2005)[2]

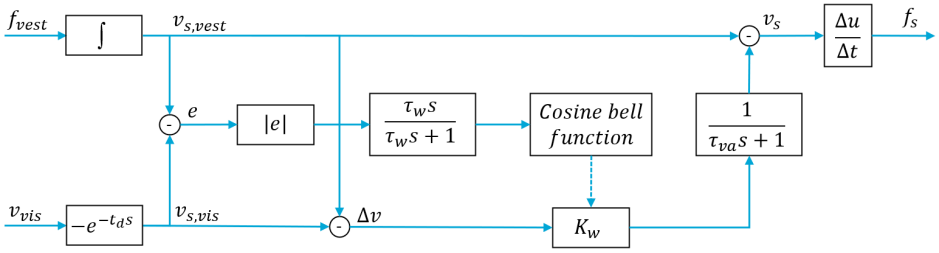

Figure 5-2: Modified visual-vestibular translational model by Telban and Cardullo (2005), included in the red $TELBAN$-block in Figure 5-1.

model for translational motion by Telban and Cardullo (2005) is used to integrate visual and vestibular information into one perceived acceleration signal (Subsection 4-2-4). A modified version of this model is included in the red $TELBAN$-block, which replaces the original otolith dynamics (OTO-block) in the 6DOF-SVC model.

The modified visual-vestibular interaction model is depicted in Figure 5-2.[1] Some modifications compared to the original model of Telban and Cardullo (2005) are made. Since the otolith dynamics are modeled as unity in the 6DOF-SVC model, they are left out of this model. Furthermore, the visual input has changed from visual acceleration to visual velocity, since humans cannot see visual acceleration as discussed in Subsection 3-1-3. Last modification is the differentiation of the perceived velocity output. This results in a perceived specific force output that is used as input to the 6DOF-SVC model again.

Figure 5-3 shows frequency responses of the current model. In this simulation, a two-hour translational sinusoidal signal acted on the vestibular x-axis with a peak acceleration ampli-

[1]The inputs $\boldsymbol{f_{vest}}$ and $\boldsymbol{v_{vis}}$ have been flipped around compared to the order in Figure 5-1. This is done to adhere to the original structure of the model in Figure 4-15.

[2]Note that the $\boldsymbol{v_{vis}}$ is used for visual velocity while $\boldsymbol{v_s}$ and $\boldsymbol{\hat{v}_s}$ represent the subjective vertical and expected subjective vertical, respectively.

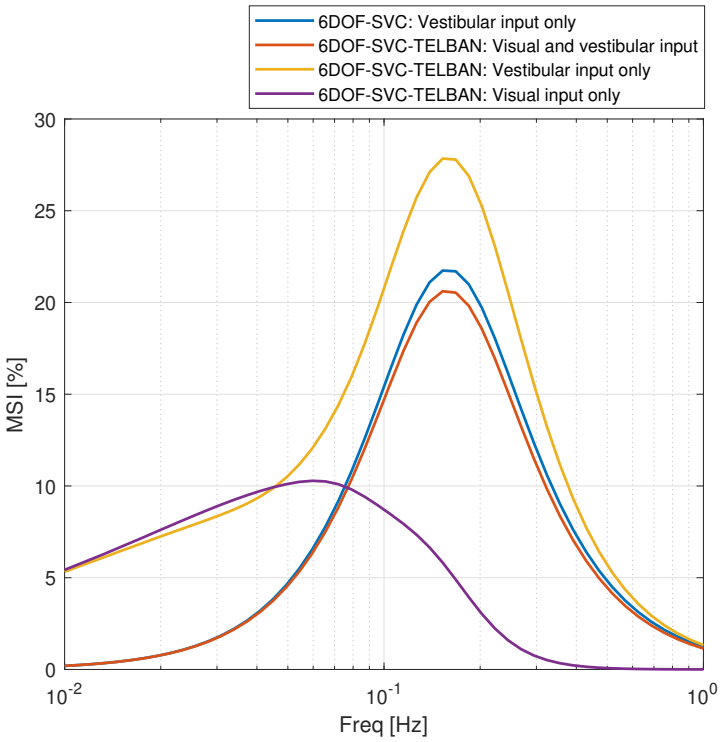

Figure 5-3: 6DOF-SVC model with visual translation extension simulation results

tude of 3 m/s^2. The visual velocity input signal was an integrated version of the vestibular acceleration signal. The parameters used for this simulation are equal to those used by Wada et al. (2020) and Braccesi and Cianetti (2011), seen in Table 4-1 and Table 4-5, respectively. The figure includes three different condition for the 6DOF-SVC model with TELBAN extension, which are the congruent visual and vestibular input, the vestibular input only, and the visual input only conditions. As a reference, the original 6DOF-SVC model responses to the same input signals are also shown in the figure. The congruent visual and vestibular inputs of the 6DOF-SVC-TELBAN model have similar MSI values compared to the original model. Setting the visual input to zero while keeping the vestibular input the same, produces higher MSI values. This condition could be compared to sitting in a car with all windows blocked, a condition tested by Griffin and Newman (2004) that also raised MS, as discussed in Section 3-2. Last, the vestibular input is set to zero while keeping the visual input the same; a condition which is not realistic for autonomous vehicles but can happen in simulator conditions. Within this condition MS decreases, but the peak notably shifts towards a lower value compared to the other two conditions. This shift is consistent with the results of Duh et al. (2004), which showed that MS was the highest with conflicting signals at 0.06 Hz. Furthermore, the visual system acts as a low-pass filter for translational motion (Bos et al., 2008), making the shift towards lower frequencies logical.

A problem with the approach presented in this section is that it does not comply to the observer model theory, as described by Bos et al. (2008). This theory states that the internal model should be an exact copy of the primary path, which is not the case with the

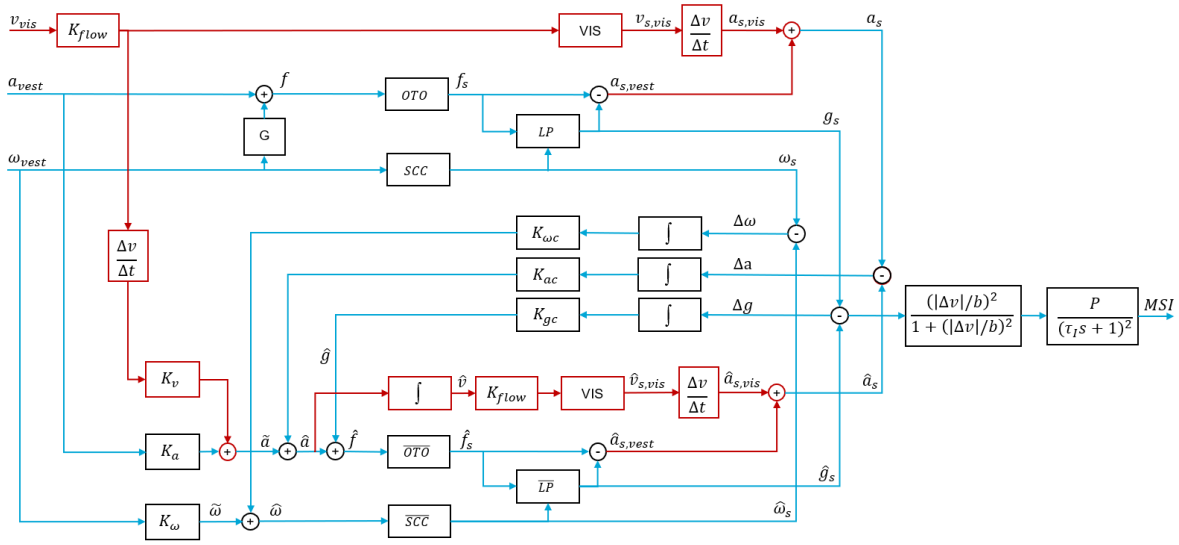

Figure 5-4: 6DOF-SVC model with visual translation input by using the observer model approach.[3]

current approach. The visual-vestibular dynamics within the $TELBAN$-block are missing in the internal model. Furthermore, the differentiation of perceived velocity into perceived specific force is an assumption that has not been validated yet. Therefore, making it hard to scientifically back-up the decisions made for this model. For the reasons mentioned above, further research into this model has been discontinued. Another method to include visual translation into the 6DOF-SVC model is presented in the next section.

5-1-2 Observer Model Approach

Another approach, which is adhering to the observer model theory, is presented in Figure 5-4. This design is based on the motion perception model of Bos et al. (2008), discussed in Subsection 3-1-3. Again, additions to the model are colored red, whereas the original model parts are colored black or blue. Figure 3-3 shows a method to combine linear visual velocity with inertial accelerations felt by the vestibular system. Here, linear vection is calculated with a low-pass filter and is added to the integrated sensed inertial acceleration. Since the 6DOF-SVC model only considers linear accelerations, and no linear velocities, it has been chosen to differentiate the visual response $\boldsymbol{v_{s,vis}}$ instead of integrating the vestibular repsonse $\boldsymbol{a_{s,vest}}$. This results in the combined sensed acceleration $\boldsymbol{a_s}$. A low-pass filter is included within the upper VIS-block in Figure 5-4, to represent the dynamics of the visual system. For preliminary simulations, the time constant of this filter was set at 5 s, equal to the time constant of the low-pass filter on the otolith afferents.

The observer theory states that an exact copy of the primary dynamics is included in the internal model, hence the same visual dynamics and differentiation are added at the bottom of the model. Differentiation of the expected sensed visual velocity $\boldsymbol{\hat{v}_{s,vis}}$ results in the expected sensed visual acceleration $\boldsymbol{\hat{a}_{s,vis}}$. This signal is again added to the expected sensed

[3] In this model the symbol for the subjective vertical signals has been changed from $\boldsymbol{v}$ to $\boldsymbol{g}$, to prevent confusion with the symbol for the velocity signals $\boldsymbol{v}$.

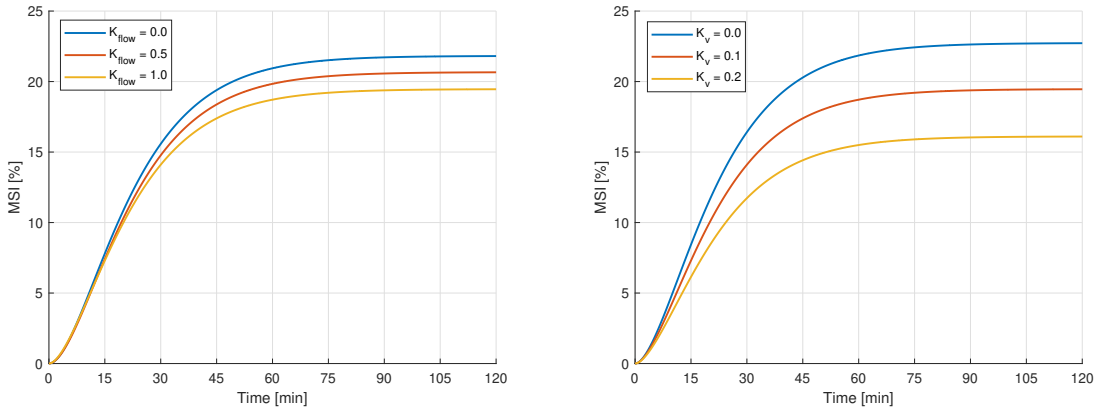

(a) Influence of K_{flow} on simulation results of the 6DOF-SVC model with visual translation

(b) Influence of K_v on simulation results of the 6DOF-SVC model with visual translation

Figure 5-5: Parameter sensitivity analysis of the 6DOF-SVC model with visual translation

vestibular acceleration $\hat{\boldsymbol{a}}_{\boldsymbol{s,vest}}$, to calculate the combined expected sensed acceleration $\hat{\boldsymbol{a}}_{\boldsymbol{s}}$. The sensed acceleration $\boldsymbol{a}_{\boldsymbol{s}}$ and the expected sensed acceleration $\hat{\boldsymbol{a}}_{\boldsymbol{s}}$ are subtracted from each other, leading to the conflict signal $\boldsymbol{\Delta a}$. This signal is used to update the input to the internal model, equivalent to the original 6DOF-SVC model (Kamiji et al., 2007). Bos et al. (2008) states that the internal model only takes one input for each type of motion, that is, there are no separate visual and vestibular inputs. For this reason, the input to the internal visual dynamics is calculated by integrating the expected acceleration $\hat{\boldsymbol{a}}$.[4]

Vection strength is influenced by the amount of optical flow present in the visual scene (Correia Grácio et al., 2014). To account for this effect, an optical flow gain K_{flow} has been added to the primary and internal dynamics of the model. This gain scales the visual velocity to a perceived visual velocity signal. More optical flow (e.g., driving in an urban area with building close to the road) results in higher experienced vection strength, making K_{flow} close to one. Visual velocity $\boldsymbol{v}_{\boldsymbol{vis}}$ is scaled down with low optical flow fields, which occurs when driving in rural areas, i.e., there are no objects close to the road. In this way, the amount of visual information used for motion perception is influenced by the amount of optical flow present in the visual scene of the observer.

The last addition to the 6DOF-SVC model is the anticipation path on the left-hand side of Figure 5-4. It is expected that more visual information leads to more anticipation of upcoming motions. Therefore, part of the visual motion is used to update the expected acceleration signal $\hat{\boldsymbol{a}}$, which is the input to the internal model. The perceived visual velocity is differentiated and scaled by gain K_v to update the acceleration signal. Similar to the values of K_a and K_ω, the value of K_v depends on the controllability of self-motion (i.e., active or passive self-motion). For preliminary simulations, the value of K_v was set to 0.1, equal to K_a and K_ω.

[4]The internal visual dynamics path now includes both an integrator and a differentiator. These could be omitted since they are both linear operators. However, to adhere to the physical principals they are kept in the model.

The influence of K_{flow} on the preliminary simulation results is shown in Figure 5-5a. Again, the parameters presented in Table 4-1 (with $K_v = 0.1$) are used for this simulation. As input to the model, the x-axis of $\boldsymbol{a_{vest}}$ was set to a sinusoidal signal with a peak acceleration amplitude of 3 m/s^2 and frequency of 0.16 Hz. The $\boldsymbol{v_{vis}}$ signal was simply an integrated version of $\boldsymbol{a_{vest}}$. The vestibular rotational velocity $\boldsymbol{\omega_{vest}}$ was kept at zero. When the gain K_{flow} is set to zero, the proposed model is equal to the original 6DOF-SVC model shown in Figure 4-5, as all paths added to the model are zero. Increasing the value of K_{flow}, decreases the final value of MSI, while keeping the shape of the MS development curve similar. Here, high values of K_{flow} would represent driving through urban areas with lots of optical flow, while low values of K_{flow} would represent driving through rural areas with low optical flow. Figure 5-5b shows the influence of K_v on the simulated MS values. The input signals are equal to those described above, with K_{flow} set to one. Higher values of K_v clearly decrease MSI.

The main reason why increasing K_v or K_{flow} decreases MSI is the anticipation path on the left side of the proposed model. More information about the actual motion is available for the internal model, making the expected motion $\hat{\boldsymbol{a}}$ closer to the actual motion $\boldsymbol{a}$. The expected motion $\hat{\boldsymbol{a}}$ is an input to the internal model while the actual motion $\boldsymbol{a}$ is an input to the primary dynamics. When these two inputs are closer to each other, the conflict signals between the sensed motion and expected sensed motion ($\boldsymbol{\Delta\omega}$, $\boldsymbol{\Delta a}$, $\boldsymbol{\Delta g}$) are reduced. Since $\boldsymbol{\Delta g}$ is used for the MSI calculation, the predicted MS is lower for higher values of K_v and K_{flow}. Interestingly, the visual dynamics added in the primary path and internal model, only increases the predicted MSI. This can be deduced from the results shown in Figure 5-5, as the predicted MSI with $K_{flow} = 1.0$ and $K_v = 0.0$ (blue graph in Figure 5-5b) is higher than the predicted MSI with $K_{flow} = 0.0$ and $K_v = 0.1$ (blue graph in Figure 5-5a), considering that the former case eliminates the anticipation path and the latter case is equal to the original 6DOF-SVC model. This result shows that the added visual dynamics does not have the desired effect. Congruent visual translation is expected to decrease MS, which was seen in the experiments described in Section 3-2. Moreover, this model is not stable at all frequency-amplitude combinations. Certain combinations cause the MSI to rise to unreasonably high values.

The results shown in Figure 5-5 are mainly determined by the newly added anticipation path on the left side of the model (Figure 5-4). A more simple approach can be taken to achieve the same results. Instead of adding the visual translational dynamics to the original model of Kamiji et al. (2007) (Figure 4-5), only the anticipation gains K_a and K_ω can be altered to adhere to the visual condition. More congruent visual translational information could increase the anticipation gain for acceleration K_a. Results of this approach can be found in Figure 5-6. The same simulation parameters as used in Figure 5-5 have been used. Since this simulation only includes longitudinal accelerations, only the anticipation gain K_a is changed between zero and one with steps of 0.2. As clearly visible, higher anticipation gains causes lower MSI values. With K_a being equal to one, there would be no MSI, as the sensory conflict signals are equal to zero. Further research is needed to correctly model the influence of visual translation on MS. The goal of the experiment, elaborated on in the next chapter, is to gain more insights into the correct way of modeling the influence of visual translation on MS.

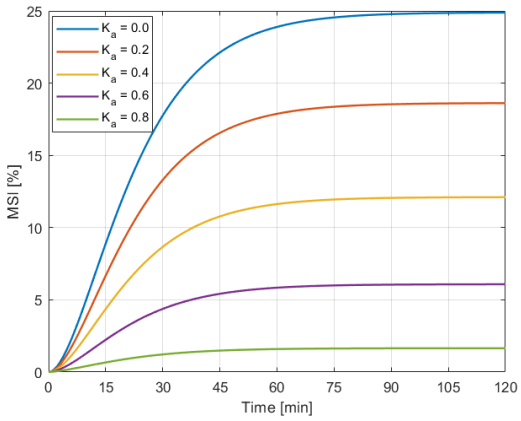

Figure 5-6: Influence of K_a on simulation results of the original 6DOF-SVC model by Kamiji et al. (2007)

5-2 Experiment Design Proposal

To test the validity of the proposed model in the previous chapter, a human-out-of-the-loop experiment will be executed. Experiment results could help in tuning the gain parameters of the proposed model. The experiment will also produce meaningful data, as an experiment like this is missing in the literature. There is lots of data available on VIMS, which only involves visual translational motion. However, an experiment with a combination of physical and visual translational motion and visual motion in the peripheral view is lacking. The experiment design proposal is elaborated on in the following section.

5-2-1 General Experiment Design

This research will contain a human-out-of-the-loop experiment, that simulates driving in an AV. As the goal of this research is to quantify the relation between visual translational information and MS, the experiment will only include translational movements. This means that the experiment only involves accelerations and decelerations in the longitudinal direction, while driving on a straight road. Curently, MS is heavily researched in the automotive industry, due to the rapid introduction of AV. For this reason, a simulated AV ride was chosen for the experiment. From earlier experiments it is known that MS only gradually increases within a period of several minutes to two hours (McCauley et al., 1976). Therefore, the experiment duration is set at 30 minutes, to capture the initial MS development.

The experiment will involve three different visual conditions, which are the baseline, low optical flow, and high optical conditions. During these conditions the physical motion will be identical, while the visual motion will differ. A schematic representation of the visual conditions can be found in Figure 5-7. As stated before, the experiment will simulate an AV ride, hence the visual scene includes a forward view of a road. A baseline condition is shown in Figure 5-7a, which is a static visual scene of a straight road. The results of this condition will be used as a reference to the other two conditions. Figure 5-7b illustrates the low optical flow condition, which represents driving through a rural area. It includes a moving center line

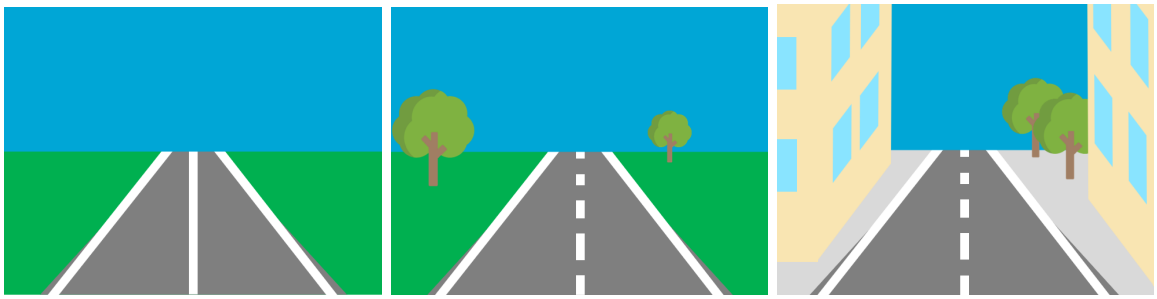

(a) Baseline condition

(b) Low optical flow condition

(c) High optical flow condition

Figure 5-7: Schematic representation of the three visual conditions during the experiment

and an occasional tree next to the road, from which some visual motion can be deducted. A high optical flow condition is shown in Figure 5-7c. This condition simulates a ride through an urban area with lots optical flow created by high buildings, cars parked to the side of the road, pedestrians, etc.

It is expected that the baseline condition will result in the highest MS, since the visual-vestibular conflict is the highest. Subjects will feel the physical motion while there is no visual motion. With lots of congruent visual information, it is predicted that a subject can better estimate the expected motion signals (see Section 5-1). Hence, it is expected that the high optical flow condition will result in the lowest MS. The low optical flow condition will generate some visual motion information, but not as much as the high optical flow conditions. Therefore, it is suspected that these MS values are between the two other conditions. To prevent any habituation or cross-over effects in the results, the three visual conditions will be performed on three different days. As a result of having three conditions, six different orders can be made. Therefore, the number of participants has to be a multiple of six, to prevent having any order effects in the results. Due to resource restrictions, only eighteen participants will perform the experiment.

Correia Grácio et al. (2014) discovered that FoV and depth cues are important to correctly estimate self-motion from visual motion in the surge direction. A wider FoV will increase the amount of visual flow in the peripheral view, which improves the self-motion estimation. The high optical flow condition will therefore also include a lot of motion in the peripheral area. However, the FoV of the visual motion stimuli is limited by the visual system of the simulator used in this experiment. Consequently, as Correia Grácio et al. (2014) recognized, the visual motion amplitude must be set higher than the physical motion amplitude for equally perceived cues. What's more, is that the weighing of visual motion differs per individual. VIMS is highly depended on this factor (Kuiper et al., 2018). This phenomenon is important for the current experiment and must be taken into account when reviewing the experiment results. Unfortunately, due to time and resource restrictions, this visual dependency value cannot be determined per participant.

During the experiment the participants are asked to verbally communicate their level of sickness with the MIsery SCale (MISC) for subjective assessment of MS. This is an eleven-point scale, which is shown in Table 5-1. Every 30 seconds the participant is asked to communicate the number corresponding to the MS symptoms they experience. Since MS symptoms signif-

Table 5-1: MIsery SCale for subjective assessment of MS, adapted from Bos et al. (2005)

Symptom		Score
No problems		0
Uneasiness (no typical symptoms)		1
Dizziness, warmth, headache, stomach awareness, sweating,...		
	vague	2
	slight	3
	fairly	4
	severe	5
Nausea		
	slight	6
	fairly	7
	severe	8
	(near) retching	9
Vomiting		10

icantly differ per individual, MISC ratings of all eighteen participants are averaged, making the experiment a within-subject design. Appropriate statistical tests will be performed to determine if any significant differences between the three visual conditions are present. It is hard to compare the MSI predicted by the MS model with the average MISC ratings from the experiment. They are not the same, as the former predicts the percentage of people that would vomit and the latter is based on symptom severity. For this reason, the shape of the two parameter graphs will be compared, as it is thought that these show similar developments.

5-2-2 Apparatus

To subject the participants to the visual and physical motion cues, the SIMONA Research Simulator (SRS) is used. The SRS is located at the faculty of Aerospace Engineering at the Delft University of Technology and can be seen in Figure 5-8. SRS has a 6DOF hydraulic motion base, capable of realistically simulating road vehicle motions. The visual system consists of three Digital Light Processing (DLP) projectors and creates a collimated 180-degree horizontal by 40-degree vertical FoV. A computer generated outside view of the three condition described in Subsection 5-2-1 will be shown to the participants. The SRS is also equipped with a surround sound system, which will be used to mask actuator noise by playing engine sounds. This will also enhance the simulation experience.

As the participant's head movement is important for MS development, an accelerometer will be attached to the head of the participants. This sensor will be used to investigate if any correlation between head movement and MS is present during the experiment. Furthermore, it is essential that the head rotations will be kept at a minimum during the experiment. To prevent head rotations induced by the movement of the participant's head, all participants

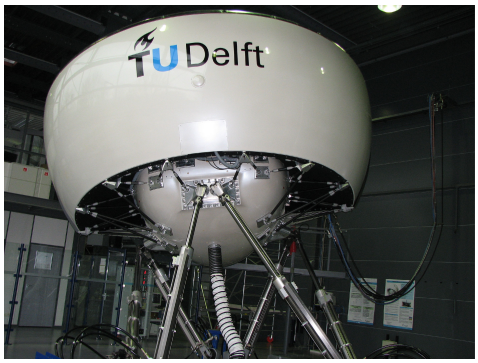

Figure 5-8: SIMONA Research Simulator

are asked to wear a neck brace. The accelerometer will help quantify the amount of head rotations, which are used to test the validity of the experiment results.

5-2-3 Motion Profile

The motion profile of the experiment will contain accelerations and decelerations in the longitudinal x-direction. All three conditions will have the exact same visual and physical motion profile. Only the content that is shown in the visual scene will differ. An example motion profile is shown in Figure 5-9, but this is not final yet. The simulated vehicle will constantly switch between two constant velocities. Parameters such as the maximal acceleration and deceleration amplitude, the maximum jerk value, the minimal and maximal velocity, are still to be determined.

Since the SRS has a limited motion space in the surge direction, low-frequency acceleration values cannot be simulated with translational motions only. A solution often used for this problem is tilt coordination. Here, the gravitational acceleration is used to create an illusion of constant acceleration, by tilting the simulator. Due to this rotation, part of the gravitational acceleration will act in the x-axis of the simulator reference frame, creating the illusion of forward acceleration. Although the rotational rates are very low, a participant might still feel these rotations. The tilt coordination creates a visual-vestibular conflict, as the visual field is not rotating. This conflict will influence the MS symptoms and need to be taken into account when evaluating the final results of the experiment.

5-2-4 Experiment Procedures

A total of eighteen participants will be recruited among students of the Delft University of Technology. Ahead of the experiment, all participants will fill in the Motion Sickness Susceptibility Questionnaire (MSSQ) form (Golding, 2006a). The MSSQ will provide a measure of the motion sickness susceptibility of the participants. In this way it can be verified that the group of participants is representative of the general population. Age might be a confounding factor in this experiment, since all participants will probably be younger than 30. Experiments performed by Jones et al. (2019) confirmed that MS susceptibility decreases with age.

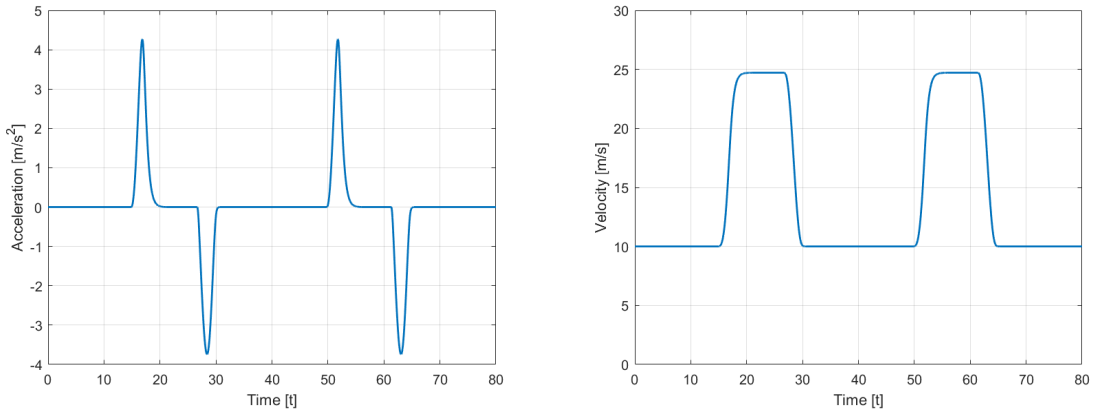

(a) Acceleration motion profile **(b)** Velocity motion profile

Figure 5-9: Preliminary motion profile used in the experiment

Participants will receive a safety briefing, together with a general briefing about the experiment procedures before the experiment. Before entering the simulator, the participants are asked to wear the accelerometer and the neck brace. After taking place inside the SRS, the seat will be adjusted such that every participant's eye height is located at the Design Eye-height Reference Point (DERP). This will make sure that all participants see the same visual field. Participants are asked to maintain a relaxed body posture and to keep looking at the center point of the visual field. After all safety procedures are finished, the experiment is started. During the experiment, participants verbally communicate their MISC value after every 30-seconds-interval sound cue. The simulated vehicle ride will take 30 minutes, after which the motion is stopped. For another fifteen minutes, participants need to communicate their MISC values to also measure the MS recovery. Additionally, after each experiment session a questionnaire about the experienced MS symptoms, the realism of the simulated vehicle motion, and the influence of the visual field will need to be filled in.

5-3 Conclusions

Although the literature leans towards the idea that linear vection is not needed for VIMS, the role of vection during MS experienced in road vehicles is not studied yet (Keshavarz et al., 2015). For this reason, the research objective presented in Section 1-2 was formulated. The current chapter discussed in what manner this research objective will be achieved. Two methods to include visual translation into the 6DOF-SVC model have been presented. The first method used the visual-vestibular translational model by Telban and Cardullo (2005), that merges accelerations felt by the vestibular system with the velocity seen by the visual system, based on the conflict between the two. Preliminary simulations of this model showed promising results that agreed with experiment data from the literature. However, the modeling approach used was hard to justify with physical processes happening in the CNS and did not adhere to the observer model theory. Consequently, another method was proposed. This method used the motion perception model of Bos et al. (2008) to combine visual translation and vestibular accelerations. These dynamics were added to the primary path and the inter-

nal model, adhering to the observer model theory. This method produced realistic results, but only at certain frequencies. Further research is needed to corectly model the influence of visual translation on MS.

To test the validity of the proposed model, a human-out-of-the-loop experiment will be executed. Participants will partake in three visual conditions, which are the baseline, the low optical flow, and the high optical flow conditions. It is expected that MS will decrease when the amount of optical flow is increased. The experiment will produce meaningful data, as an experiment like this is missing in the literature. Results could also help autonomous car manufactures with designing their new car, as correct visual translational information might be important for diminishing MS.

Chapter 6

Conclusions

This chapter will give a brief summary of the literature research that was performed. The literature research questions presented in Section 1-2 will be answered in Section 6-1. Additionally, a short research outlook is presented in Section 6-2.

6-1 Literature Study Conclusions

MS is defined as a malady caused by passive self-motion that contains certain types of dynamic and kinematic properties, in which the visual and vestibular systems play an important role. Several theories exist to explain MS, including the sensory mismatch theory, SVC theory, velocity storage theory, and the postural instability theory. In all theories verticality perception plays an important role (Bertolini & Straumann, 2016). The SVC theory is best suited for the application to autonomous vehicles, since rotational and translational motions are taken into account and seated passengers do not require postural stabilization. These findings give answers to literature research questions one and two.

Vision is one of the motion-sensitive systems, which together with the vestibular and somatosensory systems are responsible for motion perception (Cardullo et al., 2011). Signals from all these systems are integrated into one perceived motion signal by our CNS. The visual system can distinguish three types of information about self-motion or self-orientation from the visual scene. These are visual translation, visual rotation and the visual vertical (Bos et al., 2008). This information answers the third literature research question. Furthermore, conducted experiments in the literature did find an influence of the visual scene on MS severity. Providing a wide or narrow forward view reduced subject illness ratings while driving in a road vehicle (Griffin & Newman, 2004), indicating that a view of the road ahead is important for diminishing MS symptoms. Significant changes in MS were also observed when road vehicle passengers were given a task that prevented them from seeing the visual environment (Kuiper et al., 2018). Interestingly, no significant changes in MS were found during for-and-aft motion while changing the visual field (Butler & Griffin, 2006). An influence of the visual scene was only observed when rotational motions were added (Butler & Griffin, 2009). The

last two experiments only used a relatively small visual field, which might explain why no influence was observed in the first experiment. These experiments do demonstrate that the visual field can either increase or decrease MS severity, which answer the fourth literature research question.

The 6DOF-SVC model by Kamiji et al. (2007) is able to accurately predict MS development and shows a close approximation with experiment results. However, this model lacks the influence of visual motion. Model extensions for visual rotation and the visual vertical are proposed, but these only work separately for now, and experiments to verify the validity of these extensions are still needed (Liu et al., 2022; Wada et al., 2020). It became clear that the role of the visual system for MS is still underrepresented in the MS prediction models, which answers the fifth and last literature research question.

6-2 Research Outlook

To fully answer the main and sub research questions, further research is necessary. As presented in Section 5-1, the current visual translation model proposals do give promising results. However, not all frequency-amplitude combinations lead to realistic MS values. For this reason, more work on these models is required. As the research objective states, a human out-of-the-loop experiment will be conducted to verify the reliability of the model. A first proposal of this experiment is presented in Section 5-2. However, before the experiment can be executed, more work is required in designing the visual conditions, the motion profile, and the post-experiment questionnaires.

During the experiment, participants will be exposed to three different visual conditions while the physical motion stays the same. The conditions contain a baseline, a low optical flow, and high optical visual scene. The experiment results will help answer the main research question and reach the research objective. After all the data analysis has been carried out, the last step is to formulate future research recommendations.

Bibliography

Akamatsu, M., Green, P., & Bengler, K. (2013). Automotive technology and human factors research: Past, present, and future. *International Journal of Vehicular Technology*, *2013*, 1–27.

Akçelik, R., & Biggs, D. C. (1987). Acceleration profile models for vehicles in road traffic. *Transportation Science*, *21*(1), 36–54.

Angelaki, D. E., & Cullen, K. E. (2008). Vestibular system: The many facets of a multimodal sense. *Annual Review of Neuroscience*, *31*(1), 125–150.

Begg, D. (2014). *A 2050 vision for London: What are the implications of driverless transport?* (Tech. Rep.). Clear Chanel.

Benson, A. J., Hutt, E. C., & Brown, S. F. (1989). Thresholds for the perception of whole body angular movement about a vertical axis. *Aviation, Space, and Environmental Medicine*, *60*(3), 205—213.

Berthoz, A., Pavard, B., & Young, L. R. (1975). Perception of linear horizontal self-motion induced by peripheral vision (linear vection) basic characteristics and visual-vestibular interactions. *Experimental Brain Research*, *23*(5), 471–489.

Bertolini, G., & Straumann, D. (2016). Moving in a moving world: A review on vestibular motion sickness. *Frontiers in Neurology*, *7*(14), 1–11.

Bles, W., Bos, J. E., De Graaf, B., Groen, E., & Wertheim, A. H. (1998). Motion sickness: Only one provocative conflict? *Brain Research Bulletin*, *47*(5), 481–487.

Bonato, F., Bubka, A., Palmisano, S., Phillip, D., & Moreno, G. (2008). Vection change exacerbates simulator sickness in virtual environments. *Presence: Teleoperators and Virtual Environments*, *17*(3), 283–292.

Bos, J. E., & Bles, W. (1998). Modelling motion sickness and subjective vertical mismatch detailed for vertical motions. *Brain Research Bulletin*, *47*(5), 537–542.

Bos, J. E., & Bles, W. (2002). Theoretical considerations on canal-otolith interaction and an observer model. *Biological cybernetics*, *86*(3), 191–207.

Bos, J. E., Bles, W., & Groen, E. L. (2008). A theory on visually induced motion sickness. *Displays*, *29*(2), 47–57.

Bos, J. E., & Correia Grácio, B. J. (2015). Perceived radial translation during centrifugation. *Journal of Vestibular Research*, *25*(3-4), 119–124.

Bos, J. E., MacKinnon, S. N., & Patterson, A. (2005). Motion sickness symptoms in a ship motion simulator: Effects of inside, outside and no view. *Aviation, Space, and Environmental Medicine*, *76*(12), 1111–1118.

Braccesi, C., & Cianetti, F. (2011). Motion sickness. Part i: Development of a model for predicting motion sickness incidence. *International Journal of Human Factors Modelling and Simulation*, *2*(3), 163–187.

Brandt, T., & Daroff, R. B. (1980). The multisensory physiological and pathological vertigo syndromes. *Annals of Neurology: Official Journal of the American Neurological Association and the Child Neurology Society*, *7*(3), 195–203.

Brandt, T. H., Dichgans, J., & Koenig, E. (1973). Differential effects of central versus peripheral vision on egocentric and exocentric motion perception. , *16*(5), 476–491.

Butler, C. A., & Griffin, M. J. (2006). Motion sickness during fore-and-aft oscillation: Effect of the visual scene. *Aviation, Space, and Environmental Medicine*, *77*(12), 1236–1243.

Butler, C. A., & Griffin, M. J. (2009). Motion sickness with combined fore-aft and pitch oscillation: Effect of phase and the visual scene. *Aviation, Space, and Environmental Medicine*, *80*(11), 946–954.

Calderone, J. B., & Kaiser, M. K. (1989). Visual acceleration detection: Effect of sign and motion orientation. *Perception & Psychophysics*, *45*(5), 391–394.

Cardullo, F., Sweet, B., Hosman, R., & Coon, C. (2011). The human visual system and its role in motion perception. In *AIAA Modeling and Simulation Technologies Conference.*

Cheung, B. S., Howard, I. P., & Money, K. E. (1991). Visually-induced sickness in normal and bilaterally labyrinthine-defective subjects. *Aviation, Space, and Environmental Medicine*, *62*(6), 527–531.

Clark, T. K., Newman, M. C., Karmali, F., Oman, C. M., & Merfeld, D. M. (2019). Mathematical models for dynamic, multisensory spatial orientation perception. *Progress in Brain Research*, *248*, 65–90.

Correia Grácio, B. J., Bos, J. E., van Paassen, M. M., & Mulder, M. (2014). Perceptual scaling of visual and inertial cues. *Experimental Brain Research*, *232*(2), 637–646.

Dichgans, J., & Brandt, T. (1978). Visual-vestibular interaction: Effects on self-motion perception and postural control. In *Perception* (pp. 755–804). Berlin, Heidelberg: Springer.

Diels, C., & Bos, J. E. (2016). Self-driving carsickness. *Applied Ergonomics*, *53*, 374–382.

Diels, C., Ye, Y., Bos, J. E., & Maeda, S. (2022). Motion sickness in automated vehicles: Principal research questions and the need for common protocols. *SAE International*, *5*(2), 1–14.

Duh, H. B.-L., Parker, D. E., Philips, J. O., & Furness, T. A. (2004). "Conflicting" motion cues to the visual and vestibular self-motion systems around 0.06 hz evoke simulator sickness. *Human Factors*, *46*(1), 142–153.

Feenstra, P. J., Bos, J. E., & van Gent, R. N. H. W. (2011). A visual display enhancing comfort by counteracting airsickness. *Displays*, *32*(4), 194–200.

Fukuda, T. (1976). Postural behaviour and motion sickness. *Acta Oto-Laryngologica*, *81*(3-6), 237–241.

Gibson, J. J. (1950). *The perception of the visual world.* Houghton Mifflin.

Golding, J. F. (2006a). Motion sickness susceptibility. *Autonomic Neuroscience*, *129*(1-2), 67–76.

Golding, J. F. (2006b). Predicting individual differences in motion sickness susceptibility by questionnaire. *Personality and Individual Differences*, *41*(2), 237–248.

Golding, J. F., & Gresty, M. A. (2015). Pathophysiology and treatment of motion sickness. *Current Opinion in Neurology*, *28*(1), 83–88.

Griffin, M. J., & Newman, M. M. (2004). Visual field effects on motion sickness in cars. *Aviation, Space, and Environmental Medicine*, *75*(9), 739–748.

Haslwanter, T., Jaeger, R., Mayr, S., & Fetter, M. (2000). Three-dimensional eye-movement responses to off-vertical axis rotations in humans. *Experimental Brain Research*, *134*(1), 96–106.

Hosman, R. J. A. W., & Vaart, J. C. (1983). Perception of roll rate from an artificial horizon and peripheral displays. In *19th Annual Conference on Manual Control.*

Inoue, S., Liu, H., & Wada, T. (2023). *Revisiting motion sickness models based on SVC theory considering motion perception* (Tech. Rep.). SAE Technical Paper.

Jalgaonkar, N., Schulman, D. S., Ojha, S., & Awtar, S. (2021). A visual-vestibular model to predict motion sickness response in passengers of autonomous vehicles. *SAE International Journal of Advances and Current Practices in Mobility*, *3*(5), 2421–2432.

Jones, M. L. H., Le, V. C., Ebert, S. M., Sienko, K. H., Reed, M. P., & Sayer, J. R. (2019). Motion sickness in passenger vehicles during test track operations. *Ergonomics*, *62*(10), 1357–1371.

Kamiji, N., Kurata, Y., Wada, T., & Doi, S. (2007). Modeling and validation of carsickness mechanism. In *SICE Annual Conference 2007* (pp. 1138–1143).

Keshavarz, B., Riecke, B. E., Hettinger, L. J., & Campos, J. L. (2015). Vection and visually induced motion sickness: How are they related? *Frontiers in Psychology*, *6*, 472.

Khalid, H., Turan, O., Bos, J. E., & Incecik, A. (2011). Application of the subjective vertical–horizontal-conflict physiological motion sickness model to the field trials of contemporary vessels. *Ocean Engineering*, *38*(1), 22–33.

Kitahara, M., & Uno, R. (1967). XII equilibrium and vertigo in a tilting environment. *Annals of Otology, Rhinology & Laryngology*, *76*(1), 166–178.

Kuiper, O. X., Bos, J. E., & Diels, C. (2018). Looking forward: In-vehicle auxiliary display positioning affects carsickness. *Applied Ergonomics*, *68*, 169–175.

Lappe, M., Bremmer, F., & van den Berg, A. V. (1999). Perception of self-motion from visual flow. *Trends in Cognitive Sciences*, *3*(9), 329–336.

Liu, H., Inoue, S., & Wada, T. (2022). Motion sickness modeling with visual vertical estimation and its application to autonomous personal mobility vehicles. In *2022 ieee intelligent vehicles symposium (iv)* (pp. 1415–1422).

Mayne, R. (1974). A systems concept of the vestibular organs. In H. H. Kornhuber (Ed.), *Vestibular System Part 2: Psychophysics, Applied Aspects and General Interpretations. Handbook of Sensory Physiology, vol 6 / 2* (pp. 493–580). Springer.

McCauley, M. E., Royal, J. W., Wylie, C. D., O'Hanlon, J. F., & Mackie, R. R. (1976). *Motion sickness incidence: Exploratory studies of habituation, pitch and roll, and the refinement of a mathematical model* (Tech. Rep.). Human Factors Research Inc.

Merfeld, D. M. (1995). Modeling the vestibulo-ocular reflex of the squirrel monkey during eccentric rotation and roll tilt. *Experimental Brain Research*, *106*(1), 123–134.

Merfeld, D. M., Young, L. R., Oman, C. M., & Shelhamert, M. J. (1993). A multidimensional model of the effect of gravity on the spatial orientation of the monkey. *Journal of Vestibular Research*, *3*(2), 141–161.

Mittelstaedt, H. (1983). A new solution to the problem of the subjective vertical. *Naturwissenschaften*, *70*(6), 272–281.

Monen, J., & Brenner, E. (1994). Detecting changes in one's own velocity from the optic

flow. *Perception*, *23*(6), 681–690.

Money, K. E. (1970). Motion sickness. *Physiological Reviews*, *50*(1), 1–39.

Newman, M. C. (2009). *A multisensory observer model for human spatial orientation perception* (Unpublished doctoral dissertation). Massachusetts Institute of Technology.

Oman, C. M. (1982). A heuristic mathematical model for the dynamics of sensory conflict and motion sickness. *Acta Oto-Laryngologica*, *94*(sup392), 4–44.

Probst, T., Krafczyk, S., & Büchele, W. (1982). Visuelle prävention der bewegungskrankheit im auto. *Archiv für Psychiatrie und Nervenkrankheiten*, *231*, 409–421.

Raphan, T. H., Matsuo, V., & Cohen, B. (1979). Velocity storage in the vestibulo-ocular reflex arc (VOR). *Experimental Brain Research*, *35*(2), 229–248.

Reason, J. T., & Brand, J. J. (1975). *Motion sickness*. Academic Press.

Reavley, C. M., Golding, J. F., Cherkas, L. F., Spector, T. D., & MacGregor, A. J. (2006). Genetic influences on motion sickness susceptibility in adult women: A classical twin study. *Aviation, Space, and Environmental Medicine*, *77*(11), 1148–1152.

Reid, L. D., & Nahon, M. A. (1985). *Flight simulation motion-base drive algorithms: Part 1. Developing and testing equations* (Tech. Rep.). University of Toronto.

Riccio, G. E., & Stoffregen, T. A. (1991). An ecological theory of motion sickness and postural instability. *Ecological Psychology*, *3*(3), 195–240.

Robinson, D. A. (1977). Linear addition of optokinetic and vestibular signals in the vestibular nucleus. *Experimental Brain Research*, *30*(2), 447–450.

Rolnick, A., & Bles, W. (1989). Performance and well-being under tilting conditions: The effects of visual reference and artificial horizon. *Aviation, Space, and Environmental Medicine*, *60*(8), 779—785.

Rolnick, A., & Lubow, R. E. (1991). Why is the driver rarely motion sick? The role of controllability in motion sickness. *Ergonomics*, *34*(7), 867-879.

Salter, S., Diels, C., Herriotts, P., Kanarachos, S., & Thake, D. (2019). Motion sickness in automated vehicles with forward and rearward facing seating orientations. *Applied Ergonomics*, *78*, 54–61.

Schmidt, E. A., Kuiper, O. X., Wolter, S., Diels, C., & Bos, J. E. (2020). An international survey on the incidence and modulating factors of carsickness. *Transportation Research Part F: Traffic Psychology and Behaviour*, *71*, 76–87.

Stoffregen, T. A., & Smart Jr, L. J. (1998). Postural instability precedes motion sickness. *Brain Research Bulletin*, *47*(5), 437–448.

Telban, R. J., & Cardullo, F. M. (2001). An integrated model of human motion perception with visual-vestibular interaction. In *AIAA Modeling and Simulation Technologies Conference and Exhibit.*

Telban, R. J., & Cardullo, F. M. (2005). *Motion cueing algorithm development: Human-centered linear and nonlinear approaches* (Tech. Rep.). State University of New York.

Turner, M., & Griffin, M. J. (1999). Motion sickness in public road transport: Passenger behaviour and susceptibility. *Ergonomics*, *42*(3), 444–461.

Tyler, D. B., & Bard, P. (1949). Motion sickness. *Physiological Reviews*, *29*(4), 311–369.

Van der Steen, F. A. M. (1998). *Self-motion perception* (Unpublished doctoral dissertation). Delft University of Technology.

Wada, T., Fujisawa, S., & Doi, S. (2018). Analysis of driver's head tilt using a mathematical model of motion sickness. *International Journal of Industrial Ergonomics*, *63*, 89–97.

Wada, T., Kamij, N., et al. (2015). A mathematical model of motion sickness in 6DOF motion and its application to vehicle passengers. *arXiv preprint arXiv:1504.05261*.

Wada, T., Kawano, J., Okafuji, Y., Takamatsu, A., & Makita, M. (2020). A computational model of motion sickness considering visual and vestibular information. In *2020 IEEE International Conference on Systems, Man, and Cybernetics (SMC)* (pp. 1758–1763).

Young, L. R. (1978). Visually induced motion in flight simulation. In *AGARD Symposium on Flight Simulation.*

Zacharias, G. (1977). *Motion sensation dependence on visual and vestibular cues* (Unpublished doctoral dissertation). Massachusetts Institute of Technology.

Part III

Thesis Apendices

Appendix A

6DOF-SVC Model with Visual Translation

This appendix shows a more extensive analysis of the proposed 6DOF-SVC model with visual translation extension. The proposed model is shown in Figure A-1, where the additions to the model of Wada et al. (2020) are shown in red. More information about the design choices and rational of the model can be found in Part I. In the following, all parameters of the original 6DOF-SVC model were kept identical to those used by Wada et al. (2020). Furthermore, the model output was calculated for different sinusoidal signals in the x-direction (for-and-aft oscillatory motion). These signals were chosen because the model's response to different input frequencies could easily be observed. Only translational motions in the x-direction were chosen since visual translation in the y- and z-directions does not appear in car driving. However, other applications, such as virtual reality gaming, could introduce these visual translations. Therefore, further research is needed to determine whether visual translation in the y- and z-directions has an effect on MS and should be included in the 6DOF-SVC model.

A-1 Frequency Analysis

Figure A-2 shows the frequency response of the model shown in Figure A-1. The x-component of the vestibular acceleration signal a_{vest} was set to a sinusoidal signal ($a_x(t) = Asin(2\pi ft)$) with an amplitude $A = 5$ m/s^2. The y- and z-component were kept at zero. The visual velocity signal v_{vis} was the time integrated version of a_{vest}. All other inputs (i.e., ω_{vest} and ω_{vis}) were set to zero. The MSI values reached after 30 minutes of motion for different frequencies is plotted in Figure A-2.

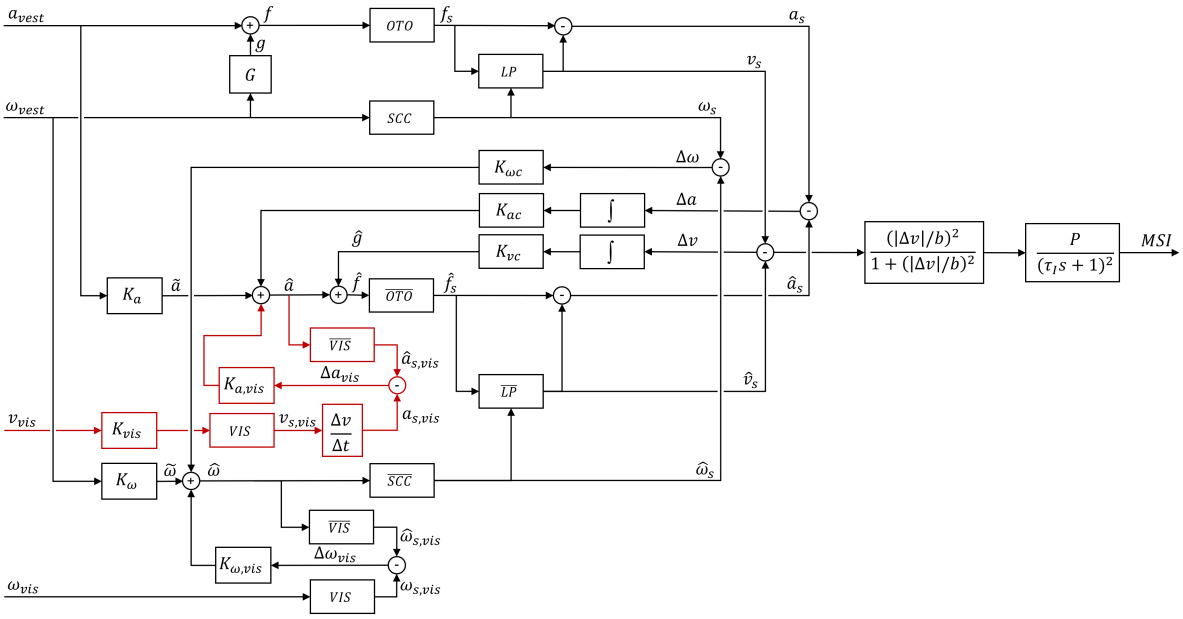

Figure A-1: 6DOF-SVC model with visual translation extension (shown in red)

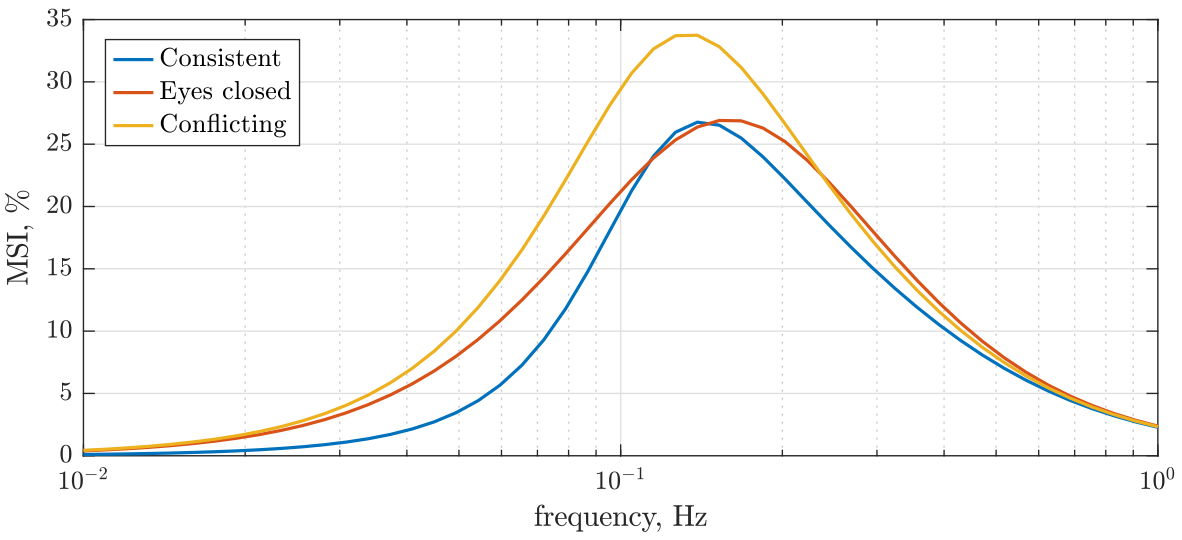

Figure A-2: Frequency responses of the 6DOF-SVC model with visual translation extension for consistent visual and vestibular information, eyes closed, and conflicting visual and vestibular information. The MSI value after 30 minutes of oscillatory motion is shown ($a_x(t) = Asin(2\pi ft)$ with $A = 5$ m/s^2)

The values for the visual gains used for the simulations are shown in Table A-1. Three conditions were tested, which were a consistent visual and vestibular information condition, an eyes closed condition (eliminating the visual influence), and a conflicting visual and vestibular information condition. The values of K_{vis} and $K_{a,vis}$ were both set to one for the consistent condition, as the input signals a_{vest} and v_{vis} were consistent. The value of $K_{a,vis}$ was set to zero for the eyes closed condition, as this eliminates the influence of visual translation on the

model (the value of K_{vis} is not important here), and returns the model to the original model of Wada et al. (2020). The conflicting condition mimics a scenario in which physical motion is present but not seen in the visual environment. The gain of $K_{a,vis}$ is set to one as visual movement is expected since the eyes are open. However, the visual movement is not seen resulting in a value of zero for K_{vis}.

Table A-1: Visual gains used for the frequency responses of the 6DOF-SVC model with visual translation

	K_{vis} [-]	$K_{a,vis}$ [-]
Consistent	1	1
Eyes closed	-	0
Conflicting	0	1

The results in Figure A-2 show an increase in MSI for the conflicting scenario compared to the eyes closed scenario (i.e., the original 6DOF-SVC model (Wada et al., 2020)). This is especially true for the lower frequencies (< 0.2 Hz), which is caused by the low-pass filter included within the visual dynamics (VIS and $\overline{VIS}$). The influence of visual translation at higher frequencies (> 0.2 Hz) is low, making the conflict signal Δa_{vis} in the model almost zero. This results in a similar MSI behavior for the eyes closed and conflicting scenarios at high frequencies, as could be observed from the figure. Furthermore, the consistent visual and vestibular motion scenario has lower MSI values for low frequencies (< 0.1 Hz) than those in the eyes closed scenario, which could also be explained with the low-pass filter included within the visual dynamics. This is because the influence of visual translation is highest in this frequency region. However, the peak value of the consistent and eyes closed scenarios are almost equal in height but at a slightly different location. Apparently, the visual dynamics decrease the peak frequency of MSI. Again, the MSI in the consistent scenario only slightly differs from that of the eyes closed scenrio at higher frequencies (> 0.2 Hz), as the influence of visual translation is low at these frequencies, making the conflict signal Δa_{vis} almost zero. More research is required to confirm whether visual translation effects the frequency response of MS as shown in Figure A-2, as the experiment presented in this thesis report does not provide enough evidence.

A-2 Visual Gains Analysis

A small sensitivity analysis to see the effect of the visual gains $K_{a,vis}$ and K_{vis} on the model's output was carried out. Figure A-3 shows the influence of increasing the visual acceleration gain $K_{a,vis}$ on the MSI ouput of the model. The value of $K_{a,vis}$ is based on the type of visual information (e.g., consistent, conflicting or eyes closed), similar to how the value of $K_{\omega,vis}$ is determined in Wada et al. (2020). The more credible the visual environment is, the higher the value of the visual acceleration gain $K_{a,vis}$. Figure A-3 illustrates that the MSI decreases when the value of $K_{a,vis}$ increases. The input to this model was again a sinusoidal signal on the x-component of the inertial acceleration ($a_x(t) = Asin(2\pi ft)$ with $A = 5$ m/s^2 and $f = 0.06$ Hz). The visual velocity was the integrated version of the inertial acceleration, while all other inputs were set to zero. It should be noted that this graph is highly depended on the

frequency of the input signal a_x. Increasing the input frequency lowers the effect of $K_{a,vis}$ on the MSI, resulting in decreasing distances between the MSI development lines in Figure A-3. Figure A-2 also shows this effect, the influence of $K_{a,vis}$ is depended on the distance between the consistent (blue) and eyes closed (red) scenarios.

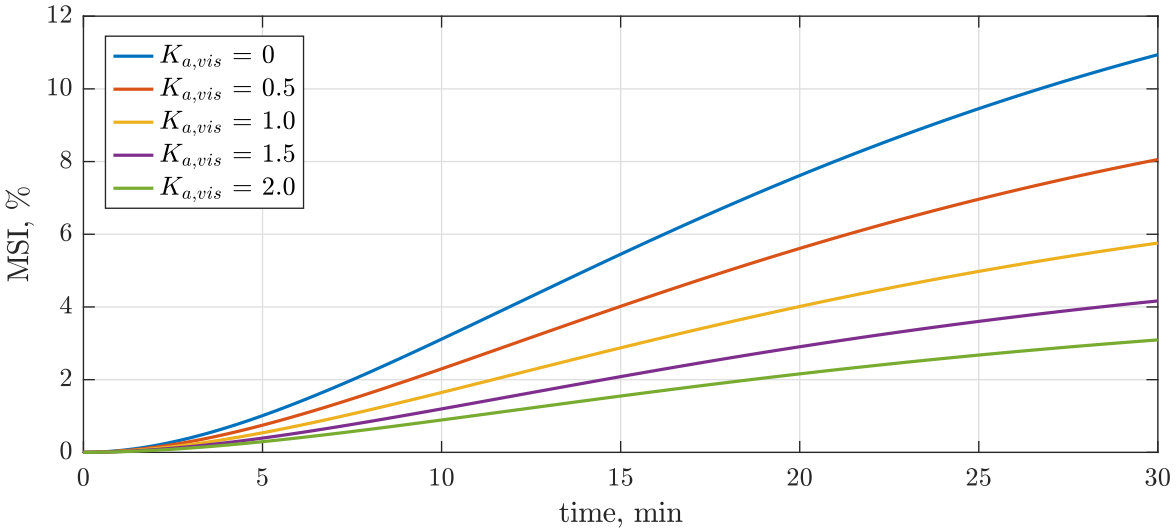

Figure A-3: Influence of $K_{a,vis}$ on the MSI ouput of the 6DOF-SVC model with visual translation extension ($a_x(t) = Asin(2\pi ft)$ with $A = 5$ m/s^2 and $f = 0.06$ Hz, $K_{vis} = 1$)

Figure A-4 shows the influence of increasing the visual gain K_{vis} on the MSI ouput of the model. The visual velocity is scaled by visual gain K_{vis} that has a value between zero (no global optical flow rate and low visual fidelity) and one (high optical flow rate and high visual fidelity). The same input signals as used in the previous sections are used here. As visible from the graph, increasing visual gain K_{vis} decreases the MSI. Again, this figure is highly depended on the frequency of the input signal a_x. The smaller the distance between the eyes closed (red) and conflicting (yellow) scenarios in Figure A-2, the lower the influence of K_{vis} on the MSI development is. The MSI lines of Figure A-4 are closer to each other when the inpuit frequency is increased.

A-3 Experiment Motion Analysis

The physical and visual motions presented to the participants during the experiment are different from a real-life driving scenario. First, tilt coordination is used that presents rotational physical motions, and second, the physical motions are scaled down by the motion filter, which creates an amplitude difference between the physical and visual motions. These phenomena cause a incongruent physical and visual motion inputs to the model, which changes the behavior of the model. Figure A-5 shows the influence of visual gains $K_{a,vis}$ and K_{vis} on MSI values for designed and simulator motions. Figures A-5a and A-5c show the results for the designed motion (congruent visual and physical motion) and have similar behavior as the results resented in the previous chapter. Figures A-5b and A-5d show the results for the simulator motion (incongruent visual and physical motion). As seen in Figure A-5b, the effect of $K_{a,vis}$ on MSI is different for the simulator motion compared to the effect for the

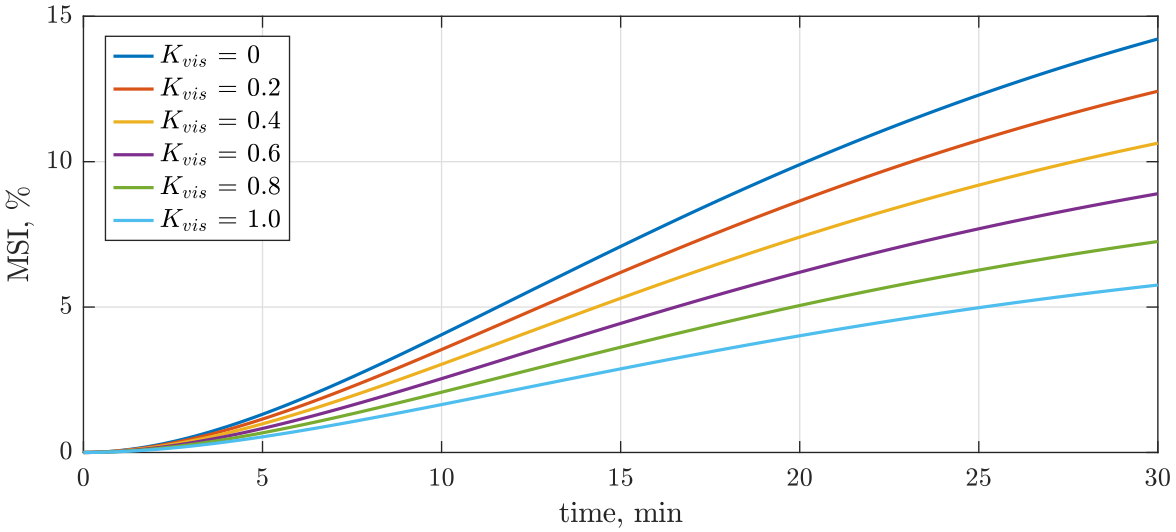

Figure A-4: Influence of K_{vis} on the MSI ouput of the 6DOF-SVC model with visual translation extension ($a_x(t) = Asin(2\pi ft)$ with $A = 5$ m/s^2 and $f = 0.06$ Hz, $K_{a,vis} = 1$)

designed motion. Since the amplitudes of a_{vest} and v_{vis} do not match, a conflict between these two signals exist. The amplitude of the visual velocity is higher than the amplitude of the simulator motion (due to motion filtering), which results in an unrealistic visual acceleration conflict signal Δa_{vis}. Setting the influence of this conflict signal too high (by increasing $K_{a,vis}$ to values higher than 3), only worsens the internally estimated acceleration signal $\hat{a}$, which therefore increases the MSI output.

The analysis above suggests that the current model is not well suited for simulated environments. Amplitude differences between visual and physical translational movements can be accepted by the CNS (as shown by Correia Grácio et al. (2014)). The visual gain K_{vis} in the model can correct for this amplitude difference, but it not known whether the CNS actually applies such a gain on the observed visual velocity. Furthermore, the value of visual acceleration gain $K_{a,vis}$ is probably not constant during simulated environments as this is depended on whether the CNS decides to use the visual translational information for self-motion perception. Telban and Cardullo (2005) proposed a self-motion perception model that takes the amplitude and duration of the conflict between visual and physical cues into account for determining the influence of the visual cues. Implementing this in the current model could be a solution for the problem presented above.

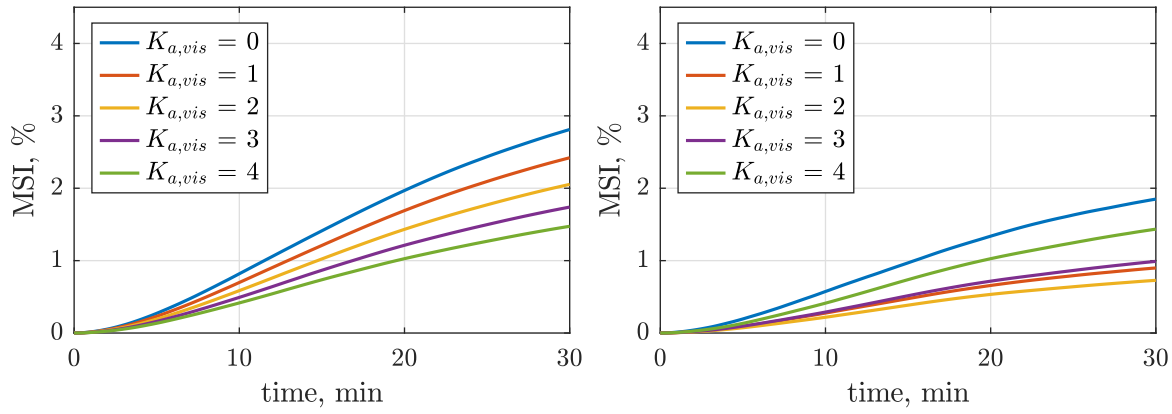

(a) Influence of $K_{a,vis}$ on designed motion ($K_{vis} = 1$)

(b) Influence of $K_{a,vis}$ on simulator motion ($K_{vis} = 1$)

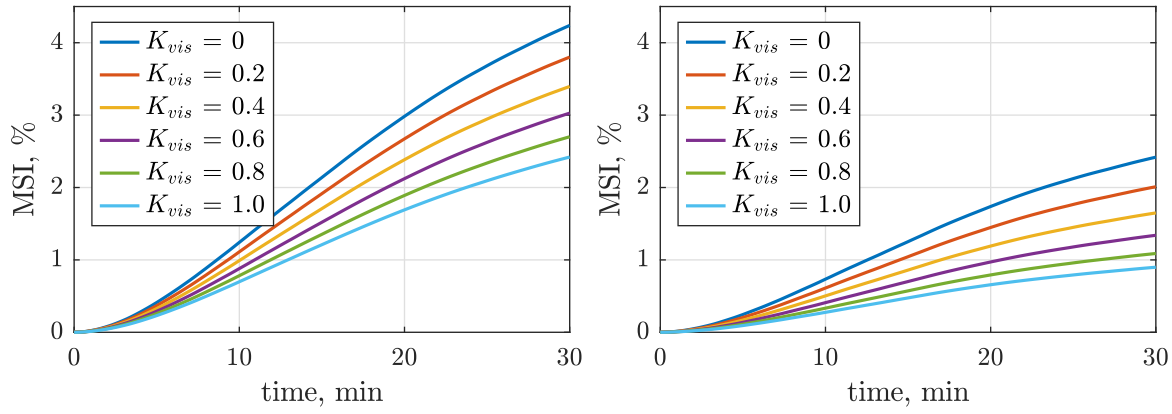

(c) Influence of K_{vis} on designed motion ($K_{a,vis} = 1$)

(d) Influence of K_{vis} on simulator motion ($K_{a,vis} = 1$)

Figure A-5: Influence of visual gains $K_{a,vis}$ and K_{vis} on MSI values for designed and simulator motions

Appendix B

Motion Profile and Motion Tuning

This appendix contains the designed motion profiles and simulator motions after motion tuning of the experiment.

B-1 Motion Profile

As discussed, the motion profile featured three velocities that usually appear in urban driving: 30, 50 and 70 km/h. Figure B-1 shows the designed velocity profiles of the three acceleration and three deceleration maneuvers.

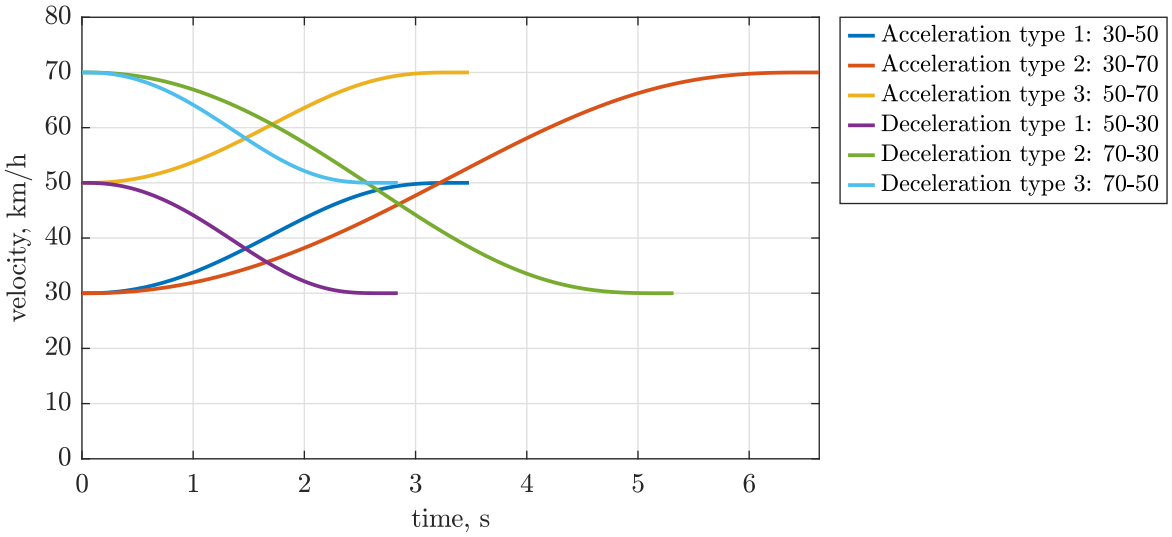

Figure B-1: Velocity profiles of the three acceleration and three deceleration maneuvers

Figure B-2 shows the designed acceleration profiles of the three acceleration and three deceleration maneuvers. The kinematic polynomial acceleration model of Akçelik and Biggs

(1987) was used to create these profiles (see Part I for an overview of the design choices). Acceleration type 1 and 3, and deceleration type 1 and 3 have equal acceleration profiles, therefore, only one of these is shown in the figure.

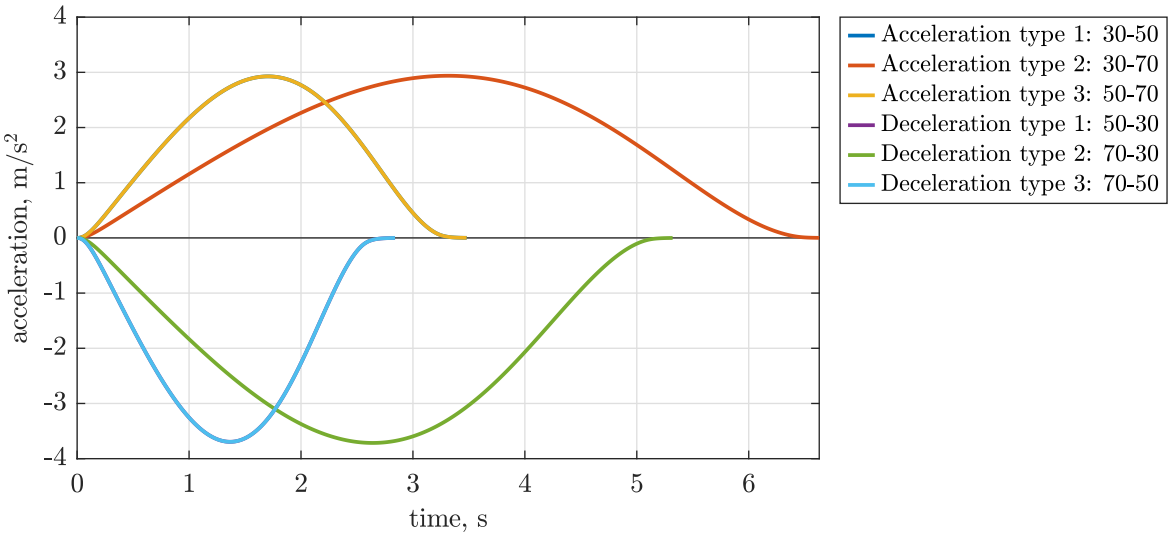

Figure B-2: Acceleration profiles of the three acceleration and three deceleration maneuvers (acceleration type 1 and 3, and deceleration type 1 and 3 have equal acceleration profiles)

The jerk profiles of the designed motion profile are shown in Figure B-3. As is visible, the jerk of the short deceleration maneuvers is higher than that of the other maneuvers. Later it was found that these high jerk values caused an "error" in the motion filer used for motion tuning (explained in the next section).

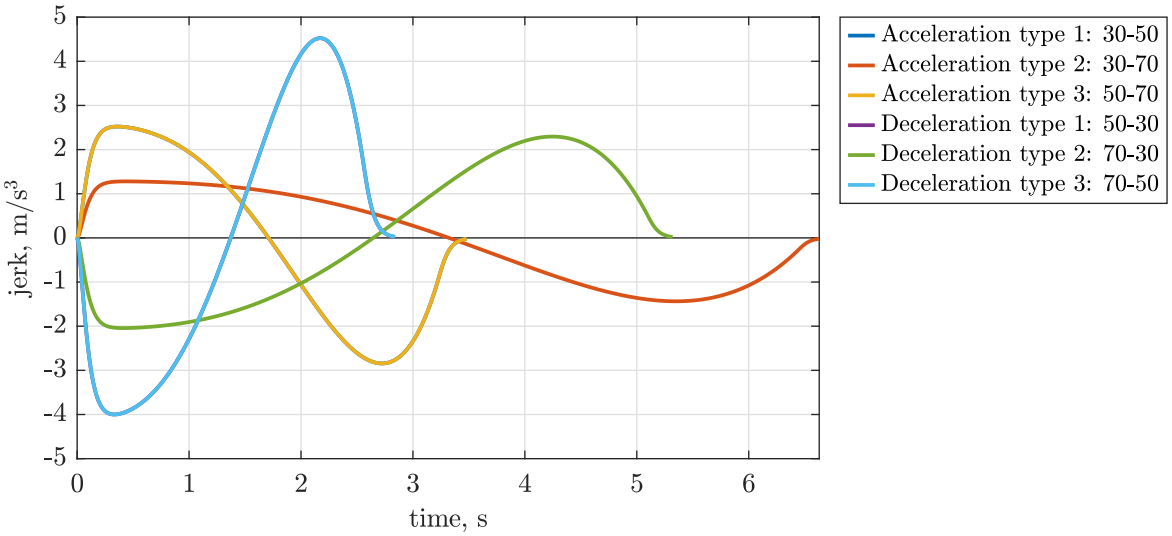

Figure B-3: Jerk profiles of the three acceleration and three deceleration maneuvers (acceleration type 1 and 3, and deceleration type 1 and 3 have equal jerk profiles)

The complete 30-minute motion profile existed of 134 maneuvers. Each type of maneuver occurred 22 times, which, together with the start and end maneuvers, made a total of 134

maneuvers. These maneuvers were pseudo-randomly ordered and the duration of the constant-velocity phases in between maneuvers was between six and twelve seconds. This value was dependent on the minimum amount of time required for prepositioning of the simulator, combined with some variation time to prevent anticipation of upcoming maneuvers. See Part I for a figure of the complete velocity profile of the experiment.

B-2 Motion Tuning

A classical washout filter (as shown in Figure B-4) was used to translate the designed vehicle motion profile into simulator motions that remain within the motion envelope of the SRS. The designed motion profile only featured specific forces, meaning that the vehicle angular rates input signal was set to zero. The filter's output were simulator positions and attitude. In the current experiment, only for-and-aft motions were considered, resulting in only longitudinal motion of the simulator (surge, heave, and pitch movements). For an overview of the filter settings used in the current experiment, see Part I.

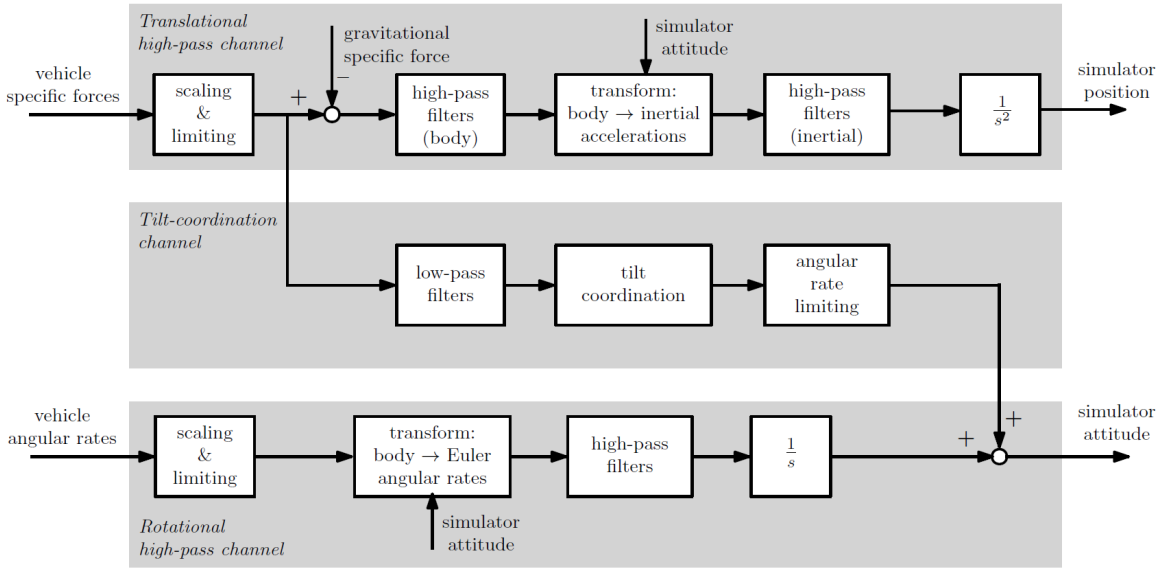

Figure B-4: Classical washout filter used to translate the designed motion profile to simulator motions (Reid & Nahon, 1985)

Figure B-5 shows the specific force of the head in the x-direction (surge) for the designed motion profile (blue) and the motion filtered simulator motion (red). Seconds 10 until 70 of the motion profile are shown, as these include all maneuver types (see text in the figure). The specific force in the simulator includes translational movements and the additional gravity component created by the tilt coordination. The figure clearly shows that the amplitude of the simulator motion is substantially lower than the designed motion. Additionally, some lag is created as the simulator is still moving after the designed motion has ended. Furthermore, the simulator motion also shows the prepositioning of the simulator (small acceleration values between maneuvers).

The longer acceleration (30→70) and the longer deceleration (70→30) simulator movements have a similar specific force profile to that of the designed motion profile, i.e., the shape of

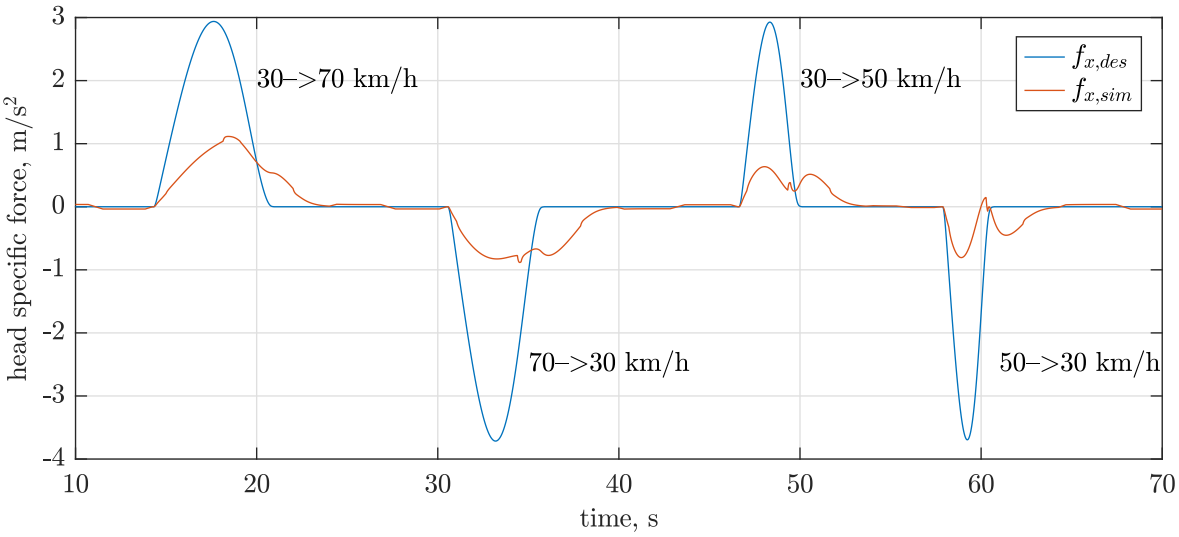

Figure B-5: The specific force of the head in the x-direction (surge) for the designed motion profile (blue) and the simulator motion after motion filtering (red). Seconds 10 until 70 are shown as these include all maneuver types (indicated by the velocities in the figure)

the graphs are similar (neglecting the amplitude reduction and additional lag). However, the specific force profile of the shorter acceleration (30→50) and the shorter deceleration (50→30) show a decrease in the experienced acceleration. Especially for the shorter deceleration, since the specific force value becomes positive for a short moment. This phenomenon was caused by the angular rate limiting in the tilt coordination channel (Figure B-4). Figure B-6 shows the required pitch angle by tilt coordination and the simulator pitch angle after angular rate limiting. As clearly visible, the required change in pitch, i.e., the required pitch rate, was substantially higher than what is allowed by the tilt rate limiter for the short deceleration maneuver (50→30). As a matter of fact, all maneuvers were limited by the tilt rate limiter as seen by the straight lines in the simulator pitch angle, but the discrepancies were highest for the short deceleration. The high required pitch rate was caused by the designed motion profile, as the high jerk values of the short deceleration (Figure B-3) are correlated with a high pitch rate. Furthermore, the natural frequency set in the tilt coordination's low-pass filter also contributed to the high required pitch rates, as a lower value would have lowered the maximum required pitch rate. Because these high pitch rates could not be achieved, the gravitational acceleration component in the simulator specific force profile (Figure B-5) was lower than required by the tilt coordination channel, making the specific force too low and therefore unrealistic.

This unrealistically simulated short deceleration maneuver was also noticed by the participants, since comments during or after the experiment described a two-phase braking maneuver or a small "tap" felt during braking. Some participants also noted that this maneuver was the most provocative during the experiment, especially as this two-phase braking is not seen in the visual motion. To investigate whether this maneuver did indeed cause more MS, the average increase in mean MISC after a specific maneuver occurred within the 30 seconds before a MISC "beep" is shown in Figure B-7 for all three conditions. As seen, the average increase in mean MISC for the 70→50 maneuver is high under all conditions. However, it is striking that this is not observed for the 50→30 maneuver (especially for BL, as this value

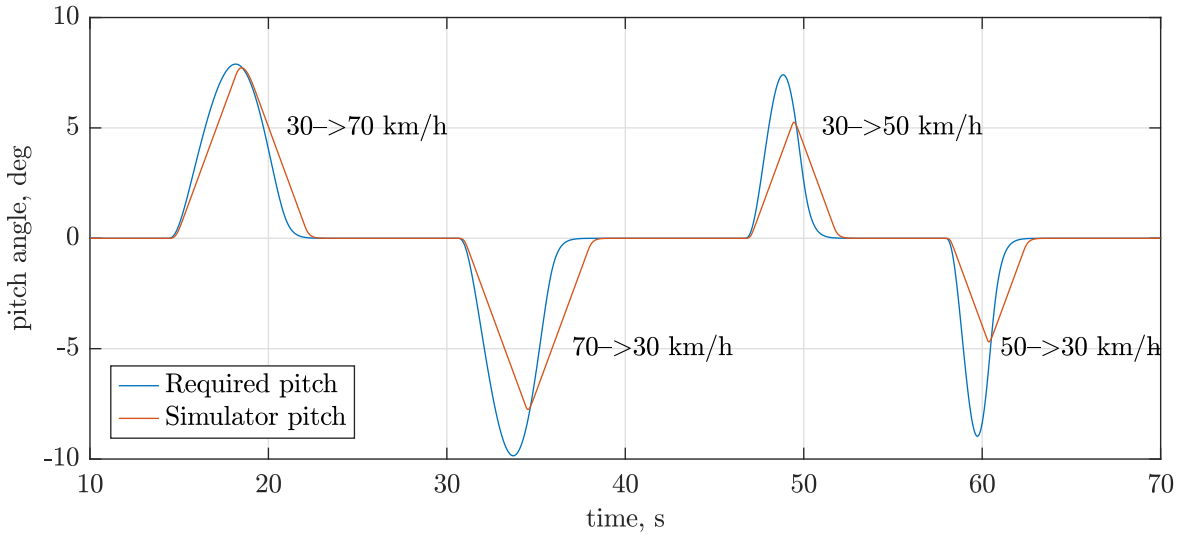

Figure B-6: The required pitch angle (blue) by tilt coordination and the simulator pitch angle (red) after angular rate limiting. Seconds 10 until 70 are shown as these include all maneuver types (indicated by the velocities in the figure)

is negative), as the simulator motions of both maneuvers are identical. Hence, this analysis could not confirm that the slow deceleration maneuvers (70→50 and 50→30) were most provocative. Furthermore, it is interesting that the average increase in the mean MISC for BL is high for the slow maneuvers 30→70 and 70→30. These maneuvers have the highest motion amplitudes (in terms of specific force) and are lacking any visual information. This could be a possible explanation for the values found.

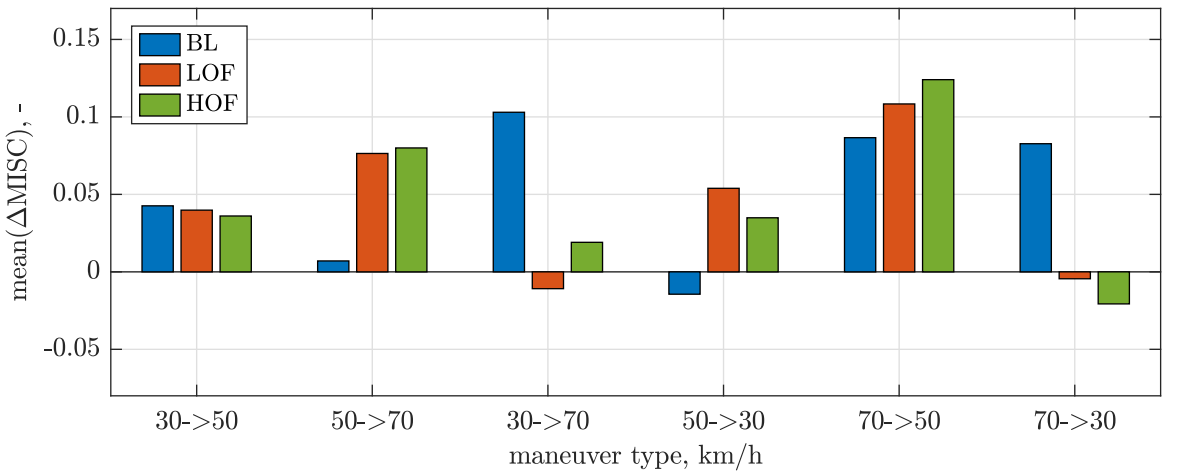

Figure B-7: The average increase in mean MISC after a specific maneuver occurred in the 30 seconds before a MISC "beep"

Appendix C

Experiment Results

This appendix contains results of the experiment that are not shown in Part I. The following sections present the following:

- The **head motion analysis** that was carried out before the experiment to investigate the effectiveness of the neck brace that was worn by the participants during the experiment.
- The individual **differences in mean MISC** values between LOF/HOF and BL conditions
- The **MSSQ distribution** of the experiment participants
- The occurrence and severity of **all 24 MS symptoms** asked for in the MS checklist
- The **physical and visual motion assessment** seven-point likert scale questions that were asked after each experiment session.
- The **subjective motion comfort assessment** which were questions asked after the last experiment trial.

C-1 Head Motion Analysis

A head motion experiment was carried out before the experiment to investigate the effectiveness of the neck brace that was worn by the participants during the experiment. A small experiment was conducted with one participant who executed two runs: one session without neck brace and one session with neck brace. All other variables were kept equal to those of the original experiment. The two sessions were performed with visual motions from the HOF condition. To measure the effectiveness of the neck brace, the participant was instructed to wear an angular rate sensor on the head. Furthermore, the participant had no knowledge about the goal of the experiment and was instructed to keep looking forward and keep a relaxed body posture.

The resulting head pitch rates of the two conditions are shown in Figure C-1. The experiment did not cover the full 30-minute motion profile of the original experiment as this was not needed to examine the effectiveness of the neck brace. As clearly visible, the pitch rate of the condition with neck brace shows substantially less spread than the pitch rate without neck brace. The SD of the head pitch rate for sessions with and without neck brace was 1.97 deg/s and 8.71 deg/s, respectively. This indicates that the neck brace indeed reduced head rotations.

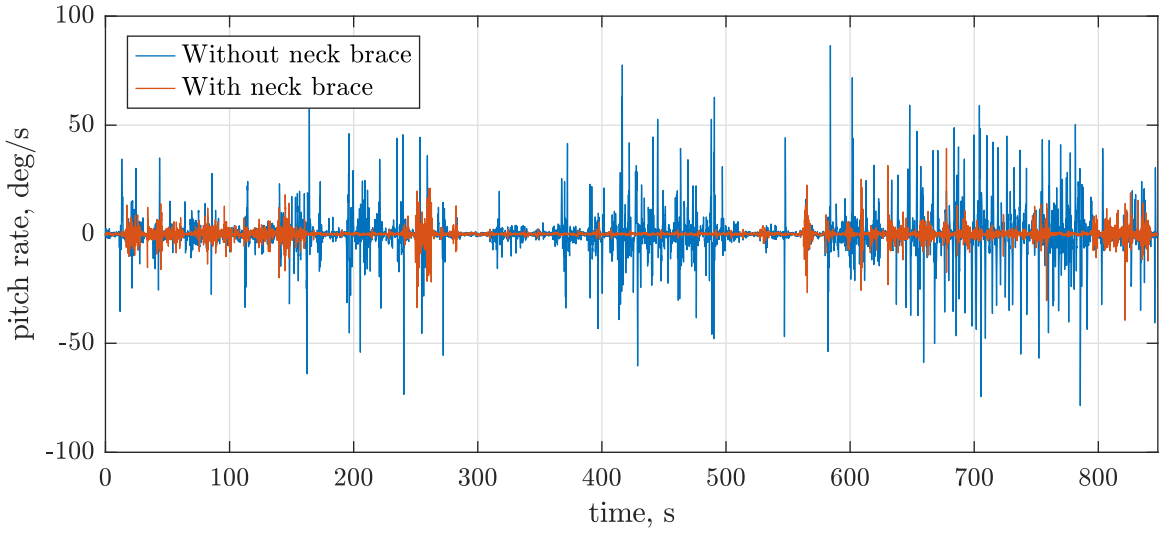

Figure C-1: Head pitch rate of subject with and without neck brace

C-2 MISC

Figure C-2 shows the individual differences in mean MISC values between LOF/HOF and BL conditions. These values were the average MISC value of the complete 30-minute motion exposure of LOF (orange) and HOF (green) compared to the average MISC value of BL (blue). This is a different way of showing the individual preferences compared to the participant reduction values used in Part I, but uses the same information. The $T1$, $T2$, and $T3$ values indicate in which trial the condition was performed.

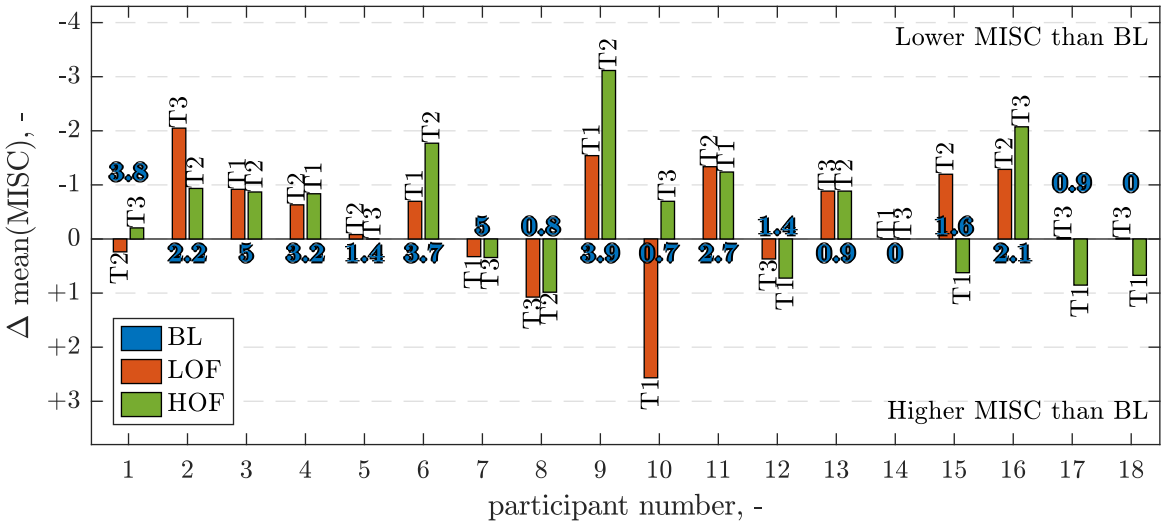

Figure C-2: Individual differences in mean MISC values between LOF/HOF and BL conditions

C-3 MSSQ

Figure C-3a shows the MSSQ values of the participant represented in a boxplot format. The median MSSQ score of the participants was 6.2 ($\mu = 7.33$, $\sigma = 6.35$) which is around the 30th percentile of MS susceptibility (Golding, 2006b). Figure C-3b displays the MSSQ boxplots for all six condition orders, which includes three participants per boxplot. This figure was made to investigate whether large differences in MSSQ values existed between the six different condition orders. As seen, the median of order group HOF→LOF→BL is higher than the others. Furthermore, the spread of the MSSQ values differs per condition order. These differences could have affected the mean MISC values of the experiment, however, with only three participants per order group it is challenging to keep these MSSQ values equal across all order groups.

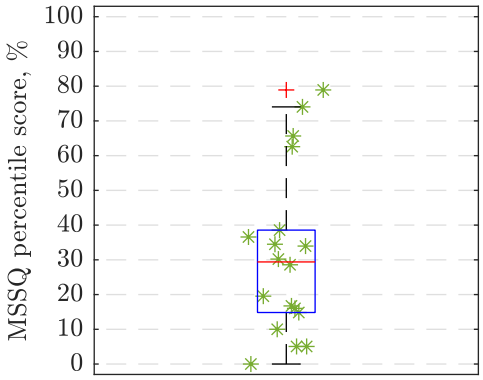

(a) Boxplot representation of the participants' MSSQ values (each green star is an individual participant)

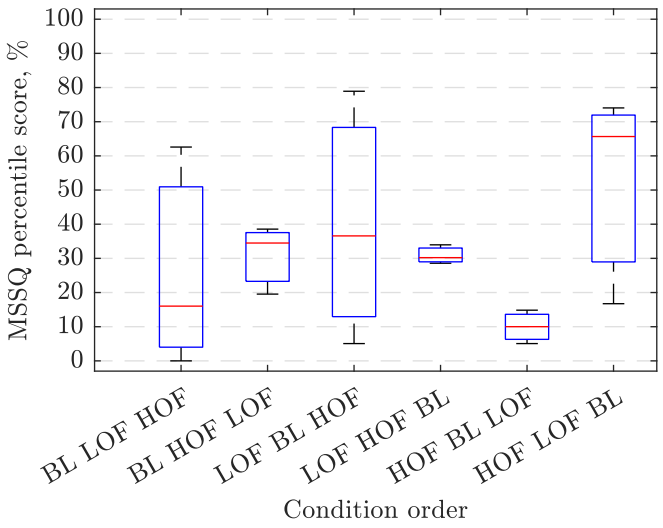

(b) Boxplot representation of the participants' MSSQ values per condition order

Figure C-3: MSSQ representations

C-4 MS Symptoms

The occurrence and severity of all 24 symptoms asked for in the MS checklist are shown in Figure C-4. No clear condition preference could be observed from this figure.

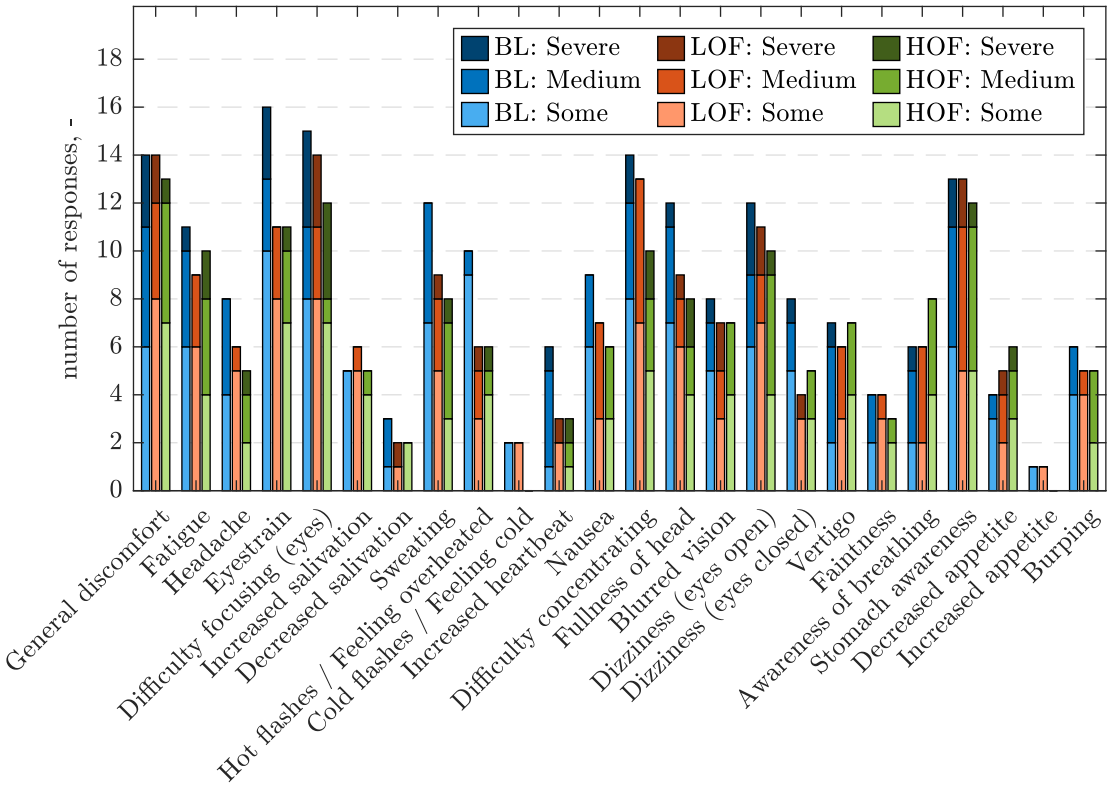

Figure C-4: All 24 symptoms asked for in the MS checklist

C-5 Physical and Visual Motion Assessment

The answers to the seven-point likert scale questions assessing the physical and visual motion are presented below. Figures C-5 - C-8 represent the physical motion assessment and Figures C-9 - C-11 represent the visual motion assessment that were all asked after each experiment session. Figure C-12 shows answers to the additional seven-point likert scale questions that were asked after the last experiment session only. Furthermore, Figure C-13 shows the participants' estimated minimum and maximum visual velocities of all three conditions. As could be seen, the spread of the maximum visual velocity in BL is large, meaning that participant had difficulties with estimating the maximum velocity when no visual cues are present. The minimum velocity of BL even shows that some participants experienced negative velocities (going backwards). For LOF and HOF is the estimated minimum and maximum close to the actual velocities.

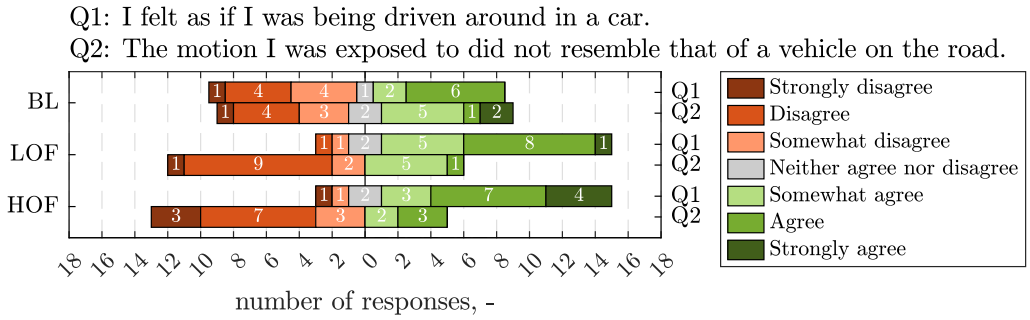

Figure C-5: Physical motion assessment questionnaire - question and counter question 1

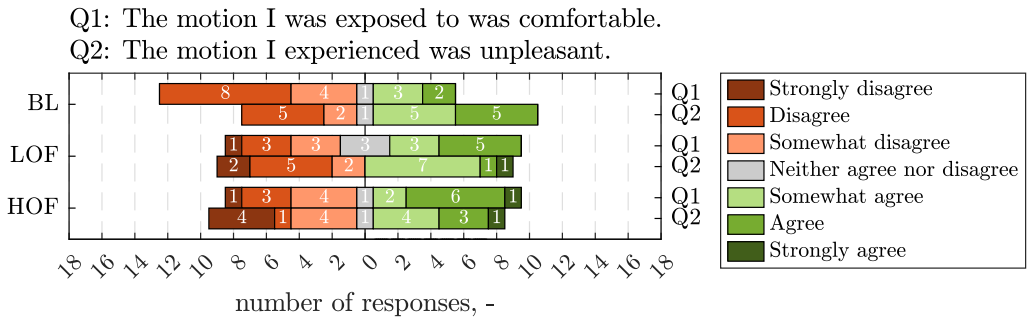

Figure C-6: Physical motion assessment questionnaire - question and counter question 2

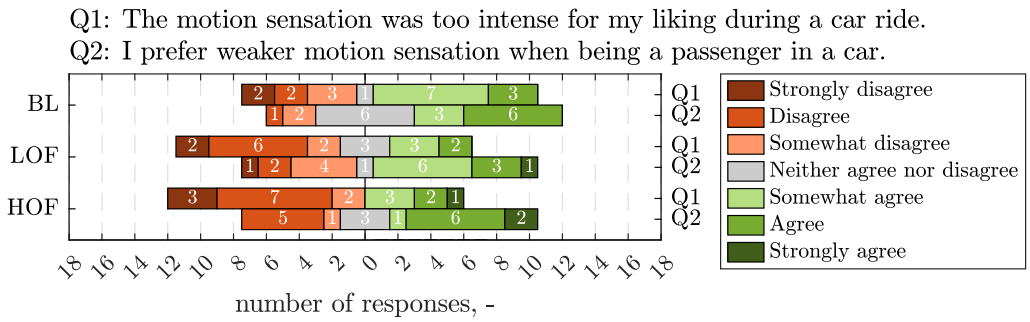

Figure C-7: Physical motion assessment questionnaire - question and counter question 3

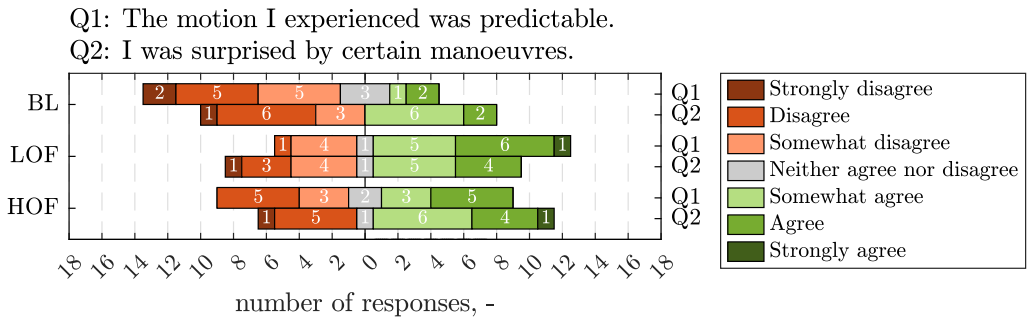

Figure C-8: Physical motion assessment questionnaire - question and counter question 4

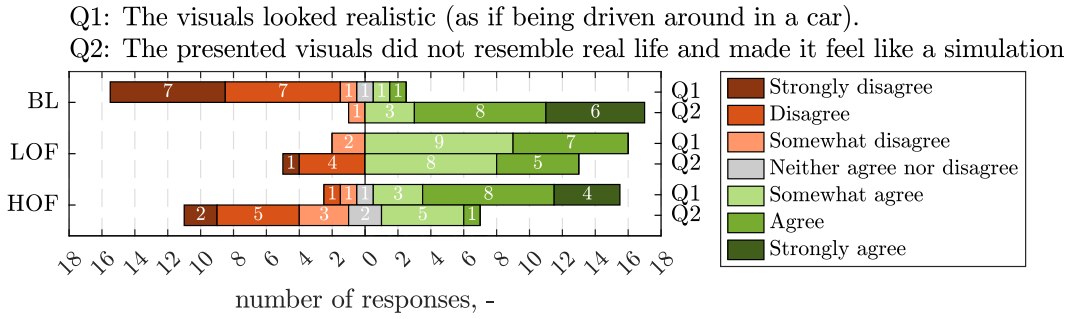

Figure C-9: Visual motion assessment questionnaire - question and counter question 1

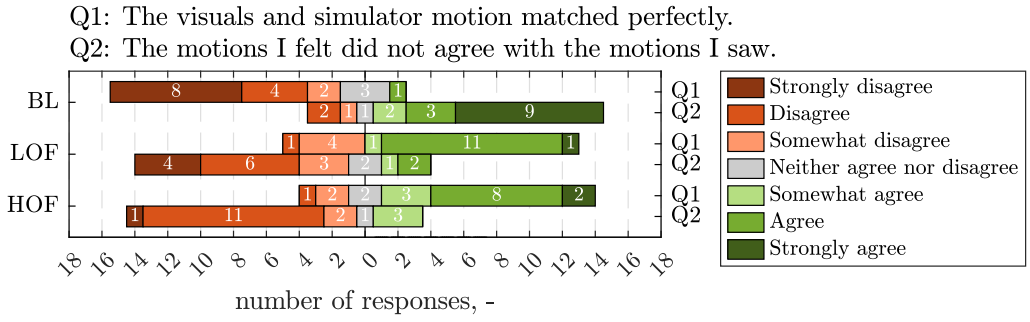

Figure C-10: Visual motion assessment questionnaire - question and counter question 2

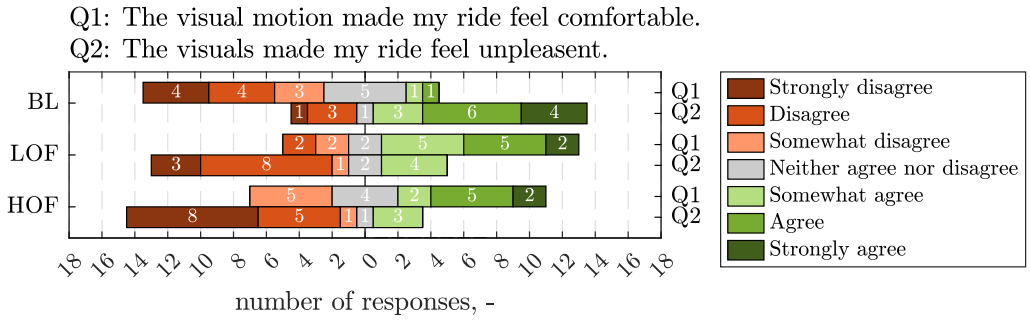

Figure C-11: Visual motion assessment questionnaire - question and counter question 3

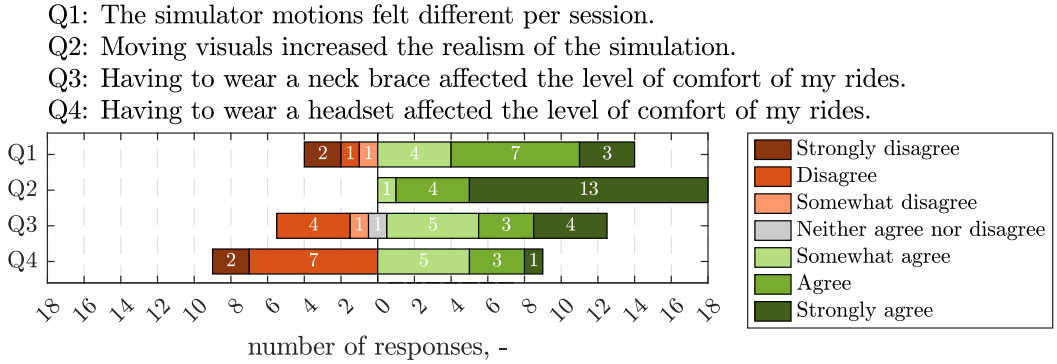

Figure C-12: Remaining questions after all experimental sessions

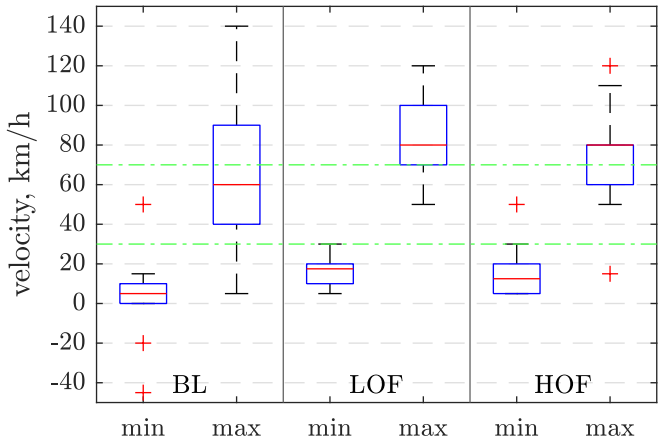

Figure C-13: Visual velocity estimations of all three sessions. The dotted green lines represent the actual minimum and maximum visual velocities

C-6 Subjective Motion Comfort Assessment

Figures C-14 and C-15 show the results of the subjective motion comfort and driving behavior assessment. After all three sessions, participants rated the conditions in terms of level of comfort and driving behavior. Both questions asked for a rating between one and seven, which ranged from 'extremely uncomfortable' to 'extremely comfortable' and 'extremely aggressive driving behavior' to 'extremely defensive driving behavior', respectively. The level of comfort is different for BL compared to LOF and HOF, while the driving behavior does not show any differences between the conditions. Figure C-16 shows a similar question to the previous driving behavior assessment, however, these answers were given right after each individual session. No clear differences or conclusions could be conducted from this figure. Last, Figure C-17 shows the results of the survey question asked after letting the participants know that the simulator motion was identical throughout all sessions. The majority answered "No" or "A bit", meaning that for most participant this was not a surprise. All participants were (recent graduate) students from Delft University of Technology which caused them to recognize early that the physical motion would probably stay the same if the visual motion changes (only one independent variable), which could explain these results.

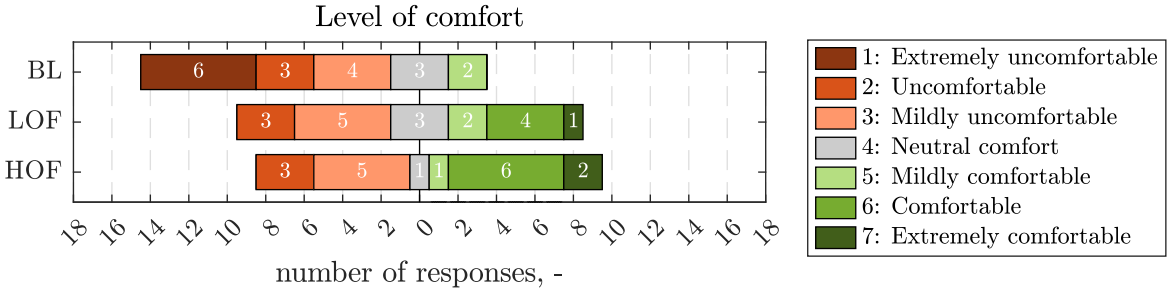

Figure C-14: Level of comfort assessment (after last experiment session)

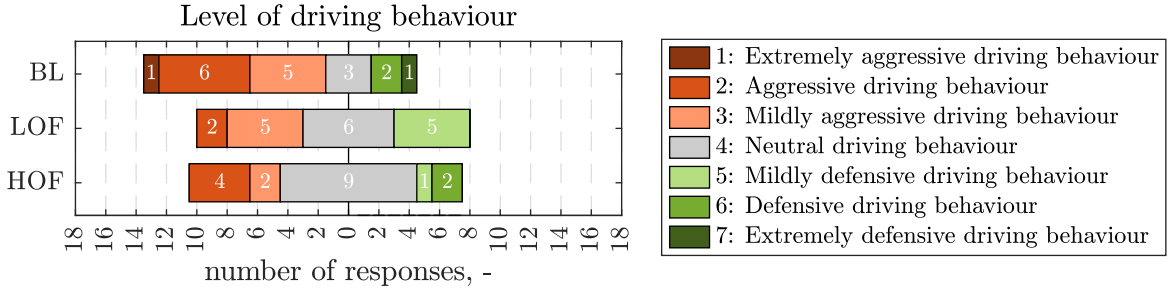

Figure C-15: Level of driving behavior assessment (after last experiment session)

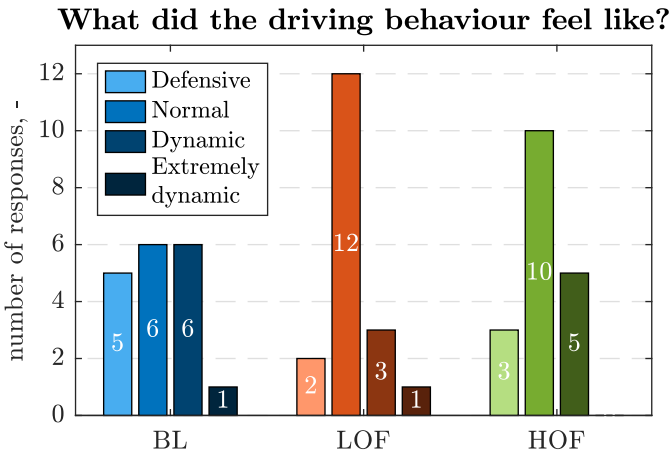

Figure C-16: Level of driving behavior assessment (after each experiment session)

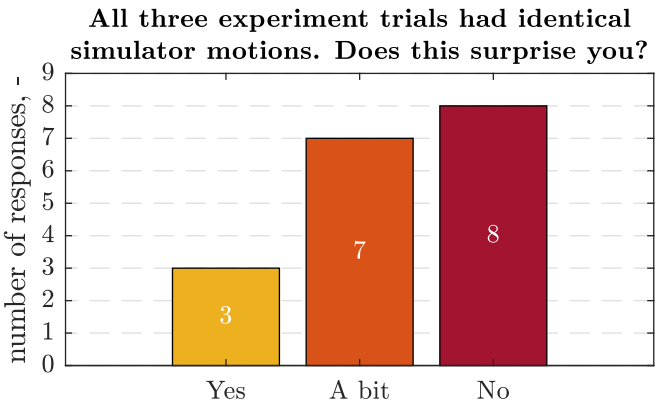

Figure C-17: Answers to the survey question asked after letting the participants know that the simulator motion was identical throughout all sessions

Appendix D

Individual Participant Results

The following pages include the results of each individual participant that completed all three experiment conditions. The results include:

- A table containing **general information** of the participant, the order of the conditions, and the reduction values $\overline{R}_{\text{LOF}}$ and $\overline{R}_{\text{HOF}}$
- The **MISC values** communicated during the 30-minute motion exposure and 10-minute recovery period. The figures of participants who were unable to complete the full session are missing MISC values for the time points that were not completed. Their recovery was still recorded and shown in the figures.
- The occurance ans severity of **MS symptoms** that were experiences in all three conditions.
- **Level of comfort and driving behaviour ratings**. After all three sessions, participants rated the conditions in terms of level of comfort and driving behavior. Both questions asked for a rating between one and seven, which ranged from 'extremely uncomfortable' to 'extremely comfortable' and 'extremely defensive driving behavior' to 'extremely aggressive driving behavior', respectively.
- **Comments** given in the open questions. These include experienced symptoms that were not mentioned in the symptom checklist, general comment of the session's experience, any remaining comment(s) after a session, and a general comment after all three sessions have been completed. Some participants refer to conditions with letters A, B, and C. This because the survey did not include the official condition names to prevent the participants from having any knowledge of the experiment goal. As a reference: A = BL, B = LOF, C = HOF.

Participant 1

This page shows the individual results of participant 1.

Table D-1: General information of participant 1

Age [years]	Gender [M/F]	MSSQ [%]	Condition order	$\overline{R}_{\text{LOF}}$ [-]	$\overline{R}_{\text{HOF}}$ [-]
24	M	62.6	BL→LOF→HOF	-0.03	0.03

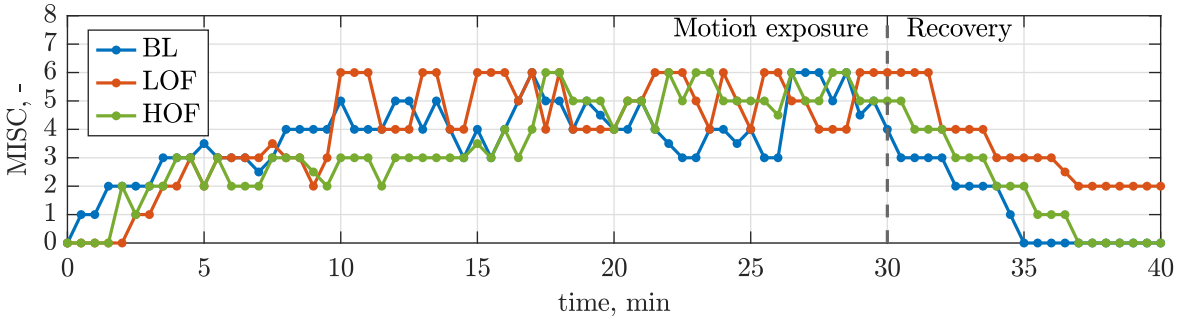

Figure D-1: MISC values of participant 1 for all conditions

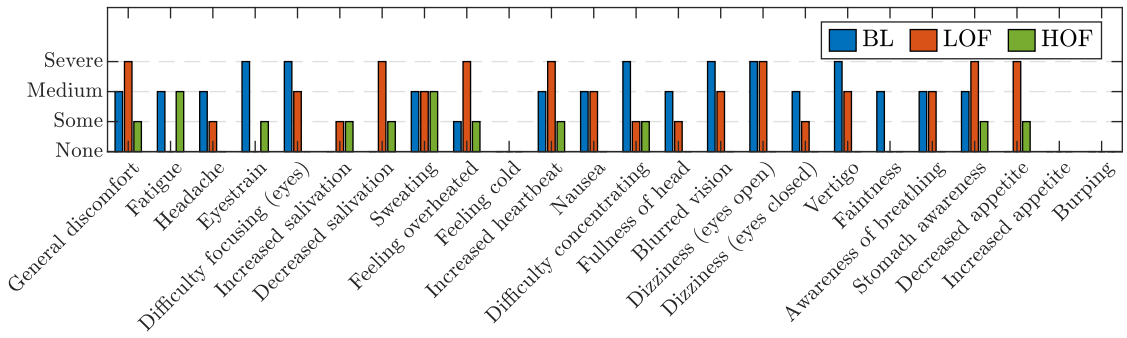

Figure D-2: MS symptoms of participant 1 for all conditions

Table D-2: Comfort and driving behaviour ratings of participant 1

	Comfort level [-]	Driving behaviour level [-]
BL	1: Extremely uncomfortable	7: Extremely aggressive driving behaviour
LOF	2: Uncomfortable	6: Aggressive driving behaviour
HOF	2: Uncomfortable	6: Aggressive driving behaviour

Baseline

Other experienced symptoms:

-

Comment of the session's experience:

Found it quite difficult to distinguish when going into number 6 when comparing it with heavy other symptoms at 5

Remaining comments of this session:

-

Low Optical Flow

Other experienced symptoms:

-

Comment of the session's experience:

The visuals helped in my experience to feel like i was more in a real car ride then with the first experiment. I was more aware of what was happening

Remaining comments of this session:

-

High Optical Flow

Other experienced symptoms:

-

Comment of the session's experience:

In the beginning it felt actually way more comfortable then the first and second session. But eventually the discomfort became higher again as time past. It did take longer i think before the real discomfort came up

Remaining comments of this session:

-

Comment of all sessions:

A: Was very uncomfortable not necessary because i felt really "misselijk" but because of the discomfort of the visuals not representing the feedback my body got from the movement. Especially my head was full, trouble focussing and concentrating. Furthermore i hard a hard time recognizing the movement as breaking and accelerating.

B: The extra visuals helped a lot in the feeling of being in a car. This was my second session and i directly picked up that when i was accelerating or breaking. However the "misselijkheid" came more in to the forefront of this sessions. Since that feeling came up a lot more, especially after breaking a couple of times after each other and then fairly quickly accelerating for a long time. This was not the most uncomfortable ride, however when looking at "misselijkheid" it was.

C: The first few minutes, if i have to guess probably 15, this ride was relatively comfortable compared to the other two. I only felt like 2's or 3's mostly and i think that was because of the nice visualization of the world and the corresponding movement that came with it. Also the buildings may have helped as a distraction the first few minutes. However after a certain amount of time almost the same feeling came back as in B with the "misselijkheid" where multiple times breaking and accelerating made me "misselijk". I did however feel that the feeling of "misselijkheid" went away quicker then in scenario B.

Overall something i noticed is that every time i was in the simulation the longer i was in there the worse i felt compared to the beginning of that simulation. And it never stayed relatively consistent during the whole simulation

Participant 2

This page shows the individual results of participant 2.

Table D-3: General information of participant 2

Age [years]	Gender [M/F]	MSSQ [%]	Condition order	$\overline{R}_{\text{LOF}}$ [-]	$\overline{R}_{\text{HOF}}$ [-]
27	M	34.5	BL→HOF→LOF	0.86	0.27

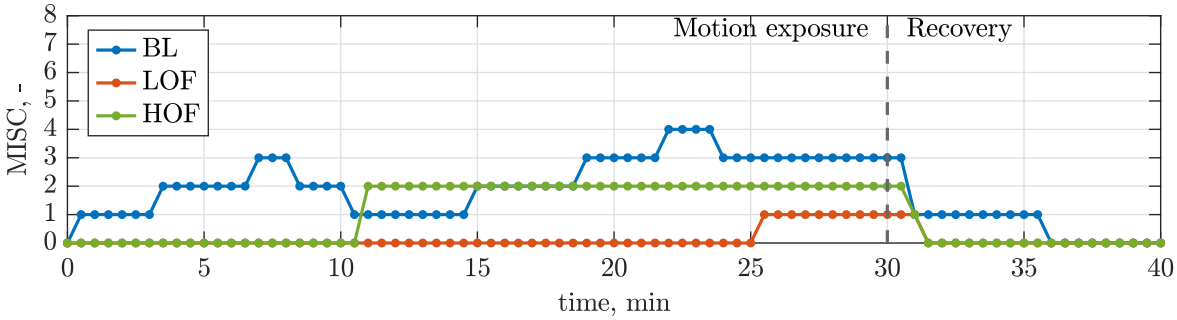

Figure D-3: MISC values of participant 2 for all conditions

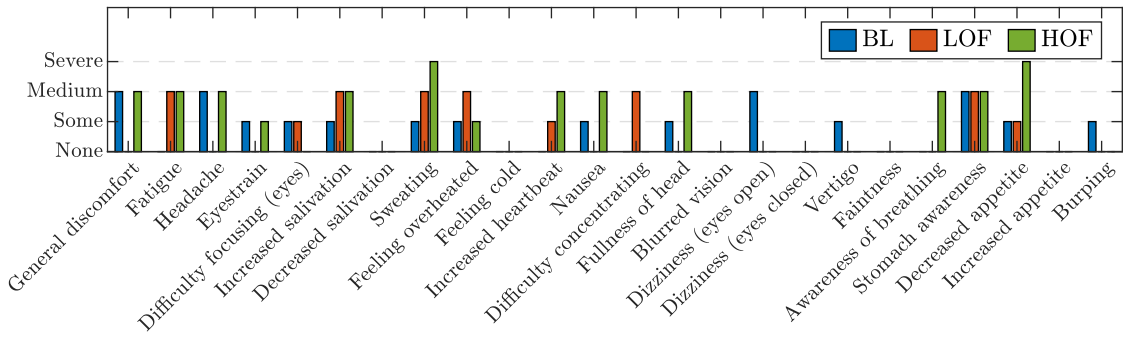

Figure D-4: MS symptoms of participant 2 for all conditions

Table D-4: Comfort and driving behaviour ratings of participant 2

	Comfort level [-]	Driving behaviour level [-]
BL	1: Extremely uncomfortable	6: Aggressive driving behaviour
LOF	4: Neutral comfortability	4: Neutral driving behaviour
HOF	5: Mildly comfortable	4: Neutral driving behaviour

Baseline

Other experienced symptoms:

No

Comment of the session's experience:

It felt weird that I could not really see based on the visuals if I was moving or not. The only indicator I had that I was moving was when I could see that the yellow middle line ended. Also, I couldn't see the horizon moving up and down when accelerating or braking even though I felt some sort of pitch movement of the simulator.

Remaining comments of this session:

I feel like the neck brace is adding some discomfort during the experiment. It makes your neck a bit sweaty and applies some pressure to you head.

Low Optical Flow

Other experienced symptoms:

-

Comment of the session's experience:

This ride felt the most comfortable out of the three sessions. Because I gave a lot of 0's, I was really trying to concentrate on how i felt to see if I maybe needed to increase the number. This sometimes made me forget about the simulator motion all together to a point where I wasn't really actively aware of it. The acceleration and deceleration still felt unpredictable since there wasn't really a reason (traffic lights or other traffic) to chance the speed of the vehicle. This session I did not really feel that the neck brace was uncomfortable even though I previous sessions I did find it uncomfortable. I am sure that I put on the neck brace just as tight as in the other sessions.

Remaining comments of this session:

-

High Optical Flow

Other experienced symptoms:

-

Comment of the session's experience:

Having these visuals made the ride a lot more comfortable. The accelerating and braking were unpredictable since there never really was a reason to brake or accelerate (no traffic lights or other traffic). In general I do feel that the braking and accelerating felt realistic. I also felt like I that part of the discomfort was caused by the neck brace applying pressure to my head. Compared to the first session the temperature also felt cooler than before.

Remaining comments of this session:

I think i filled in all my thoughts in the previous section.

Comment of all sessions:

In A and C it felt as a relief to take of the neck brace. In B not as much. I find it difficult to asses the differences in driving behavior between the different sessions. For all i know the driving behavior could be exactly the same every session. Session C might also have been less comfortable compared to session B since in session C I was paying more attention to all the surrounding buildings and parked cars. In session B the environment was not really that diverse so I was more relaxed.

Participant 3

This page shows the individual results of participant 3.

Table D-5: General information of participant 3

Age [years]	Gender [M/F]	MSSQ [%]	Condition order	$\overline{R}_{\mathrm{LOF}}$ [-]	$\overline{R}_{\mathrm{HOF}}$ [-]
18	F	28.6	LOF→HOF→BL	0.15	0.30

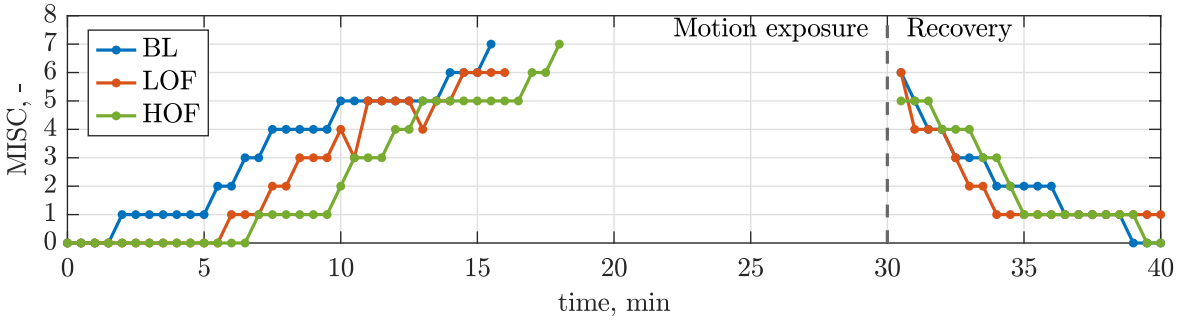

Figure D-5: MISC values of participant 3 for all conditions

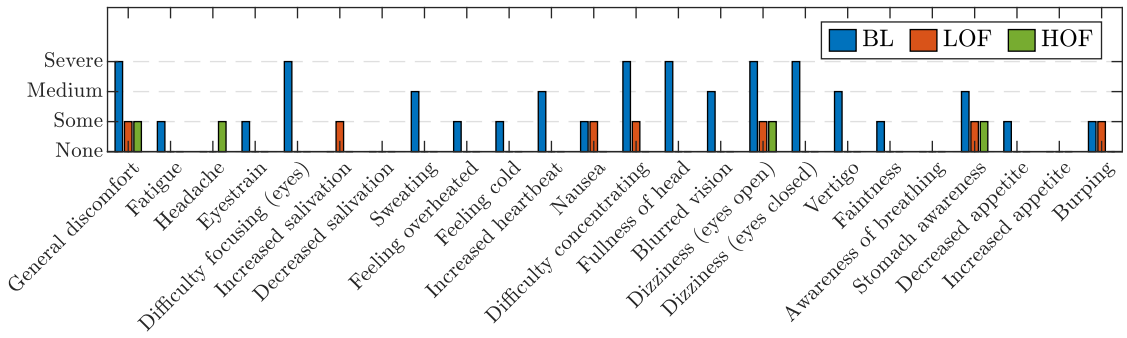

Figure D-6: MS symptoms of participant 3 for all conditions

Table D-6: Comfort and driving behaviour ratings of participant 3

	Comfort level [-]	Driving behaviour level [-]
BL	2: Uncomfortable	4: Neutral driving behaviour
LOF	6: Comfortable	4: Neutral driving behaviour
HOF	6: Comfortable	4: Neutral driving behaviour

Baseline

Other experienced symptoms:

-

Comment of the session's experience:

This time I was more aware of the motion of the simulator and its moves. I actually felt as if I was being held up and down instead of being driven in a car. It was way easier to bear the diziness and stomach awareness but it still made the ride more and more uncomfortable as I progressed. The lack of "moving visuals" had an impact on that I think.

Remaining comments of this session:

-

Low Optical Flow

Other experienced symptoms:

-

Comment of the session's experience:

Whenever the car simulation would stop, that's when I felt the symptoms the most. When the car would accelerate, I felt fine, but the change in velocity made me feel dizzy.

Remaining comments of this session:

-

High Optical Flow

Other experienced symptoms:

-

Comment of the session's experience:

On slower velocities I was able to concentrate and actually enjoy the ride, right after that when the velocity started to increase, I really felt like quickly moving and I was having a bit of blurry vision.

Remaining comments of this session:

-

Comment of all sessions:

In terms of comfortability I preferred C on lower velocities. The moving visuals actually made it feel as if I was in a car driving around the city, but at higher velocities and with abrupt brakes I wasn't able to focus on anything. In B, on higher velocities the symptoms were quite bearable. The visuals were quite familiar but unrealistic as I felt that I was driving towards nowhere. In motion C I was more likely to feel more symptoms in a shorter time than in B. Motion A felt just static, which made me aware of the motion of the simulator. It felt like an unpleasant ride up and down, maybe similar to a motion of a swing even. In A I felt less symptoms, but because of the motion I felt dizzy really quick. In general, A was the best in terms of bearing the symptoms and C was the worse. I was the most comfortable at the beginning of the motion in C though.

Participant 4

This page shows the individual results of participant 4.

Table D-7: General information of participant 4

Age [years]	Gender [M/F]	MSSQ [%]	Condition order	$\overline{R}_{\text{LOF}}$ [-]	$\overline{R}_{\text{HOF}}$ [-]
22	F	74.0	HOF→LOF→BL	0.11	0.15

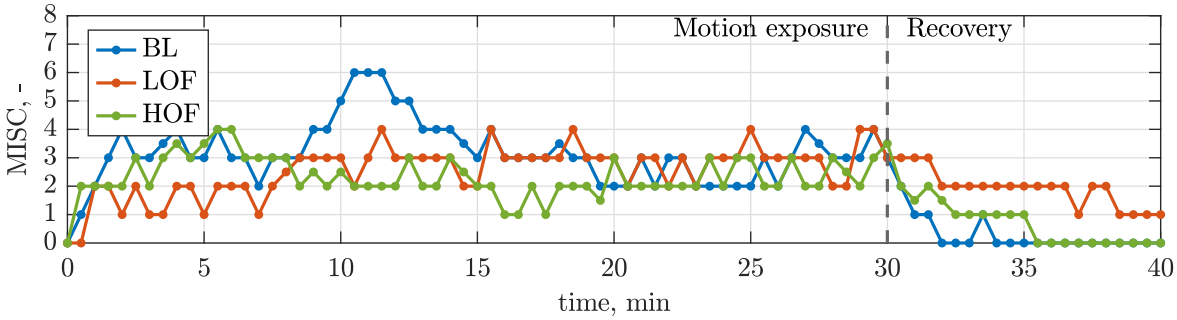

Figure D-7: MISC values of participant 4 for all conditions

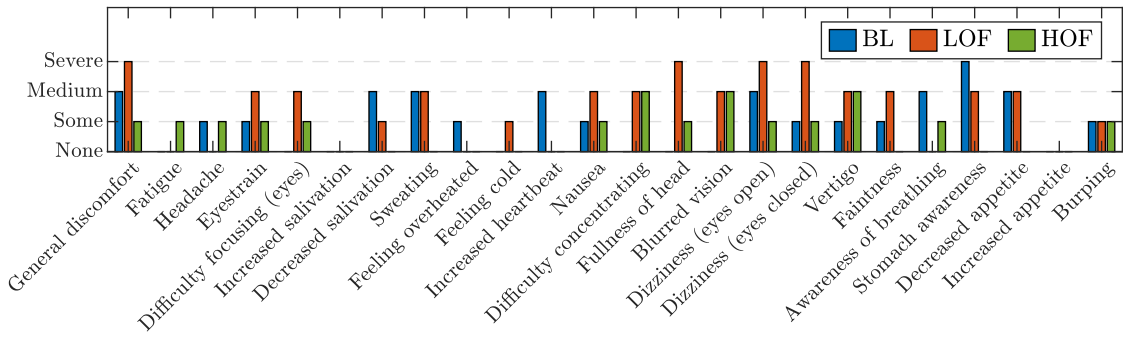

Figure D-8: MS symptoms of participant 4 for all conditions

Table D-8: Comfort and driving behaviour ratings of participant 4

	Comfort level [-]	Driving behaviour level [-]
BL	1: Extremely uncomfortable	6: Aggressive driving behaviour
LOF	2: Uncomfortable	4: Neutral driving behaviour
HOF	3: Mildly uncomfortable	4: Neutral driving behaviour

Baseline

Other experienced symptoms:

-

Comment of the session's experience:

It was not very comfortable, because the motion of the vision was standing almost still/ there was no visual movement. But the motion I felt was stronger, so it made me a little nauseous

Remaining comments of this session:

-

Low Optical Flow

Other experienced symptoms:

Een beetje een brok in mijn keel gevoel

Comment of the session's experience:

The experience was not that pleasant, but still okay.

Remaining comments of this session:

-

High Optical Flow

Other experienced symptoms:

-

Comment of the session's experience:

De vertraging was erg haperuig en dat is wat mij vooral draaierig maakte. Verder vond ik de opbouwende versnellingen en vertragingen niet vervelend. Ik zou niet zeggen dat het hele wilde bewegingen waren, maar omdat je die schokken niet verwacht werd ik wel een beetje duizelijk met een beetje hoofdpijn.

Remaining comments of this session:

-

Comment of all sessions:

I feel like the motion of the three different simulations was very similar. But because of the different visuals it made the overall experience different. In A, the experience was uncomfortable because it did not match the visuals with the motion. Also the visuals were very plain, so it was not really noticeable when the visuals were moving. I preferred the visuals of B, but the motion was still unpleasant. And at C the motion was also not very pleasant, but it felt like the motion and the visuals did match the best. So I preferred C, then B and lastly A .

Participant 5

This page shows the individual results of participant 5.

Table D-9: General information of participant 5

Age [years]	Gender [M/F]	MSSQ [%]	Condition order	$\overline{R}_{\text{LOF}}$ [-]	$\overline{R}_{\text{HOF}}$ [-]
20	F	16.0	BL→LOF→HOF	0.03	0.00

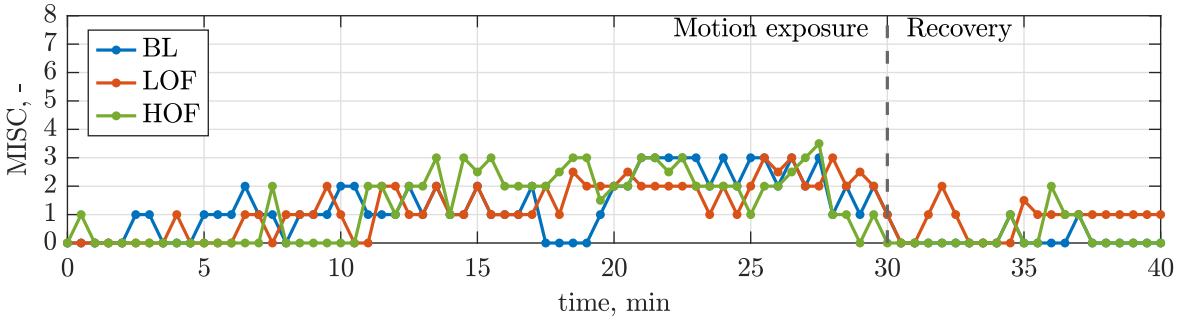

Figure D-9: MISC values of participant 5 for all conditions

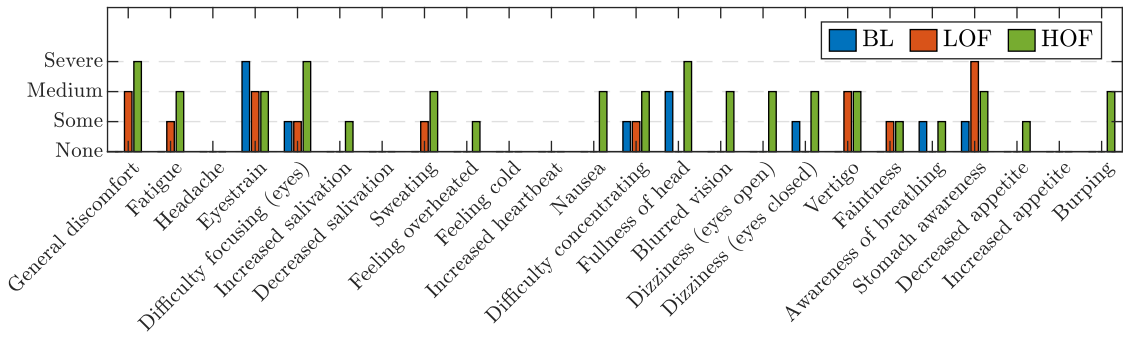

Figure D-10: MS symptoms of participant 5 for all conditions

Table D-10: Comfort and driving behaviour ratings of participant 5

	Comfort level [-]	Driving behaviour level [-]
BL	2: Uncomfortable	5: Mildly aggressive driving behaviour
LOF	3: Mildly uncomfortable	5: Mildly aggressive driving behaviour
HOF	3: Mildly uncomfortable	5: Mildly aggressive driving behaviour

Baseline

Other experienced symptoms:

-

Comment of the session's experience:

It sometimes felt as if I in a little boat at sea

Remaining comments of this session:

-

Low Optical Flow

Other experienced symptoms:

-

Comment of the session's experience:

It felt as if I was getting ready for take off in an airplane, due to the visuals. If it was only motion it was like the climax of an attraction in an amusement park (think of Joris and the Draak or something). I did feel quite comfortable

Remaining comments of this session:

-

High Optical Flow

Other experienced symptoms:

-

Comment of the session's experience:

It was like taking a drive around the city, very calm. As if you were in the car with someone who just got their driver's license, because you sometimes felt a feedback as if you were driving a stick. (in Dutch: je voelde soms ineens een bam wanneer je aan het doorschakelen bent en de koppeling niet goed vasthebt)

Remaining comments of this session:

-

Comment of all sessions:

The first one was more as if I was floating, the second one felt more like an airplane about to take off and the third one was just a drive around the city. The third one does have my preference because it feels more familiar due to the surrounding as well

Participant 6

This page shows the individual results of participant 6.

Table D-11: General information of participant 6

Age [years]	Gender [M/F]	MSSQ [%]	Condition order	$\overline{R}_{\text{LOF}}$ [-]	$\overline{R}_{\text{HOF}}$ [-]
24	M	30.2	LOF→HOF→BL	0.10	0.32

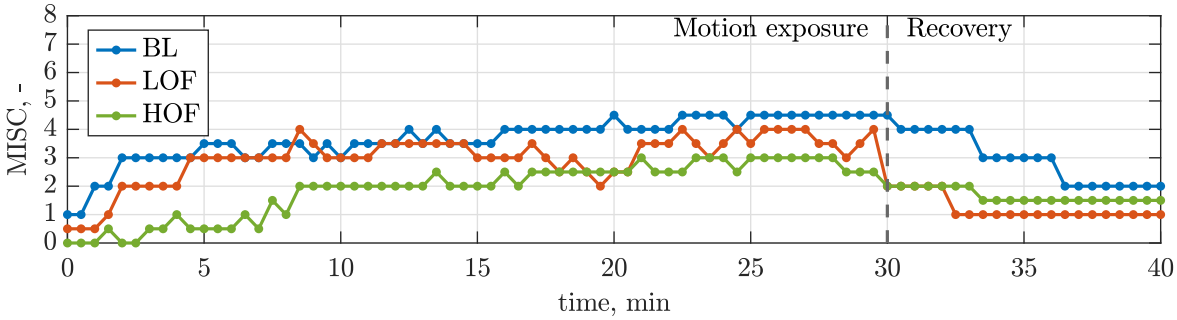

Figure D-11: MISC values of participant 6 for all conditions

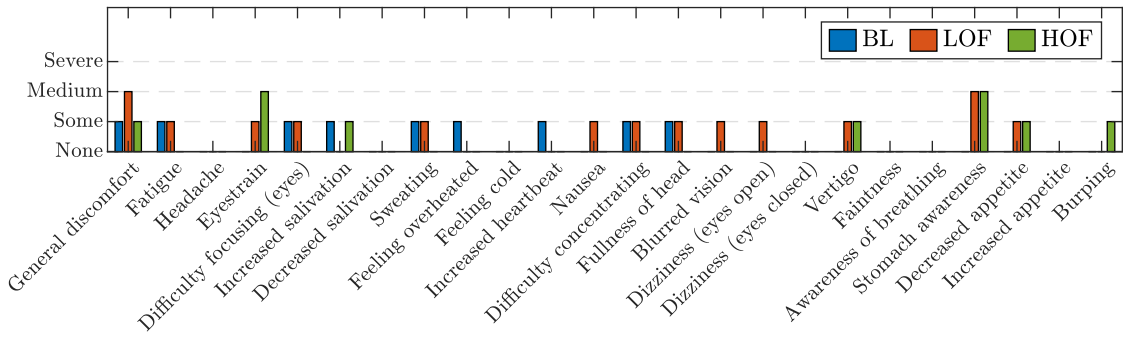

Figure D-12: MS symptoms of participant 6 for all conditions

Table D-12: Comfort and driving behaviour ratings of participant 6

	Comfort level [-]	Driving behaviour level [-]
BL	4: Neutral comfortability	2: Defensive driving behaviour
LOF	5: Mildly comfortable	4: Neutral driving behaviour
HOF	6: Comfortable	6: Aggressive driving behaviour

Baseline

Other experienced symptoms:

-

Comment of the session's experience:

I did not relate the motion and the visuals to driving anymore. I could just accept the motion and did not get any discomfort from that as i know of. The visuals gave me way more of a hard time. Also some questions related to driving i could not really answer that well (like the last about velocity) because i did not see the simulation as driving anymore.

Remaining comments of this session:

-

Low Optical Flow

Other experienced symptoms:

-

Comment of the session's experience:

In general it was intuitive, only sometimes there were a few movements that surprised me (sudden changes in the movement of the simulation) and gave me a bit of a disoriented feeling. for the rest it was fun!

Remaining comments of this session:

-

High Optical Flow

Other experienced symptoms:

-

Comment of the session's experience:

was a pretty pleasant ride. On some points it was a tiny bit uncomfortable but that did not get worse and worse during the ride. The visuals helped as there where some constant changes in scenery

Remaining comments of this session:

-

Comment of all sessions:

Second question, for baseline i did not relate it to driving anymore so i don't really have a opinion on aggression levels in driving style for that one

Participant 7

This page shows the individual results of participant 7.

Table D-13: General information of participant 7

Age [years]	Gender [M/F]	MSSQ [%]	Condition order	$\overline{R}_{\text{LOF}}$ [-]	$\overline{R}_{\text{HOF}}$ [-]
22	F	78.9	LOF→BL→HOF	-0.30	-0.02

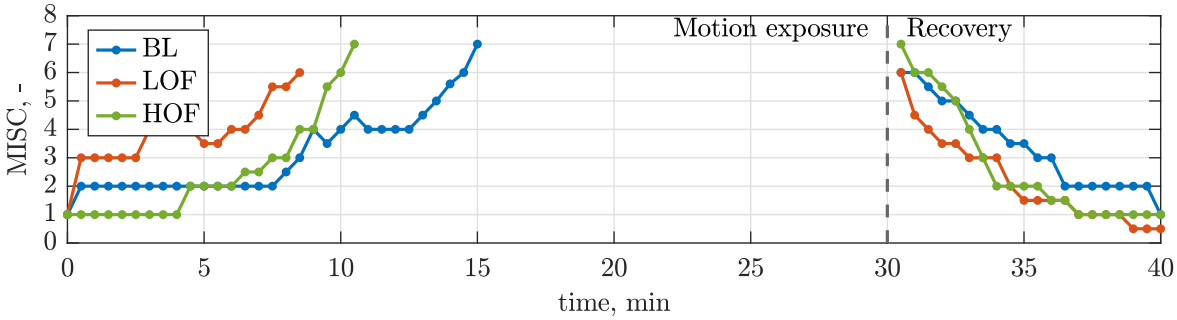

Figure D-13: MISC values of participant 7 for all conditions

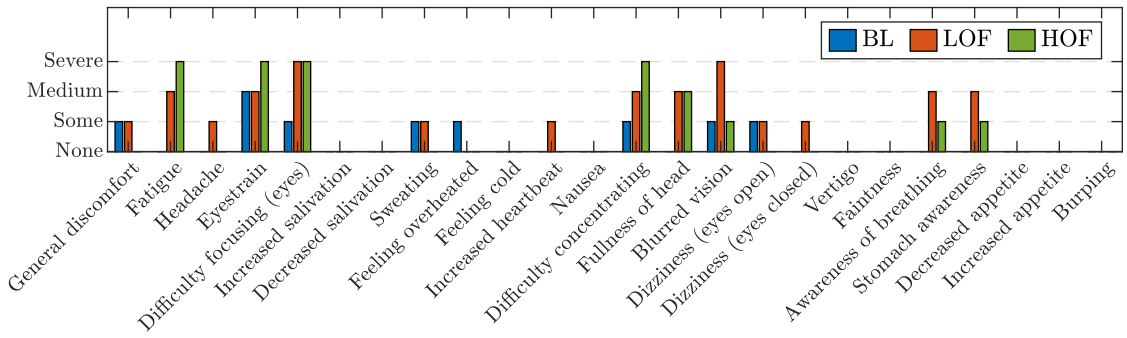

Figure D-14: MS symptoms of participant 7 for all conditions

Table D-14: Comfort and driving behaviour ratings of participant 7

	Comfort level [-]	Driving behaviour level [-]
BL	1: Extremely uncomfortable	4: Neutral driving behaviour
LOF	3: Mildly uncomfortable	5: Mildly aggressive driving behaviour
HOF	6: Comfortable	2: Defensive driving behaviour

Baseline

Other experienced symptoms:

-

Comment of the session's experience:

It did not always feel like I was in a car. Sometimes it felt like I was in a plane during take-off/landing, so more like I was going up or down in stead of forward or backwards. It also sometimes felt like I was going backwards, last time I did not have this feeling. The visuals did not feel pleasant. I could not focus on anything and this became worse the longer I was in it. Normally my method for not becoming sick is to focus on things far away and that was now impossible as there were only a couple of lines far away that were difficult to focus on. It did help when the simulator ended to focus on things in the simulator that were relatively far away but looking at the visual did not make me feel that amazing.

Remaining comments of this session:

I feel better now than I did after the last trial. Today I experienced a really different type of uncomfortableness/sickness. Last time it was more nausea and feeling my stomach. This time it was more dizziness and not being able to focus and my head spinning. During both trials it did not feel great but the dizziness is fading away quicker than the nausea was.

Low Optical Flow

Other experienced symptoms:

Feeling shaky (handen een beetje aan het beven/trillen en ook toen ik opstond erna dat ik een beetje rillerig was)

Comment of the session's experience:

I could not anticipate the movements of the car because it suddenly went faster and slower without any warning/reason. In a normal car you see something happening in front of you and know that you will slow down so you can anticipate it, now it just happened without reason. The movements were also quite harsh. It reminded me of being in a car with adaptive cruise control as those also can break or increase speed quite harshly.

Remaining comments of this session:

It did not feel good but it was a nice experience.

High Optical Flow

Other experienced symptoms:

-

Comment of the session's experience:

Visuals were nice. When I focus on things far away I get less sick so it was nice that there were enough things to focus on. Sometimes I focused on things that came closer and when the car then suddenly increased speed or slowed down, I became a bit less comfortable (iets misselijker). The car still did not drive like a normal car would. It was unpredictable when it would increase speed or slow down and these movements were also quite harsh. This was not nice.

Remaining comments of this session:

-

Comment of all sessions:

I preferred experiment B or C as these felt more like a car. A did not necessarily make me sicker but it was a different kind of sickness (like being twirled around on an office chair instead of being in a car). B and C did not differ that much, C was more fun to look at the different visuals while B was a bit boring. However, sometimes at C I looked a while at one thing and therefore I was more surprised by some movements as I was focusing less on the simulator movements. In B there was not much to see so I was quite focused on the movements and therefore always mentally prepared for a movement (I still couldn't predict them but I was just constantly kind of bracing myself and during C I did not constantly brace myself).

Participant 8

This page shows the individual results of participant 8.

Table D-15: General information of participant 8

Age [years]	Gender [M/F]	MSSQ [%]	Condition order	$\overline{R}_{LOF}$ [-]	$\overline{R}_{HOF}$ [-]
22	F	38.6	BL→HOF→LOF	-0.41	-0.39

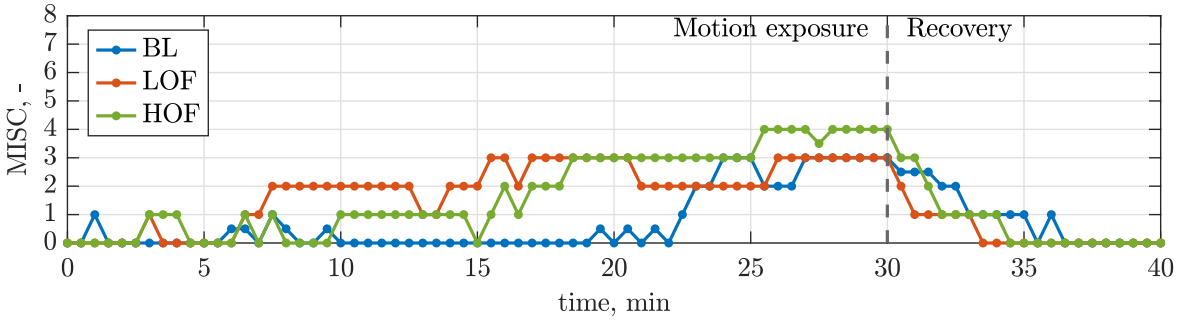

Figure D-15: MISC values of participant 8 for all conditions

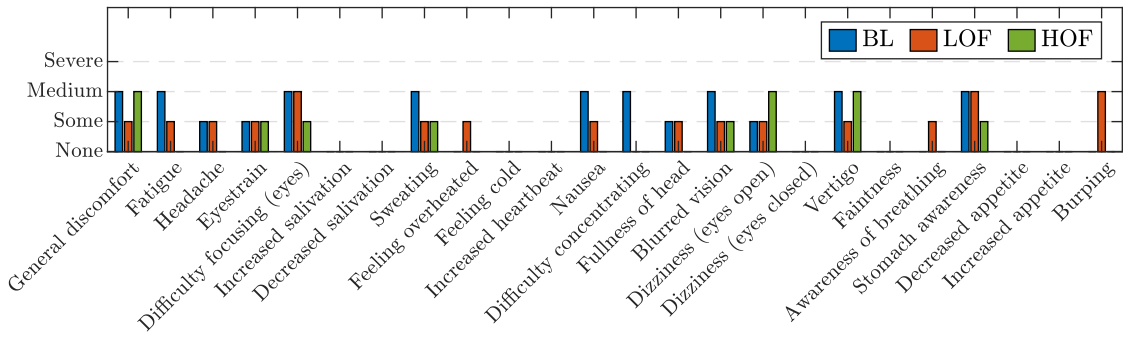

Figure D-16: MS symptoms of participant 8 for all conditions

Table D-16: Comfort and driving behaviour ratings of participant 8

	Comfort level [-]	Driving behaviour level [-]
BL	3: Mildly uncomfortable	5: Mildly aggressive driving behaviour
LOF	3: Mildly uncomfortable	5: Mildly aggressive driving behaviour
HOF	3: Mildly uncomfortable	5: Mildly aggressive driving behaviour

Baseline

Other experienced symptoms:

No

Comment of the session's experience:

I would describe the ride as slightly uncomfortable. Half of the time I felt like I was was standing still and the other half of the time I think the simulator was moving. This - together with the feeling that I was moving up and down - made it not feel like a car ride at all.

Remaining comments of this session:

-

Low Optical Flow

Other experienced symptoms:

-

Comment of the session's experience:

I experienced today's ride as quite boring. Obviously the visuals did not change much and after a certain time I got used to the motion. It was slightly uncomfortable however as the longer the ride took I got a little dizzier

Remaining comments of this session:

-

High Optical Flow

Other experienced symptoms:

no

Comment of the session's experience:

The experience was a lot more realistic than previous time. However, since I was constantly 'in motion' I became quite dizzy at a certain moment. I think my dizziness would have been less if I would have 'stood still' for a while during the experiment.

Remaining comments of this session:

-

Comment of all sessions:

In experiment A I did not feel like being driven around in a car, as there was no visual motion. That is, every time the simulator stood still I felt like I stood still. In the second and third experiment, the visuals made me feel in motion the whole time. When the simulator stood still, I felt like driving with constant velocity.

With regards to comfortability and driving behaviour I did not experience any differences between the three experiments, as in my opinion the motions in all three experiments were very similar (if not the same?!). So the visuals in experiment B and C definitely made the ride more realistic, but in terms of comfortability not much changed for me.

Participant 9

This page shows the individual results of participant 9.

Table D-17: General information of participant 9

Age [years]	Gender [M/F]	MSSQ [%]	Condition order	$\overline{R}_{\text{LOF}}$ [-]	$\overline{R}_{\text{HOF}}$ [-]
21	M	34.0	LOF→HOF→BL	0.25	0.68

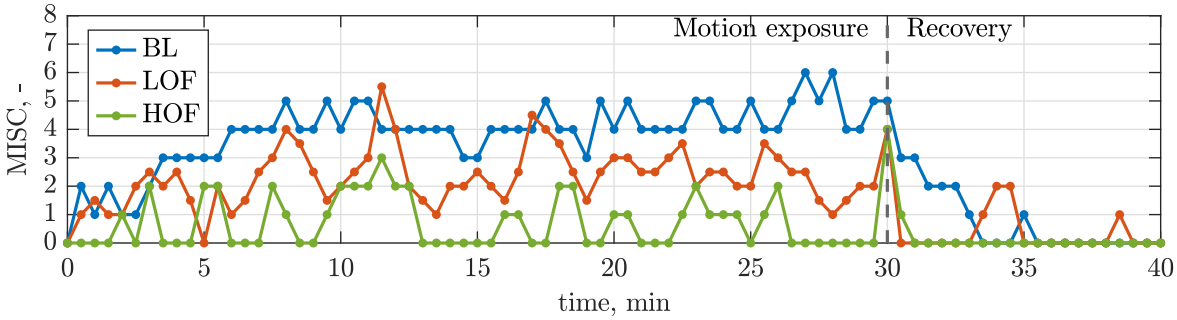

Figure D-17: MISC values of participant 9 for all conditions

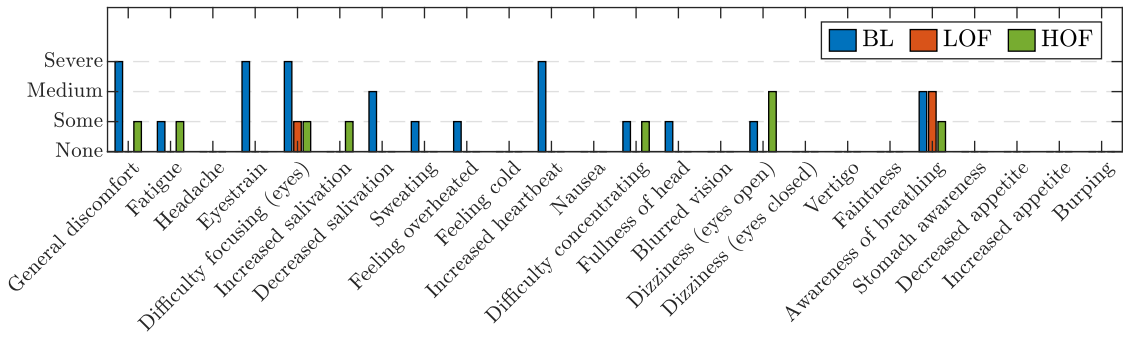

Figure D-18: MS symptoms of participant 9 for all conditions

Table D-18: Comfort and driving behaviour ratings of participant 9

	Comfort level [-]	Driving behaviour level [-]
BL	3: Mildly uncomfortable	6: Aggressive driving behaviour
LOF	2: Uncomfortable	3: Mildly defensive driving behaviour
HOF	6: Comfortable	4: Neutral driving behaviour

Baseline

Other experienced symptoms:

-

Comment of the session's experience:

It sucked. The visuals presented didn't match the motion of the simulator, sometimes it almost felt like it was contradicting the motions felt. Combined with the continues engine sound which did not increase nor decrease whilst accelerating or braking made it almost impossible to distinguish what speed I was traveling at, or if I was even traveling at al.

Remaining comments of this session:

-

Low Optical Flow

Other experienced symptoms:

The feeling that what was seen did not match the feeling that was felt. (long feeling of braking when already going very slow)

Comment of the session's experience:

The smooth parts were nice, also whilst breaking. The more erratic motion felt way less comfortable, with hard breaking, heavy differentiating speeding up. Long periods of slight breaking were also not very nice, if the breaking itself was very light. 1 smooth motion of medium breaking, and the same with accelerating where most preferred.

Remaining comments of this session:

-

High Optical Flow

Other experienced symptoms:

I felt a little bit lulled to sleep. Going in, and coming out I didn't feel tired at all, but halfway through I became a little sleepy and unfocussed. This resolved as soon as the simulator ended

Comment of the session's experience:

The experience was more comfortable. The houses and buildings gave focus point, which allowed a better deception of the driven speed. This increased the feeling of realism, and made it feel more like a car ride. If you discount certain moments where the car drove very slow without clear reason, it felt a lot more realistic then the first session. The movements also felt smoother, with less bumps and shocks. This improved the comfort of being in the simulator and during heavy breaking.

Remaining comments of this session:

I am not sure if it is because I got used to the feeling of the simulator, but it al felt smoother this time around. The given focus points in the buildings, slightly more predictable driving behavior and the decrease in shocks and bumps together made the ride feel pretty comfortable. The movements at some points almost felt soothing, and had a calming effect. Sometimes the increases in speed or heavy moments of breaking did have a dizzying effect.

Comment of all sessions:

Session A felt very uncomfortable. The motions and visuals did match which made it very difficult to get comfortable or predict what was going to happen. Session B felt slightly less uncomfortable, which may have been caused by it being my first session. Overall the visuals made it better, but lack of reasons for the car to suddenly brake or accelerate still made the driving unpredictable, which made it again difficult to get comfortable. Session C felt the most comfortable. The buildings and side roads made braking slightly more realistic and helped in preparing. It also made it easier to distinguish the speed traveled at, making the entire ride more pleasant and comfortable

Participant 10

This page shows the individual results of participant 10.

Table D-19: General information of participant 10

Age [years]	Gender [M/F]	MSSQ [%]	Condition order	$\overline{R}_{\text{LOF}}$ [-]	$\overline{R}_{\text{HOF}}$ [-]
23	F	36.6	LOF→BL→HOF	-0.64	0.91

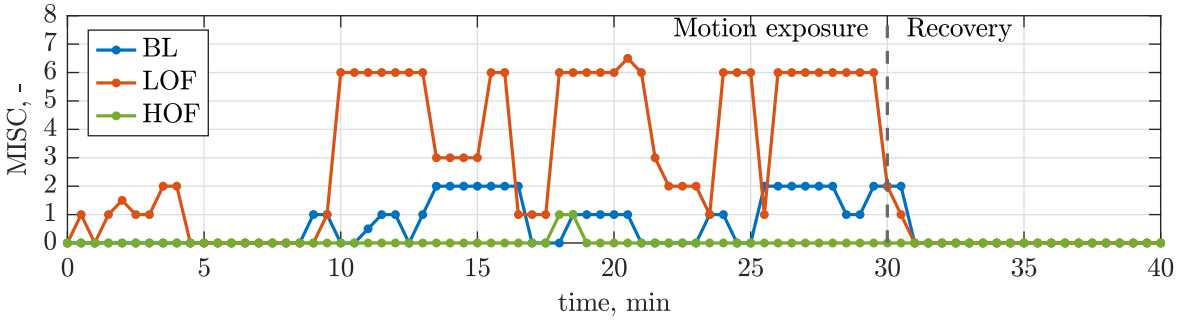

Figure D-19: MISC values of participant 10 for all conditions

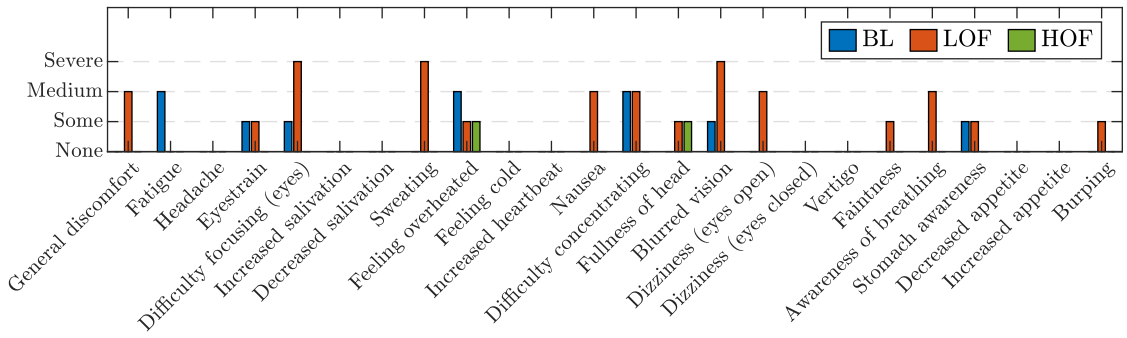

Figure D-20: MS symptoms of participant 10 for all conditions

Table D-20: Comfort and driving behaviour ratings of participant 10

	Comfort level [-]	Driving behaviour level [-]
BL	1: Extremely uncomfortable	6: Aggressive driving behaviour
LOF	3: Mildly uncomfortable	5: Mildly aggressive driving behaviour
HOF	6: Comfortable	4: Neutral driving behaviour

Baseline

Other experienced symptoms:

-

Comment of the session's experience:

Werd wat verveeld doordat het beeld hetzelfde bleef, daardoor moeilijk om te focussen. Verder voelde het meer alsof de achterkant of voorkant omhoog kwam, meer een soort achtbaan. Doordat het beeld hetzelfde bleef had ik niet het gevoel van in de auto zitten.

Remaining comments of this session:

-

Low Optical Flow

Other experienced symptoms:

-

Comment of the session's experience:

Hoe ik mij voelde ging erg op en neer tijdens de rit. Soms voelde de simulator meer alsof ik omhoog ging en omlaag ging dan dat het voelde alsof ik afremde of heel hard ging. Vooral de momenten dat er werd afgeremd en momenten dat ik wat om mij heen keek werd ik wat misselijk. Daarnaast kon ik mij moeilijk focussen op het beeld.

Remaining comments of this session:

-

High Optical Flow

Other experienced symptoms:

-

Comment of the session's experience:

Het beeld werd slomer als de bewegingen ook slomer gingen en andersom, dat was fijn.

Remaining comments of this session:

-

Comment of all sessions:

Ik heb gemerkt dat het beeld veel met mij doet. Ik kan mij namelijk ook voorstellen dat alle drie dezelfde bewegingen waren en dat ik vooral meer voelde als het beeld niet overeenkwam of dat ik het moeilijk vond om te focussen. Bij B had ik daar namelijk het meest moeite mee, wellicht omdat het de eerste sessie was maar ook omdat dat beeld niet heel scherp was (dat is nu mijn beleving). Verder vond ik A vooral heel saai en het moeilijkst te interpeteren, omdat het beeld totaal niet meebewoog met de bewegingen die ik voelde.

Participant 11

This page shows the individual results of participant 11.

Table D-21: General information of participant 11

Age [years]	Gender [M/F]	MSSQ [%]	Condition order	$\overline{R}_{\text{LOF}}$ [-]	$\overline{R}_{\text{HOF}}$ [-]
24	M	16.7	HOF→LOF→BL	0.33	0.29

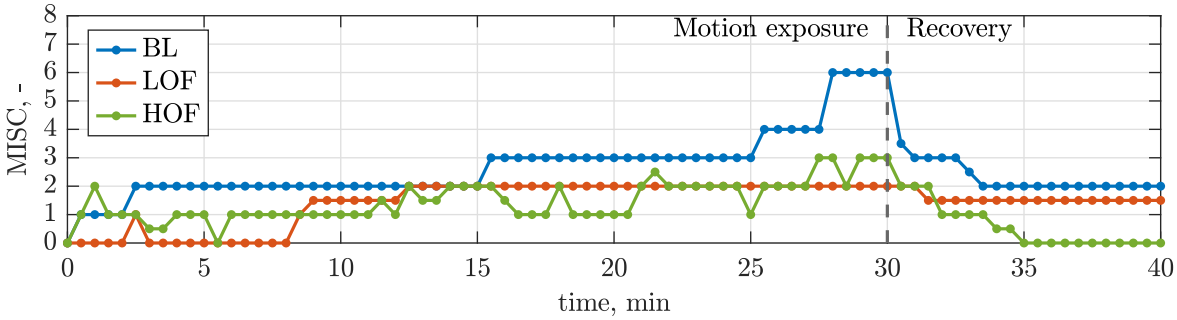

Figure D-21: MISC values of participant 11 for all conditions

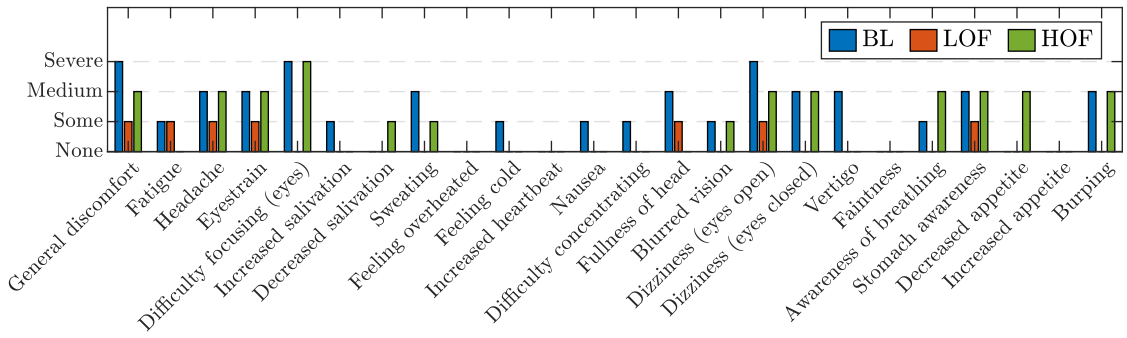

Figure D-22: MS symptoms of participant 11 for all conditions

Table D-22: Comfort and driving behaviour ratings of participant 11

	Comfort level [-]	Driving behaviour level [-]
BL	3: Mildly uncomfortable	5: Mildly aggressive driving behaviour
LOF	6: Comfortable	3: Mildly defensive driving behaviour
HOF	7: Extremely comfortable	4: Neutral driving behaviour

Baseline

Other experienced symptoms:

-

Comment of the session's experience:

To be honest, I really don't know the speed i was going, due to there being no reference points, it was not possible for me to detect that.

In general de expereince of today was far less comfortable then the previous two sessions, I was looking to find a horizon that would match what i was feeling. But it was not there of course. this resulted in not being able to relax like in the previous sessions.

Remaining comments of this session:

-

Low Optical Flow

Other experienced symptoms:

-

Comment of the session's experience:

It was harder to judge the speed and acceleration due to a lack of reference points (just a few trees) compared to the previous time (city scape).

I noticed that I focused less on the individual movements because i was already somewhat used to them. Therefore I focussed more on the visuals, but they were quite boring. there was little detail to focus on and keep concentrated. This resulted in me trying to entertain myself in other ways, by looking around the cabin or wandering off in my head with other thoughts.

Remaining comments of this session:

I noticed some flickering in the left side of my field of view. I don't know if this was part of the experiment or technical defects or that I made them up. At some point they also disapeared and i didn't notice them again.

High Optical Flow

Other experienced symptoms:

-

Comment of the session's experience:

Normally when you are driving, you are responding to the traffic around. But in the simulation there was nothing the car was responding to, which was a bit weird at first. In general the movements felt quite natural, like how you would experience them in a car, however sometimes there were smoother movements, for example when the acceleration was leveling off, those felt more comfortable.

Remaining comments of this session:

-

Comment of all sessions:

Preference go's to the city scape. There are far more reference points to determine your speed, acceleration. But besides that there are also details in the landscape that can keep you distracted/entertained, while that was not the case in the highway scene.

The highway scene was quite comfortable. It was harder to determine the speed and acceleration than in the city, but a rough estimation could be made. It was however really boring, which meant I was searching for other distractions, like looking to the inside of the cockpit.

Participant 12

This page shows the individual results of participant 12.

Table D-23: General information of participant 12

Age [years]	Gender [M/F]	MSSQ [%]	Condition order	$\overline{R}_{LOF}$ [-]	$\overline{R}_{HOF}$ [-]
25	F	14.8	HOF→BL→LOF	-0.12	-0.21

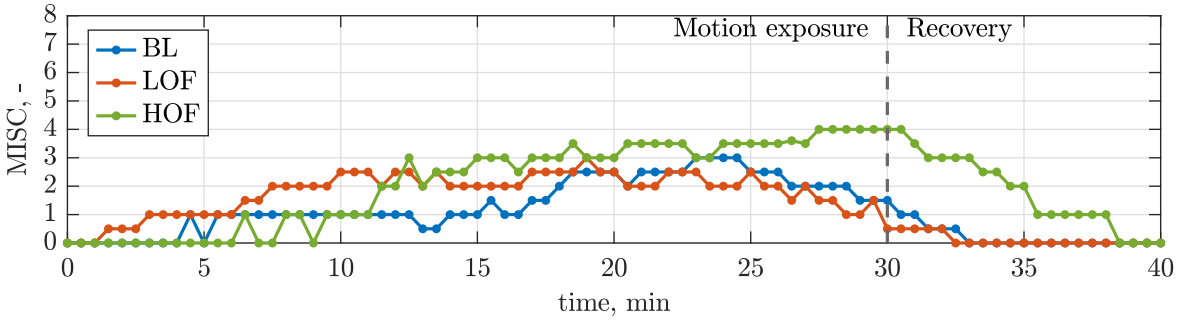

Figure D-23: MISC values of participant 12 for all conditions

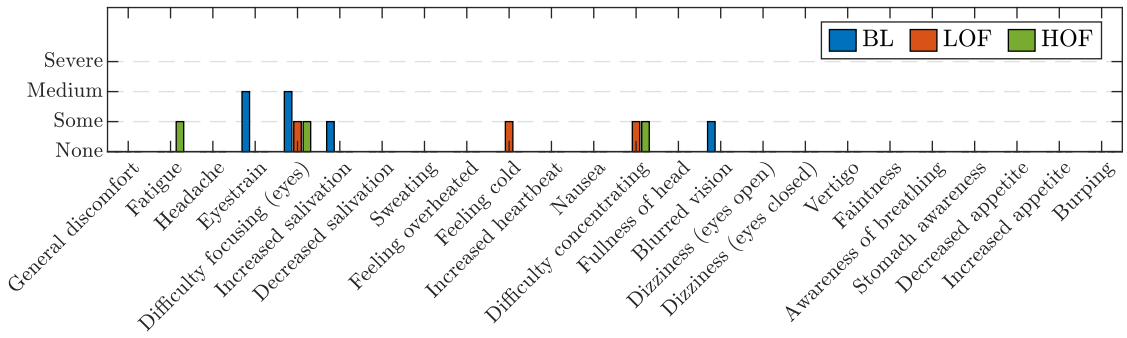

Figure D-24: MS symptoms of participant 12 for all conditions

Table D-24: Comfort and driving behaviour ratings of participant 12

	Comfort level [-]	Driving behaviour level [-]
BL	3: Mildly uncomfortable	2: Defensive driving behaviour
LOF	4: Neutral comfortability	4: Neutral driving behaviour
HOF	6: Comfortable	4: Neutral driving behaviour

Baseline

Other experienced symptoms:

-

Comment of the session's experience:

I wasn't entirely sure all the time if the car was going forwards or backwards

Remaining comments of this session:

-

Low Optical Flow

Other experienced symptoms:

-

Comment of the session's experience:

Since it's just a scale of 0-10 for everything together, it is difficult to distinguish between different things (for example, feeling your stomach and getting warm flashes) if they are about the same on the scale. The number remains the same but the experience is different

Remaining comments of this session:

-

High Optical Flow

Other experienced symptoms:

feeling tensed

Comment of the session's experience:

It felt a bit weird to go over bumps in the road, but not see them as the projected road was smooth

Remaining comments of this session:

-

Comment of all sessions:

Condition C was the least pleasant, not just because of the driving but I think also because so many different buildings were flashing by. Condition B was a lot more comfortable (and the one I prefer most), since the view was more predictable. During condition A, it was just hard to tell how fast the simulation was going because of the lack of reference, however, it was a lot more preferable than condition C.

Participant 13

This page shows the individual results of participant 13.

Table D-25: General information of participant 13

Age [years]	Gender [M/F]	MSSQ [%]	Condition order	$\overline{R}_{LOF}$ [-]	$\overline{R}_{HOF}$ [-]
22	F	19.5	BL→HOF→LOF	1.00	1.00

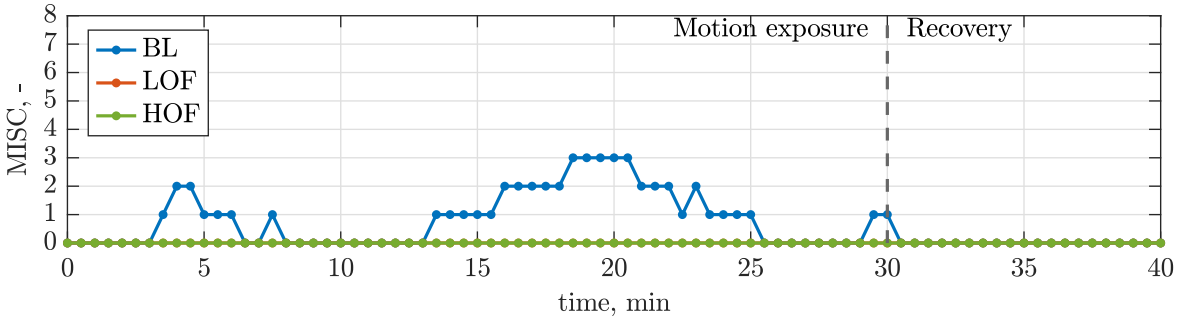

Figure D-25: MISC values of participant 13 for all conditions

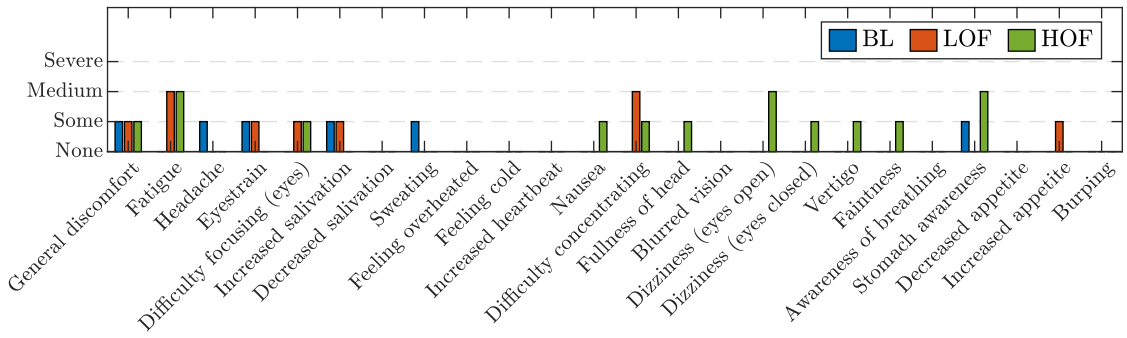

Figure D-26: MS symptoms of participant 13 for all conditions

Table D-26: Comfort and driving behaviour ratings of participant 13

	Comfort level [-]	Driving behaviour level [-]
BL	5: Mildly comfortable	4: Neutral driving behaviour
LOF	6: Comfortable	3: Mildly defensive driving behaviour
HOF	2: Uncomfortable	6: Aggressive driving behaviour

Baseline

Other experienced symptoms:

Beetje licht in mijn hoofd

Comment of the session's experience:

Wanneer ik langer ik de diepte staarde werd mijn orientatie minder. Naarmate de rit langer duurde hadden de bewegingen daarom meer effect op mijn reactie daarop. Ik werd dan ook sneller lichter in mijn hoofd.

Remaining comments of this session:

-

Low Optical Flow

Other experienced symptoms:

no

Comment of the session's experience:

Er gebeurde wat om mij heen, zoals de bomen de langs mij gingen. Hierdoor was het makkelijker te focussen en had ik meer gevoel van hoe hard ik zou gaan en wanneer er hard of zachter werd afgeremd.

Remaining comments of this session:

-

High Optical Flow

Other experienced symptoms:

no

Comment of the session's experience:

Het was prettig dat er om mij heen veel gebeurde. Daardoor was er meer besef van hoe hard ik ging of wanneer er versneld werd of afgeremd werd. Hierdoor staarde ik minder in een lege diepte wat prettig was.

Remaining comments of this session:

-

Comment of all sessions:

De stad gaf mijn voorkeur. Dit omdat er veel om mij heen gebeurde. Dit maakte niet alleen het concentreren makkelijker, maar gaf ook meer gevoel aan wat de auto deed. Daarna komt de 'rural area' dit omdat hier ook verschil was met wat er om mij heen gebeurde, maar minder als in de stad. Het concentreren bleef wel een stuk makkelijker dan bij de 'baseline'. Ik had bij de 'baseline' eigenlijk niet echt het gevoel dat ik zelf controle had over wat er gebeurde en het voelde doordat het beeld het zelfde bleef uitzichtloos wat mij duizelig maakte.

Participant 14

This page shows the individual results of participant 14.

Table D-27: General information of participant 14

Age [years]	Gender [M/F]	MSSQ [%]	Condition order	$\overline{R}_{\text{LOF}}$ [-]	$\overline{R}_{\text{HOF}}$ [-]
26	M	5.1	LOF→BL→HOF	0.00	0.00

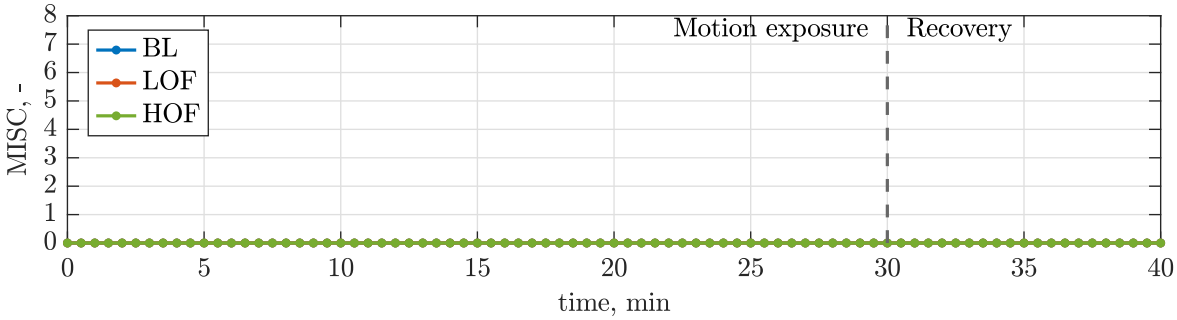

Figure D-27: MISC values of participant 14 for all conditions

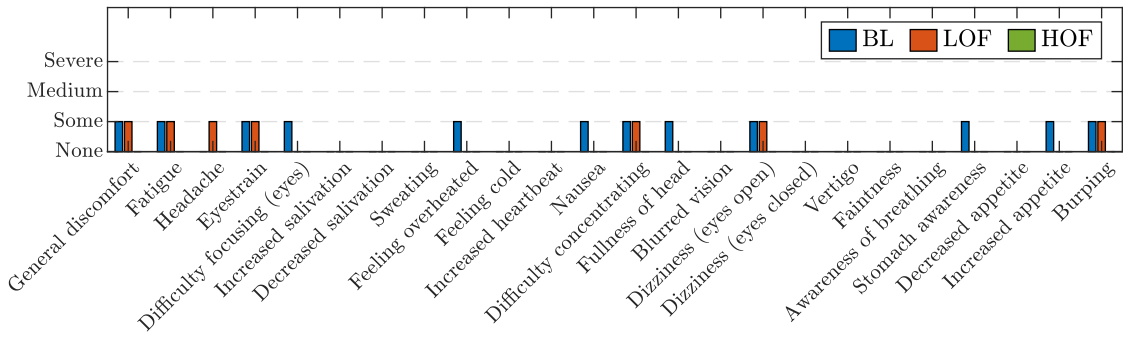

Figure D-28: MS symptoms of participant 14 for all conditions

Table D-28: Comfort and driving behaviour ratings of participant 14

	Comfort level [-]	Driving behaviour level [-]
BL	1: Extremely uncomfortable	6: Aggressive driving behaviour
LOF	6: Comfortable	4: Neutral driving behaviour
HOF	7: Extremely comfortable	4: Neutral driving behaviour

Baseline

Other experienced symptoms:

-

Comment of the session's experience:

It felt very monotonous despite the changes in motion. At times it felt like the car was driving backwards.

Remaining comments of this session:

-

Low Optical Flow

Other experienced symptoms:

-

Comment of the session's experience:

It felt like a going through a linear rollercoaster but then slowed down many times. Probably because of the recurring elements of breaking, accelerating and bumps feeling a bit repetitive.

Remaining comments of this session:

-

High Optical Flow

Other experienced symptoms:

-

Comment of the session's experience:

Very relaxed. My mind wandered quickly and the simulation drew little attention to itself. The visuals had a nice variation to them.

Remaining comments of this session:

-

Comment of all sessions:

The urban area was the most comfortable and felt like a relaxed ride. The rural area caused a slight eye strain/less focus due to my gaze being more fixated to a single point rather than switching focus to varying objects in the urban experience. The baseline was the least comfortable, keeping my eyes focused was harder and the motion felt a lot more prominent.

Participant 15

This page shows the individual results of participant 15.

Table D-29: General information of participant 15

Age [years]	Gender [M/F]	MSSQ [%]	Condition order	$\overline{R}_{LOF}$ [-]	$\overline{R}_{HOF}$ [-]
22	M	65.7	HOF→LOF→BL	0.62	-0.17

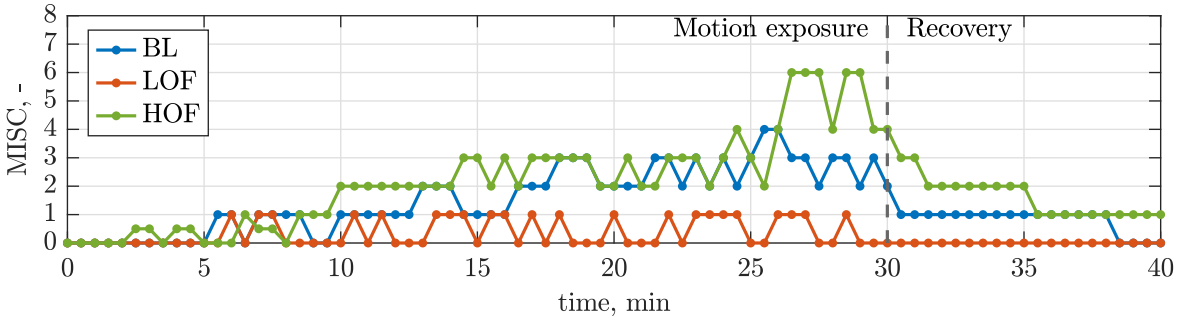

Figure D-29: MISC values of participant 15 for all conditions

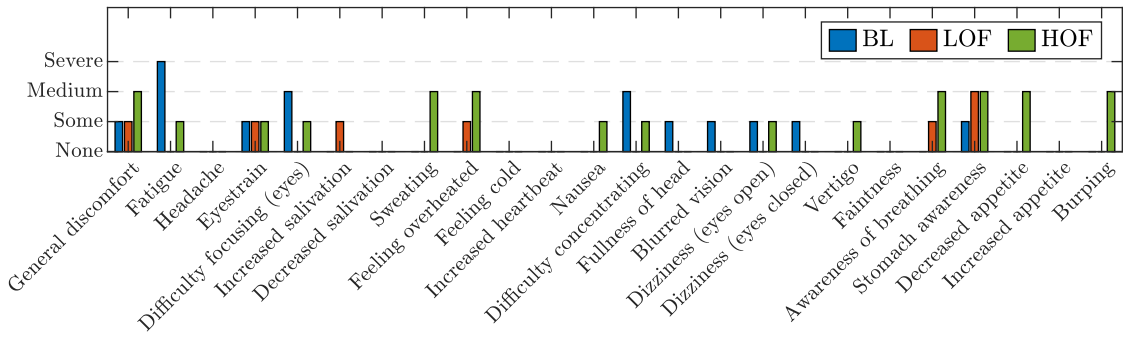

Figure D-30: MS symptoms of participant 15 for all conditions

Table D-30: Comfort and driving behaviour ratings of participant 15

	Comfort level [-]	Driving behaviour level [-]
BL	2: Uncomfortable	5: Mildly aggressive driving behaviour
LOF	4: Neutral comfortability	5: Mildly aggressive driving behaviour
HOF	3: Mildly uncomfortable	6: Aggressive driving behaviour

Baseline

Other experienced symptoms:

-

Comment of the session's experience:

I think that the visuals on a screen made it worse than if i would have no visuals

Remaining comments of this session:

-

Low Optical Flow

Other experienced symptoms:

-

Comment of the session's experience:

Felt like a calmer ride than previous session (C).

Remaining comments of this session:

-

High Optical Flow

Other experienced symptoms:

-

Comment of the session's experience:

The not linear acceleration was extra uncomfortable

Remaining comments of this session:

The neckbrace made me less comfortable than in a normal situation.

Comment of all sessions:

The rural area was by far the most comfortable, the rural area seemed more busy, but this was also my first session.

Participant 16

This page shows the individual results of participant 16.

Table D-31: General information of participant 16

Age [years]	Gender [M/F]	MSSQ [%]	Condition order	$\overline{R}_{\text{LOF}}$ [-]	$\overline{R}_{\text{HOF}}$ [-]
22	M	0.0	BL→LOF→HOF	0.45	1.00

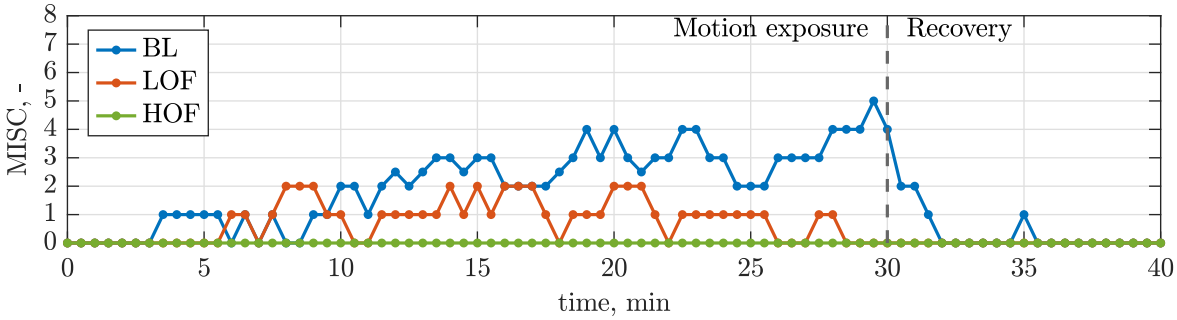

Figure D-31: MISC values of participant 16 for all conditions

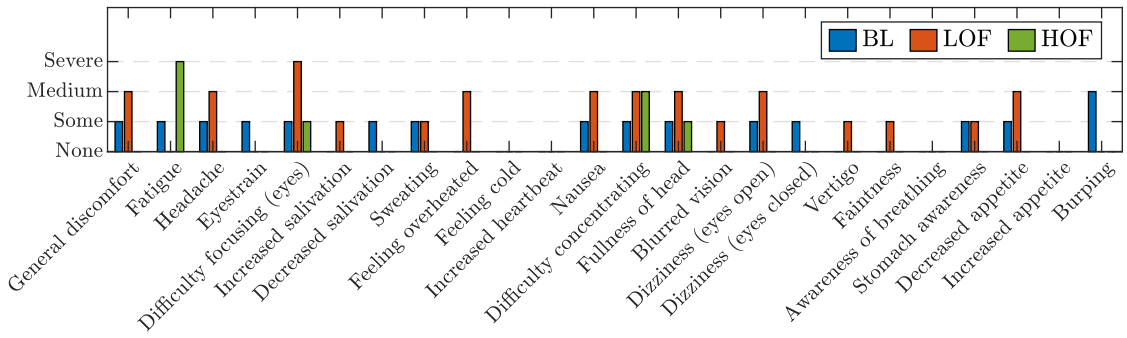

Figure D-32: MS symptoms of participant 16 for all conditions

Table D-32: Comfort and driving behaviour ratings of participant 16

	Comfort level [-]	Driving behaviour level [-]
BL	4: Neutral comfortability	1: Extremely defensive driving behaviour
LOF	5: Mildly comfortable	6: Aggressive driving behaviour
HOF	2: Uncomfortable	4: Neutral driving behaviour

Baseline

Other experienced symptoms:

-

Comment of the session's experience:

I felt a bit of dizziness at some points, but that was perhaps the influence of the visuals. The motions sometimes felt like I was going up and down but never reaching a climax thus leaving a bit of tension.

Remaining comments of this session:

It was very fun!

Low Optical Flow

Other experienced symptoms:

-

Comment of the session's experience:

It was a more pleasant ride than the first time. The movement on the screen matched the simulations movement well and time passed by quicker than last time. It was a little more sleep inducing as well. The only thing that did not match the simulation of a car that well was the bump back up after simulating a breaking movement. This was the only time that I really became aware that it was a simulation.

Remaining comments of this session:

It was a way better pass time than last time.

High Optical Flow

Other experienced symptoms:

-

Comment of the session's experience:

It was difficult for me to stay awake, only the beeps every 30 seconds kept me awake. Especially when the car was accelerating or decelerating the swinging motion was sleep inducing. All together it was a pleasant experience though.

Remaining comments of this session:

-

Comment of all sessions:

The last two sessions (B and C) were really comfortable, but it was hard to keep focus and I had a constant feeling of dozing off. The first session was not nice at all and I was happy when it ended.

Participant 17

This page shows the individual results of participant 17.

Table D-33: General information of participant 17

Age [years]	Gender [M/F]	MSSQ [%]	Condition order	$\overline{R}_{LOF}$ [-]	$\overline{R}_{HOF}$ [-]
19	F	10.0	HOF→BL→LOF	0.01	-0.33

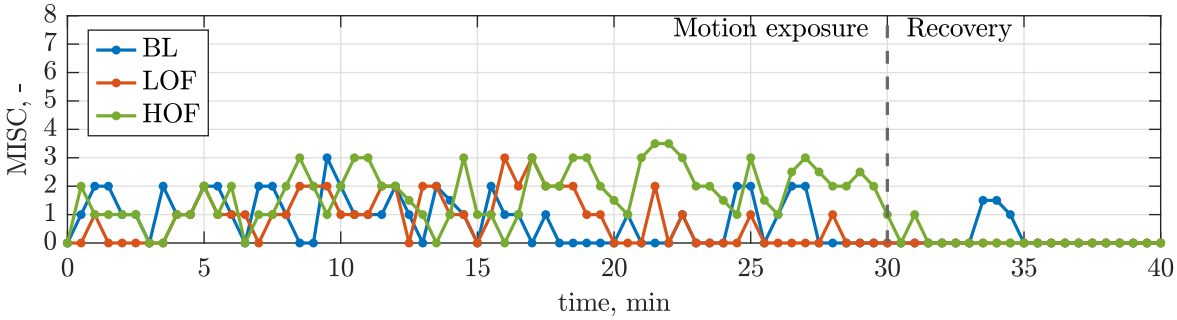

Figure D-33: MISC values of participant 17 for all conditions

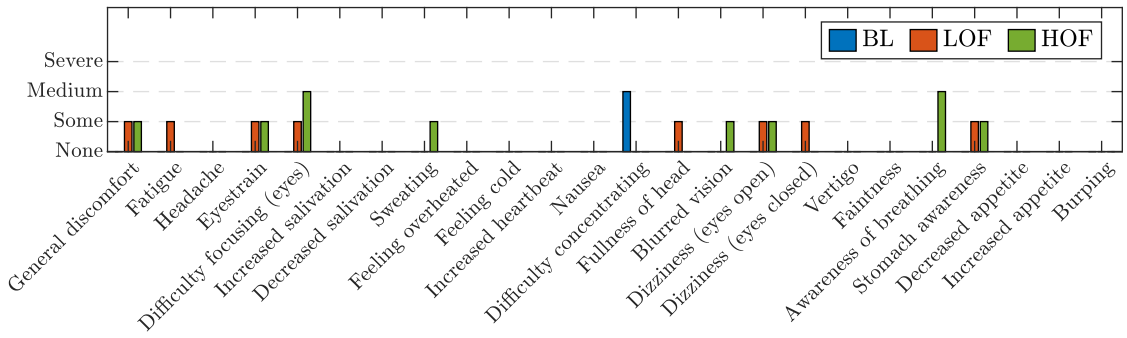

Figure D-34: MS symptoms of participant 17 for all conditions

Table D-34: Comfort and driving behaviour ratings of participant 17

	Comfort level [-]	Driving behaviour level [-]
BL	5: Mildly comfortable	6: Aggressive driving behaviour
LOF	3: Mildly uncomfortable	3: Mildly defensive driving behaviour
HOF	4: Neutral comfortability	3: Mildly defensive driving behaviour

Baseline

Other experienced symptoms:

-

Comment of the session's experience:

The movement was a bit shaky but generally pretty okay. Sometimes the stops and accelerating was a bit abrupt but overall pretty comfortable. The movement that went back and forth made me very sleepy and made it a bit hard to focus on the road. The road itself was also not very stimulating and made it also harder to concentrate and not fall asleep. The movement was also very slow and carefull mostly.

Remaining comments of this session:

-

Low Optical Flow

Other experienced symptoms:

-

Comment of the session's experience:

It was quite comfortable with a few abrupt acceleration and stops but overall pretty nice. Did become a bit sleepy

Remaining comments of this session:

-

High Optical Flow

Other experienced symptoms:

No

Comment of the session's experience:

Unpleasant, the ride had unpredictable movement. Stopping and accelerating seemingly random which made me feel unpleasant (dizzy and aware of my stomach). The stopping and accelerating also was done too quickly in my opinion.

Remaining comments of this session:

-

Comment of all sessions:

B was quite comfortable with not too many abrupt movements and visuals were the most realistic. The other experiments had more abrupt movements and were therefore more uncomfortable.

Participant 18

This page shows the individual results of participant 18.

Table D-35: General information of participant 18

Age [years]	Gender [M/F]	MSSQ [%]	Condition order	$\overline{R}_{\text{LOF}}$ [-]	$\overline{R}_{\text{HOF}}$ [-]
22	M	5.1	HOF→BL→LOF	1.00	-0.95

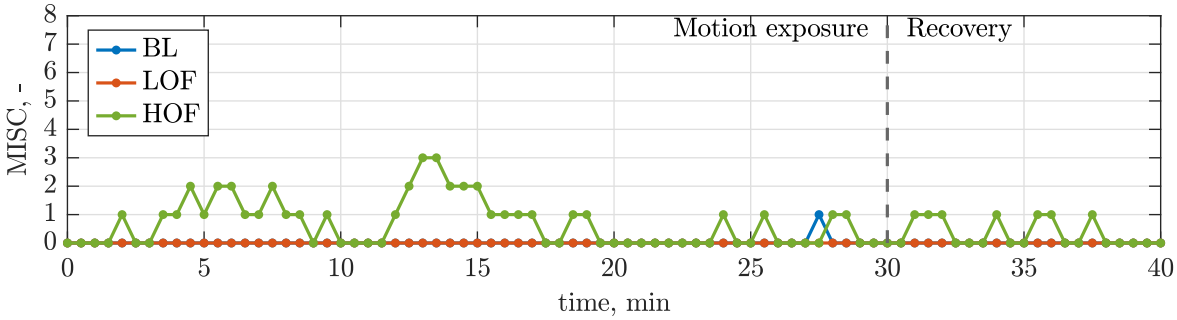

Figure D-35: MISC values of participant 18 for all conditions

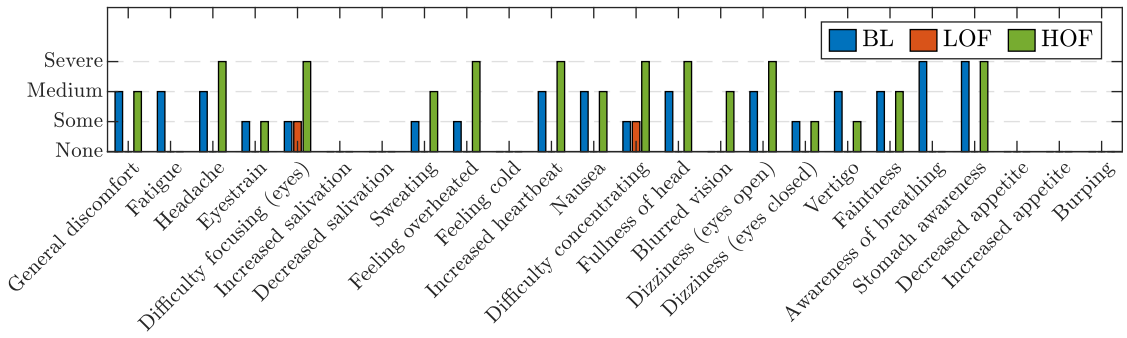

Figure D-36: MS symptoms of participant 18 for all conditions

Table D-36: Comfort and driving behaviour ratings of participant 18

	Comfort level [-]	Driving behaviour level [-]
BL	4: Neutral comfortability	5: Mildly aggressive driving behaviour
LOF	7: Extremely comfortable	3: Mildly defensive driving behaviour
HOF	3: Mildly uncomfortable	2: Defensive driving behaviour

Baseline

Other experienced symptoms:

-

Comment of the session's experience:

It was easier to keep focusing on the end of the road then the first session because there weren't many surroundings that could make me a bit dizzy.

Remaining comments of this session:

-

Low Optical Flow

Other experienced symptoms:

-

Comment of the session's experience:

The visuals matched good with the feeling of the simulator.

Remaining comments of this session:

-

High Optical Flow

Other experienced symptoms:

-

Comment of the session's experience:

Because there is no traffic around it's hard to predict when you will (de)accelerate and therefor you sometimes get surprised what can make you feel a bit discomfortable.

Remaining comments of this session:

-

Comment of all sessions:

my preference was the rural area because you could really estimate the speed that you were riding and compared to the urban city there was not so much that could make you very dizzy.

Appendix E

Experiment Briefing

This appendix contains all information provided to the participants before participating in the experiment, including:

- Email communication
- Informed consent form
- Experiment briefing
- MISC used in the briefing
- Checklist verbal briefing

Email communication

Dear Participant,

Thank you for your availability. You are scheduled for the following 3 sessions.
Trial 1: ±90min
Monday 17 February 13:00
Trial 2: ±60min
Wednesday 19 February 9:00
Trial 3: ±70min
Friday 21 February 11:00

Please let me know if you are still available in these timeslots and mark them in your personal calendar.

Location: `https://goo.gl/maps/zwh4VANiV3guikvm6`
The experiment will take place at the SIMONA Research Simulator at the Faculty of Aerospace Engineering. I will pick you up in the main hall of the Aerospace Faculty. Please be sure to be there 5 min in advance.
Expectation:
You can find the experiment briefing attached to this email. Before your first trial all procedures will be discussed, and I will make sure you understand and agree. A consent form needs to be signed for using your (anonymous) results of the experiment. After this, I will talk you through all steps in the progress of the simulator run in the SIMONA Research Simulator. The second and third trial require a shorter start-up time.
Preparation:
Being fit for the trials is also important since the experiment is about comfort. Therefore, (excessive) alcohol or drugs use in the **24h** before each experiment trial is strongly discouraged. In order to have the best experience, make sure that you have eaten before the trial and that you are well rested.
SIMONA safety video: `https://www.youtube.com/watch?v=PXijsyJ3hro`
Before participating in the experiment trials, it is important to watch the SIMONA safety video and read the briefing and the informed consent form. It is allowed to do this on location, however, it is faster and may be more convenient to do this before the first trial.
Corona
Please be aware that this experiment will follow the corona guideline set by the faculty, which may be stricter than you expect. We will try to keep our distance during the experiment and avoid close contact. Please check if you have any COVID-19-related symptoms beforehand, please let me know as the experiment will then be rescheduled.
Cancelation:
If you cannot participate for any other reason, please let me know in advance. You do not have to state a reason, we can check if another timeslot would fit.
If you have any other questions beforehand, please let me know via email or by phone (below).

See you soon and best regard,
Mitchel Elbertse

Experiment Consent Form – Investigating Motion Comfort in Automated Vehicles

Please tick the appropriate boxes	**Yes**	**No**
I have read and understood the experiment briefing, or it has been read to me. I have been able to ask questions about the study and my questions have been answered to my satisfaction.	○	○
I consent voluntarily to be a participant in this study and understand that I can refuse to answer questions and I can withdraw from the study at any time, without having to give a reason.	○	○
I understand that I will be compensated for my participation in the form of a Bol.com gift card with €10,- credit for each experiment session that I attempt. This is independent of whether I decide to withdraw from the study before having taken part in all experiment sessions, or whether an experiment session is aborted prematurely. It also does not depend on any of my answers provided during the study.	○	○
I understand that taking part in the study involves being asked to provide verbal feedback on my motion discomfort development on a frequent basis, while being exposed to simulator motion.	○	○
I understand that taking part in the study involves the risk of developing temporary physical and/or mental discomfort caused by being exposed to simulator motion, as the goal of the experiment is to investigate the motion (dis)comfort development of vehicle passengers.	○	○
I confirm that the researcher has provided me with detailed safety and operational instructions for the SIMONA Research Simulator and that these instructions are fully clear to me.	○	○
I confirm that the researcher has provided me with detailed safety instructions to ensure my experiment sessions can be performed in line with current RIVM COVID-19 regulations *at all times* and that these instructions are fully clear to me.	○	○
I understand that information I provide will be used for scientific reports and/or publications, in which the researcher will not identify me by name, and that my confidentiality as a participant in this study remains secure.	○	○
I understand that personal information collected about me that can identify me, such as my name and my age, will not be shared beyond the study team.	○	○
I understand that this research is funded by and performed in collaboration with an industry partner, who will only receive anonymized data collected in this research.	○	○
I give permission for the anonymized motion discomfort history questionnaire, symptoms checklists, verbal motion discomfort ratings and other comfort questionnaires that I provide to be archived in a secure data repository, so they can be used for future research and learning.	○	○
I understand that at all times I can request for my participant data to be removed from the secure data repository.	○	○
I understand that this research study has been reviewed and approved by the TU Delft Human Research Ethics Committee (HREC). I am aware that I can report any problems regarding my participation in the experiment to the researcher using the contact information below.	○	○
I confirm that I currently do not have any COVID-19 symptoms.	○	○

Signatures

_____	_____	_____	Part. no.: _____
Name of participant	Signature	Date	(Filled out by researcher)

I, as researcher, have accurately read out the information sheet to the potential participant and, to the best of my ability, ensured that the participant understands to what they are freely consenting.

_M. Elbertse_____	_____	_____
Researcher name	Signature	Date

Contact responsible researcher:	Mitchel Elbertse	M.Elbertse@student.tudelft.nl	+31 6xxxxxxxx
Contact research supervisor:	Rowenna Wijlens	R.Wijlens@tudelft.nl	+31 6xxxxxxxx

Experiment Briefing

Investigating Motion Comfort in Automated Vehicles

First of all, thank you for taking part in this experiment! You will be participating in a motion experiment in the SIMONA Research Simulator (SRS) at the Faculty of Aerospace Engineering of the TU Delft. This briefing will provide you with a short introduction on what to expect and what is expected from you as a participant.

Your participation in this experiment is completely voluntary, which means you have the right to withdraw from the experiment at any given time without having to give a reason. The experiment has been approved by the *Human Research Ethics Committee* of the TU Delft and will be performed in line with current RIVM COVID-19 regulations at all times as well as with additional guidelines of the faculty and facility. All data collected during this experiment will, of course, be made completely anonymous, but can still always be deleted on your request.

The experiment will consist of three separate experiment sessions. We would like to ask you not to discuss the experiment with any other participants before they, as well as you, have completed all three sessions, as this could influence the experiment results.

Experiment Goal

The goal of this experiment is to investigate passengers' motion comfort in self-driving vehicles, including their reaction to different visual environments. The results of this experiment can be used to make recommendations on self-driving vehicle design to ensure that passengers feel as comfortable as possible during their ride.

Experiment Procedures

The experiment will consist of three separate experiment sessions, which will take place a few days apart. Each session will take approximately *60 to 75 minutes*. All sessions will consist of a briefing, a simulated drive in the simulator and a debriefing, which consists of filling in a motion discomfort symptoms checklist and questionnaires on the experienced motion and visual environments. In all sessions, you will be exposed to 30 minutes of simulator motion. The time schedule for the three experiment sessions is shown below.

Introduction (only the first session) ±15 min	**Briefing** ±5 min	**Simulator motion** ±30 min	**Recovery period** ±10 min	**Questionnaires** ±15/20 min

Experiment Tasks / Expectations

The experiment will simulate a condition where you are a passenger of a self-driving vehicle. Therefore, you do not have to provide any steering or gas/brake pedal inputs. Instead, you will be asked to have a relaxed body posture and keep looking forward. Furthermore, you are asked to wear a *neck brace* and *headset* during the experiment.

The tasks for you as a participant during your time in the simulator are as follows:

- Relax your body and keep looking forward.
- Wear a neck brace and headset.
- Every 30 seconds, you will be notified with a beep that requests you to verbally communicate your motion discomfort level on the scale that is presented in front of you.
- For 10 minutes directly after the simulator motion has ended, you will be asked to remain seated and verbally communicate your motion discomfort level every 30 seconds on the scale that is presented in front of you.
- Enjoy the ride!

Please remember that you have the right to stop at any given moment. The researcher may also make this decision if this seems better for you. It is *not* the goal to get you very nauseous or sick.

Lastly, thank you for your participation and do not hesitate to contact us in case of any questions or remarks!

Contact responsible researcher:	Mitchel Elbertse	M.Elbertse@student.tudelft.nl	+31 6xxxxxxxx
Contact research supervisor:	Rowenna Wijlens	R.Wijlens@tudelft.nl	+31 6xxxxxxxx

English

Symptoms		MISC
No problems at all		0
Uneasy (no typical symptoms)		1
Dizziness, warmth, headache, stomach awareness, sweating, …, but NO nausea	vague	2
	slight	3
	fairly	4
	severe	5
Nausea	slight	6
	fairly	7
	severe	8
	(near) retching	9
Vomiting		10

Nederlands

Symptomen		MISC
Geen enkel probleem		0
Niet helemaal lekker (zonder herkenbaar symptoom)		1
Duizeligheid, warm, hoofdpijn, bewust van de maag, zweet, …, maar GEEN misselijkheid	vaag	2
	beetje	3
	nogal	4
	ernstig	5
Misselijkheid	beetje	6
	nogal	7
	ernstig	8
	(bijna) kokhalzen	9
Overgeven		10

Briefing checklist experiment – Motion Sense Mitchel

General

- Participation is completely voluntary.
- You can withdraw at any moment.
- Data is anonymized but can be removed at any time.
- **Sign consent form!**

Experiment

- Three separate sessions in simulator.
- Passenger in self-driving vehicle → no steering or gas/brake pedal inputs
- Goal: investigate passengers' motion comfort in self-driving vehicles.

Procedures

- Each session lasts around 60-75 minutes.
- Introduction (first session) → Briefing sim → Simulator motion → Recovery → Questionnaires.
- Compare all session in the end!

SIMONA procedures

- Watch safety video → Questions?
- Seat belt
- Seat adjustment
- Emergency buttons
- Communication

Tasks

- Relax your body and keep looking forward.
- Wear a neck brace and headset.
- MISC beeps every 30 seconds, for 30 minutes + 10 minutes recovery → stay seated.
- It is allowed to think out loud.
- Enjoy the ride!

Please remember that you have the right to stop at any given moment. The researcher may also make this decision if this seems better for you. It is **not** the goal to get you very nauseous or sick.

Appendix F

Experiment Checklist

This appendix contains the experiment checklist for the beginning of the day, during the experiment, and the end of the day. This checklist was used to ensure that each experimental session progressed in an equal way. Additionally, the briefing checklist is included that ensured that all participants had the same instructions before the start of the experiment.

Checklist SIMONA – Motion Sense Mitchel – Start of day

General

- Find supervisor
- SIMONA **ON** (panel downstairs)

Control room

- Logbook SIMONA
- Screens **ON**

SIMONA control panel

- EFIS2 **ON** (everything else **OFF**)
- Airco **ON**
- Cabin lights **ON** (for boarding participant)

SIMONA cabin

- Check sick bags
- Install headset (check volume, upright = neutral)
- Check loose items in cabin

Motion System

- Visual check if ready → Environment ready button
- Disconnect bridge
- Motion system **ON**
    - **Write down time!**
    - During warmup, ΔP should be around 110 bar (warm-up)
    - If ΔP around 160 bar, turn **OFF** → wait → **ON** again
- After warmup, take SIMONA out of the buffers
    - Environment ready
    - Select all actuators
    - CManual
    - Small ticks on UP → continuous UP until almost halfway →continuous DOWN again
    - CManual End
    - After taking out of buffers, ΔP should be around 160 bar
- Check whether everything is working by running own project for 2 minutes with motion (projectors can stay off at this time)
- Motion system **OFF**
    - **Write down time!**
- Connect bridge

Visual system

- Turn all projectors **ON**
    - **Write down time!**

Checklist SIMONA – Motion Sense Mitchel - Experiment

(Safety) briefing

- SIMONA safety video (if needed)
- Experiment briefing (if needed)
- MISC table explanation
- Communication explanation (don't touch headset buttons)
- Neck brace
- Informed consent form

Start of Experiment

- Subject in SIMONA
- Check seatbelt
- Check eye height (DERP) and forward position subject
- Check environment
- Check communication
    - Tab From USB:
        - Three inputs to 0dB
        - Select output: Pilot headset
    - Tab Cockpit:
        - Desktop Mic: Headset
        - Headset Mic: Pilot (to hear MISC beep??)
    - Tab Volumes:
        - Check that control room voice is not too loud
- **Select visual condition in start-up script**
- Check dueca_mod.py settings
    - MISC language
    - Motion / ImageShower / HeadSet TRUE
- Start DUECA → Screens will change (Unity starts)
- Shuttle Door Open / Seatbelts Unfastened lights turned **OFF**
- Cabin lights **OFF**
- Visual check if ready → Environment ready button
- Disconnect bridge
- Motion system **ON**
    - **Write down time!**
    - Take SIMONA out of the buffers if necessary (OFF for >70min)
- ~~IF motion system fails: Reset Host2MCCEXPERIMENTAL~~
- IF alarms on Simulink or participant takes seatbelt off too early: confirm alarm, reset alarms

Experiment

- Go to **HOLD**
    - SIMONA **UP**
- Go to **ADVANCE**
    - Ask if ready
    - Ask first MISC score
    - Countdown
    - Start own timer
    - Stop at MISC = 7 or MISC = 3 * 6

End of Experiment

- Tell to remain seated with seatbelt ON
- Go to **INACTIVE**
  - SIMONA **DOWN**
- Go to **STOP**
- Motion system **OFF**
  - **Write down time!**
- Connect bridge
- Wait for recovery period to finish
- Free subject
  - Seatbelt off
  - Headset off
- **Questionnaire!**
- **Do not talk to other subjects!!!**
- Debrief
  - Bol.com voucher
- Clean all equipment
  - Cabin
  - Doorhandles
  - Headset
  - Neckbrace

End of Day

- Visual system **OFF**
  - **Write down time!**
- Screens control room off

Appendix G

Experiment MISC Rating Card

This appendix contains the MISC rating card that was used to monitor the participants' verbally communicated MISC scores during the experiment sessions.

MIsery SCale (MISC) rating card
Motion Sense Mitchel

Participant number: _____

Age: _____ **M / V / X**

Trial 1: BL / LOF / HOF
Date: ___ / ___ /2023
Time: ___ : ___

Trial 2: BL / LOF / HOF
Date: ___ / ___ /2023
Time: ___ : ___

Trial 3: BL / LOF / HOF
Date: ___ / ___ /2023
Time: ___ : ___

		T1	T2	T3			T1	T2	T3			T1	T2	T3
0	00:00				**37**	18:30				**59**	29:30			
1	00:30				**38**	19:00				**60**	30:00			
2	01:00				**39**	19:30				**1/61**	(3)0:30			
3	01:30				**40**	20:00				**2/62**	(3)1:00			
4	02:00				**41**	20:30				**3/63**	(3)1:30			
5	02:30				**42**	21:00				**4/64**	(3)2:00			
6	03:00				**43**	21:30				**5/65**	(3)2:30			
7	03:30				**44**	22:00				**6/66**	(3)3:00			
8	04:00				**45**	22:30				**7/67**	(3)3:30			
9	04:30				**46**	23:00				**8/68**	(3)4:00			
10	05:00				**47**	23:30				**9/69**	(3)4:30			
11	05:30				**48**	24:00				**10/70**	(3)5:00			
12	06:00				**49**	24:30				**11/71**	(3)5:30			
13	06:30				**50**	25:00				**12/72**	(3)6:00			
14	07:00				**51**	25:30				**13/73**	(3)6:30			
15	07:30				**52**	26:00				**14/74**	(3)7:00			
16	08:00				**53**	26:30				**15/75**	(3)7:30			
17	08:30				**54**	27:00				**16/76**	(3)8:00			
18	09:00				**55**	27:30				**17/77**	(3)8:30			
19	09:30				**56**	28:00				**18/78**	(3)9:00			
20	10:00				**57**	28:30				**19/79**	(3)9:30			
21	10:30				**58**	29:00				**20/80**	(4)0:00			
22	11:00				Comments Trial 1:									
23	11:30													
24	12:00													
25	12:30													
26	13:00													
27	13:30				Comments Trial 2:									
28	14:00													
29	14:30													
30	15:00													
31	15:30													
32	16:00				Comments Trial 3:									
33	16:30													
34	17:00													
35	17:30													
36	18:00													

Appendix H

Questionnaires

This appendix contains the **registration questionnaire** and the **post trial questionnaire** that were conducted within Qualtrics. The former was used for the registration of the participants and contained a brief explanation of the experiment, the participant requirements, questions to gather general information about the participants, and the MSSQ used to measure the participants' susceptibility to MS. The post trial questionnaire included the MS symptoms checklist, physical and visual motion assessments, and subjective comfort assessment. The latter was included in the full experiment comparison that was only shown after the participants completed all three sessions.

Registration Questionnaire

Start of Block: Introduction

Introduction **Welcome to the survey for participation in a Motion Comfort experiment.**
This survey will take approximately 10 minutes.

This survey serves to inform and present some basic information about a motion comfort experiment being performed in the SIMONA Research Simulator. In case you are interested in taking part in this experiment, this form will obtain some required information about you. The input you give will be used to select the most suitable participants. After the selection you will hear by email if you are selected to participate in the experiment.

This experimental research is performed to gather data for the MSc thesis research of Mitchel Elbertse. The experiment takes place at the Faculty of Aerospace Engineering at the Delft University of Technology, under supervision of Prof. Dr. Ir. Max Mulder, Dr. Ir. Rene van Paassen and PhD candidate Rowenna Wijlens. The purpose of the experiment is to create a better understanding of passengers' comfort in autonomously driving vehicles.

The goal of this experiment is to investigate passengers' motion comfort in self-driving vehicles, including their reaction to different visual environments. The results of this experiment can be used to make recommendations on self-driving vehicle design to ensure that passengers feel as comfortable as possible during their ride.

Expectations of the experiment:
The experiment will take place in the SIMONA Research Simulator at the Faculty of Aerospace Engineering at the Delft University of Technology. The experiment consists of 3 separate trials, planned on 3 separate days. Each trial consists of a **30 min** simulator drive and will take around **60-90 min** in total. During the experiment you are asked to wear a neck brace and a headset. For each actively participated trial, you will receive a €10,- bol.com voucher as a compensation for your time.

The data of this survey will be used to select the participants most suitable to participate in the experiment. All data gathered before, during, and after the experiment will be made anonymous, however, for scheduling purposes, it is required to provide your email address. To ensure privacy, all external contact is done using TU Delft supported software or (email) servers.

Note that only the main researcher (Mitchel Elbertse) will have access to your response form. None of the personal data you provide (e-mail address, name and, optionally, phone number) will be shared with any other party. Your participation in this study is entirely voluntary and you

can withdraw at any time. Your response form and any contact details that you will provide (e.g. e-mail address) will be deleted as soon as the experiment ends.

If you have any questions, please feel free to contact me:

Mitchel Elbertse
M.Elbertse@student.tudelft.nl
+31 6 xxxxxxxx

End of Block: Introduction

Start of Block: Availability

Q10 **Availability**
This experiment consists of three separate sessions (**60-90 min**) on three separate days. If you are invited to participate in the experiment based on (the results of) this questionnaire, you will receive more information and a detailed planning with all session options.

The experiment sessions will take place from **13-02-2023**, till **03-03-2023**. It is required to do the three separate trials in a 7-10 day period. Please indicate your availability in this period below.

- ○ **Yes**, I am very flexibel, thus this should fit in my schedule
- ○ **Maybe**, I will try to fit the 3 trials in, but I am not sure yet

End of Block: Availability

Start of Block: Participant requirements

Q11 **Participant requirements**
It is important that participants have correctly functioning motion sensors. This means that you do not suffer from: Inner ear problems (e.g., stability issues) Significant eyesight problems (that are not solved with glasses/etc.)
Other requirements: No claustrophobia (you will be in the closed cockpit of the SIMONA Research Simulator for approximately 40min without breaks) Not participated in other similar motion (dis)comfort experiment(s) recently (<6 months)
If you're in doubt about fulfilling one of the aforementioned requirements, feel free to contact me (contact details displayed on home page).

- ○ I understand, and I am fulfilling these requirements

End of Block: Participant requirements

Start of Block: Basic info

Q16 **General information**

Q12 1/3 - How susceptible to motion sickness do you consider yourself to be?

- Not at all
- Slightly
- Moderately
- Very much

Q13 2/3 - Please state your gender

- Male
- Female
- Non-binary / third gender
- Prefer not to say

Q14 3/3 - Please state your age

_____

End of Block: Basic info

Start of Block: Block 4

Q17 **Motion Sickness Susceptibility**
The following questions are designed to find out how susceptible to motion sickness you are,

and what sorts of motion are most effective in causing that sickness. Sickness here means feeling queasy or nauseated or actually vomiting.

Q18 1/2 - For each of the following types of transport or entertainment please indicate, **as a CHILD (before age 12)**, how often you **Felt Sick or Nauseated**:

	Not Applicable - Never Travelled	Never Felt Sick	Rarely Felt Sick	Sometimes Felt Sick	Frequently Felt Sick
Cars	○	○	○	○	○
Buses or Coaches	○	○	○	○	○
Trains	○	○	○	○	○
Aircraft	○	○	○	○	○
Small Boats	○	○	○	○	○
Ships, e.g., Channel Ferries	○	○	○	○	○
Swings in playgrounds	○	○	○	○	○
Roundabouts in playgrounds	○	○	○	○	○
Big Dippers, Funfair Rides	○	○	○	○	○

Q19 2/2 - For each of the following types of transport or entertainment please indicate, **over the LAST 10 YEARS**, how often you **Felt Sick or Nauseated**:

	Not Applicable - Never Travelled	Never Felt Sick	Rarely Felt Sick	Sometimes Felt Sick	Frequently Felt Sick
Cars	○	○	○	○	○
Buses or Coaches	○	○	○	○	○
Trains	○	○	○	○	○
Aircraft	○	○	○	○	○
Small Boats	○	○	○	○	○
Ships, e.g., Channel Ferries	○	○	○	○	○
Swings in playgrounds	○	○	○	○	○
Roundabouts in playgrounds	○	○	○	○	○
Big Dippers, Funfair Rides	○	○	○	○	○

End of Block: Block 4

Start of Block: Block 5

Q21 **Contact information**

Please enter your email address (TU Delft email address if possible).

This is used for contact and experiment scheduling.

Q22 If you have any comments or scheduling constraints, feel free to leave them here:

_____

Q23 **Please complete the survey by clicking the blue arrow below**

End of Block: Block 5

Post Trial Questionnaire

Start of Block: Default_questions

Q3 **Post-experiment-session questionnaire**

This questionnaire is meant to record your experience of today's experiment session.

!!!
You are asked to leave subjective textual comments. In order to protect your own privacy, please make sure that your comments do not contain any personal information.
!!!

However, your comments can be very valuable for the results of this experiment.

Page Break

Q1 What is your participant number? (ask the main researcher)

_____

Q3 Which experiment *condition* did you perform today? (ask the main researcher)

- A
- B
- C

Q4 Which experiment session number did you perform today?

- First experiment session
- Second experiment session
- Third experiment session

End of Block: Default_questions

Start of Block: Questions_per_trial

Q14 **Motion Sickness Symptoms**

Q6 The following checklist is designed to capture how you were feeling during and right after exposure to the simulator motion. Please tick whether/to which extent you were/are experiencing the symptoms stated below.

	None	Some	Medium	Severe
General discomfort	○	○	○	○
Fatigue	○	○	○	○
Headache	○	○	○	○
Eyestrain	○	○	○	○
Difficulty focusing (eyes)	○	○	○	○
Increased salivation	○	○	○	○
Decreased salivation	○	○	○	○
Sweating	○	○	○	○
Hot flashes / Feeling overheated	○	○	○	○
Cold flashes / Feeling cold	○	○	○	○
Increased heartbeat	○	○	○	○
Nausea	○	○	○	○
Difficulty concentrating	○	○	○	○
Fullness of head	○	○	○	○

Blurred vision	○	○	○	○
Dizziness (eyes open)	○	○	○	○
Dizziness (eyes closed)	○	○	○	○
Vertigo	○	○	○	○
Faintness	○	○	○	○
Awareness of breathing	○	○	○	○
Stomach awareness	○	○	○	○
Decreased appetite	○	○	○	○
Increased appetite	○	○	○	○
Burping	○	○	○	○

Q8 Did you experience any other symptoms not mentioned above?

_____

Page Break

Q15 **Simulator Motion and Visuals**

Q5 The following questions are designed to find out how you would judge the motion you were exposed to. Judging **solely** the **simulator motion** you were exposed to (thus, not considering, amongst others, visuals and sound), to which extent do you agree with the following statements? Please provide the appropriate answers.

	Strongly disagree	Disagree	Somewhat disagree	Neither agree nor disagree	Somewhat agree	Agree	Strongly agree
I felt as if I was being driven around in a car.	○	○	○	○	○	○	○
The motion I experienced was unpleasant.	○	○	○	○	○	○	○
The motion sensation was too intense for my liking during a car ride.	○	○	○	○	○	○	○
The motion I experienced was predictable.	○	○	○	○	○	○	○
The motion I was exposed to did not resemble that of a vehicle on the road.	○	○	○	○	○	○	○
The motion I was exposed to was comfortable.	○	○	○	○	○	○	○

I prefer weaker motion sensation when being a passenger in a car.	○	○	○	○	○	○	○
I was surprised by certain manoeuvres.	○	○	○	○	○	○	○

Q7 The following questions are designed to find out how you would judge the presented **visuals** you were exposed to. To which extent do you agree with the following statements? Please provide the appropriate answers.

	Strongly disagree	Disagree	Somewhat disagree	Neither agree nor disagree	Somewhat agree	Agree	Strongly agree
The visuals looked realistic (as if being driven around in a car).	○	○	○	○	○	○	○
The visuals and simulator motion matched perfectly.	○	○	○	○	○	○	○
The visuals made my ride feel unpleasent.	○	○	○	○	○	○	○
The presented visuals did not resemble real life and made it feel like a simulation.	○	○	○	○	○	○	○

The motions I felt did not agree with the motions I saw.	○	○	○	○	○	○	○
The visual motion made my ride feel comfortable.	○	○	○	○	○	○	○

Q9 Please indicate what the driving behaviour that you experienced during today's experiment session felt like.

- ○ Defensive: cautious driving behaviour
- ○ Normal: neutral driving behaviour
- ○ Dynamic: aggressive driving behaviour
- ○ Extremely dynamic: extremely aggressive driving behaviour

Q12 What was the minimum and maximum velocity during your ride today?

- ○ Minimum velocity (km/h): _____
- ○ Maximum velocity (km/h): _____

Q18 Please leave a comment about your general experience of today's ride.

_____

End of Block: Questions_per_trial

Start of Block: Full_experiment_comparison

Q13 **Full Experiment Comparison**

The following questions will ask you to compare all three experiment sessions with each other, as you have completed them all.

Q10 Please indicate to what extent you agree with the following statements related to all three sessions.

	Strongly disagree	Disagree	Somewhat disagree	Neither agree nor disagree	Somewhat agree	Agree	Strongly agree
The simulator motions felt different per session.	○	○	○	○	○	○	○
Moving visuals increased the realism of the simulation.	○	○	○	○	○	○	○
Having to wear a neck brace affected the comfortability of my rides.	○	○	○	○	○	○	○
Having to wear a headset affected the comfortability of my rides.	○	○	○	○	○	○	○

Q15 Please rate the level of **comfortability** of the rides you experienced in all three sessions in the matrix below. Give each condition a score between 1-7, in which a 1 is extremely **uncomfortable** and a 7 is extremely **comfortable**. You are allowed to put multiple conditions at the **same level** of comfortability.

	1: Extremely **Uncom-fortable**	2: **Uncom-fortable**	3: Mildly **uncom-fortable**	4: Neutral comfortability	5: Mildly **com-fortable**	6: **Com-fortable**	7: Extremely **com-fortable**
A: Baseline (no visual motion)	○	○	○	○	○	○	○
B: Rural area (highway)	○	○	○	○	○	○	○
C: Urban area (city)	○	○	○	○	○	○	○

Q17 Please rate the **driving behaviour** of the rides you experienced in all three sessions in the matrix below. Give each condition a score between 1-7, in which a 1 is extremely **defensive/cautious** driving behaviour and a 7 is **aggressive** driving behaviour. You are allowed to put multiple conditions at the **same level** of driving behaviour.

	1: Extremely **defensive** driving behaviour	2: **Defensive** driving behaviour	3: Mildly **defensive** driving behaviour	4: Neutral driving behaviour	5: Mildly **aggressive** driving behaviour	6: **Aggressive** driving behaviour	7: Extremely **aggressive** driving behaviour
A: Baseline (no visual motion)	○	○	○	○	○	○	○
B: Rural area (highway)	○	○	○	○	○	○	○
C: Urban area (city)	○	○	○	○	○	○	○

Q22 Please describe your preference and/or experiences of the 3 different conditions in a couple of words.

_____

_____

_____

_____

_____

Page Break

Q20 All three experiment trials had **identical simulator motions**.

Does this surprise you?

- ○ Yes
- ○ A bit
- ○ No

Q25 Please explain why (not)?

_____

_____

_____

_____

_____

Page Break

Q23 Thank you very much for participating in this 3-trials experiment! All experimental output will be anonymously processed and will contribute to his research field, as well as my MSc thesis.

Please remember: Do not talk about the experiment with other participants as this could influence the results.
Do not forget to ask for your bol.com voucher!
Please click the arrow below to finish the questionnaire!

If you have any general comments/remarks left about the full experiment, please leave them here.

_____

_____

_____

_____

_____

End of Block: Full_experiment_comparison

Start of Block: Ending_per_trial

Q19 Any other remarks/thoughts of the trial you did today?

_____

_____

_____

_____

_____

Q16 Thanks for filling in the questionnaire!

Please remember: Do not talk about the experiment with other participants as this could influence the results. Try to remember today's session as it is required to compare all sessions after the final trial.
Do not forget to ask for your bol.com voucher!

Please click the arrow below to finish the questionnaire!

End of Block: Ending_per_trial